Inferential Active Disturbance Rejection Control of Distillation Columns

by

Fahad Khamis Sanad Al Kalbani

A thesis submitted in partial fulfilment
of the requirements for the degree of
Doctor of Philosophy
School of Chemical Engineering and Advanced Materials
Newcastle University

United Kingdom

October 2018

Abstract

The distillation column is an important processing unit in the chemical and oil refining industry. Distillation is the most widely employed separation method in the world's oil plants, chemical and petrochemical industrial facilities. The main drawback of the technique is high energy consumption, which leads to high production costs. Therefore, distillation columns are required to be controlled close to the desired steady state conditions because of economic incentives. Most industrial distillation columns are currently controlled by conventional multi-loop controllers such as proportional-integral-derivative (PID) controllers, which have several shortcomings such as difficulty coping with sudden set-point jumps, complications due to the integral term (I), and performance degradation due to the effect of noise on the derivative term (D). The control of ill-conditioned and strongly non-linear plants such as high purity distillation needs advanced control schemes for high control performance. This thesis investigates the use of active disturbance rejection control (ADRC) for product composition control in distillation columns. To the author's knowledge, there are few reported applications of ADRC in the chemical industry. Most ADRC applications are in electrical, robotics and others. Therefore, this research will be the first to apply the ADRC scheme in a common chemical processing unit, and can be considered as a first contribution of this research.

Initially, both PI and ADRC schemes are developed and implemented on the Wood–Berry distillation column transfer function model, on a simulated binary distillation column based on a detailed mechanistic model, and on a simulated heat integrated distillation column (HIDiC) based on a detailed mechanistic model. Process reaction curve method and system identification tools are used to obtain the 2×2 multi-input multi-output (MIMO) transfer function of both binary and HIDiC for the purpose of PI tuning where the biggest log-modulus tuning (BLT) method is used. Then, the control performance of ADRC is compared to that of the traditional PI control in terms of set-point tracking and disturbance rejection. The simulation result clearly indicates that the ADRC gives better control performance than PI control in all three case studies.

The long time delay associated with product composition analysers in distillation columns such as gas chromatography deteriorates the overall control performance of the ADRC scheme.

To overcome this issue an inferential ADRC scheme is proposed and can be considered as a second contribution of this research. The tray temperatures of distillation columns are used to estimate both the top and bottom product compositions that are difficult to measure on-line without a time delay. Due to the strong correlation that exists in the tray temperature data, principal component regression (PCR) and partial least square (PLS) are used to build the soft sensors, which are then integrated into the ADRC. In order to overcome control offsets caused by the discrepancy between soft sensor estimation and actual compositions measurement, an intermittent mean updating technique is used to correct both the PCR and PLS model predictions. Furthermore, no significant differences were observed from the simulation results in the prediction errors reported by both PCR and PLS.

The proposed inferential ADRC scheme shows effective and promising results in dealing with non-linear systems with a large measurement delay, where the ADRC has the ability to accommodate both internal uncertainties and external disturbances by treating the impact from both factors as total disturbances that will then be estimated using the extended state observer (ESO) and cancelled out by the control law. The inferential ADRC control scheme provides tighter product composition control that will lead to reduced energy consumption and hence increase the distillation profitability. A binary distillation column for separating a methanol–water mixture and an HIDiC for separating a benzene–toluene mixture are used to verify the developed inferential ADRC control scheme.

Dedication

This dissertation is dedicated to my parents and my wife.

Acknowledgements

Usually I look back at the last three years of my PhD journey and wonder whether I did any work at all, or if I just channelled the intellect, support, and energy of everyone around me into a coherent curriculum vitae, attaching my name to it in each process. If Newcastle University allowed it, I would list everyone in this thesis as co-authors, but I expect they will have to settle for a brief, inadequate mention here at the beginning.

This PhD thesis is a culmination of an excellent working relationship with my supervisor Jie Zhang, to whom I am eternally thankful and grateful. Jie provided continuous support during my PhD and generously gave me huge guidance during the critical issues I normally faced. His vast experience in process control theories and his willingness to share his knowledge has supported me during my three and half years of research.

I am also greatly indebted to my parents who in some way contributed to my PhD journey by sacrificing a lot of being away from them for more than three years. Completing and getting this PhD certificate is a valuable gift for them for all support and love they still give me. I am trying to make them very proud of me.

I also have strong appreciation for both Dr. Thomas Bisgaard and Dr. Jakob Kjosted from Denmark Technical University (DTU) who guided and supported me in developing a mechanistic simulation model for the heat integrated distillation column (HIDiC) in order to apply both the control algorithm and investigate their performance in a complex distillation model.

My company, Petroleum Development of Oman (PDO) for their generous support and scholarship they provided me with. Their trust in me and my capabilities generate my motivation to achieve my targets and return to the company as soon as possible to work hard again with them and adhere to my commitment.

Writing this thesis was a lovely experience with cherished friends who gave empathy and enthusiasm in just the right doses. The wonderful companionship of Muhanna Al Ghafri, Sultan Al Rashdi, Mohammed Al Rashdi, and many other friends ensures that I can only look back over the last few years with a feeling of reminiscing and fondness.

The endless encouragement and unconditional love provided by my beloved family provided a secure anchor during the difficult and hard times, thank you.

As long as I am writing names down, I cannot neglect indicating my best friend Talal Al Mandhari, a most constant friend since elementary school. He's provided me a lot of encouragement and support over the years.

Lastly, Nasra Al Waili, my beloved wife who is doing a BSc degree in bioscience program at Cardiff University. She came with me to Newcastle University when I was in a critical situation during my PhD journey, away from her study, family, friends and responsibilities. Her support can be summed up in the following fact: she stayed with me at the hospital many times when I got a strong infection, and she is giving me strong support by providing a comfortable and productive environment to write my thesis in a short duration of time and in a good manner.

Table of Contents

List of Figures

List of Tables

Chapter 1 Introduction

1.1 Background

The refining process of crude oil produces different oil products. The separation process of these products necessarily requires a distillation column. Among all common technologies, distillation columns are the most frequently used facility in the oil and chemical industries for the separation of liquid mixtures. Indeed, distillation is the most preferred separation method at various industrial scales with more than 40,000 columns in operation worldwide (Kiss, 2014). A general distillation column consists of a vertical column where trays or plates are used to increase the separation of components. A condenser and reboiler are used as heat duties. The reboiler provides the required heat for necessary vaporisation from the column bottom, and then the vapour is condensed by the condenser. Part of the condensed vapour is used as reflux whilst the rest is collected in a reflux drum and withdrawn as a top product.

Notably, almost every product in the market includes chemicals that have passed through a distillation column. Despite their flexibility and simplicity, the total efficiency of distillation columns is quite low due to irreversible energy loss associated with mass transfer such as re-mixing in separation, pressure heat, and drop transfer. Distillation has been in use for a decade and is often observed as a mature technology, but it consumes a significant percentage of the total heating in the world's process industry. It is a major energy consumer in the petrochemical and chemical industry. Most distillation column operations require a vast amounts of energy and account for more than 32.9% of the total energy used in the refining and bulk chemical processes industry (Figure 1.1) and more than 95% of the energy consumed in separation processes (World Energy Council, 2016). The minimum energy expected to be consumed in distillation columns depends on temperature span and operating pressures (Kiss, 2014). It is very possible that it will remain the choice of separation technology for the next decade, but radial modifications and changes need to be made to reduce energy consumption. Reducing or minimising the energy consumption of a distillation column is not a straightforward task. First, distillation columns come in various

configurations with different operating objectives. These kinds of variances lead to a different operational degree of freedom and distinct dynamic behaviours. Moreover, many columns are subject to significant interactions among the control loops and have frequent limits and constraints on their operation that complicates dynamic behaviour and makes it more difficult to control and optimise. As a result, specialised control configurations are required to minimise the energy consumption to control both top and bottom product stream compositions.

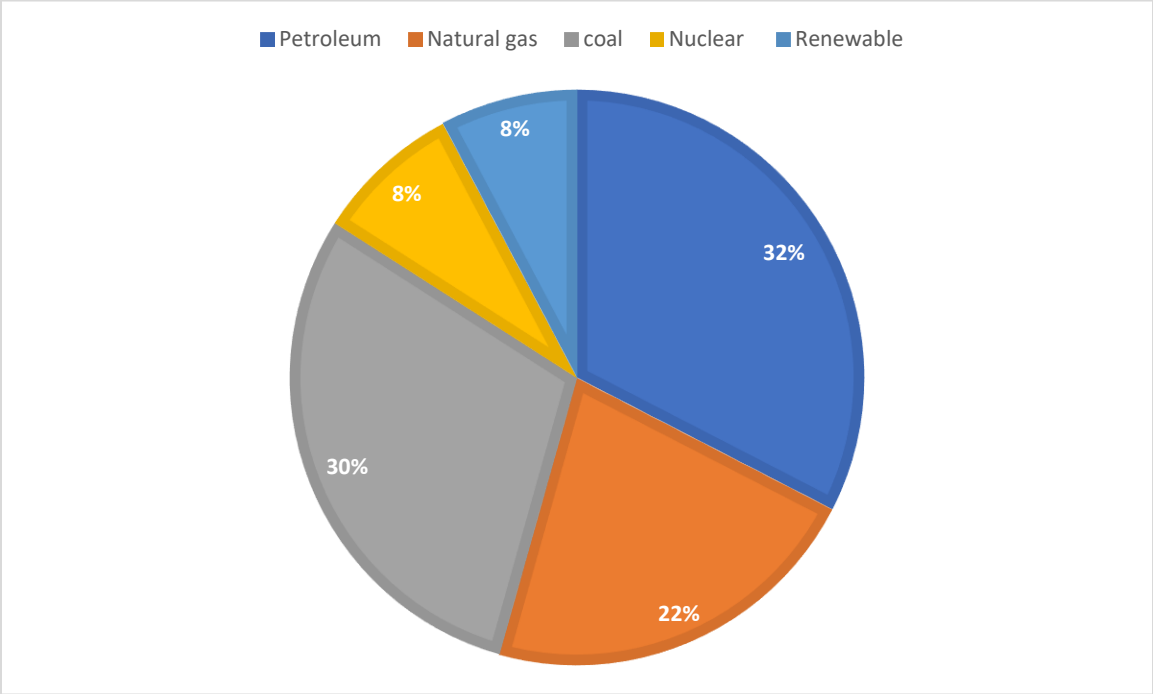

Figure 1.1: Industrial energy consumption worldwide, 2016 (World Energy Council, 2016)

Waheed et al. (2014) observed that distillation columns require high energy consumption for the entire processing system that accounts for around 95% of the total energy used in the chemical industry, and an estimated 3% of the total energy consumption (Waheed et al., 2014; Jeffries et al, 2016; Orozco et al., 2016; Manikandan et al, 2017). It is very clear that energy consumption has a large impact on the overall production and operational costs of such processing units, where it can produce greater than 50% of both capital and plant operating costs in a typical chemical plant, significantly impacting overall profitability (Kiss and Bildea, 2011). By investigating the relationship between the heat source of the reboiler and cold source on the top from the condenser, the distillation process can be considered as a heat engine which generates energy at the reboiler

stage and rejects part of temperature at the condenser stage, in order to separate the volatile components from the less volatile components (Soares Pinto et al., 2011).

Despite efforts made by researchers to control and optimise energy consumption, the issue of achieving good separation with less energy consumption still exists. There is no doubt that any reduction of energy consumption, without compromising yield and product quality, can directly create some economic benefits. Funk and his co-workers (1978) conducted a feasibility study in around 400 distillation columns and found that more than 42% of the energy consumption of distillation towers can be effectively reduced by changing and manipulating the operation parameters (Funk et al, 1978). Extensive research has been conducted to enhance the energy efficiency of distillation columns, focusing on either the efficiency of the distillation column or improving the design of optimal distillation schemes. However, there are other options for enhancing the energy efficiency of distillation operations, which include modifying the operating conditions or making changes to the design of the column, such as adjusting the reflux ratio (Abolpour et al., 2013; Waheed et al., 2014) and preheating the feed rate (Soave and Feliu, 2002). Other alternative cost-effective and attractive approaches proposed in relation to the above are to implement optimal control solutions (Fuentes and Luyben, 1983). Nevertheless, dynamic simulation models of these distillation column systems are normally required by current control methods. Improving the control technique of product compositions can have a significant effect on enhancing product quality, reducing energy consumption and protecting environmental resources (Waller et al., 1988).

Currently, the need to optimise efficiency in terms of energy consumption and enhancing the reliability of optimisation and automation results in increasing expectations towards modern industrial control applications. Control engineers have strived to solve various control issues in terms of operating industrial processes in a more accurate manner, but at the same time with lower production costs in terms of energy consumption. For example, non-linear control issues have been emerging an area of research for the last three decades. Learning the basic strategies of non-linear control design and analysis can significantly improve the control theories to overcome such practical control problems successfully. The vast majority of literature on adaptive control and adaptive estimation relies on the assumption that the system parameters are constant or slowly time varying. Traditionally, the dynamics of distillation columns are approximated by linear

models as they are simple to understand, ease the control system design and can be used in well-developed linear control theory in order to design linear controllers. Waller et al. (1988) argued that the main drawback of using these types of linear controllers is that they achieve good performance only with small changes of the nominal operating point and in a narrow range of operating conditions without a large amount of external undesired disturbance (Waller et al., 1988). In practice however, the non-linear and time-varying behaviour of the process parameters might be of significant importance. Time-varying parameters could exist due to the uncertain, complex mechanisms that are not designed or accounted for by the process model. They can also be introduced from unmeasured inputs or model plant mismatch that affects the overall process dynamics. Moreover, many industrial processes exhibit highly time-varying and non-linear behaviour across the industrial operating range. The behavioural complicacy of these types of systems causes many difficulties in design and analysis techniques that prevent researchers from providing systematic solutions to the various problems associated with non-linear systems (Precup et al., 2009). In addition, this phenomenon needs more sophisticated techniques that would enable non-linear function approximation and input–output mapping to be established.

The design of current controllers, such as model predictive control (MPC) and many others, relies heavily on an accurate mathematical model of the system under control. However, constructing such a dynamic model for any industrial system needs detailed process knowledge from specialist engineers. Commonly it is a challenge to assemble the existing knowledge into a compact and coherent mathematical design. Usually this leads to a very complex model of the dynamic system, as it is very difficult to identify which effects are relevant and should be considered in the final model, and which should be neglected. Such an approach is usually found to be very expensive and laborious. If the knowledge of the specialist is lacking, like in the case of poorly understood systems, the construction of an accurate dynamic model is actually impossible. Furthermore, some quantities such as rates and coefficients required to construct the dynamic mathematical model are often unknown, and should be estimated by conducting various dedicated experiments (Tóth, 2010). However, in many industrial cases such a model is quite difficult to design due to the many reasons investigated by Mohammedzaman and Jamab (2006):

- Lack of accurate knowledge about parameters of the overall system. Unfortunately, the use of a simplified model usually leads to performance reduction of the overall system and may lack robustness due to modelling error.
- The presence or existence of a strong non-linear dynamic at the dynamic system.

For the last decades and until now, the PID controller has been considered the backbone for most current control applications, as described in Åström and Hägglund (2006) and O'Dwyer (2009). Despite the fact that PID controllers are easy to derive, configure, implement and tune, they also produce poor performance and lack efficient handling of constraints for the critical integration processes and processes with a large time delay. Due to the above reasons, various research studies have been carried out in order to overcome the limitations of PID controllers. As a result various control techniques like PI, active disturbance rejection control (ADRC), and inferential control will be implemented in this research to investigate their performance and make a suitable analysis in each control algorithm regarding set-point tracking, robustness, and disturbance rejection.

Due to the difficulty of obtaining accurate measurements for top and bottom product compositions in distillation columns without a time delay, the integration of an ADRC algorithm and inferential control algorithm is proposed here using the secondary variables, tray temperatures, in order to control the primary variables which are top and bottom product compositions.

1.2 Significance of the study

Regarding control applications, an ideal control algorithm solution is the control system that can be implemented straightforwardly into a specifically given process. It is immediately available to use upon implementation and designed to achieve or execute a specific task without any external user intervention. Such an ideal control system is highly recommended in the industry as it provides intuitiveness and simplicity for the user as well as the effectiveness of task realisation due to both its adaptive and robust features. Moreover, there are certain difficulties in designing a robust control system in practice:

- The uncertainty description is not usually provided and should be accounted for and developed in a mathematical model.

- The choice of sensors, actuators, and their locations that specify the achievable performance of the overall system usually require some intervention from the instrument and control engineers.
- Operational aspects such as handling of constraints, sensor failures, actuator failures and stuck valves can create a bottleneck for the closed loop performance.

There are several industries that benefit from the use of intelligent, robust and expert control, ranging from electrical, electronic, food, textile, automotive to chemical industries, etc. These industries commonly include processes that show highly non-linear systems, coupled and uncertain behaviour and thus need intelligent and robust solutions for their efficient operation. However, the chemical industry is a major one due to its association with a large proportion of the world population and the huge impact on people's lives through the nature of products and operations that it provides including pharmaceuticals, food, beverages and petroleum products. One of the common processes in the chemical industry is the distillation process. It is considered as a typical unit operation in chemical engineering that requires a robust control technique due to its complexity, nonlinearities and the uncertainties of the dynamic process. Using a suitable robust and intelligent control system will lead to significant energy savings, consistent product composition quality and higher product yield. However, current control algorithms are hampered by many issues such as strong control loop interaction, lack of reliable measurements, and large system uncertainty. The application of adaptive and robust control theories can substantially enhance distillation column control.

Even after numerous advancements in robust control theories, the control of most industrial distillation columns is still being conducted based on intuition and heuristic control techniques such as multi-loop PID as some of the new control techniques have some drawbacks. Fuzzy control rules rely on expert knowledge. The Neural Network (NN) algorithm is quite comlex and not easy to implement.

The ADRC has been proposed and considered as a new paradigm to overcome the disadvantages of the conventional industrial control tools (Sun et al., 2017). Initially, the ADRC technique was applied in many applications outside the domain of chemical and process engineering, especially in electrical and electronic engineering applications. It has shown strong practical appeal and provides interesting and promising results in controlling various complex

time-varying and nonlinear systems. To the author's knowledge, there are few reported applications of ADRC in the chemical industry, which will be discussed in detail in Chapter 2. It also provides some other contributions:

- Recently there have been several studies on various approaches to reduce energy consumption, plant operational cost and reduce environmental harm in chemical process plants. Specifcally, one of these approaches is to control the operational parameters by an efficient control strategy (Contreras-Zarazúa et al., 2016; Zheng et al., 2017). ADRC is a new control technique which has strong practical appeal. It is a model free control approach and can deal with nonlinearities, time delay and loop interactions. Most of the currently reported applications of ADRC are in the motion control area. This thesis investigates using ADRC in various types of distillation columns such as the binary distillation column and HIDiC. The control techniques developed in this thesis will also be applicable to other process units in the oil and gas industry. There are many process loops that should be tuned and controlled by using various control techniques. As a result, it will assist the control engineer in acquiring several control strategies of various oil and gas industry processes.
- A time delay issue frequently occurs in many non-linear practical systems such as nuclear reactors, chemical processes, telecommunications, long transmission lines and many others (Rakkiyappan, 2011). Since time delay is the main cause of poor control performance and instability, the control of systems with time delay has received significant attention from researchers over the past years. However, current measurement tools such as gas analysis and NIR-infrared—used to measure the product composition—possess an undesired time delay of approximately 10–15 minutes (Zhang, 2001). This will affect the overall performance of the control technique and reduce its efficiency. This research aims to overcome this issue by building a soft sensor model to estimate the product compositions and integrate it within the ADRC to significantly enhance the overall control performance.

1.3 Aim and objectives

The core aim of this research is to design and develop an inferential ADRC technique to control a binary distillation column and HIDiC. Moreover, there are certain objectives that need to be executed and completed in this research:

- Implement the PI controller on a binary distillation column and HIDiC as a basis for performance comparison.
- Implement the ADRC technique on a binary distillation column and HIDiC.
- Investigate the overall performance of both (PI and ADRC) regarding set-point tracking, robustness, and disturbance rejection, the impact of model uncertainty and control loop interactions.
- Build inferential estimation models to estimate the product compositions from easy-to-measure process variables using PCR and PLS techniques.
- Integrate inferential control with ADRC and implement these on the binary distillation column and HIDiC.

1.3 Papers published

This research has led to the development of some new control strategies that have the capability of handling the modelling issue of non-linear applications and strong control loop interactions. Furthermore, another novel control strategy is introduced to overcome the measurement delay associated with product composition. The novel strategies introduced in this research are summarised below:

- A novel control technique that has the ability to control both top and bottom product compositions of a simulated binary distillation column based on a rigorous mechanistic model was introduced in this paper. A comparison was made between the performance of PI and ADRC schemes in terms of set-point tracking and external disturbance rejection which shows an efficient performance of the ADRC scheme over the conventional PI controller. This paper was presented at the 8th IEEE GCC conference and won the 3rd best paper award **(Al Kalbani, Al Hosni, and Zhang, 2015).**
- Another novel control technique was introduced by integrating static PCR based inferential control with the ADRC scheme on a binary distillation column to overcome the undesired delay introduced by the current measurement tools of product composition. This paper was presented at IFAC ADChem 2015 **(Al Kalbani & Zhang, 2015).**
- In order to improve the performance of the static model based inferential ADRC scheme, a dynamic model based inferential ADRC control was developed and it provides better control

performance compared to the static one. This paper was presented at the ICINCO 2015 conference and was short-listed for best paper award **(Al Kalbani & Zhang, 2015).**

- Due to the promising result produced from applying the ADRC scheme on the binary distillation column, the ADRC was applied to a HIDiC in order to investigate its performance in overcoming the strong loop interactions. The performance of the ADRC and PI schemes was investigated again in terms of set-point tracking and undesired disturbance rejection. This paper was presented at the 21st MMAR conference **(Al Kalbani, Zhang, Bisgaard and Huusom, 2016).**
- The static PCR model based inferential control was integrated with the ADRC scheme to overcome the measurement delay of product composition in the product composition control of a HIDiC. This paper was presented at the IEEE ICARCV 2016 conference **(Al Kalbani & Zhang, 2016).**
- The dynamic PCR model based inferential control was again integrated with the ADRC scheme to provide better performance than the static inferential ADRC scheme and overcome the measurement delay of product composition. This paper was presented at IEEE- GCC 2017 conference in Bahrain **(Al Kalbani & Zhang, 2017).**

Furthermore, the following papers are in progression to be submitted to journals:

- Dynamic PCR model based inferential ADRC of a binary distillation column.
- Dynamic PCR model based inferential ADRC of a heat integrated distillation column for separating benzene–toluene.

1.4 Thesis outline

This thesis is divided into five major chapters, in addition to this introduction chapter and conclusion in Chapter 7.

Chapter 2 presents the literature review. It starts with a brief overview of various distillation columns. It subsequently highlights various control algorithms used in refinery and chemical industrial applications with their associated drawbacks. It is shown that the PI controller is the most common control technique used in current industrial applications for approximately 90% of chemical industrial applications. Despite this fact, this type of common algorithm has several limitations that will be introduced in detail in this chapter. In addition, in order to overcome these

limitations the new control approach introduced by Han (2009) will be explained in minute detail. The structure and implementation of the ADRC scheme will be described and discussed with its associated equations in order to apply its structure on proposed case studies in this research. However, obtaining accurate measurements for the product composition of distillation columns is quite difficult and critical due to the presence of delay caused by the current measurement tools such as the gas analyser. As a result, a background overview of inferential control is introduced and its characteristics are described. Since there are various types of techniques to build the inferential control introduced and used in the existing literature, only suitable techniques for proposed case studies are discussed in this chapter.

Chapter 3 starts by presenting an overview of the Wood–Berry distillation column model, which is a well-known 2×2 (two inputs and two outputs) transfer function of a pilot plant binary distillation column for separating a mixture of methanol and water. It is used in this chapter as a first case study in this research. Prior to implementing the PI controller, the parameters of this controller are obtained using the BLT tuning technique. Then, both PI and ADRC controllers are implemented and applied to the Wood–Berry distillation column. Furthermore, the control performance of both schemes are investigated and discussed in terms of set-point tracking, loop interaction and the external disturbance rejection. The importance of these tests is to investigate the efficiency of both schemes and decide on the most suitable controller to deal with this type of strong non-linear application. The sum of squared error (SSE) is used as a control performance indicator.

In Chapter 4, a background overview of a binary distillation column is introduced. This brief background has also been highlighted in the existing literature in terms of various control schemes that have already been applied before. In contrast to the simulation using transfer functions in Chapter 3, simulation of a binary distillation column based on a nonlinear mechanistic model was implemented in order to provide a more realistic simulation. The process reaction curve technique is used to obtain the transfer function of the binary distillation column from the mechanistic model. Again the BLT approach is used to specify the PI controller parameters. Then, both PI and ADRC controllers are designed and applied to the mechanistic model based simulation to investigate their performance in terms of set-point tracking and external disturbance rejection to evaluate if the ADRC scheme will provide good results compared to the conventional PI control, and if it will be

able to overcome the PI controller limitations. Again, SSE is used as a control performance indicator.

Chapter 5 presents inferential ADRC for the product composition control in the binary distillation column. This chapter presents the current composition measurement devices such as gas analyser possessing undesired delay, which is estimated to be 10–15 minutes. It will also discuss the issues associated with the single temperature control in the binary distillation column. These issues will be overcome by designing the inferential control technique and implementing it as a feedback control loop to the ADRC controller. In this chapter, the PCR and PLS techniques are used first to build the soft sensors of the estimation model in order to integrate it with the existing ADRC scheme designed in the previous chapter. Furthermore, the main purpose of this integration is to provide a continuous measurement by soft sensors for the ADRC scheme to keep the product compositions at the desired set-point. However, the existence of control offset due to the nominal operating condition change such as set-point change in the estimated signal has been eliminated successfully using the mean updating technique.

In Chapter 6, after the promising results presented in Chapter 4 of applying the ADRC scheme to the binary distillation column, ADRC is applied to the most critical and complicated column: the HIDiC. The HIDiC is considered to be one of the most difficult distillation columns to control and handle due to the challenges it presents such as strong loops interaction. Thus, evaluating the performance of the ADRC scheme on this type of distillation column will give a clear idea about the efficiency of this type of controller compared to other existing controllers especially the PI controller. Simulation of the HIDiC in MATLAB based on the mechanistic model is developed. This chapter will start by providing an overview of the HIDiC, its components, and the overall operating principle. It is subsequently followed by obtaining the 2×2 MIMO transfer function of HIDiC using the system identification toolbox in order to apply the BLT tuning method and producing the suitable gain parameters of the PI controller. After obtaining the appropriate controller parameters, both PI and ADRC control schemes are implemented. Different tests are conducted to evaluate their performance in terms of set-point tracking and disturbance rejection. Then the introduced ADRC scheme is integrated with the inferential control scheme in order to overcome the delay associated with the measurement of the product compositions. Again, the soft sensors or estimation model in this chapter are implemented using both PCR and PLS due to the

strong collinearity associated with the secondary measurement variables (tray temperatures). Furthermore, the existence of control offset due to the nominal operating change such as set-point change in the estimated signal was eliminated successfully using mean updating technique.

Chapter 2 Literature review

2.1 Introduction

Many industrial processes are considered to be strongly time varying, non-linear and ill-conditioned plants. They are also often associated with long delays that in fact introduce an additional phase lag that significantly reduces the stability margin or simply destabilises the control system. The ecological and economical optimal operation requires tight control of the controlled product quality variables. The economic benefits of enhanced control schemes tend to be significantly underestimated.

In the last decades, the proficient and efficient use of energy has become a highly significant issue in the industrial sector, since the prices of energy as well as environmental awareness are continually increasing. Thus, industry is highly interested in approaches for minimising energy consumption (Fazlali et al., 2009). In particular, distillation is still one of the most commonly used and one of the most versatile separation methods for separating liquid mixtures in petrochemical and chemical industries, accounting for about 25–40% of total energy usage (Kiss, 2014). Due to its relatively low energy efficiency, it is often considered one of the biggest energy consumers in industrial processes. When considering energy efficiency in any type of distillation column, it is essential to account for the form of energy being consumed and the quality of cooling and heating required. Trade-offs exist between environmental impact, cost, energy sources and equipment requirements. Distillation columns consume a huge amount of energy to generate the heat required to convert liquid to vapour and then condense the vapour back to liquid via a condenser. They use more than 40% of the total energy used in the refining and bulk chemical process industry and more than 90–95% of the energy consumed in liquid separation and purification (Vazquez–Castillo et al., 2009; Jogwar and Daoutidis, 2010; White, 2012; Masoumi and Kadkhodaie, 2012; Nair and Raykar, 2017), and account for more than 3% of the energy consumption in the world (Biyanto et al., 2017; Jeffries et al, 2016). Moreover, the capital investment in these distillation systems is indicated to be at least eight billion US dollars, which can contribute to greater than 40–50% of both capital and plant operating costs in a typical chemical plant and can have a significant impact on the overall plant profitability (Kiss and Bildea, 2011; Kiss, Landaeta and Ferreira, 2012; Tarjani et al., 2017). The minimum energy expected to be consumed in distillation columns depends on various operation variables such as temperature spans and operating pressures, so the optimisation of these variables leads to reduced energy demand while meeting product quality and quantity

requirements (Kiss, 2013).

This chapter is organised as follows. Section 2.2 gives brief background information about binary distillation column and HIDiC. Section 2.3 introduces one of the commonly used controller, the proportional – integral and derivative controller, and its advantages and limitations. Then, the concept of ADRC is introduced in Section 2.4 with its main components and associated mathematical equations. Section 2.5 presents brief information about the Kalman filter with its constructed mathematical equations. Section 2.6 provides background information about the observer that is used to observe the state variables that are inaccessible and not available to measure by direct measurement tools. Then, the concept of the inferential estimator with background information about the PCR and PLS are outlined in Section 2.7. Finally, a summary is given in Section 2.8.

2.2 Distillation columns

The distillation column is probably the most common and important process unit, and has been intensively investigated and analysed in the chemical engineering sector during the past few decades (Keller and Humphrey, 1997; Al-Muslim et al., 2003; Rivero, Rendón and Gallegos, 2004; Alhajji and Demirel, 2015; Demirel, 2013; Shin et al, 2015; Zhang and Liu, 2017). Distillation is a thermal separation technique for separating a mixture of two or more liquid materials into their component fractions of required purity according to the difference in volatility of the components. Note that distillation refers to a unit operation of a physical separation process. However, the combination of different distillation process operations lead to the introduction of new distillation processes such as a dividing wall column (Harmsen, 2010), or with a chemical reaction, leading to the introduction of chemical reactive distillation (Sharma and Singh, 2010; Sundmacher et al, 2005), and other chemical process operations (Schmidt-Traub and Górak, 2006).

Distillation has various applications such as the separation of crude oil into different oil cuts (e.g. diesel, gasoline, kerosene, etc.), water desalination and purification, the separation of air into its components (e.g. nitrogen, oxygen, and argon), and the production of distilled beverages or the distillation of fermented solutions with high alcohol content (Forbes, 1970). Distillation has been

the subject to vast development due to the petrochemical industry and as such it is one of the most significant techniques in the global energy supply system (Harmsen, 2010).

2.2.1 Binary distillation columns

Binary distillation columns constitute a major part of most chemical industries such as petrochemical production, liquor production and coal tar processing for the separation of feed mixtures. Figure 2.1 presents a schematic diagram of a conventional binary distillation column that illustrates some of the desired inputs and components present in a large-scale distillation column. The feed is composed of a mixture of the two components that need to be separated. The feeding tray separates the column into a rectifying or enriching section (upper part of the column) and a stripping section (lower part of the column). Separation occurs due to both mass transfer and intensive heat transfer between the liquid flow and counter-currently rising vapour flow (Rehm, 2009). The separation process of the two components in the feed composition can occur due to the fact that the boiling mixture's vapour will be richer in components compared to the component that has a lower boiling point. Hence, when this vapour is condensed and cooled the condensate will contain more volatile components. Meanwhile, the remaining feed mixture will contain a higher proportion of the less volatile component.

The feed mixture is usually fed in the middle of the column. The vapour component is produced by the reboiler that is supplied by sufficient heat. The steam moves up through trays inside the distillation column to reach the top part and then rises out to be liquefied in a condenser. At that point liquid from the condenser enters into the reflux drum. At the final stage the distillate and top product are collected from the drum as a pure product. In addition, part of the pure product from the reflux drum is fed back close to the top, while the impure is produced at the bottom channel (Kiss, 2013). The trays of a binary distillation column indicate distillation stages, where some of the vapour leaving up the column is condensed by the condenser. The distillation column trays are characterised by many bubble caps or holes to allow the vapour to pass through. Their intended purpose is to increase the contact time between liquid and vapour in the column. If there are two components in the feed mixture (as in the case study considered in this research), a greater amount of the volatile component will vaporise and a larger amount of non-volatile components will remain in the liquid condensate. In other words, the component with the lower boiling point

will condense in the top condenser and the substances with a higher boiling point will move out from the bottom of the column as a condensed liquid (Miccio and Cosenza, 2014).

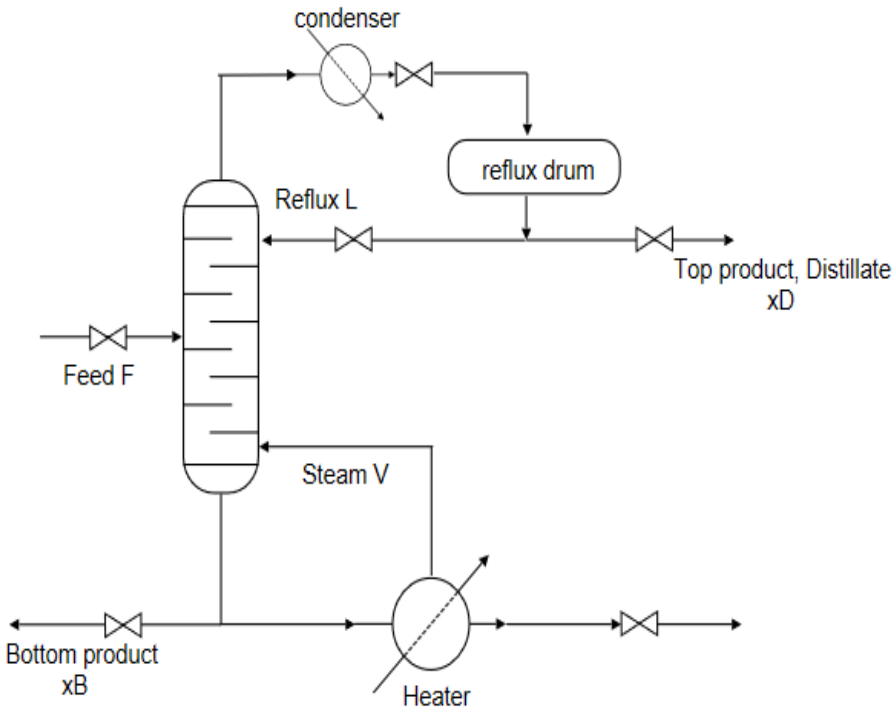

Figure 2.1: Schematic of a binary distillation column

The separation process of a binary column requires a large amount of heat from the reboiler to boil up the liquid mixture. This heat is then lost when liquefying the overhead vapour at the condenser. Despite its substantial energy consumption, the binary distillation column continues to be widely used in many industrial applications for separation and purification (Jana, 2010). Thus, there is a need for successful and efficient control techniques to increase the profitability and productivity of a plant. In distillation column control, the overhead distillate composition x_D and bottom composition x_B are usually selected as the controlled variables. When the reflux flow rate L and vapour boil up rate V are used as manipulated variables for controlling the product compositions of binary distillation columns, the increase of reflux flow rate always increases the purification of the top product composition (Feng et al., 2006). The rates of the manipulated variables are normally limited. Specifically, the extremely high reboiler rate and high reflux rate cause column flooding. However, the extremely low rates in these manipulated variables enlarge the spaces between liquid and vapour and might cause column channelling, which will lead to damaging the column itself (Skogestad, 1997).

2.2.2 Heat Integrated Distillation Columns (HIDiC)

In a typical chemical plant, the separation processes occurring in the distillation column are the main energy consumers and account for around 40–70% of both operating and capital costs (Ruiz et al., 2010). Unexpectedly, the thermal efficiency provided by the conventional distillation column is about 5–20% (Nair and Raykar, 2017). The low thermodynamic efficiency is usually associated with the substantial energy wastage existing in the process of distillation, which occurs due to the large difference between condenser and reboiler temperatures. Moreover, the thermal energy recovered in the condenser stage cannot be used to heat other flows in the same distillation column (Ponce et al., 2015). To increase heat separation and reduce energy consumption, a greater temperature should be provided in the reboiler part and drawn-off at a low temperature in the condenser. Due to the intensive energy consumption and low thermal efficiency, the distillation column has become a potential applicant for minimising its utility demand. Furthermore, various attempts are being made to introduce a successful systemic technique for enhancing the efficiency of the distillation process.

Almost 80 years ago, the concept of heat integration was originally proposed to improve energy efficiency. So far, several studies have been introduced on optimal design and synthesis of heat integrated distillation schemes (Gross et al., 1994). The concept of a thermally coupled distillation column was first introduced by Brugma in 1937. This energy efficient separation operation technique was re-introduced again by Wright (Wright, 1949) and then discussed and investigated by Petlyuk (Petlyuk et al, 1965). The heat transfer principle from the rectifying to the stripping section in a single unit was initially introduced by Freshwater (Freshwater, 1961). In order to improve the energy efficiency of the distillation column, the heat pump principle is usually implemented as an operative means of re-using the rejected heat (Null, 1976; King, 2013). This is normally referred to as heat pump assisted distillation columns. While it is a useful method for saving energy, it suffers from strict requirements imposed by the feed mixtures to be separated.

In 1967, Freshwater and Pike introduced the internal heat integration between the rectifying and stripping sections of a distillation column (Freshwater and Pike, 1967). This technique was initially presented for gas separation processes (Haselden, 1958). The advantages of this approach have been further systematised and clarified through various numerical solutions based on the second law of thermodynamics (Shimizu and Mah, 1983). Using the same principle of internal

heat integration, a secondary reflux and vaporisation distillation column was introduced. This type of distillation column included internal heat integration between part of the rectifying and stripping sections. Next, the principle of internal heat integration was extended to the whole rectifying and stripping sections (Shimizu et al., 1985; Shimizu and Mah, 1983).

A complete comparison was introduced between the benefits of the HIDiC and the traditional distillation column (Lueprasitsakul et al., 1990; Takamatsu et al, 1996). Since 1990, various heat integrated distillation schemes have been investigated and presented (Glenchur and Govind, 1987; Naito et al., 2000). A new scheme of HIDiC was designed that has alternating trays of stripping and enriching sections (Feng et al., 2006). Then, the efficiency was further improved by introducing a unique structure of HIDiC that has neither a trim condenser nor a trim reboiler; this column is commonly referred to as an ideal-heat integrated distillation column (i-HIDiC). The operation of i-HIDiC proves that it is more energy efficient than the general HIDiC, which includes both the condenser and reboiler along with the presence of an internal heat integration structure (Takamatsu et al, 1996).

The HIDiC is one of the technologies introduced to reduce the energy consumption by 20–40% compared to the conventional distillation process due to the heat exchange strategy especially in the separation of close to boiling mixtures (Masoumi and Kadkhodaie, 2012). The heat exchange process occurs when heat is propagated and produces condensation or vaporisation due to the pressure difference between the rectifying and stripping sections (Suphanit, 2010a). As a result, the ideal structure of HIDiC has neither a condenser nor a reboiler, and thus has a huge amount of energy reduction (Nakaiwa et al., 2000). The heat transfer occurs in the stripping and rectifying sections. The operation of both the rectifying and stripping sections is similar to a diabetic column that allows heat to leave or enter any particular stage along the column section. Furthermore, instead of rejecting heat through the main condenser and generating the heat through the main reboiler, the rectifying section distributes the total heat rejection, while the total heat absorption is distributed along the stripping section. The utility load required in the main reboiler or the main condenser can hence be reduced. The difference in pressure between the two column sections that is adjusted via a throttling and a compressor valve should be large enough to driving a positive temperature between the two sections (Suphanit, 2011b). Moreover, the implementation of this technology pursues minimising the emissions of carbon dioxide and reducing the total annual cost

(TAC) of this fundamental separation process. Figure 2.2 presents the schematic diagram of an ideal HIDiC.

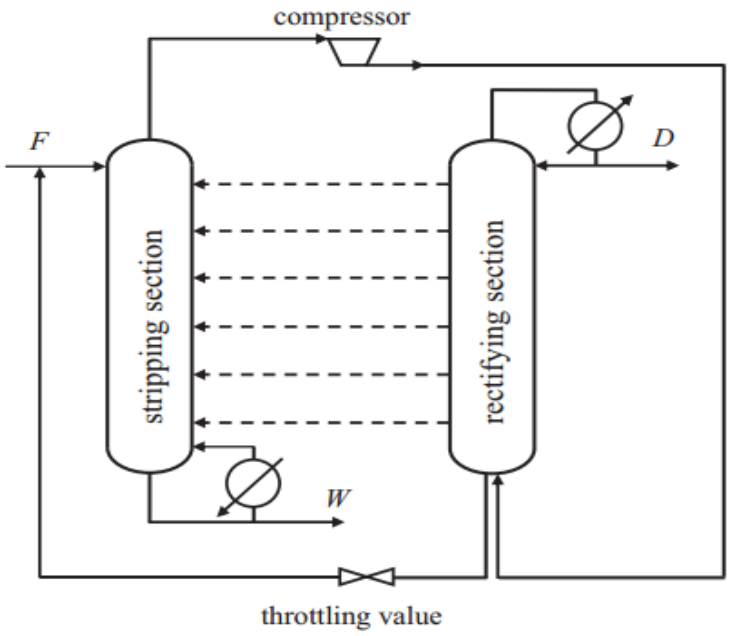

Figure 2.2: Schematic of an ideal HIDiC (Nakaiwa et al., 2000)

It is very likely that distillation will continue to be the process chosen for liquid mixture separation for the next decade as it is still labelled "as the technique of choice for many current purification and separations" but it needs to make radical modifications and changes to reduce energy consumption. With rising environmental concerns and growing energy awareness there is a need to minimise energy use in all industry sectors (Kiss, 2013).

The distillation column is commonly considered to be a non-linear and time varying system and its model is typically required in control and optimisation. Obtaining an accurate model is challenging. Even if the model system is accurate, the dynamic model of the system has numerous parameters that present a range of difficulties to controlling this type of system.

2.3 Control of distillation columns

2.3.1 Control of binary distillation columns

A review of the existing literature regarding control schemes reveals various schemes applied to the Wood–Berry distillation column. The main idea of applying various control strategies to a distillation column is to select one of the many possible control strategies that meet process operational needs. Acharya, Dumpa and Dan (2016) provide a comprehensive study of control of the Wood–Berry binary distillation. They applied a multi-loop PID and decoupled PID controller in order to control the binary distillation column. In addition, the introduced decoupled PID controller showed high performance compared with that of the conventional PID controller, especially in a strong loop interaction. The main drawback of their work is that the decoupling PID controller reduced the impact of loop interactions only, without improving the overall performance of the PID controller (Acharya et al, 2016). Costa and colleagues applied the conventional PID scheme on the Wood–Berry binary distillation column and quadruple tank (Costa, de Almeida and Angélico, 2012). The tuning parameters of the PID controller were tuned using both genetic algorithm (GA) and particle swarm optimisation (PSO). Their results show that both GA and PSO tuning techniques with the exiting of the decoupling structure were able to produce a good dynamic performance from the PID controller. A major disadvantage to their research is the overshoot associated with the sudden set-point change that leads to deterioration in the overall performance of the PID controller.

Dumpa et al. (2016) presented a comparative analysis of various control techniques for the Wood–Berry distillation column. Different control schemes such as internal model controller (IMC), lead-lag IMC, Smith predictor IMC and feed forward IMC controller were considered, applied and compared based on their performance. Each individual controller has a specific implementation and working principle. For example, the IMC controller approach has the advantage of robust to model uncertainty and trade-offs between the overall performance and robustness, the lead-lag IMC approach is used to improve settling time and reduce overshoot percentage, and the feed-forward IMC controller is implemented along with feedback control to reduce external disturbance and reject it. In brief, the overall performance of all implemented controllers are promising but it is better to find a controller with a specific known design and one capable of providing improved performance in terms of disturbance rejection, robustness to model uncertainty and set-point tracking.

Mishra et al. (2013) applied MPC to the Wood–Berry model in order predict the control variable. The MPC scheme provides various important advantages such as addressing the static and dynamic interaction between input, output and disturbance variables.

Olesen et al. (2013) introduced a new technique for tuning the autoregressive exogenous input (ARX)-based MPC scheme of multivariate processes. The MPC scheme is designed and implemented based on a state space model. The tuning technique of the MPC parameters can be done numerically by minimising the integrated absolute error (IAE). They applied their technique on the Wood–Berry model and a cement mill. The introduced technique provided improved control performance with improved robustness capability but performs poorly under external disturbances generated from both feed flow rate and feed composition.

Adel, Elamvazuthi and Hanif (2009) used a Supervisory Control and Data Acquisition (SCADA) system in order to monitor and control the binary distillation column. They applied the conventional PI controller on the Wood–Berry distillation column. The parameters of the PI controller were determined using four different tuning methods: Coohen–Coon, multi-loop, Ziegler–Nichols, and minimal Integral of Time-Weighted Absolute Error (ITAE). The simulation results showed that comparatively, ITAE is the most suitable tuning technique. These results are then used in the creation of a graphical user interface (GUI). In their research, the Wood–Berry binary distillation column exhibited very high overall performance. Both product compositions settled down to their set-points with little overshoot, but the effect of external disturbance on the overall performance of their controller was not investigated.

Kadhar and colleagues (2015) proposed the design of a non-fragile multivariable PI controller for an industrial MIMO dynamic system using a diversity controlled self adaptive differential evolution with local search (DCSaDE-LS) scheme. The proposed technique was formulated as a single optimisation problem with the objective of evaluating robustness performance against the non-fragileness constraint. The robustness and non-fragileness of the proposed controller was investigated under -40% to 40% variations in nominal operating process and controller parameters. Real-time level temperature reactors and Wood–Berry distillation processes were considered a case study system. The simulation result showed that the DCSaDE-LS-designed non-fragile multivariable PI controller has improved time domain performance, and better non-fragileness and robustness than the reported multivariable PI controller et al, 2015).

Tufa and Ka (2016) evaluated the effect of model plant mismatch (MPM) on the overall performance of MPC and a systemic technique to specify the mismatch threshold in which the performance deterioration can be significantly considered. The Wood–Berry distillation model is used as a simulation case study with the MPC scheme to evaluate the efficiency of the proposed approach. The simulation result demonstrated that a 70% increase in the overall integral error (OIE) for the set-point tracking issue is found to be an acceptable limit for the performance deterioration of the MPC scheme (Tufa and Ka, 2016).

Uddin et al. (2016) compared the performances of the ARX model and auto regressive moving average with exogenous input (ARMAX) model for detection of model plant mismatch. A Wood–Berry distillation column was used as a simulation case study with the MPC scheme to evaluate the efficiency of both proposed approaches. The simulation result showed that both ARX and ARMAX models were able to identify the MPM introduced in the simulation model with little difference in magnitude of partial correlation coefficients. Furthermore, the ARMAX models gave higher accuracy with less computational complexity compared to ARX models (Uddin et al., 2016).

2.3.2 Control of HIDiC

Early in 1976, the first research in this area was published by Tyreus and Luyben (1976) to investigate the control issue of double effect distillation. They investigated the control of three different heat integration schemes: feed-split, light-split reverse, and light-split forward (integration). They suggested that the light-split reverse is the most controllable configuration. Weitz and Lewin (1996) studied the light-split reverse scheme using the disturbance cost as a control parameter variable and a similar conclusion was suggested. Wang and Lee (2002) introduced a non-linear PI control for a binary high purity heat integrated distillation column with a light reverse/split scheme. Zhu, Hong and Wang (2004) discussed the implementation issues of a two level control approach of dynamic integrated Real Time Optimisation (RTO) and nonlinear MPC for the HIDiC. They considered four nonlinear schemes: data reconciliation and state estimation, economic operation optimisation, parameter estimation and nonlinear MPC. The simulation results indicated that the proposed technique is effective to realise such advanced strategy on a rigorous model of an industrial sized plant (Zhu, Hong and Wang, 2004). Fukushima

et al. (2006) gave dynamic simulation models for various types of HIDiC. Furthermore, the dynamic and controllability of HIDiC were evaluated and compared with the Conventional Distillation Column (CDiC). They also introduced a suitable control system for the HIDiC (Fukushima et al, 2006).

In order to control the system successfully, reliably, regularly, and efficiently, measurement should be provided. At the same time, environmental regulation dictates strict refinery emissions and product quality specifications.

2.4 Proportional–Integral and Derivative control (PID)

Currently, industrial control applications are based on a PID controller in over 95% of cases (Chunzhe et al., 2015). Investigating the widespread industrial use of conventional PID schemes, it can be clearly observed that even for a small percentage of enhancements in the design structure, a PID controller might have an enormous effect on practical applications. Furthermore, due to the structural limitations of conventional PID controllers, they might not produce the desired performance for complex systems. The main reason behind this is that PID is an error feedback control scheme where the control action is determined by control error only. The derivative term of the PID controller only gives a 'one step' estimation of error, hence the disturbance and uncertainties of a complex process cannot be estimated well, which leads to slow compensation (Tan and Fu, 2015; Chen et al., 2017).

Han (2009) mentioned that the PID controller was first introduced by Minorsky in 1922. The PID controller is defined mathematically as:

$$u(t) = k_c \left(e(t) + \frac{\int_0^t e(\tau) d\tau}{\tau_I} + \tau_D \frac{de(t)}{dt} \right) \tag{2.1}$$

Where:

k_c represents the controller gain

τ_I represents the integral constant

τ_D represents the derivative constant

e represents the error signal

2.4.1 PID controller tuning in SISO systems

Despite the significant development that occurred in advanced control theory, the PID controller is still the most common controller used in process control due to its implementation simplicity and remarkable effectiveness (Deshpande, 1989; Koivo and Tanttu, 1991). According to Almodaresi and Bozorg (2017), more than 95% of industrial applications are still using PI controllers, particularly when the requirement of mathematical models are not too rigorous and when dominant process dynamics are of the first or second order (Almodaresi and Bozorg, 2017). Although the PID controller has only three tuning parameters, it is not a straight forward task to find their optimal values without a systematic procedure (Skogestad, 2003). In addition, suitable PID tuning techniques are extremely desirable due to their widespread use (Tavakoli et al, 2006). Currently there are a number of techniques for tuning PID controller parameters (Skogestad, 2001; Cominos and Munro, 2002; Garcia et al, 2007). The efficient selection of the tuning method can produce an efficient output performance with less error signal between the desired set-point and the output performance.

The ZN PI controller setting can be calculated from the values of ultimate gain K_u and ultimate period P_u as:

$$K_{\mathrm{ZN}} = \frac{K_u}{2.2} \tag{2.2}$$

$$\tau_{\mathrm{ZN}} = \frac{P_u}{1.2} \tag{2.3}$$

Where:

K_{ZN} represents the controller gain

τ_{ZN} represents the reset time

K_u represents the ultimate gain

P_u represents the ultimate period

In the frequency domain, the ultimate gain K_u is effectively the gain margin G_m, which indicates the amount of system gain amplification that will make the dynamic system become marginally unstable:

$$K_u = G_m \tag{2.4}$$

Consequently, the dynamic system will oscillate with a constant magnitude and the ultimate period, P_u, which is related to the phase crossover frequency ω_G as:

$$P_u = \frac{2\pi}{w_G} \tag{2.5}$$

2.4.2 Tuning PI in multi-loop systems

Due to energy integration and the fact that product quality is generally influenced by multiple factors, most modern industrial processes are MIMO systems. Multivariable control requires maintaining various controlled variables at their desired set-points. For easier control implementation and tuning, it is desirable to apply well established single loop PID tuning techniques to these MIMO processes (Grosdidier and Morari, 1987). However, compared with Single Input Single Output (SISO) systems, MIMO systems are more difficult to control due to the existence of control loop interactions. Adjusting controller parameters of one loop impacts the overall performance of other loops which may lead to destabilisation of the entire dynamic system (Xiong and Cai, 2006).

Luyben (1986) introduced a simple and practical multi-loop controller tuning technique called the Biggest Log-Modulus tuning (BLT). It is an interactive strategy for tuning the PI controller applied for an MIMO system. It is considered an extension to the Ziegler–Nichols method as it is based on the ZN tuning technique for each individual loop and a single detuning factor is introduced to meet the stability criterion considering the interactions between loops

(Nandong and Zang, 2014). In this technique the ZN tuning rules are first applied to the diagonal elements of the transfer function matrix of an MIMO process by treating them as SISO processes.

After acquiring the ZN tuning parameters, a detuning factor *F* is applied to the controller parameters:

$$K_c = \frac{K_{ZN}}{F} \tag{2.6}$$

$$\tau_I = F\,\tau_{ZN} \tag{2.7}$$

The detuning factor *F* specifies the stability of each individual loop where a larger value of *F* will lead to a more stable system but the load and set-point tracking responses are more sluggish and vice versa.

For a given detuning factor *F*, the closed loop log modulus L_{cm} can be calculated as:

$$L_{cm} = 20 \log \left| \frac{w}{1+w} \right| \tag{2.8}$$

$$w = -1 + \det\left(I + G_p G_c\right) \tag{2.9}$$

Where G_c is a diagonal (n x n) matrix of PI controller transfer functions, G_p is (n x n) matrix representing the process transfer functions associating the n controlled variables to the n manipulated variables (Luyben, 1986).

Then, the detuning factor *F* will be varied until the biggest L_{cm} over the entire frequency is equal to some selected specified number $[L_{cm}]^{max}$. This specified number is usually equal to double the system dimension:

$$L_{cm}^{max} = 2n \tag{2.10}$$

2.4.3 Limitations of PID

Commonly, the conventional PID controller is the first choice for industrial control engineers, but it is hard for a controller to provide an effective control signal to uncertain, non-linear and coupled systems despite all mentioned advantages (Xu and Wang, 2017). Gao (2006c) also argued that the simplicity of the PID controller leads to some fundamental limitations, especially in digital control applications that consist of powerful and new compact digital processors (Gao, 2006c). Due to this fact, Han (2009) highlighted various major limitations that exist in the PID control framework (Han, 2009). These limitations, with the corresponding conceptual and technical solutions, are as follows:

I. Set-point jump

Here, a sudden change at the set-point signal leads to a sudden jump in the manipulated signal or the controller output. As a result it produces some undesired overshoot. For example, this kind of sudden jump can lead to frequent fluctuations that may destroy the valve easily. To overcome this limitation, it is of great importance to design a transient profile in order to force the controlled variable to follow the set-point changes gradually. The speed of the transient profile should vary in accordance with applications and should be selected accordingly (Gao, 2006d).

II. Noise degeneration in the derivative control *D*

Despite the advantages of *D* control in reducing the overshoot of error change, most practitioners prefer to use the PI controller in most real applications instead of PID control. Increasing the differential control factor k_d will accelerate the response of the system and remove the unnecessary overshoot and offset. However, it makes the system sensitive to measurement noise and reduces the anti-jamming ability of the plant (Cao et al., 2008). The main method to overcome and resolve this kind of issue is by effectively estimating the total amount of noise and removing it from the control law (Gao, 2006c; Han, 2009).

III. Oversimplification in the form of linear weighted sum control law

A loss of performance in and the oversimplification of the control law in the arrangement of the linear weighted sum is another limitation of PID control. The control law of the PID control consists of a linear combination of present or current error, the accumulative errors over an interval

of time in the past and the error variation predictions for the future, which are manually tuned to obtain the desired performance (Chen et al, 2007).

As a result, Han (2009) indicates that this linear combination ignores other parameters that are more effective and should be considered and thus make the PID controller more powerful (Han, 2009). In order to overcome this limitation, non-linear feedback where the error signal can be reduced or reach the desired set-point more quickly in certain finite cases is introduced.

IV. Complication due to the integral term *I*

The integral term means the summation of an error signal over an interval of time to eliminate the steady state offsets. In fact most control loop actions reach the desired steady state due to the effect of the integral term *I* (Han, 2009). Despite all previous advantages, the utilisation of the integral term in any control loop introduces unwanted performance issues such as integral windup, a decrease in the stability margin due to phase lag characteristics, unacceptable saturation, and large settling time (Maurya and Bhandari, 2016). Moreover, Cao et al. (2008) argued that if the integral parameter k_i is too high, it would make the dynamic quality of the system weaker and result in closed loop system instability.

According to Xia et al. (2007), in order to overcome the conventional PID defects and control the distillation column, the new proposed control scheme should have the following characteristics:

- Overcome the PID key weakness or limitations.
- Tolerate large uncertainties in a physical process.
- Capable of estimating the controlled variable from accessible and measurable variables, since quite often in the chemical industry the controlled variable cannot be measured directly due to the undesired delay or is too expensive to measure. The control action can then be generated based on the estimated signal (Chen et al., 2016).
- Easy to understand and implement in vast industrial applications.
- Easy to tune, optimise, and operate.
- Capable of controlling and eliminating the frequent occurrence of disturbance.
- Capable of eliminating the impact of strong loop interactions.

It should combine the advantage of conventional PID controllers with the best advantages of modern control paradigms such as the state observer (Xie and Long, 2009). As a result, a highly successful solution was introduced by Han for processes that are time varying, non-linear and full of uncertainties, both external and internal parameters. This scheme is called Active Disturbance Rejection Control (ADRC). ADRC is gradually gaining recognition and consideration, owing to its excellent quality control and unique philosophy. It prefers to use non-linear functions in the design of the control law and the observer, which is potentially more successful in disturbance, uncertainty and enhancing system dynamics (Li, Qi, et al., 2015).

2.5 The concept of ADRC

The principle of ADRC was pioneered in 1995 by Jinqing Han who worked in the Chinese Academy of Science (Han, 2009). However the term ADRC was systemically introduced for the first time into English scientific literature in 2001 by Zhiqiang Gao (Gao, Huang and Han, 2001; Gao, 2006c; Gao, 2006d). It was introduced, developed and matured in the last twenty years by different groups of researchers around the world (Han, 2009; Huang and Xue, 2014; Gao, 2014b; Zheng and Gao, 2014), and it has been used in various applications in much of the relevant literature in recent years. Miklosovic et al. (2006) claim that the main idea of ADRC is very intuitive and that ADRC focuses on disturbance rejection as the central task, and the ‘active’ part is introduced by mitigating disturbance before it enters the system. ADRC is a departure from both model based multivariable and PID control paradigms and brings together the advantages of PID (i.e. error based) and modern control concept (i.e. state observer; (Gao, 2006c). It is independent of the mathematical model of the controlled plant. In other words, ADRC is an error driven scheme and has the capability to access and control the plant without an accurate model (Lu and Wang, 2012). It deliberately assumes an integrator mathematical plant model and handles all modelling errors as disturbance estimations. The conventional disturbance concept as something coming from outside the system is broadened in the ADRC scheme to include internal dynamics, and its latter removal makes design and tuning of the controller a simple task (Gao, 2015a). Its use of real time estimation and compensation eliminates the steady state error between the input and output with the help of Non-Linear Weighted Sum (N-LWS) and Extended State Observer (ESO). The undesired external disturbance and system uncertainties can be estimated and compensated

instantaneously at each sampling time, effectively and accurately (Kai and Yanlei, 2010). Furthermore, the ADRC scheme has various features over existing control algorithms such as fast control response, strong disturbance estimation and rejection, a simple tuning algorithm, not requiring an accurate mathematical model and physical measurement of the disturbances (Zhu et al., 2011). According to Figure 2.3, the ADRC scheme has three main components: Transient Profile Generator (TPG), ESO, and N-LWS.

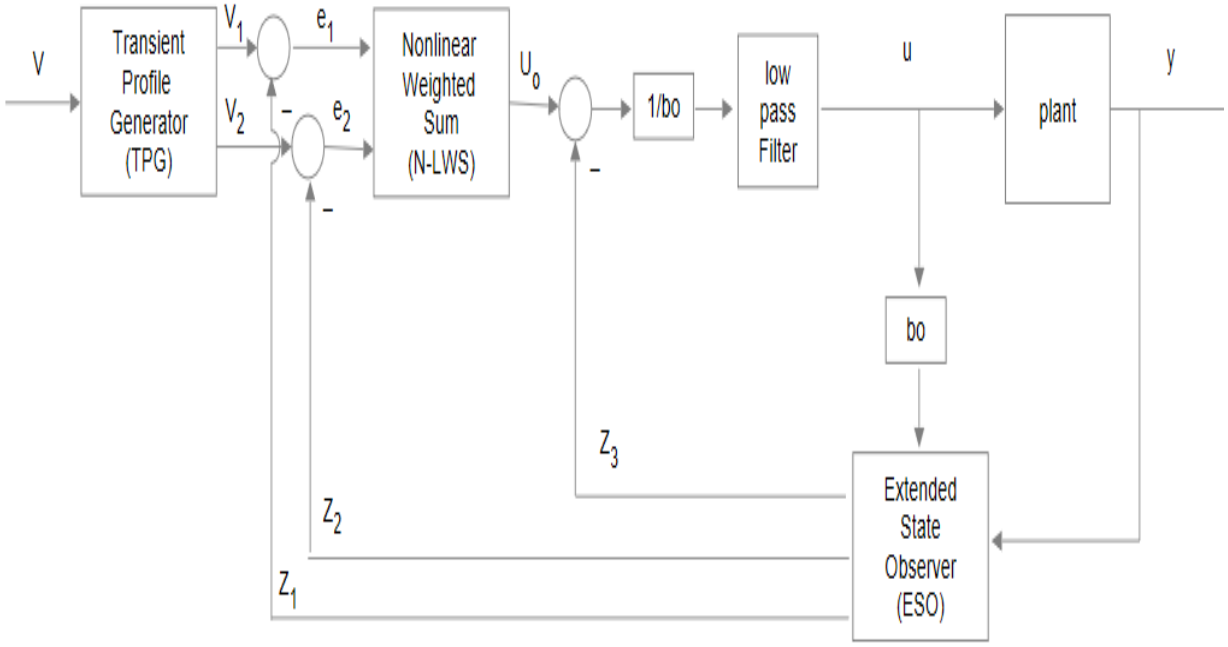

Figure 2.3: ADRC schematic (Han, 2009)

i. Transient Profile Generator

In tracking, the desired output trajectory or reference must be carefully produced to make it physically feasible for the output to follow. It is helpful to keep the tracking error to a minimum (Sun et al., 2017). This is the idea behind the reference generator and has been widely applied and practiced in many industrial applications under different names such as soft start in power electronics or motion profile in servo systems. It is able to minimise the oscillation and overshoot and increase system robustness. As a result, the s-curve and trapezoidal profile are usually used in a motion profile to avoid actuator saturations and to save energy. Han was very much aware of

such existing profile generators and he introduced a clever and simple reference generator called the TPG, as a component in the structure of the ADRC (Gao, 2015a). TPG designs the reasonable differential signal to achieve the target of noise suppression and arranges a transition process for the output signal to produce a smooth output signal from the differential signal of the input signal. It is also proposed to solve the issue of overshoot and rapidity of the PID control scheme by preserving the response speed of the system (Sun et al., 2017; Han, 2009):

The desired transient profile generator can be designed as follows:

$$\begin{cases} \dot{v}_1 = v_2 \\ \dot{v}_2 = -r\, sign(v_1 - v + \frac{v_2|v_2|}{2\,r}) \end{cases} \tag{2.11}$$

Referring to equation 2.11, v represents the desired set-point, v_1 is the desired transient trajectory, v_2 is the derivative of the desired transient trajectory, r is one of the ADRC design parameters that plays an essential role in adjusting the speed of the TPG. Furthermore, it is well known that the continuous time solution represented in this equation may introduce significant numerical errors in the discrete time implementation. To overcome this issue, a discrete time solution can be represented below (Han, 2009):

$$\begin{cases} v_1 = v_1 + hv_2 \\ v_2 = v_2 + h\, fhan \end{cases} \tag{2.12}$$

Where *fhan* represents Han function $fhan\,(v_1, v_2, r_0, h_0)$ which can be obtained by the following equations:

$$
\begin{cases}
d = hr^2 \\
a_0 = h\, v_2 \\
g = v_1 + a_0 \\
a_1 = \sqrt{d(d + 8|y|)} \\
a_2 = a_0 + (sign(y)(a_1 - d))/2 \\
s_y = (sign(y + d) - sign(y - d))/2 \\
a = (a_0 + y - a_2)s_y + a_2 \\
s_a = (sign(a + d) - sign(a - d))/2 \\
fhan = -r\,(\frac{a}{d} - sign(a))s_a - rsign(a)
\end{cases}
\tag{2.13}
$$

Where *h* represents the required smoothness for the output response.

Table 2.1: Recommended ranges for TPG tuning parameters *r* and *h* (Gao, Huang and Han, 2001; Han, 2009).

TPG tuning parameter	***Recommended range value***	***Effect***
r	***0.1 < r < 10***	Describes the required speed of the output response of the industrial application, it is a compromise between speed and stability.
h	***0.002 < h < ∞***	Describes the required smoothness of the output response of the industrial application, it is a compromise between smoothness and sluggishness.

With reference to Table 2.1, it might be noticed that the practitioners will have to make a trade-off between smoothness and sluggishness. In addition, they should select the tuning parameter values based on the industrial application and desired output.

It can be realised that the TPG operates as a filter where the proportions of the signal that exert an acceleration greater than the design parameter *r* are blocked. The TPG filter will exert the desirable performance.

One of the advantages the TPG has in the ADRC structure is its functionality in generating the derivative of signals accompanied by noise while maintaining a suitable rate of Signal-to-Noise Ratio (SNR). The importance of this characteristic is that a pure differentiator in practice is not physically implementable. This is due to the existence of noise in the feedback control and also the result of continuous discontinuities occurring at the reference signal that affect the impracticability of differentiating the error signal.

ii. Extended State Observer

Observers are dynamic functions that extract information about the system states from their inputs and outputs in real time. ESO is introduced in the context of ADRC and is independent of the mathematical model. ESO is also recognised as an estimator that plays a vital role in modern control theory. The main idea of the ESO is to estimate online variables that are usually inaccessible instrumentation-wise such as model errors, external disturbances and internal non-linear dynamics of the physical plant and to effectively compensate online for the unexpected disturbances in the control effort (Zheng and Gao, 2014). The ADRC can perfectly and successfully drive the controlled output signal to its desired value if the ESO has an accurate estimation for the external disturbances, model error and internal non-linear dynamics of the plant (Xia et al., 2007). It also acts as a low pass filter that reduces the effect of measurement noise in the feedback control loop (Zhao et al., 2011).

The parameters of ESO are selected and tuned in accordance with the essential conditions of the error dynamics stability (Han, 2009). ESO adopts a double channel compensating technique to redesign the system model and alter the uncertain, non-linear system to be approximately certain and linear (Xia et al., 2007). According to Figure 2.3, the output signal y and the control signal u are fed as inputs to the ESO, which then generates three output signals consisting of z_1, z_2, and z_3. z_1 traces y, z_2 traces the differentiation of y and z_3 traces the disturbances. As a result ESO can be designed and implemented as follows (Li, Xia, et al., 2015):

$$\begin{cases} e_1(t) = z_1(t) - v_1(t) \\ e_2(t) = z_2(t) - v_2(t) \\ z_1(t+k) = z_1(t) + kz_2(t) - \beta_1 e(t) \\ z_2(t+k) = z_2(t) + k(z_3(t) + b(u) - \beta_2 e(t) \\ z_3(t+k) = z_3(t) - \beta_3 e(t) \end{cases} \quad (2.14)$$

Where:

k represents the sampling interval.

b represents the tuning parameter.

e represents the error signal between the estimation outputs of ESO component and the output signal of the TPG.

β_1, β_2, and β_3 represents the linear observer gain that can be calculated by:

$$\beta_1 = 1, \beta_2 = \frac{1}{3k}, \beta_3 = \frac{2}{64k^2} \quad (2.15)$$

The design gains β_1, β_2 and β_3 affect the performance of ESO and if selected properly, can enable ESO to produce very good observation for the error variable, the error differential variable and the total disturbance of the controlled system. For example, the parameter β_3 determines the lag degree of the observed estimation z_3 of the total disturbance the system is subjected to. A larger gain of β_3 leads to a smaller lag of the observed estimation z_3 of the total amount of disturbance. If the gain parameter β_3 is too large it will make some oscillation of the estimated value of the total disturbance and produce an inaccurate estimation. Han (2009) suggested that the above tuning rule is valid for sampling times between 0.0001 and 1000.

iii. Non-Linear Weighted Sum

ADRC is a non-linear controller configuration that is independent of the plant model and has the capability to enhance the overall dynamic performance compared to the traditional PID scheme without substantially increasing the computational complexity (Gong et al., 2012; Shao and Wang, 2015). The N-LWS implements feedback linearisation to generate state variable error. This state variable error signal can be obtained by calculating the difference between the TPG output and ESO state variables, revealing that the control signal of the ADRC includes both the state variable of non-linear feedback and the unknown disturbance compensate of ESO (Zheng et al, 2012).

According to the real time and online values provided by TPG and ESO, the compensation signal and control signal for the total undesired disturbance are generated by N-LWS. The main advantage of feedback linearisation of a dynamic behaviour system is the real-time compensation for the undesired disturbance, converting the dynamic system from a non-linear system to an integrator system. Moreover, it solves the contradiction between system overshoot and response rapidity. It also strengthens the controller robustness and makes the system reach a stable state quickly (Qiao and Jie, 2005). Based on the error signal *e* introduced from the calculation difference between the TPG and ESO (equation 2.14), u_o can be calculated by the following equation:

$$u_0 = fal(e, \alpha, \delta) = \begin{cases} k_p \frac{e}{\delta^{1-\alpha}} & |e| \leq \delta \\ k_p |e|^{\alpha} sign(e) & |e| > \delta \end{cases} \quad (2.16)$$

Where:

e represents the error value,

α represents the non-linear error factor. The typical value of this parameter can range between 0.25 and 1,

δ represents the filtering factor and is used to reduce the oscillation function. The typical value of this parameter can be 0.05 and 0.5

kp is the proportional gain.

The *fal* function was introduced by Han (2009) and plays an important role in the ADRC scheme, where when $|e| \leq \delta$, *fal* filter function is a first order inertial filter that removes the high frequency noise (Han, 2009). When $|e| \geq \delta$, the output signal will reach the desired set-point rapidly. Thus, the *fal* function filter not only has a significant filtering impact on noise, but also a good tracking speed. δ and α are two essential variables to be predetermined (Dong and Zhang, 2015). Finally, and upon the observation of Figure 2.3, the control signal *u* can be calculated by the disturbance rejection equation:

$$u = \frac{u_0 - z_3}{b} \quad (2.17)$$

Where the parameter b is the compensation factor to specify the compensation intensity. In terms of the stability analysis and smoothing the output control signal, the control signal *u* is passed

through a low pass filter to remove any undesired overshoot and increase the quality and stability of the generated control signal. The form of a discrete low pass filter is:

$$F(n) = f_c \times F(n-1) + u(n) \times (1 - f_c) \quad (2.18)$$

Where:

f_c represents the filter constant between 0 and 1, corresponding to no filtering impact on the original control signal and extreme filtering impact on the selected original control signal.

F represents the filtered control signal.

However, it can be realised from the above components that the common idea of an ADRC controller is to divide the process design into two main parts (Madoński and Herman, 2011):

- The first part is responsible for compensating for model uncertainties that can be designed by input and output data using the ESO.
- The second part is responsible for realising and achieving the desired performance for the N-LWS and TPG compensated system.

2.6 ADRC applications

Due to its simplicity, the ADRC algorithm can be easily implemented in a wide range of applications. The key in ADRC applications is the reformulation of the control problem as that of disturbance rejection control, as shown in several applications such as internal combustion, space applications, power generation, aeronautics, high energy physics and process control (Gao, 2006). Texas Instruments and Parker are adopting the ADRC algorithm to replace the predominant PID in motion control and process control respectively (Gao et al, 2001). Moreover, Goforth (2004) and Zheng, Gao and Gao (2012) argue that the parameterised ADRC not only offers much improved performance, but it can be tuned easily.

Dinh et al. (2017) designed an ADRC for integrated missile guidance and control based on ESO and sliding mode control (SMC). The integrated model was designed as a block strict feedback nonlinear system where the target manoeuvres, modelling errors and unmodelled non-linearities are considered unknown uncertainties that have been estimated and compensated online

by the designed ESO. The simulation results demonstrated dynamic performance in terms of dynamic response and noise tolerant performance. The MATLAB simulation indicates that smooth missile trajectories and small miss distances are achieved, and the system is robust against system uncertainties and undesired external disturbance.

The position tracking control issue of the electrical cylinder in the presence of inertia load, friction load and nonlinear disturbance due to its transmission process is addressed by Peng et al. (2017). They applied ADRC to compensate for the external disturbance and make a continuous and accurate transition. A TPG component is used for providing a transition process to force the output process to follow the desired set-point and avoid any overshoot. ESO is designed to estimate the unmeasurable internal disturbance, internal uncertainties and external uncertainty of servo motion for better performance. The N-LWS is used to produce a reasonable control signal. Experimental and simulation results show that ADRC produces very strong robustness and adaptability compared with conventional PID control algorithms.

Zhang et al. (2017) applied ADRC to solve the issue of reduction ratio uncertainty, time varying load torque disturbance, and the initial deviation of the eccentric shaft mechanical zero that exists in a continuous casting mould vibration displacement system driven by a servo motor. TPG is used to provide a transition process of eccentric shaft angular displacement with a differential signal that forces the eccentric shaft angular displacement to change softly. To reject disturbance and improve control robustness, an ESO is used to estimate and compensate the external disturbance that leads to enhanced disturbance rejection capability. N-LWS is then used to enhance stability and rapidity of the control system. Finally, the experiments and simulation results show that the ADRC scheme has the advantages of fast response, high accuracy and strong robustness against internal and external disturbance in the control system.

Dong and Zhang (2015) applied ADRC on an aero engine to realise the acceleration and deceleration process in a more flexible and controllable manner. Comparison between the proposed ADRC scheme and the conventional PI controller are conducted based on a nonlinear model to investigate the flexibility and effectiveness of the proposed control scheme. The simulation results show that the ADRC scheme can reduce overshoot of the turbine temperature, which consequently extends its lifetime.

Zhang et al. (2017) used ADRC for furnace pressure control in a thermal power plant. Maintaining a stable pressure in a furnace guarantees the efficiency and safety of combustion. Multi-loop coupling and frequent external disturbance make this system difficult to maintain at an anticipated furnace pressure. Through simulation and experiment on a 100 MW power plant, the effectiveness of ADRC is demonstrated by fast response, rejecting the external disturbance, and coping well with uncertain dynamics in the absence of a detailed mathematical model.

Wang et al. (2017) studied the stability of a floating wind turbine where the output of the turbine is significantly affected by uncertainty introduced from the inaccuracy of a mathematical model and the external disturbances generated from wind and waves. They applied the ADRC scheme to control the floating wind turbine. The experiment and simulation results show that the proposed control scheme has better performance on floating wind turbine power control.

Motion control: the superior performance of an ADRC in response to load changes in non-linear applications is highlighted by Gao (2006c). Chong and Zhang (2010) present an ADRC specifically designed for a missile servo system with large loads. A comparison has been made between the ADRC and the conventional PID and it shows that ADRC offers an effective robust performance and capability of large load disturbance rejection. According to the results of more than 168 benchmark tests on an industrial motion control platform that characterises the performance of both existing industrial controllers and ADRC, the promising potential of the ADRC algorithm is shown as a reasonable solution in the manufacturing industry (Tian and Gao, 2009). Other difficult issues concerning position control of the servo system such as motional disturbance, smoothing input signal and hard matching between parameters due to the system's strict stability requirements are solved to achieve a quick and precise response in position control by utilizing a novel idea that combines the soft computing technique of fuzzy logic and ADRC (Xiong and Cai, 2006).

Microelectromechanical systems (MEMS) Gyroscope: the main advantage of ADRC is its tracking performance capability that is employed in vibrational MEMS gyroscopes by Zheng et al. (2007). A demodulation strategy is used to estimate the time-varying rotation to control the sense and drive axes of the vibrational gyro. The extensive possibilities of research in the domain of MEMS sensors like pressure sensors and micro-accelerometers using ADRC are also mentioned. The successful and effective hardware implementation of ADRC on MEMS

gyroscopes is also analysed and discussed by Dong et al. (2008). Stability analysis shows promising results and proves the theoretical establishment of applying the ADRC algorithm in MEMS gyroscopes where the core issue is disturbance rejection (Zheng et al., 2009). It also shows the robustness of the ADRC algorithm against parameter variations (Hou et al., 2001).

Velocity regulation and web tension: successful implementation of ADRC in velocity regulation and web tension is detailed in Zhou and Gao (2007) and Kotina et al. (2011). The zero steady state control error without the integrator term and better command following in the transient stage are demonstrated.

In addition to the areas mentioned above, the ADRC algorithm concept has been successfully applied by Chen et al. (2007) to solve a range of issues related to human postural sway. Among several control problems in thermal power plants the key problematic issue is that of disturbance rejection.

ADRC has been configured in Parker Hannifin Extrusion plant in North America by LineStream Technologies and it is claimed to have resulted in energy conservation of 50% (Desai et al, 2018).

It has been noticed however that the applications of the ADRC scheme applied in process control is less than in motion control. This gives as motivation to consider a process control application where the dynamic plant is difficult to identify.

2.7 Kalman filter

Generally, it is essential to get measurements of controlled variables in order to control them. Unfortunately, many controlled variables are either too difficult or too expensive or even impossible to measure. Some controlled variables cannot be measured due to the lack of suitable sensors. Distillation columns are broadly used in the chemical and petroleum industries and it is usually hard to obtain accurate and reliable product composition measurements without a large time delay. Many composition analysers like gas chromatography commonly have a substantial time delay of around 10 to 20 minutes because of long dead times for sensors located far downstream and the time involved to heat the sample and purge the sample line. A further

drawback is that the reliability of composition analysers is usually quite low. Moreover, using this type of analyser in a distillation column composition control will consequently involve high maintenance costs. As a result, the achievable composition control performance is reduced significantly (Miklosovic et al, 2006). Schemes for dealing with unmeasured variables of dynamic systems should be used. The Kalman filter can be considered an optimal recursive data processing algorithm that operates as a state estimator for a linear system when the dynamic model for the system as well as certain characteristics of measurement and undesired external noises are identified (De Assis and Maciel Filho, 2000). It uses all available measurements regardless of their accuracy to estimate the current value of the controlled variables. Figure 2.4 shows the typical application in which a Kalman filter could be implemented advantageously for estimation purposes where the dynamic system (e.g. mobile robot, motor, chemical process, satellite) is affected by a known set of external disturbance and control signals, and its outputs are measured by measuring devices, and available measurements concerning system behaviour are solely given by the inputs and observed outputs (Ribeiro, 2004; Welch and Bishop, 2006).

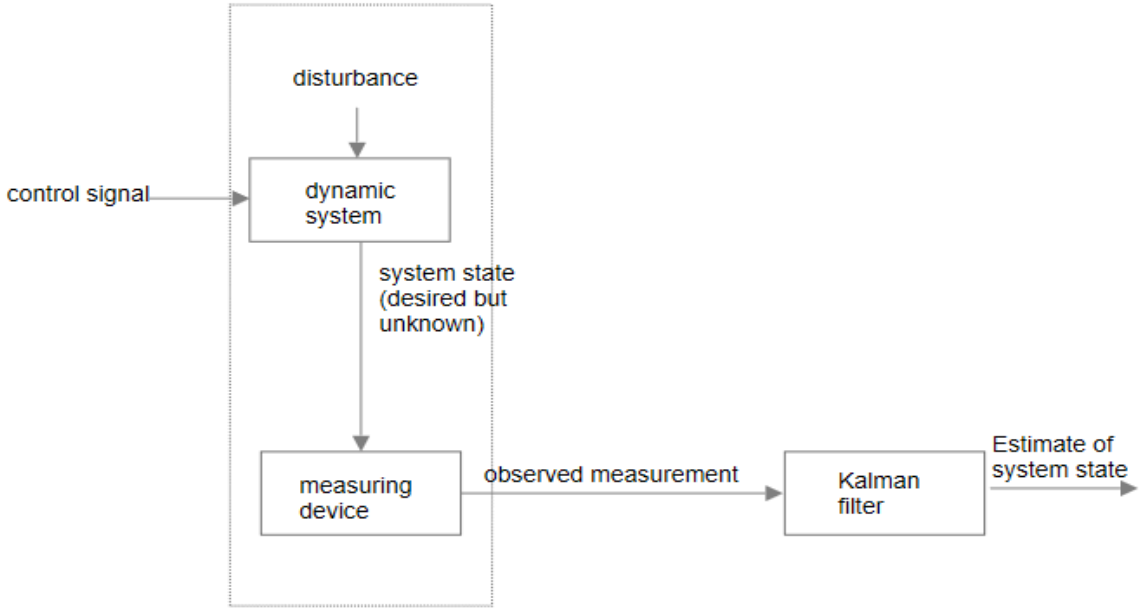

Figure 2.4: Typical application of a Kalman filter (Welch and Bishop, 2006)

The Kalman filter uses a state space model to estimate the state vector *x* from the measurement *z* given in the equation below (Welch and Bishop, 2006):

$$x_k = Ax_{k-1} + Bu_{k-1} + w_{k-1} \quad (2.19)$$

$$z_k = Hx_k + v_k \tag{2.20}$$

Where:

x represents the state variables.

u represents the control input signal.

w represents the input disturbance noise.

v represents the measurement noise.

z represents the available measurements.

The Kalman filter can operate in a form of feedback control signal where it first estimates the states of the process and then obtains measurement feedback. Thus, the Kalman filter has two groups of equations, time update and measurement update. Initially, the time update group project forward both the current state (x_{k-1}) and error covariance (P_{k-1}), while the second group measurement update equations correct the projected estimates by the actual measurement at that time. This process is then repeated using the corrected estimates, to produce the new estimates. Figure 2.5 presents the complete diagram of the operation of the Kalman filter.

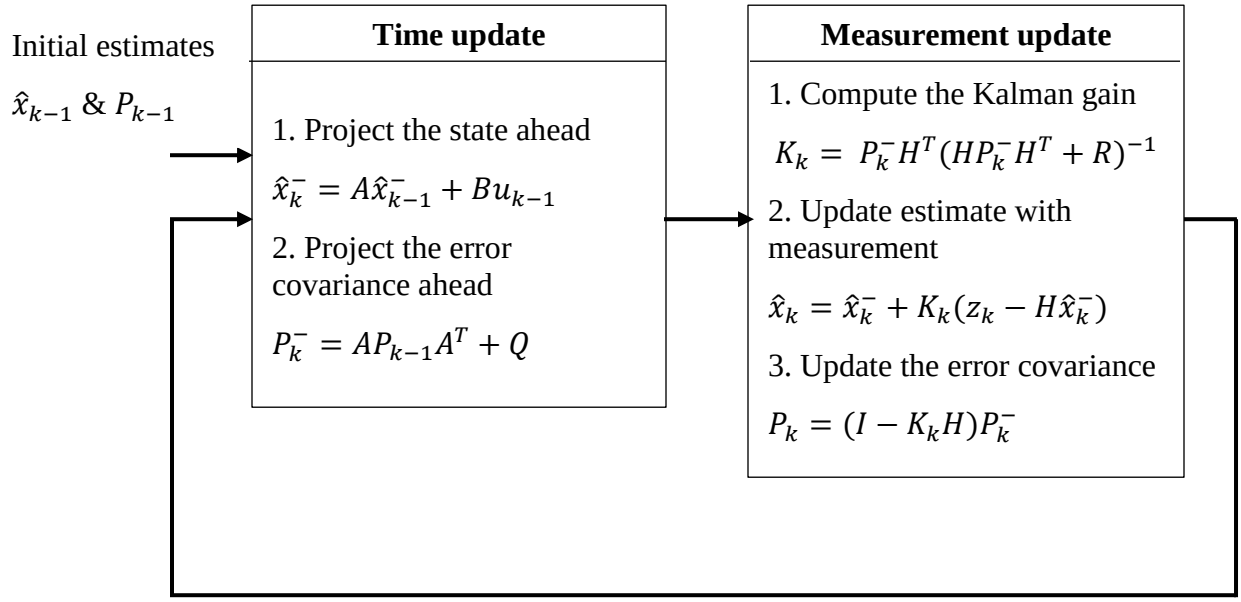

Figure 2.5: Operation of Kalman filter (Welch and Bishop, 2006)

Where:

$\hat{x}$ represents the estimated state.

A represents the state transition matrix.

u represents the control variables.

B represents the control matrix (i.e., mapping control to state variable).

P represents the state variance matrix.

Q represents the process variance matrix.

Z represents the measurement variables.

R represents the measurement error covariance.

H represents the measurement matrix.

K represents the Kalman gain.

I represents the Identity matrix.

Subscripts:

K represents the current sampling time.

k-1 represents the previous sampling time.

The Kalman filter described earlier is capable of predicting the state variables of a discrete time process that is described by a linear difference equation and it becomes a very powerful tool when estimating a noisy system. Furthermore, this filter is unable to estimate the system with non-linear behaviour. In addition, this Kalman filter is not suitable for estimating the product compositions in distillation columns that are usually nonlinear (De Assis and Maciel Filho, 2000).

2.8 Inferential measurement

The Kalman filter scheme is linear in nature and needs a mathematical model representation of the system behaviour, as well as direct output measurements, in order to estimate the state variables. However, in the case of a distillation column as mentioned before, neither a physical measuring tool to provide direct composition measurement nor any suitable dynamic model exists.

Thus, a Kalman filter may not be a suitable means to provide composition estimations for a distillation column.

Another solution to the observability issue for a distillation column system is to estimate the product compositions using an inferential measurement scheme, by the support of other output variables and estimation models connecting these two variables together. Inferential measurement is the technique by which the difficult-to-measure product quality variables can be inferred and estimated from other accessible and easy-to-measure process variables such as pressure, flow, and temperature (Guilandoust et al, 1988; Du, del Villar and Thibault, 1997) . Inferential control has been an active research area in recent years (Liao and Dexter, 2010; Oomen et al., 2011; Xie et al, 2011; Abusnina et al, 2014; Singh et al., 2016; Jeffries et al, 2016; Dekemele et al., 2016), and was first introduced by Brosilow and Tong (1978). The inferential control scheme uses the accessible outputs of the plant to infer the impact of control input changes and unmeasured noises. Guilandout et al. (1987) introduced an estimation strategy to frequently infer unmeasured outputs using measured system outputs. Unfortunately the complete implementation procedures of their system are quite difficult to follow.

Lu and Fisher (1988) introduced an algorithm for predicting the inter-sample outputs by utilising fast control input and slowly measured outputs. Lee and Morari (1997) proposed a generalised inferential control structure and discussed several optimal control issues in the MPC and IMC frameworks. The inferential control approach is more efficient and effectively utilizes the measured variables that are already available. Inherent in inferential control technology is a knowledge of the interdependencies and relationships between easy-to-measure and difficult-to-measure variables. The extraction of this knowledge and the structure in which it is used is key to the effectiveness of inferential control technology.

Kano et al. (2003) proposed a predictive inferential control scheme to control the product composition in a distillation column. Singh et al. (2005) investigated an inferential control scheme applied to a distillation column where the estimator has been designed by an artificial neural network. Abusnina, Kudenko, and Roth (2014) integrated the Kernel principal component analysis with the Gaussian process inferential control system to achieve robustness of the soft sensors during all process operating conditions.

2.8.1 Principle of inferential control

The behaviour of any system/process is specified by the system state variables that depend on the process operating conditions and control adjustments applied to them. The primary controlled variables are usually difficult to measure online for some processes (Tham et al., 1991b, 2002; Bolf et al, 2008). In order to overcome this issue, the primary controlled variables can be estimated or inferred by building and utilising a suitable mathematical model of the plant whose inputs are secondary output variables. The feasibility of the inferential measurement system is valid when the states of secondary variables reveal and reflect the primary variables states. It is also useful when the secondary measurements contain some information about the disturbance that impact the primary variable (Deshpande and Deshpande, 2012). The main purpose in designing and developing this inferential estimator model is to model the relationship between the unmeasured primary variables and measured secondary input and output variables. It provides an effective and elegant technique to improve the utilisation of currently available information. The implemented model can then be used to estimate primary variables as shown in Figure 2.6.

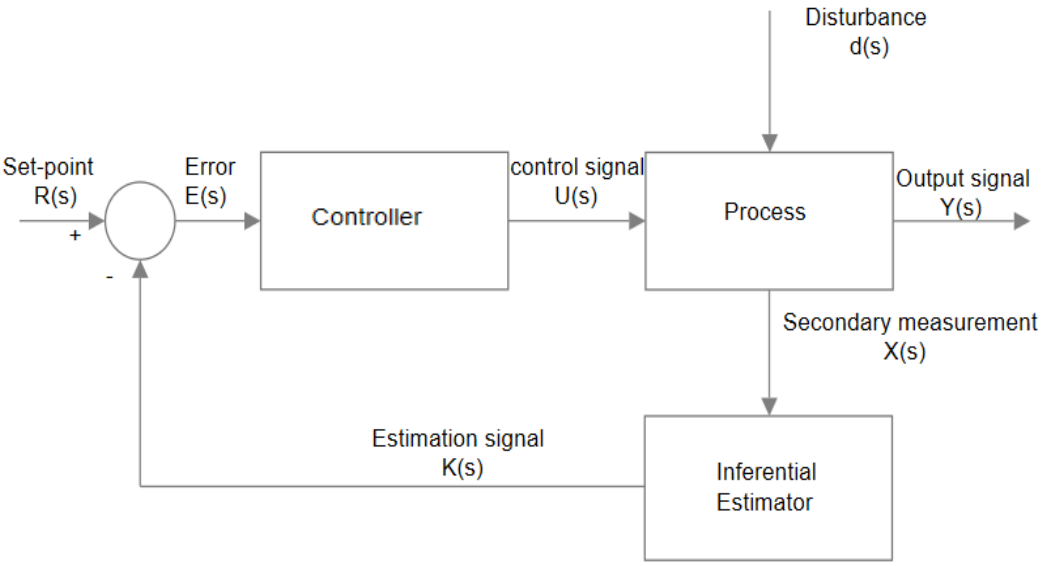

Figure 2.6: Inferential feedback control (Kadlec and Gabrys, 2008)

According Figure 2.6, samples of secondary measurements *X(s)* are taken and fed back to the inferential estimator to produce the estimation value of the output *K(s).* The estimated process outputs are then compared with the desired set-point to produce the error signal that will be the input signal to the controller. The inferential estimator can generate the estimation of difficulty to

measure primary variables at the same frequency that secondary variables are measured and then used as feedback in an inferential control algorithm (Abusnina, Kudenko and Roth, 2014). If the estimation signal of the primary outputs is sufficiently accurate, then the estimated outputs of the primary variables can be used in controlling and optimising the process. The important part of the inferential estimator is the design of the mathematical model that connects the difficult to measure primary variables with the easy to measure secondary variables.

The application of an inferential control scheme for estimation and control of the unmeasured primary variables is of great importance in the processing industry, where a vast number of secondary measured variables that are measured quickly and can be used as input signals for the inferential estimator. There are various advantages of soft sensors in comparison with traditional instrumentation (Deshpande and Deshpande, 2012; Singh, Gupta and Gupta, 2005; Andrijić et al., 2017):

- They provide more insight into the process through catching information hidden in data.
- They allow industrial users to reduce environmental impact, enhance productivity, become more energy efficient, and develop business profitability by decreasing the production costs due to the reduction of off-specification products.
- They can be simply implemented on existing hardware. Moreover, several on-line identification algorithms can be used to preserve the model when plant system parameters change.
- They entail little or no capital costs e.g. installation cost, commissioning and management of the required infrastructure.
- When there is an existing measurement delay for a controlled variable, the overall performance of the control loop can deteriorate. In such a case, inferential control is considered a good choice because it relies on secondary measurements that have relatively low levels of dead-time where soft sensors can operate in parallel with the current analysers in order to keep control loops operating quickly and properly.
- In many cases, the cost of online analysers for measuring primary variables can be excessive. Sensors for measuring secondary variables are typically cheap and less expensive to maintain.

In terms of product composition control in distillation columns, soft sensing and inferential control techniques have acquired momentum as viable replacements and complements to hardware

sensors (Fortuna et al, 2005). In the last two decades, there has been rising interest and research into the development of inferential control models, which are often called soft sensors, to provide regular on-line estimations of quality variables on the basis of their correlation with on-line process measurements (Bolder et al, 2014; Andrijić et al., 2017). Such predictive models dedicated to create real time estimates of product quality variables may help to improve system reliability, reduce the need for measuring devices and develop tight control policies (Tham et al., 1991b). Soft sensors in distillation columns can be defined as a system design consisting of mathematical algorithms that generate reliable real-time estimates of unmeasured product compositions by utilising their correlation with the accessible data of tray temperatures (Tham et al., 1991c).

2.8.2 Developing a model based software sensor

Generally, throughout the extensive literature, multivariate statistical techniques are popular when designing inferential estimators. Kresta, Macgregor and Marlin (1991) stated that the partial least squares (PLS) method could be exerted to form a good inferential estimation from a very large number of process variables. Mejdell and Skojested (1991) presented the use of a principal component regression (PCR) estimator to estimate distillation column product composition from flow rate measurements and tray temperatures. It was shown that PCR is capable of dealing with the strong collinearity between the temperature measurements leading to improved estimation performance (Mejdell and Skogestad, 1991). Moreover, Zhang (2001) reported that the inferential feedback control of distillation composition can be implemented by using PLS and PCR models. He also presented a new method for removing static estimation and control off-sets by using a mean updating technique (Zhang, 2001).

2.8.2.1 Principal Component Regression

The main principle of PCR is to use a reduced number of principal components (PCs) of the input variables to predict the response variable. The main reasons behind regressing the output response variable on the PCs rather than directly on the predictor variables is to decompose the highly correlated inputs to uncorrelated variables and hence reduce the dimensionality of the predictor variables by taking only the first few PCs. Therefore, this technique can be performed in

two steps: firstly to decompose the correlated X matrix to uncorrelated PCs, and secondly to perform regression using the first few PCs as predictor variables. The data transformation to the new coordinate system can be achieved in a way that the highest variance of data projection lies on the first coordinates (1st PC). This means that the first PC preserves as much data variability as possible in one dimension. Successively, the second PC accounts for the next highest data variance and so on (Rencher, 1998).

The predictor matrix *X* can be decomposed into the sum of *k* outer product of vectors:

$$X = \sum_{i=1}^{k} t_i \, p_i^T \tag{2.21}$$

Where k is the number of columns in *X* or number of rows in *X* if there are more columns than rows, t_i is called the *ith* score vector, and p_i called the *ith* loading vector.

The score vectors are mutually orthogonal, so are the loading vectors that are of unit length. The variation of *X* in the direction of p_i is reflected by the length of t_i. The first loading vector p_1 indicates the direction of the largest variation of *X* while p_k represents the direction of the smallest data variation in *X*.

The principal components can be calculated as:

$$T = XP \tag{2.22}$$

The linear regression of the response variable *Y* on the PCs can be written as

$$Y = TB + E \tag{2.23}$$

Where *B* represents the vector of model parameters which can be obtained by the least square estimation as shown below

$$B = (T^T T)^{-1} \, T^T Y \tag{2.24}$$

In addition, the vector of model parameters $\hat{\theta}$ for the original predictor variables can be calculated as shown in the equation below

$$\hat{\theta} = PB = (T^T T)^{-1} \, T^T Y \tag{2.25}$$

The MATLAB function (*svd*) will be used to compute the loading matrix *P* in order to be used to calculate the score matrix *T*.

$$[U, S, V] = svd(X) \tag{2.26}$$

Where:

V=*P*.

X represents the matrix data from the secondary variables (in this research, *X* is tray temperature measurements).

2.8.2.2 Partial Least Squares

Since its introduction in 1975 and similar to PCR, PLS has been recommended as one of the standard tools for designing and developing regression models when data sets are ill-conditioned or have highly correlated predictor variables compared to other traditional techniques (e.g. MLR). Both PCR and PLS techniques are similar in terms of their efforts to regress response variables on reduced dimensional latent variables (Chen et al,2017). Nevertheless, unlike the PCR technique that uses the *X* predictor variables to find the new latent variables, PLS technique uses both predictor variables *X* and response variables *Y* to find the new latent variables. These resultant latent variables are essentially playing the part of predictor variables. The core idea of the PLS technique is to extract those implicit latent variables from the predictor variables *X* that can best predict the response variables. These latent variables or underlying factors are useful for estimating the response variable as well as reducing the dimension of the predictor variables (Shepard et al, 1966; Geladi and Kowalski, 1986).

The outer relationship for the input data matrix can be written as:

$$X = TP^T + E = \sum_{i=1}^{a} t_i \, p_i^T + E \tag{2.27}$$

The outer relationship for the output data matrix can be written as:

$$Y = UQ^T + F = \sum_{i=1}^{a} u_i \, q_i^T + F \tag{2.28}$$

Where:

T and *U* represent the latent vectors for *X* and *Y* respectively.

P and *Q* are the loading vectors for *X* and *Y* respectively.

E and *F* represent the residuals matrices for *X* and *Y* respectively.

The PLS technique is used to provide a linear relationship fitting between *X* and *Y* by applying the least square regression between each pair of *t* and *u* latent vectors as given by the equation below:

$\check{u}_h = b_h t_h \qquad h = 1,2, \ldots\ldots, a$

Where $b_h = t_h^T u_h/(t_h^T t_h)$, which is equivalent to regression parameters in MLR and PCR.

2.8.2.3 Dynamic inferential model

Since the static inferential estimator is usually not efficient in some industrial processes where the relationship between soft sensor input and output variables are dynamic and for the purpose of improving the prediction accuracy of the static soft sensor, dynamic inferential estimation models should be developed. The dynamic approach of PCR and PLS modelling can be achieved by adding the past measurements of the inputs as additional model inputs (Abusnina, Kudenko and Roth, 2014). For example, the first order dynamic model can be designed and developed as:

$$y(t) = \sum_{i=1}^{k}(\theta_{i,1}\, T_i(t) + \theta_{i,2} T_i(t-1)) \tag{2.29}$$

Where:

T_i represents the secondary variables (tray temperatures).

y represents the primary variable (top and bottom compositions).

θ_i represents the model parameters associated with each individual secondary variable.

t represents the discrete time.

The 2nd order dynamic model can be written:

$$y(t) = \sum_{i=1}^{k}(\theta_{i,1}\, T_i(t) + \theta_{i,2} T_i(t-1) + \theta_{i,3} T_i(t-2)) \tag{2.30}$$

The 3rd order dynamic model can be written:

$$y(t) = \sum_{i=1}^{k}(\theta_{i,1}\, T_i(t) + \theta_{i,2} T_i(t-1) + \theta_{i,3} T_i(t-2) + \theta_{i,4} T_i(t-3)\,) \quad (2.31)$$

And so on.

It has been expected that a dynamic inferential model will give a better estimation than a static one. In this research, once the dynamic inferential model is designed it will be combined and integrated with the ADRC scheme in order to introduce the dynamic ADRC scheme, which will be applied to the binary distillation column and HIDiC.

2.9 Summary

It appears from the literature that distillation columns have been in use for a long time and are often considered mature technology, but they consume a significant percentage of the total energy in the global processing industry: they are major energy consumers in the petrochemical and chemical industries. Most operations of distillation columns involve a significant amount of energy, where they account for more than 40% of the energy used in the refining and bulk chemical processes industry and more than 95% of the energy consumed in separation processes.

Currently, many of the advanced control design methods depend on a mathematical model of the controlled plant. Moreover, many industrial plants are not only time-varying and non-linear but also extremely uncertain. Obtaining an accurate mathematical model description of physical plants is generally not accessible in industrial control, which leads to a significant dilemma for control practitioners where the essential requirement is to obtain a mathematical plant model from the uncertainty and theoretical aspects of the dynamic plant in practice. Another dilemma in designing a control system is how the undesired disturbances can be handled. In current control schemes, disturbance dilution is the main key control design objective. The common solution is to estimate and cancel the disturbance directly.

It has been noticed in the literature that most industrial applications are controlled by PID controllers. However, this PID controller has several limitations such as sudden set-point jumps, oversimplification of non-linear weighted sum control law, complication due to the integral term *I*, and noise degradation associated with the derivative term *D*. These limitations may lead to

degradation of the overall performance of the controller. In addition, Han (1995) proposed ADRC, which is independent of the mathematical model. The ADRC algorithm is proposed to replace the dominant PID controller and overcome its limitations.

In order to control a dynamic system effectively, it is essential to get real-time measurements of the controlled variables. Unfortunately, many of the controlled variables in industrial applications are either too difficult, too expensive or even inaccessible to measure. The Kalman filter and observer are not suitable schemes for non-linear processes as both techniques are linear and need a mathematical model representation of the system behaviour and direct measurement of the controlled variables. Instead, the inferential model can be considered a suitable technique to solve the difficulty of measuring the inaccessible or difficult to measure variables. The inferential model can be built using three different categories such as data based modelling techniques, hybrid techniques and multivariate statistical techniques.

The combination of the ADRC scheme and the inferential control will introduce another control scheme known as the inferential ADRC scheme, which will be applied on the distillation column in order to control it continuously and successfully.

Chapter 3 ADRC of a distillation column simulated using a MIMO transfer function

3.1 Introduction

Wood and Berry in 1973 presented the control of a binary distillation column with a 9 inch diameter and 8 trays for separating a methanol and water mixture as shown in Figure 3.1. They presented the transfer function models of the distillation column identified from experimental data as a 2×2 (two inputs and two outputs) transfer function matrix with a long time delay (Liu et al., 2017). The Wood–Berry model is considered a classical example that has been used in many previous research papers in MIMO process control (Deshpande and Ash, 1983; Shridhar and Cooper, 1997; Mantz and De Battista, 2002; Jain and Lakshminarayanan, 2007; Zheng et al, 2009).

The controlled variables are the top and bottom product compositions expressed in weight % of methanol. The reboiler boiling up rate and reflux rate are the manipulated variables expressed in lb/min. The transfer function model is given by (Ahuja, Narayan and Kumar, 2016):

$$\begin{bmatrix} Y_1(s) \\ Y_2(s) \end{bmatrix} = \begin{bmatrix} \frac{12.8\, e^{-2s}}{16.7\, s+1} & \frac{-18.9\, e^{-4s}}{21.0\, s+1} \\ \frac{6.6\, e^{-10s}}{10.9\, s+1} & \frac{-19.4\, e^{-4s}}{14.4\, s+1} \end{bmatrix} \begin{bmatrix} u_1(s) \\ u_2(s) \end{bmatrix} + \begin{bmatrix} \frac{3.8\, e^{-8.1s}}{10.9\, s+1} \\ \frac{4.9\, e^{-3.4s}}{13.2\, s+1} \end{bmatrix} . [D(s)] \quad (3.1)$$

Where:

Y_1 represents the overheads composition or top composition (weight % water).

Y_2 represents the bottom composition (weight % methanol).

u_1 represents the reflux rate (lb/min), the first manipulated variable for controlling the top composition.

u_2 represents the steam rate to the reboiler (lb/mim), the second manipulated variable for controlling the bottom composition.

D(s) represents the undesired external disturbances to which the column is subjected. In this research, the external disturbances in this model is feed flow rate (lb/min).

In the Wood–Berry distillation column, the feed entering the distillation column is a mixture of light and heavy components almost at the centre of the column, referred to as the feed stage (since the Wood–Berry distillation column consists of 8 trays, the feed tray is approximately located at the 5th tray). The light component (more volatile) exits the column from the top while the heavy component (less or non-volatile) exits the column from the bottom (Kiss and Bildea, 2011). Figure 3.1 shows the simplified schematic diagram of Wood–Berry distillation column.

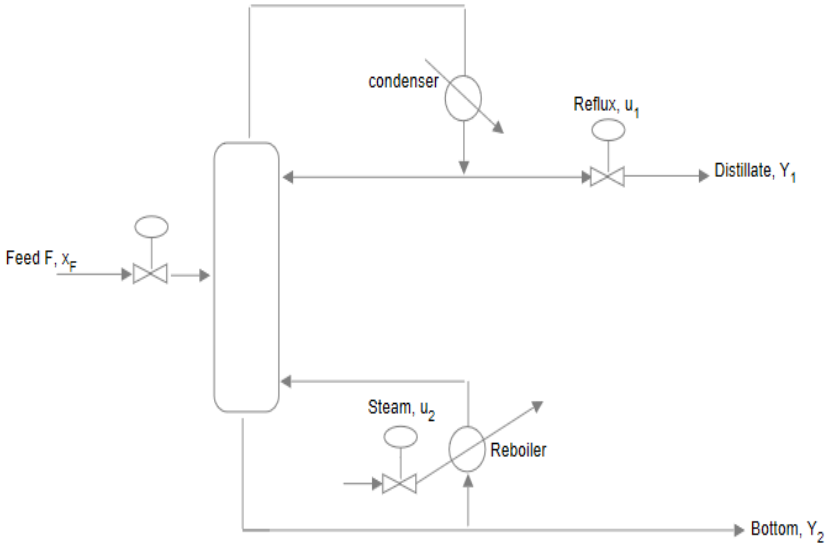

Figure 3.1: Simplified schematic of a Wood -Berry distillation column

This well-known Wood–Berry distillation column is used in the current research to investigate the effectiveness of ADRC for the control of distillation columns. This chapter is organised as follows: Section 3.2 provides a brief background on the control structure of controlling the Wood–Berry distillation column, where it starts by applying the BLT tuning approach for selecting the PI controller parameters, followed by implementing the components of ADRC scheme. In Section 3.3, both PI and ADRC schemes are investigated and evaluated by implementing various tests such as set-point tracking, strong loop interactions, system robustness and external disturbance rejection. Finally, conclusions are drawn in Section 3.4.

3.2 The control structure of the Wood–Berry column

3.2.1 Multi-loop PI control of the distillation column

Since PI control is the most common control scheme and is used in about 90% of industrial applications mentioned in the literature, the PI controller is implemented and applied to the Wood–Berry distillation column.

Selecting a suitable control configuration for dual composition control of a binary distillation column is a significant challenge. As shown in Figure 3.2, the LV control configuration is used here. In this configuration, the top composition Y_1 is controlled by first input (reflux), and the bottom composition Y_2 is controlled by second input (steam).

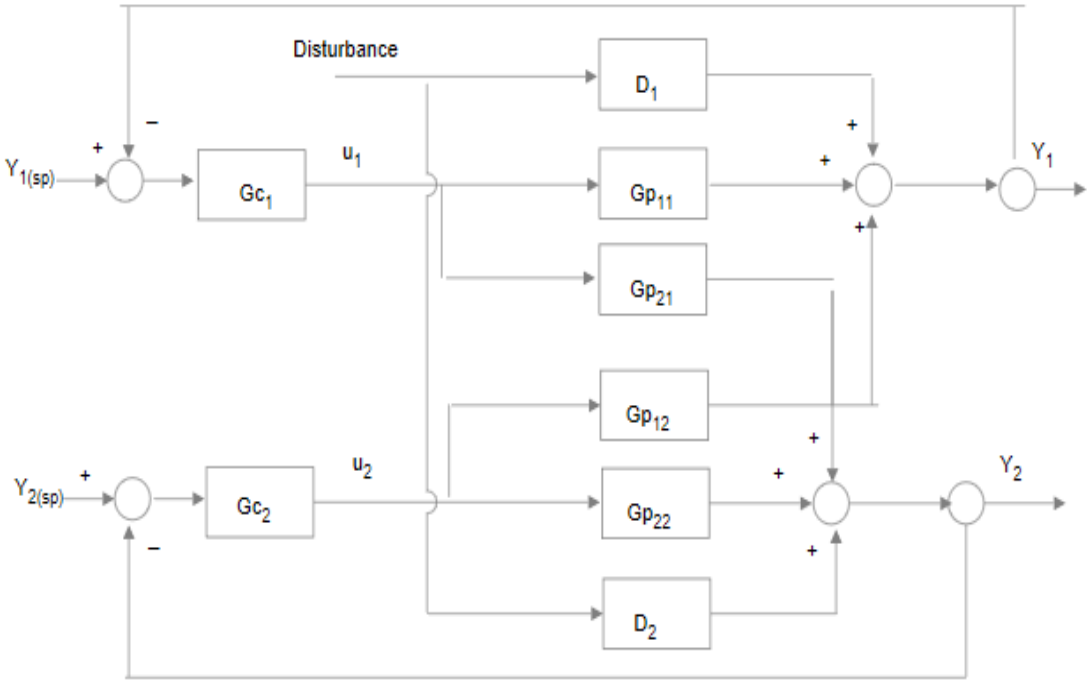

Figure 3.2: LV control pairing

The controller parameters of the multi-loop PI controller are tuned based on the BLT technique.

3.2.1.1 Tuning the PI controller parameters

ZN tuning technique:

According to the Wood–Berry model in (3.1), there are two control transfer functions to obtain:

$$\begin{bmatrix} Y_1 \\ Y_2 \end{bmatrix} = \begin{bmatrix} G_{p11} & G_{p12} \\ G_{p21} & G_{p22} \end{bmatrix} \begin{bmatrix} G_{c1} & 0 \\ 0 & G_{c2} \end{bmatrix} \begin{bmatrix} Y_{1(sp)} - Y_1 \\ Y_{2(sp)} - Y_2 \end{bmatrix} \tag{3.3}$$

In addition, the transfer function G_{p11} is used to obtain the parameters of the first controller G_{c1} and the transfer function G_{p22} is used to obtain the parameters of the second controller G_{c2}. Figures 3.3 and 3.4 shows the bode plot for G_{p11} and G_{p22} respectively.

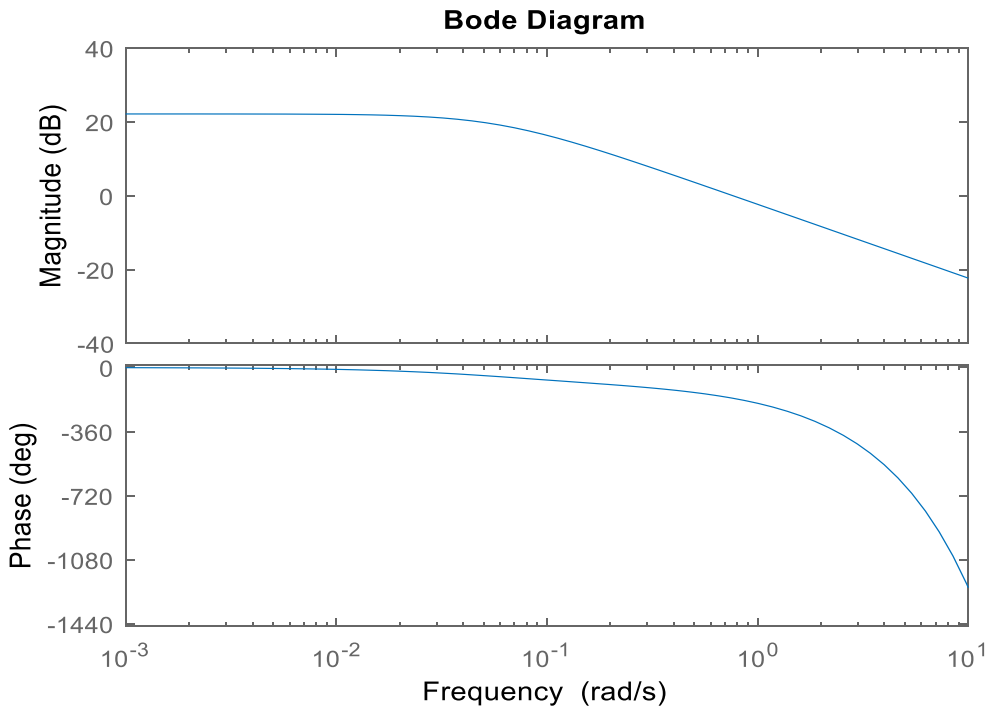

Figure 3.3: Bode plot of the transfer function G_{p11} (s)

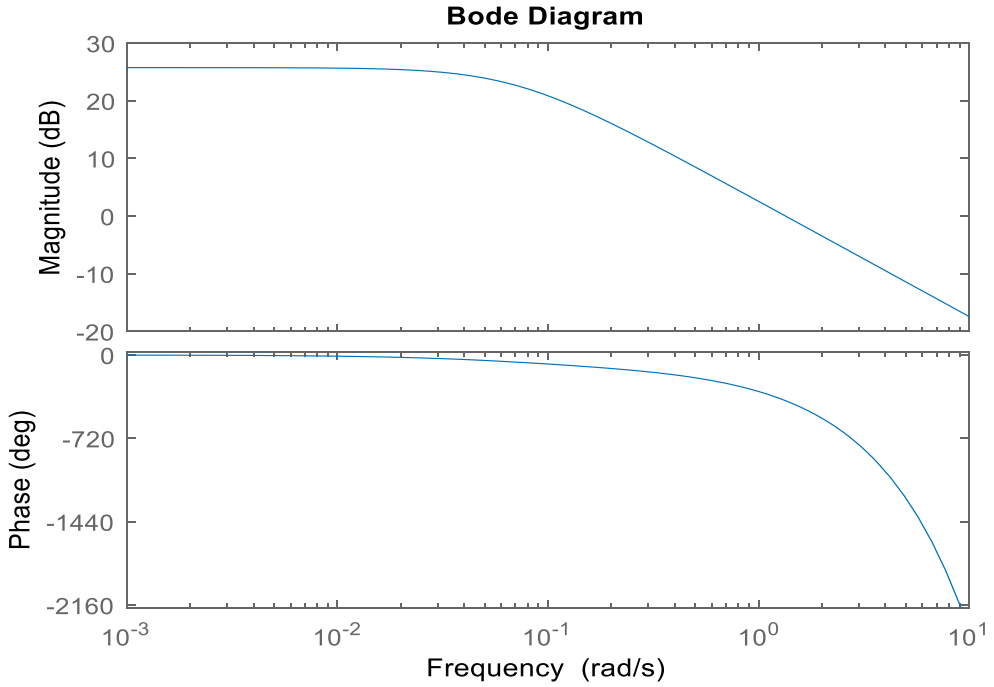

Figure 3.4: Bode plot of the transfer function G_{p22} (s)

The gain margin G_M and phase crossover frequency w_G were obtained from the above Bode plots and are used for tuning controller parameters as shown in Table 3.1.

Table 3.1: ZN tuning setting

Loop	Controller	G_M	w_G	K_C	τ_I
Y_1	G_{c1}	1.0749	0.8217	0.4886	6.3720
Y_2	G_{c2}	1.4648	1.9722	0.6658	2.6548

These parameters were further detuned using the BLT factor F (detailed in the next section).

BLT tuning technique:

According to the Wood–Berry model in Equation 3.1, the Wood–Berry distillation column is a MIMO (2×2) dynamic system and the BLT should be set as 4:

$$[L_{cm}]^{max} = 4 \tag{3.4}$$

The plot of L_{cm} is shown in Figure 3.5. It can be shown that the detuning value of F that gives the biggest L_{cm} is approximately equal to:

F = 1.3225

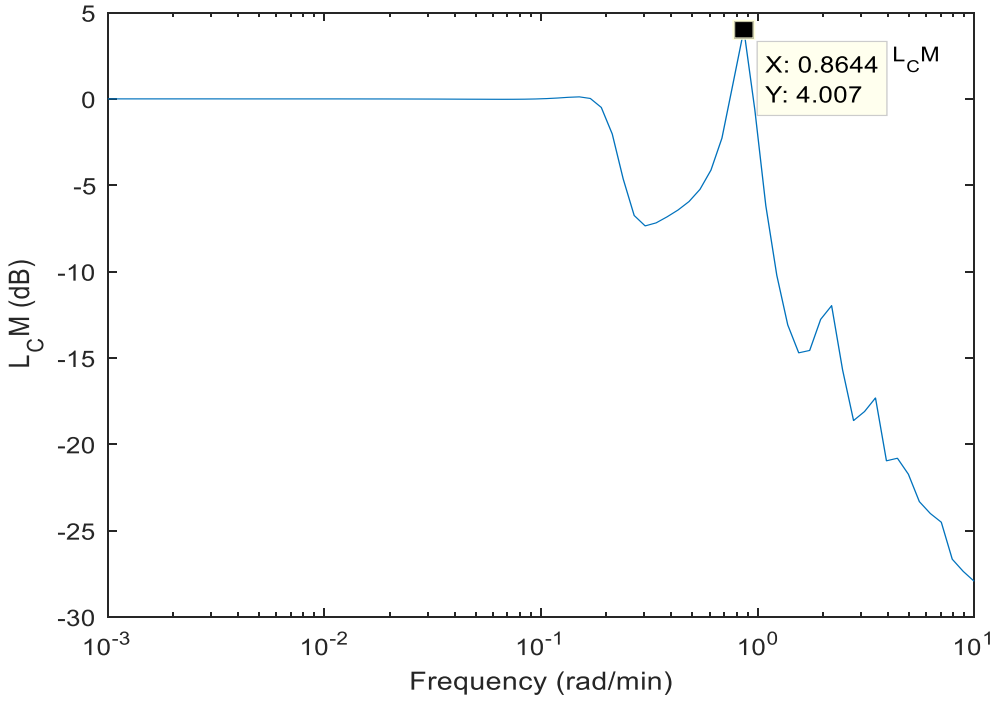

Figure 3.5: Closed loop log modulus

Using the detuned factor F, the controller parameters obtained from ZN tuning approach is further detuned and summarised in Table 3.2.

Table 3.2: BLT tuning setting

Loop	***Controller***	K_c	τ_I
Y_1	G_{c1} ***(reflux)***	0.3694	8.4272
Y_2	G_{c2} ***(steam)***	0.5035	3.5111

3.2.2 ADRC of the distillation column

In order to implement the ADRC scheme on the Wood–Berry distillation column, each part of the ADRC was designed and investigated individually.

i. TPG

The set of mathematical relationships presented in equations 2.12 and 2.13 were implemented in order to generate and simulate the full order of the discrete TPG form. As mentioned by Han (2009), the discrete TPG performance can be specified by both tuning parameters *r* and *h*, which are used to adjust the speed and smoothness of the TPG response respectively. Furthermore, after conducting various implementation experiments and according to Han (2009), Table 3.3 gives the TPG tuning values.

Table 3.3: Selected values for TPG tuning parameters *r* and *h*.

TPG tuning parameters	**Selected values**	
	Y_1	Y_2
r	1	1
h	0.9	1.1

ii. ESO

As explained in Chapter 2, ESO can be designed by implementing the set of mathematical equations in 2.14 and 2.15. Table 3.4 gives the ESO tuning values.

Table 3.4: Selected values for ESO tuning parameters.

ESO tuning parameters	**Selected values**	
	Y_1	Y_2
β_1	1	1
β_2	33.33	33.33
β_3	156.25	156.25
b	99	100

k	0.01	0.01

iii. N-LWS

Referring to Chapter 2, the N-LWS can be designed by using equations 2.16, 2.17 and 2.18 in order to produce the suitable filtered control signal f_c. Table 3.5 gives the N-LWS tuning values.

Table 3.5: Selected values for N-LWS tuning parameters.

N-LWS tuning parameters	**Selected values**	
	Y_1	Y_2
α	0.99	0.7
δ	0.5	0.25
kp	4.5	54
f_c	0.1	0.99

3.3 Investigating the performance of both control schemes

Set-point tracking, model uncertainty, control signal response, and disturbance rejection in the output response are the most important behavioural characteristics for any multivariable control system. In this section, the performance of both PI and ADRC schemes are analysed and discussed in order to investigate the efficiency of both controllers.

A. Set-point tracking performance

Multi-loop SISO controllers are usually used to control chemical processes that are MIMO. The simple controller and easy-to-handle control loop are the most attractive advantages of these control systems. Inevitably however, interactions exist between control loops upon which the design of such a controller to meet the desired specifications faced more difficulties than that for a single loop, and became an attractive research topic for years (Gagnon et al, 2003). The loop

interaction can be defined as a parameter change in one loop that might generate a significant disturbance in another control loop. This issue is introduced mainly due to the hidden feedback link or channel between the two interacting loops (Parvat et al, 2015).

The existence of loop interactions in a multi-loop control configuration might cause an undesirable effect in control performance. Furthermore, the presence of a significant amount of loop interactions among the loops can seriously deteriorate the overall performance of the decentralised controller and may even lead to unstable control systems (Garrido et al, 2011). Detection of the extent of interactions among the loops and identifying the most important loop is a difficult task, because a chemical process can have hundreds of control loops (Rahman and Shoukat Choudhury, 2011). In this research, a sequence of set-point changes in both Y_1 and Y_2 were applied in order to investigate the influence of control loop interactions. Set-point changes—especially in chemical applications—occur when the steady state changes due to a change in raw materials and product specifications. Thus, it is necessary to make the system follow up and track the new state or new set-point without violating the constraints (Kögel and Findeisen, 2013). According to Limon et al. (2016), the impact of the set-point change can be considered equivalent to a disturbance that needs to be handled properly to reduce the control error (Limon et al., 2016).

The controller set-point tracking performance is evaluated based on settling time and SSE. Figures 3.6 and 3.7 show the set-point tracking performance in Y_1 in conjunction with the interaction as a result of coupling both control loops together using both ADRC and PI schemes. Figures 3.8 and 3.9 represent the set-point tracking capability in Y_2 in conjunction with the interaction as a result of coupling both control loops together using both ADRC and PI schemes.

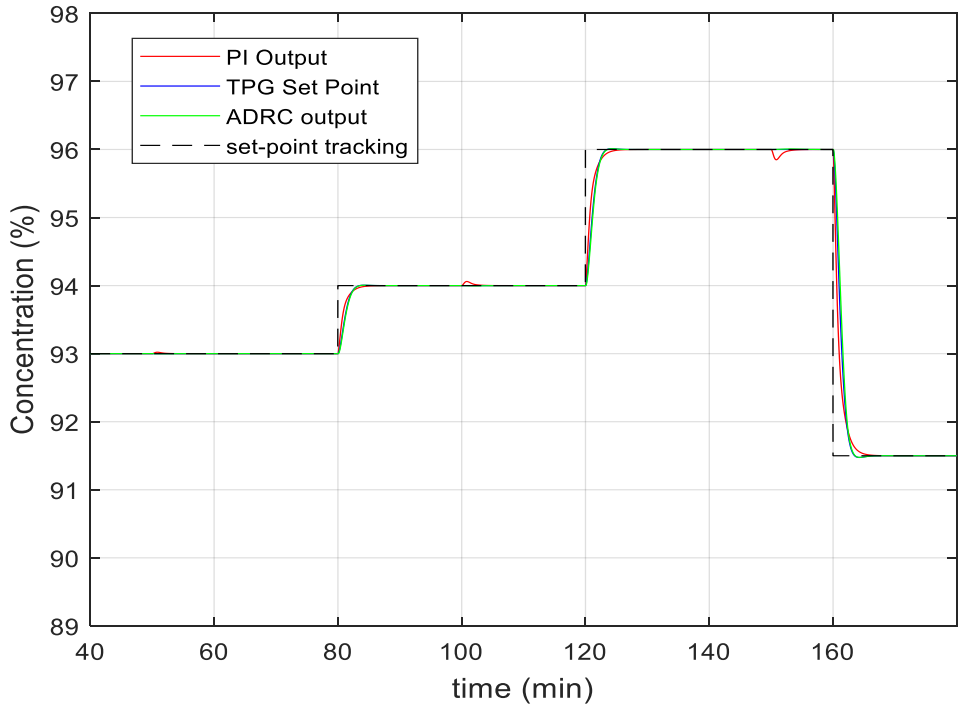

Figure 3.6: Performance of PI and ADRC schemes under the set-point tracking test for Y_1

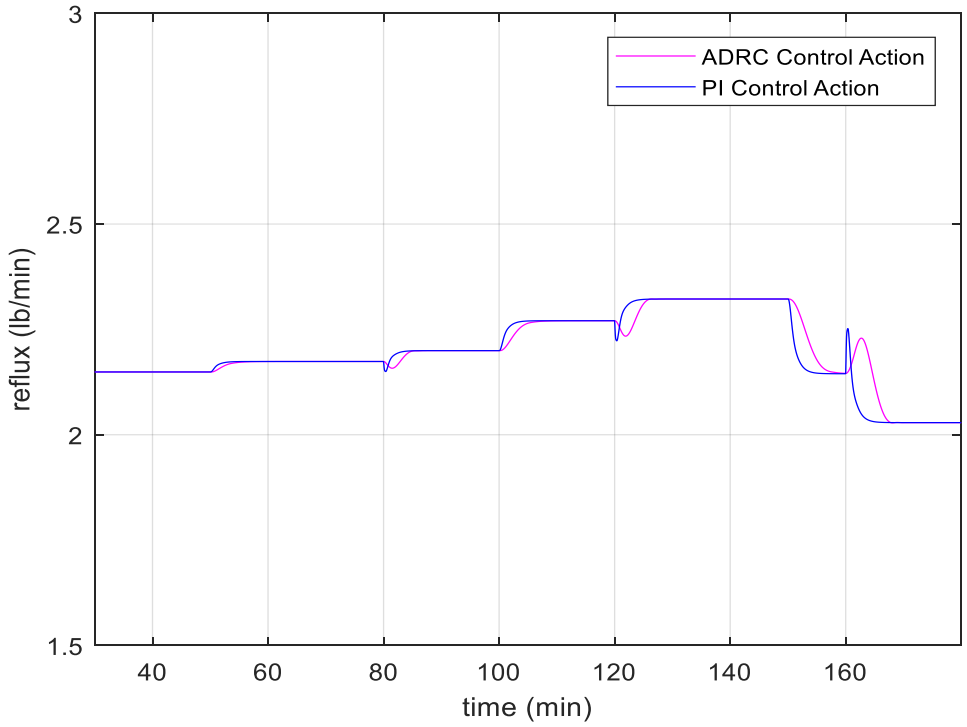

Figure 3.7: Control action of PI and ADRC schemes under the set-point tracking test for Y_1

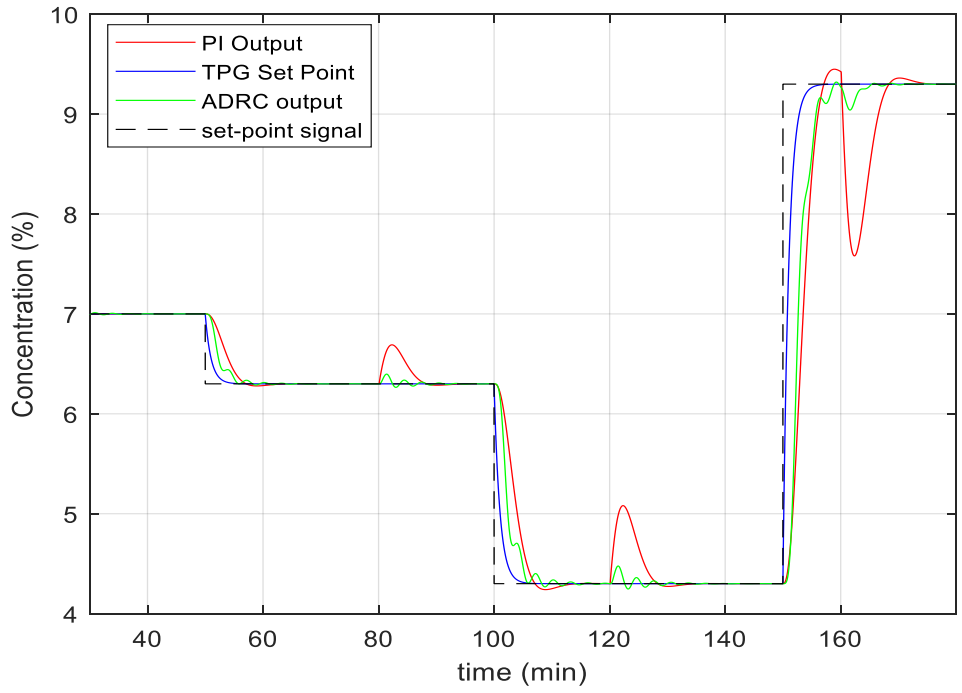

Figure 3.8: Performance of PI and ADRC schemes under the set-point tracking test for Y_2

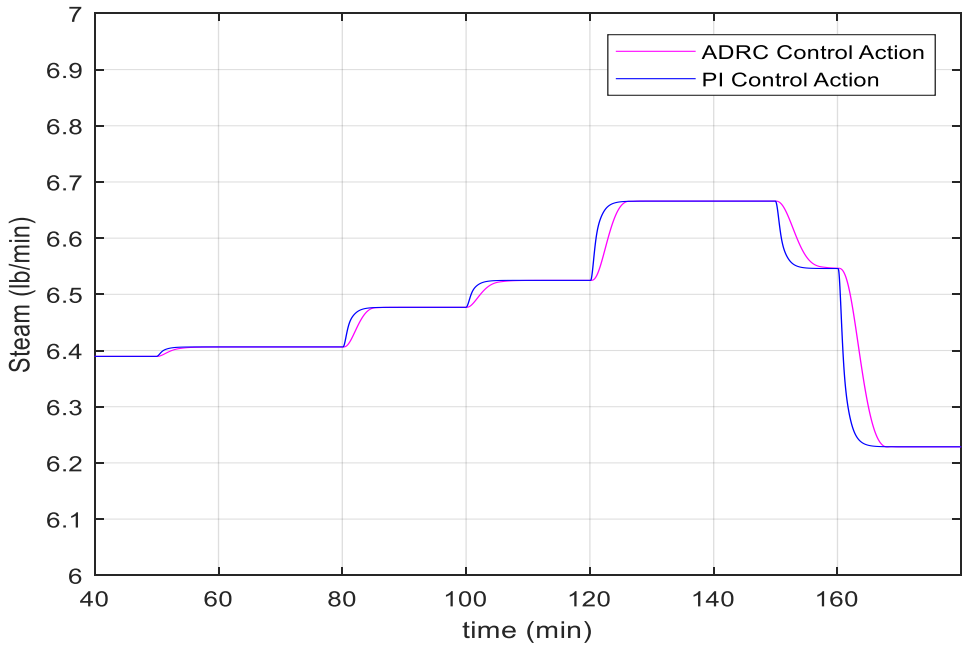

Figure 3.9: Control action of PI and ADRC schemes under the set-point tracking test for Y_2

Several points can be noticed from Figures 3.6 to 3.9:

Referring to Figures 3.6 and 3.7, the overall performance of the ADRC scheme under the set-point tracking and loop interaction tests are efficient where the controlled variables follow the TPG set-points. This is especially apparent at the top composition with no exerted signs of sluggishness or overshoot, and as soon as a set-point change is introduced in other loop, ADRC successfully and efficiently rejects this form of loop interaction and resumes tracking its desired set-point. It is also noticed that the maximum deviation from the original desired set-point was around 120 min and was found to be less than 15%—considered an acceptable percentage for the control practitioners. Overall, the ADRC scheme has the capability to estimate and reject the internal disturbance represented by loop interactions and force the output response to resume its desired set-point. Furthermore, it can also be observed from Figures 3.7 and 3.9 that the control signals exerted from the ADRC scheme are smooth, non-aggressive and non-oscillating.

The PI controller performance under loop interaction and set-point tracking is not efficient as the ADRC, where the output signal follows the desired set-point especially for the top composition. Some overshoots exist at the bottom composition that were introduced due to the strong loop interaction, where the maximum deviation from the original desired set-point was around 160 min (57%), which is impractical and not an acceptable percentage for the control practitioners. The response was also observed to oscillate before it settles to the designed set-point. Furthermore, this substantial overshoot will affect and deteriorate the overall control performance of the PI controller.

Table 3.6 gives the SSE values related to the performance of set-point tracking of both control schemes. The SSE values associated with the PI controller are significantly greater than the SSE values corresponding to ADRC in terms of set-point tracking under the presence of control loop interaction. Moreover, the greater SSE values of the PI controller reflect the large overshoot signs that make the PI controller inapplicable for real applications.

Table 3.6: SSE values associated with set-point tracking performance

Control Loops	***SSE (PI)***	***SSE (ADRC)***
Y_1	103.426	22.2875
Y_2	1436.2	480.1744

B. Controller Robustness

Control systems are designed and implemented based on simplified models of dynamic processes. The process dynamics of a plant may change during operation. The sensitivity of a closed loop control system to the variations in process dynamics is therefore considered a fundamental issue. In addition, robustness is the ability of the closed loop control system to be insensitive and unaffected to any parameter variations (Selvi et al, 2007). Controller robustness can be defined as the ability of the controller to reach or achieve satisfactory performance despite the presence of parameter variations. Generally, in a model-based control technique, deviation of a parameter value from its nominal operating value in the plant model used by the controller can be defined as model uncertainty (Limon et al., 2016).

In reality, as it is really difficult to find an accurate plant model, some assumptions are always made while modelling a process. Since the prime controller is already configured or designed, tuned and tested primarily on the dynamic simulated model rather than the real plant, it becomes an essential part to investigate the controller performance if the values of the plant parameters deviate from the originals that were specified whilst designing and tuning the controller. Furthermore, this test is implemented to assess the robustness of each controller. In this research, the modelling disparity can appear in the Wood–Berry model where the nominal plant model does not exactly match the real process dynamics. A −25% decrease in both dominant time constants τ_{11} and τ_{22} of the nominal plant model are implemented to investigate the impact of model-plant mismatches (Kalpana et al, 2017):

$$\begin{bmatrix} y_1(s) \\ y_2(s) \end{bmatrix} = \begin{bmatrix} \frac{12.8\, e^{-2s}}{16.7s\,12.5\, s+1} & \frac{-18.9\, e^{-4s}}{21.0\, s+1} \\ \frac{6.6\, e^{-10s}}{10.9\, s+1} & \frac{-19.4\, e^{-4s}}{14.4s\,10.8\, s+1} \end{bmatrix} \begin{bmatrix} u_1(s) \\ u_2(s) \end{bmatrix} \quad (3.5)$$

The set-point tracking capability of Y_1 and Y_2 applied to the updated modified transfer function using the ADRC schemes is represented in Figures 3.10 to 3.13.

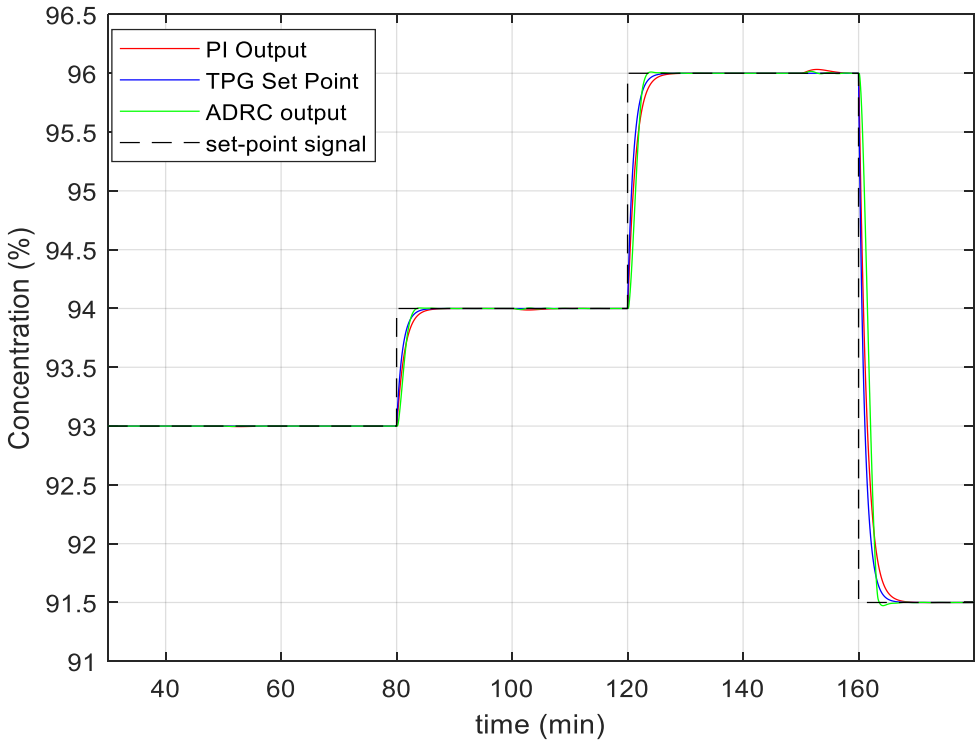

Figure 3.10: Performance of PI and ADRC schemes under the robustness test for Y_1

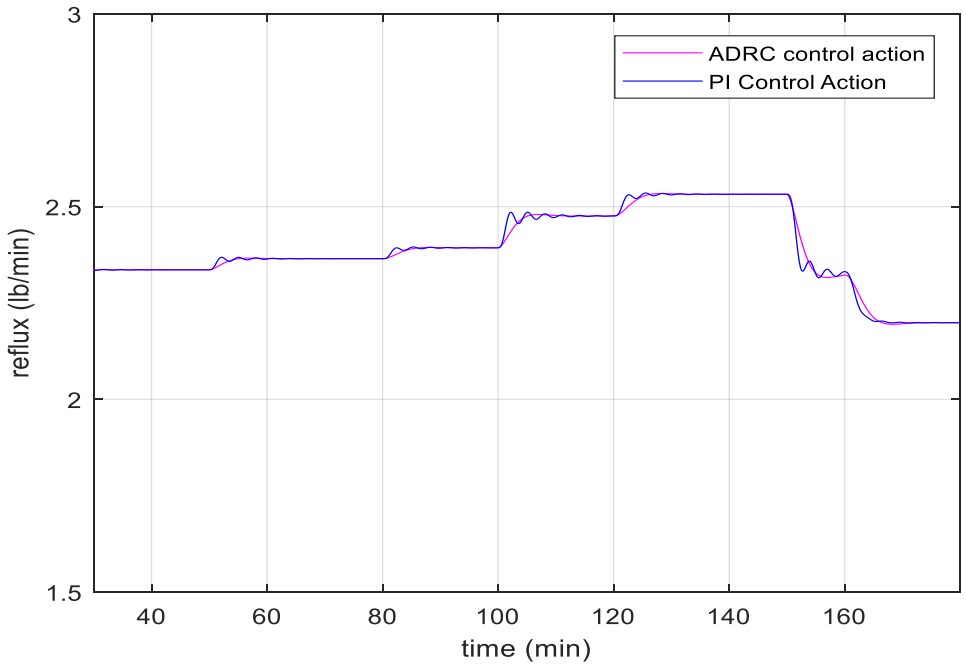

Figure 3.11: Control action of PI and ADRC schemes under the robustness test for Y_1

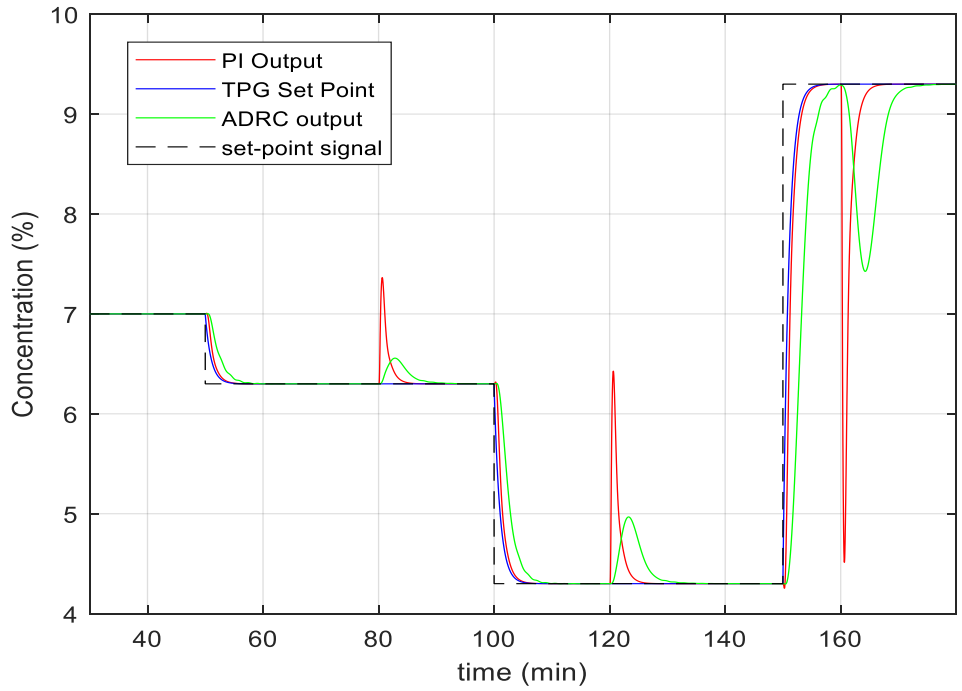

Figure 3.12: Performance of PI and ADRC schemes under the robustness test for Y_2

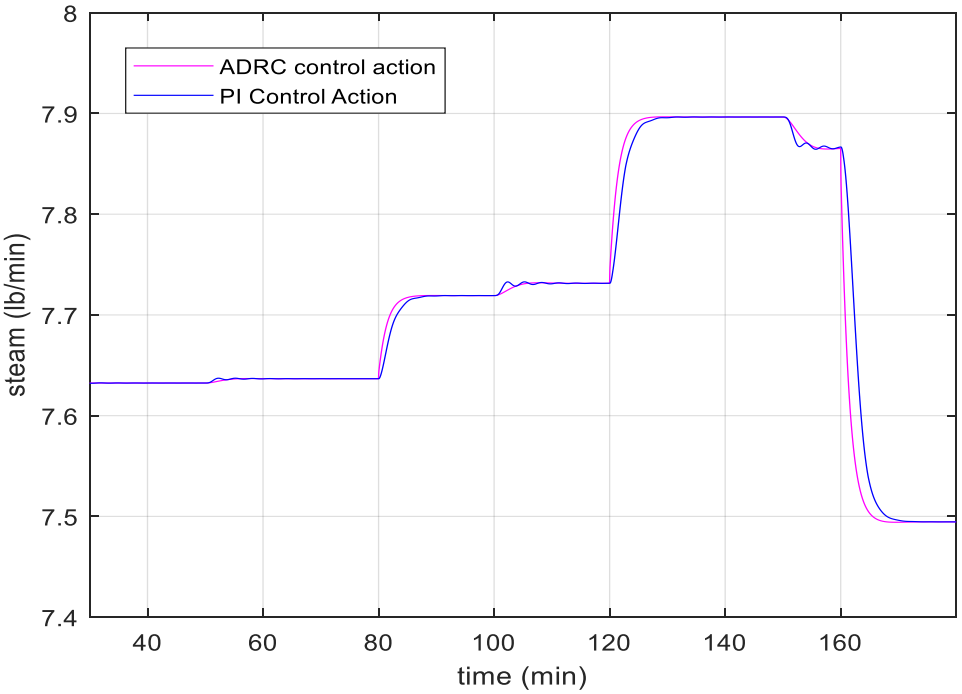

Figure 3.13: Control action of PI and ADRC schemes under the robustness test for Y_2

Upon the comparison of Figures 3.6 and 3.8 with Figures 3.10 and 3.12, several points may be noted. Referring to Figures 3.10 and 3.12, the ADRC set-point tracking performance on the modified transfer function system is similar to and as efficient as the performance on the original Wood–Berry transfer function. Moreover, and according to Figures 3.11 and 3.13, the ADRC control action exerted on the modified transfer function system is smooth non-oscillatory, which produces a smooth tracking signal. However, referring to Figures 3.10 and 3.12, the set-point tracking performance of the PI controller on the modified transfer function is as efficient as that on the original transfer function. Moreover, the PI control action exerted on the modified transfer function system is approximately oscillating with an aggressive response. As a result, the PI controller needs to be re-tuned in order to handle the variation of the plant parameters and reduce the effect of loop interactions. The SSE value of PI will be higher than the one applied to the original Wood–Berry transfer function.

Table 3.7 represents the SSE values associated with the set-point tracking performance of both control algorithms. The values of SSE associated with the PI controller are considerably greater than the SSE values associated with ADRC.

Table 3.7: SSE values associated with set-point tracking performance under the robustness test

Control Loops	***SSE (PI)***	***SSE (ADRC)***
Y_1	122.6	34.636
Y_2	2585.2	540.22

According to Table 3.7 the SSE values corresponding to the ADRC scheme are significantly less than the SSE values corresponding to the conventional PI controller. For the sake of comparison between the original and altered Wood–Berry system, and by taking the top composition Y_2 as an example, it may be observed that the SSE value increased from 480.17 to 540 for the ADRC scheme. Correspondingly, the SSE value associated with the PI controller increased dramatically from 1436.2 to 2585.2, indicating that as process variations exist in the system, the control objective becomes more challenging to achieve for both control schemes. However, it was concluded that despite the 25% modification in the dominant time constants τ_1 and

τ_2, the ADRC scheme maintained tight control performance where the process model mismatch (PMM) that was introduced as a result of process variations was successfully estimated and rejected by the presence of ESO component without re-tuning the ADRC components to compensate for this alteration.

C. External disturbance rejection

It is well known that variation in feed flow rate is one of the most common external disturbances in a distillation column, and has a huge impact on both product compositions. According to the Wood–Berry model in (3.1), the disturbance models are considered as $H_1(s) = \frac{3.8\, e^{-8.1s}}{10.9s+1}$, $H_2(s) = \frac{4.9\, e^{-3.4s}}{13.2\, s+1}$. In general, the disturbance magnitude of the distillation column is around 10–20% of the nominal value in operating points. So in this simulation, the feed disturbance of ±0.1% is added at t = 60, 90, 130 and 150 min as shown in Figure 3.14. Such type of disturbances are commonly encountered in the refinery and chemical processes as a results of changing feedstocks. The response curves of the top and bottom compositions with the impact of external disturbance under the control of the ADRC and PI controller are shown in Figures 3.15 to 3.18.

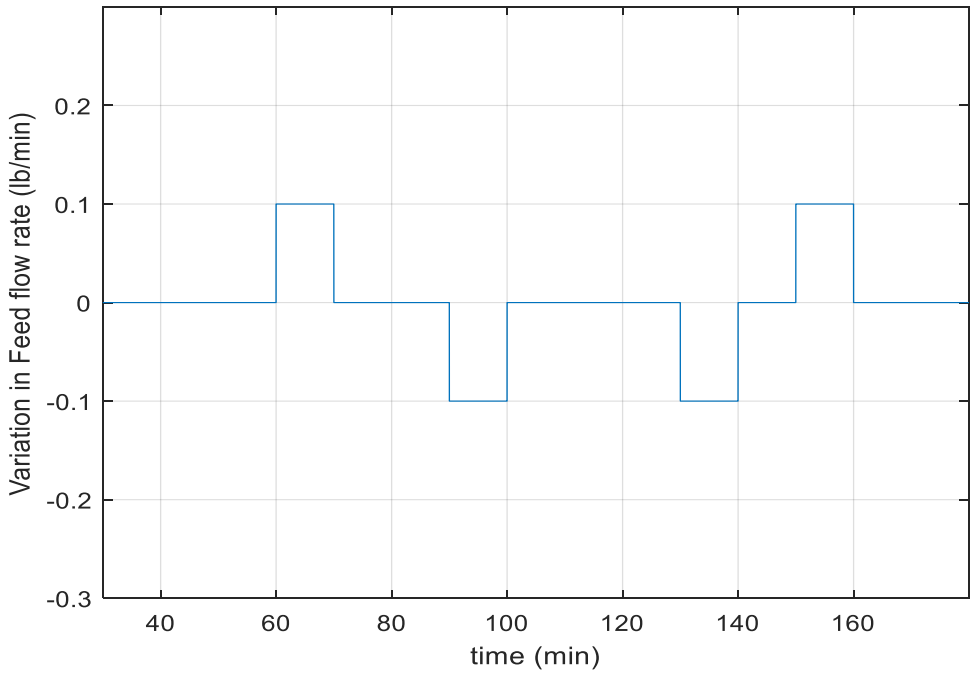

Figure 3.14: External disturbances of feed flow rate

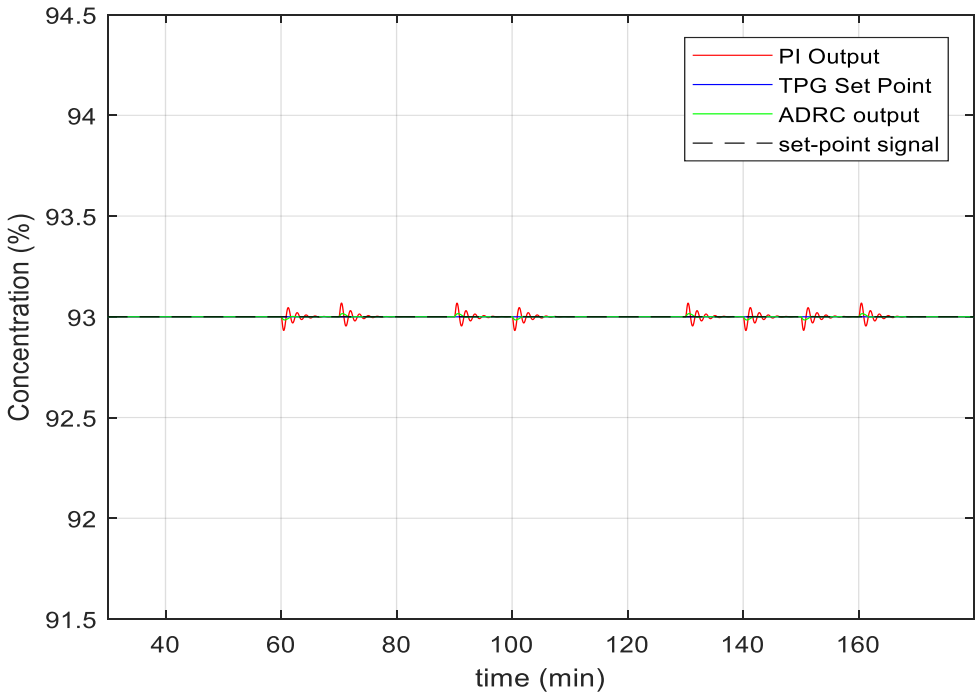

Figure 3.15: Performance of PI and ADRC schemes under the external disturbance test for Y_1

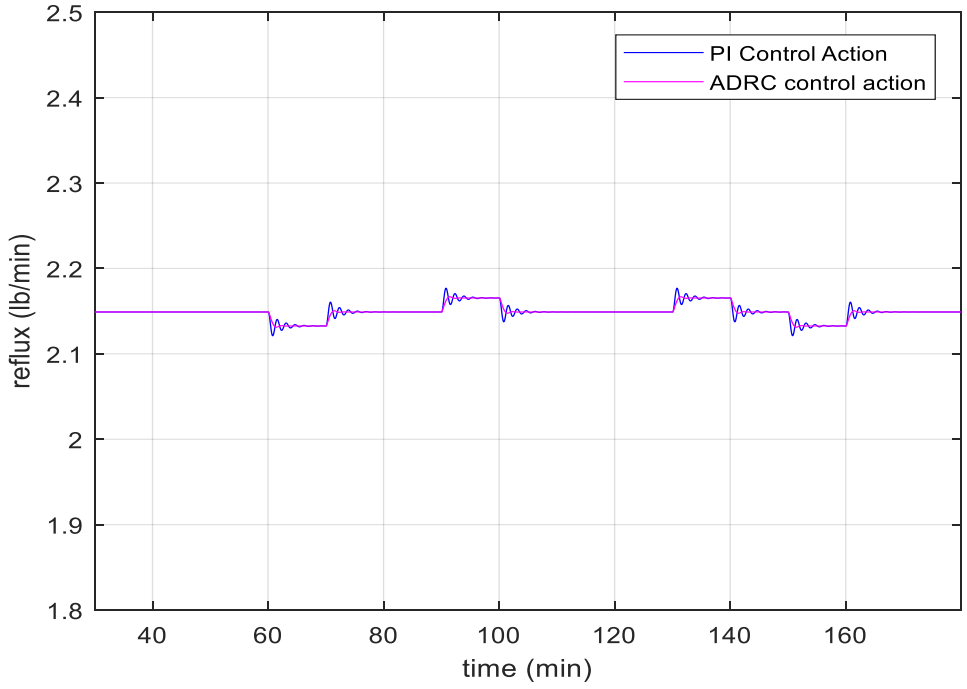

Figure 3.16: Control action of PI and ADRC schemes under the external disturbance test for Y_1

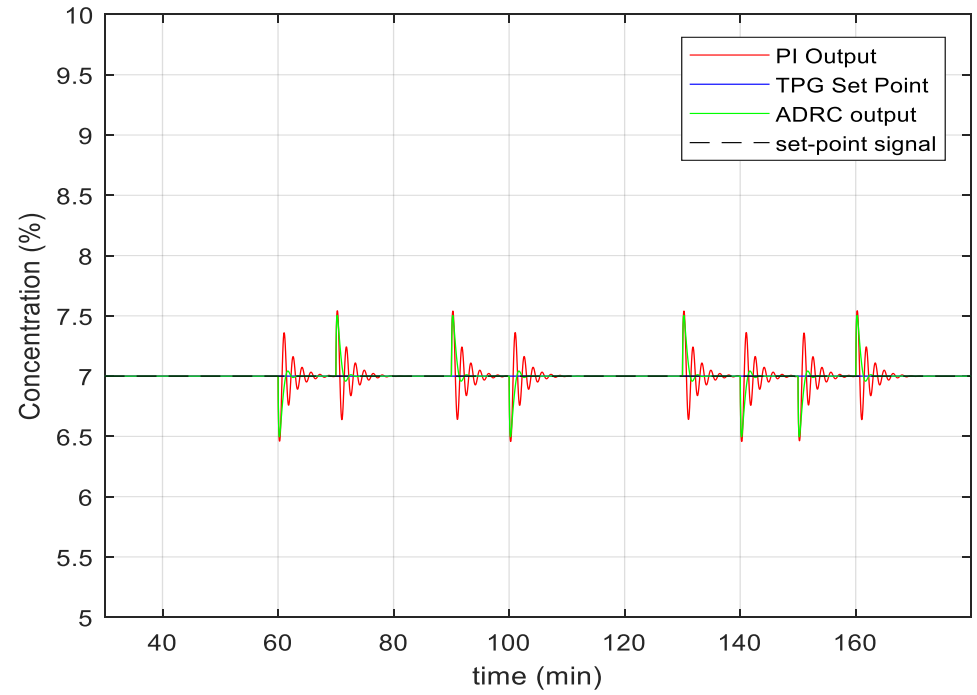

Figure 3.17: Performance of PI and ADRC schemes under the external disturbance test for Y_2

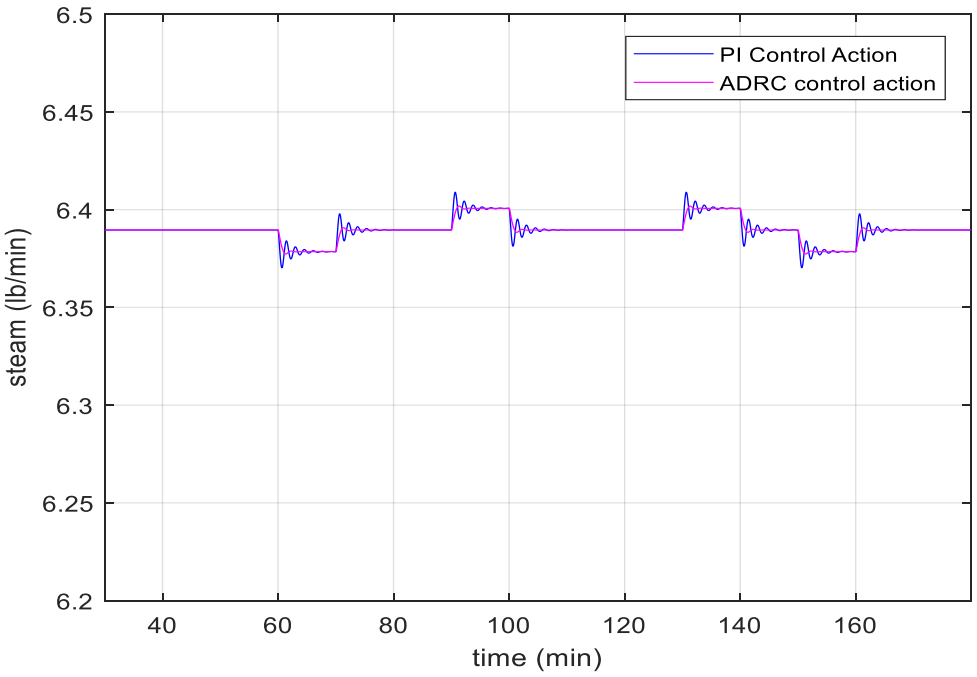

Figure 3.18: Control action of PI and ADRC schemes under the external disturbance test for Y_2

Referring to Figures 3.15 and 3.17, the overall performance of the ADRC scheme under the impact of external disturbance is very efficient. The process output response successfully follows the desired set-point with a much faster transient tracking response, quick recovery speed, small amplitudes of fluctuations, shortened settling time and less oscillation from input disturbances due to the ESO efficient estimation for the external disturbance generated from feed flow-rate. Hence, the output response of both product compositions follows the TPG response very closely. Furthermore, it can also be observed from Figures 3.16 and 3.18 that the control signal exerted from the ADRC scheme is much less sensitive to external noise variations, resulting in effective set-point tracking performance despite the impact of external disturbance. This is again due to the existence of a low pass filter that removes the sluggish response and smoothens the ADRC control signal.

Referring to Figures 3.15 and 3.17, the overall performance of the controlled process outputs of the PI controllers under the impact of external disturbance is not efficient as the ADRC performance, where the output signal follows the set-point successfully with slow recovery speed, large fluctuation amplitudes and a large settling time compared to the ADRC scheme. In addition, it can also be observed from Figures 3.16 and 3.18 that the control signals of the PI controller give a slightly aggressive and excessive response compared to the control actions of ADRC.

Table 3.8 represents the SSE values associated with the set-point tracking performance of both control algorithms. The values of SSE associated with the PI controller are considerably greater than the SSE values associated with ADRC. It can be seen from this table that the SSE values of the set-point tracking performance under the external disturbance is smaller than the previous one and this is due to the set-point changes where in previous condition there are a large serious changes of the set-point which produce an increase in SSE value while in this test, the set point signal it kept constant and the output signal follows the desired set-point in most iterations.

Table 3.8: SSE values associated with disturbance rejection performance under the external disturbance test

Control Loops	***SSE (PI)***	***SSE (ADRC)***
Y_1	21.5	0.237
Y_2	347	67.57

3.4 Conclusions

In this chapter, both ADRC and multi-loop PI control are designed and implemented on the MIMO transfer function model of the Wood–Berry distillation column. The PI controller is tuned by using the BLT tuning method. The performance of both control strategies were investigated and demonstrated in terms of set-point tracking capability, robustness in process variation, and external disturbance rejection. The SSE values were used to compare the two control schemes. The simulation results clearly indicate that the ADRC scheme performs better than PI control. The results of this chapter give motivation to implement the ADRC scheme in more complex dynamic simulations.

Chapter 4 ADRC of a distillation column simulated using a mechanistic model

4.1 Introduction

In the previous chapter, the ADRC and PI controllers were applied to the Wood–Berry distillation column represented by MIMO transfer functions. This transfer function model is a linear approximation that attempts to represent the dynamic behaviour of a distillation column in a relatively small operating range. In this chapter, both ADRC and PI controllers are applied to a binary distillation column simulated using a detailed mechanistic model. The mechanistic model is more accurate and contains tray-by-tray mass balance of the column. The control performance of both ADRC and PI controllers will be investigated in terms of set-point tracking and disturbance rejection.

This chapter is organised as follows: Section 4.2 introduces the considered distillation column in this chapter. In this section, the mechanistic model of a binary distillation column is introduced with the assumption made prior, implementing both PI and ADRC schemes. Furthermore, the 2×2 MIMO transfer function of the binary distillation model is obtained using a process reaction curve approach. Subsequently, the multi-loop control of the distillation column is represented in Section 4.3. This section starts by tuning the PI controller using the BLT technique in order to find suitable gain parameters for the PI controller. Suitable parameters of the ADRC scheme are also specified in this section. Section 4.4 investigates and evaluates both ADRC and PI by implementing various tests such as set-point tracking and external disturbance rejection. Finally, conclusions are drawn in Section 4.5.

4.2 Binary distillation columns

4.2.1 The considered distillation column

A non-linear dynamic mechanistic model-based simulation of a binary distillation column for separating a mixture of water and methanol is used in this research. The feed stream enters into the feed tray as a continuous stream with feed flow rate (F) and feed composition (x_f). Commonly, this feed tray (N_F) is located between the stripping and rectifying sections. The column obtains both distillate product stream (D) with distillate composition (x_D) and bottom product stream (B)

with the bottom composition (x_B). The column is used to separate methanol–water mixture into a distillate containing 97% methanol and a bottom stream containing 3% methanol. The water-cooled condenser (considered as tray $N + 1$) is used to completely condense the overhead vapour. The manipulated variables that are considered for product composition control purposes are the vapour flow rate (V) and reflux flow rate (L) (Fernandez De Canete et al., 2013). The rigorous mechanistic non-linear model has been developed based on detailed tray-by-tray mass and energy balances. This mechanistic model has been verified and validated using pilot plant test data and has been used in various control system studies (Tham et al., 1991a; Tham et al., 1991b). The non-linear dynamic simulations are based on the following assumptions: constant molar flow rates; constant relative volatility; constant stage pressure of 1.013×10^5 Pa; distillation tray efficiency of 100% (acts as an ideal tray); the dynamic system shows essentially ideal performance; the liquid feed at bubble point; the liquid on each distillation tray, in condenser, and reboiler are constant and completely mixed; the vapour holdup is completely neglected; vapour flow rate is constant; constant liquid holdup in the reflux drum; and finally the reflux stream is not sub-cooled.

Thus, the mathematical expression of the binary distillation model can be represented by the following equations (Al-Dunainawi and Abbod, 2016; Bendib, Bentarzi and Zennir, 2015):

- On each individual tray (excluding reboiler, condenser, feed tray and the tray immediately above the feed tray)

$$M_i \frac{dx_i}{t} = L_{i+1}x_{i+1} + V_{i-1}y_{i-1} - L_i x_i - V_i y_i \tag{4.1}$$

- Immediately above the feed stage $i = NF + 1$:

$$M_i \frac{dx_i}{t} = L_{i+1}x_{i+1} + V_{i-1}y_{i-1} - L_i x_i - V_i y_i + F_V y_F \tag{4.2}$$

- At the feed stage $i = NF$:

$$M_i \frac{dx_i}{t} = L_{i+1}x_{i+1} + V_{i-1}y_{i-1} - L_i x_i - V_i y_i + F_L X_F \tag{4.3}$$

- In the reboiler and column base:

$$M_B \frac{dx_i}{t} = L_2 - V_1 - B \tag{4.4}$$

- Total condenser:

$$\frac{dM_D}{dt} = V_{NT} - L - D \quad (4.5)$$

- Vapour-liquid equilibrium relationship for each tray:

$$y_i = \frac{ax_i}{1+(a-1)x_i} \quad (4.6)$$

- Reflux ratio:

$$R = \frac{L}{D} \quad (4.7)$$

- Total mass balance in the reboiler:

$$B = F - D \quad (4.8)$$

- Total mass balance in the condenser:

$$D = \frac{V}{R+1} \quad (4.9)$$

A description of variables and typical values is shown in Table 4.1(Díaz et al., 2016):

Table 4.1: Model variables and parameters

Symbol	Description	Typical value and unit
M*	Hold-up	0.5 kmol
V	Vapour flow rate into the condenser	19.238 g/s
L	Reflux	10.108 g/s
D	Distillate flow rate	9.13 g/s
B	Bottoms flow rate	9.1 g/s
F	Feed flow rate	18.23 g/s
A	Relative volatility	2
R	Reflux ratio	1.107
S	Steam flow rate	13.814 g/s
N	Number of trays	10
N_F	Feed tray no.	6
x_F	Feed composition	0.5
x_D	Top composition	93%
x_B	Bottom composition	7%
y_i	Vapour molar fraction on the *i*th stage	-
x_i	Liquid composition on the *i*th stage	-

* The hold-up on each individual stage including reboiler and condenser has the same value.

In order to control the top composition Y_1 and bottom composition Y_2 efficiently, reflux rate u_1 and steam rate u_2 will be used as manipulated variables respectively. The disturbances considered here are feed flow rate F and feed composition x_f disturbances. For analysing the control system of the binary distillation column, its transfer function model as shown in Figure 4.1 will be identified.

$$\begin{bmatrix} Y_1(s) \\ Y_2(s) \end{bmatrix} = G_P \begin{bmatrix} u_1(s) \\ u_2(s) \end{bmatrix} + G_d \begin{bmatrix} F(s) \\ x_f(s) \end{bmatrix} \tag{4.10}$$

In the above equation, the process model is represented by the transfer function G_p and the disturbance model is represented by G_d

$G_p = \begin{bmatrix} P_{11} & P_{12} \\ P_{21} & P_{22} \end{bmatrix}$, and $G_d = \begin{bmatrix} d_{11} & d_{12} \\ d_{21} & d_{22} \end{bmatrix}$

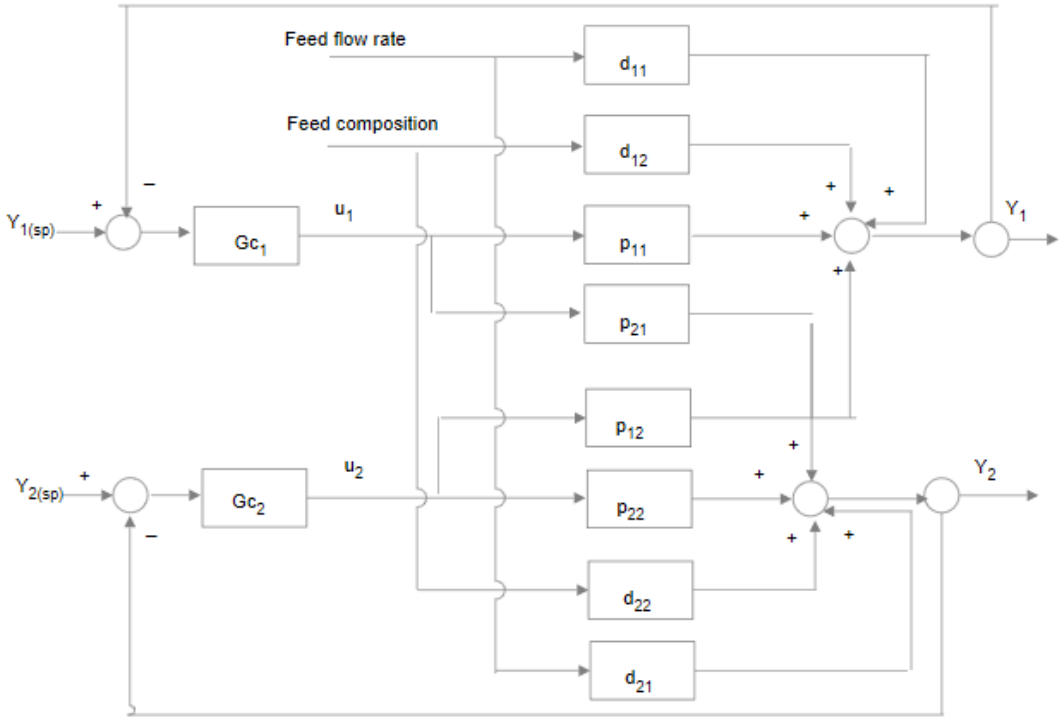

Figure 4.1: Control structure of the binary distillation column

4.2.2 Transfer function model of the distillation column

In order to obtain the transfer functions of G_p, a step change was applied on both reflux rate and steam flow rate individually and the corresponding changes in both Y_1 and Y_2 were recorded as shown in Figures 4.2 and 4.3. It is assumed that there is a 10 min time delay in the composition analyser.

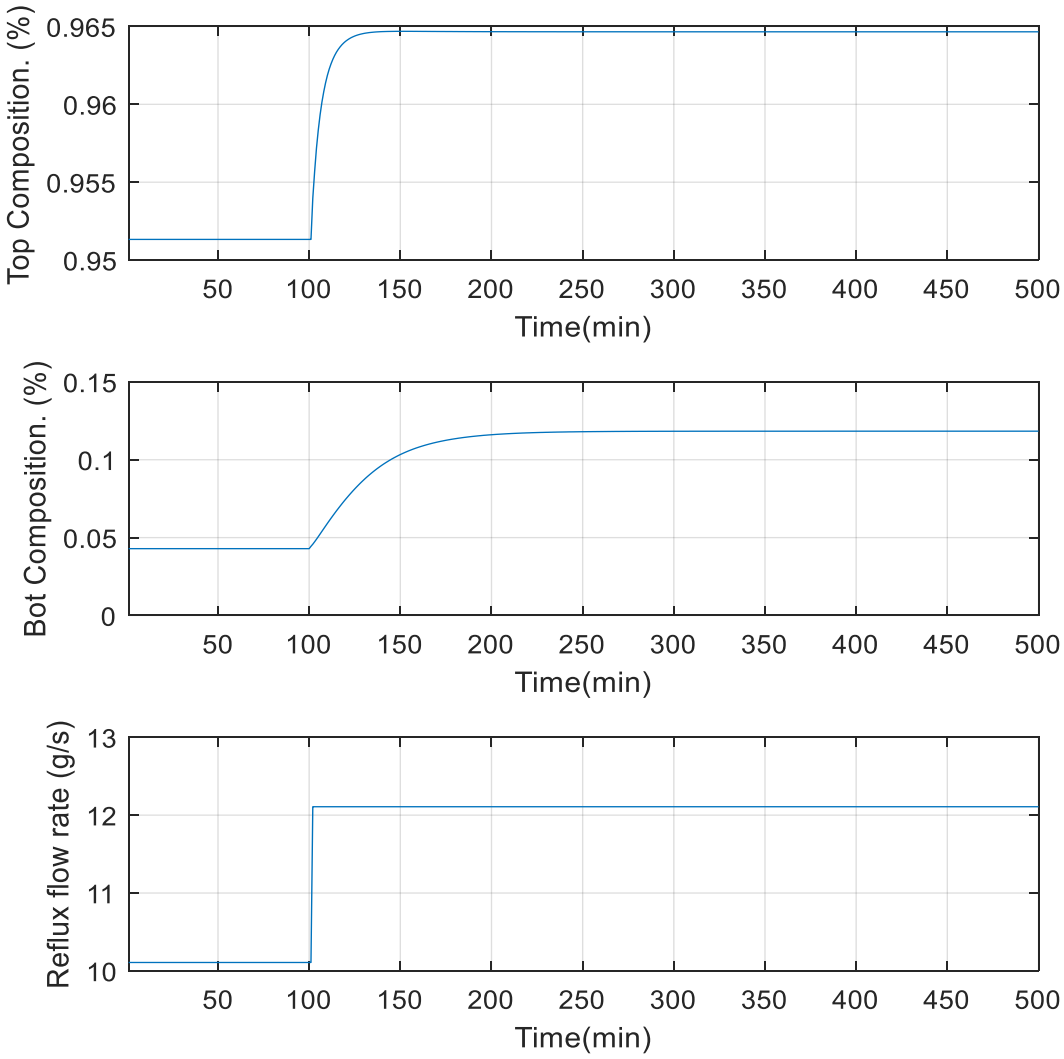

Figure 4.2: Process modelling with reflux flow rate step changes

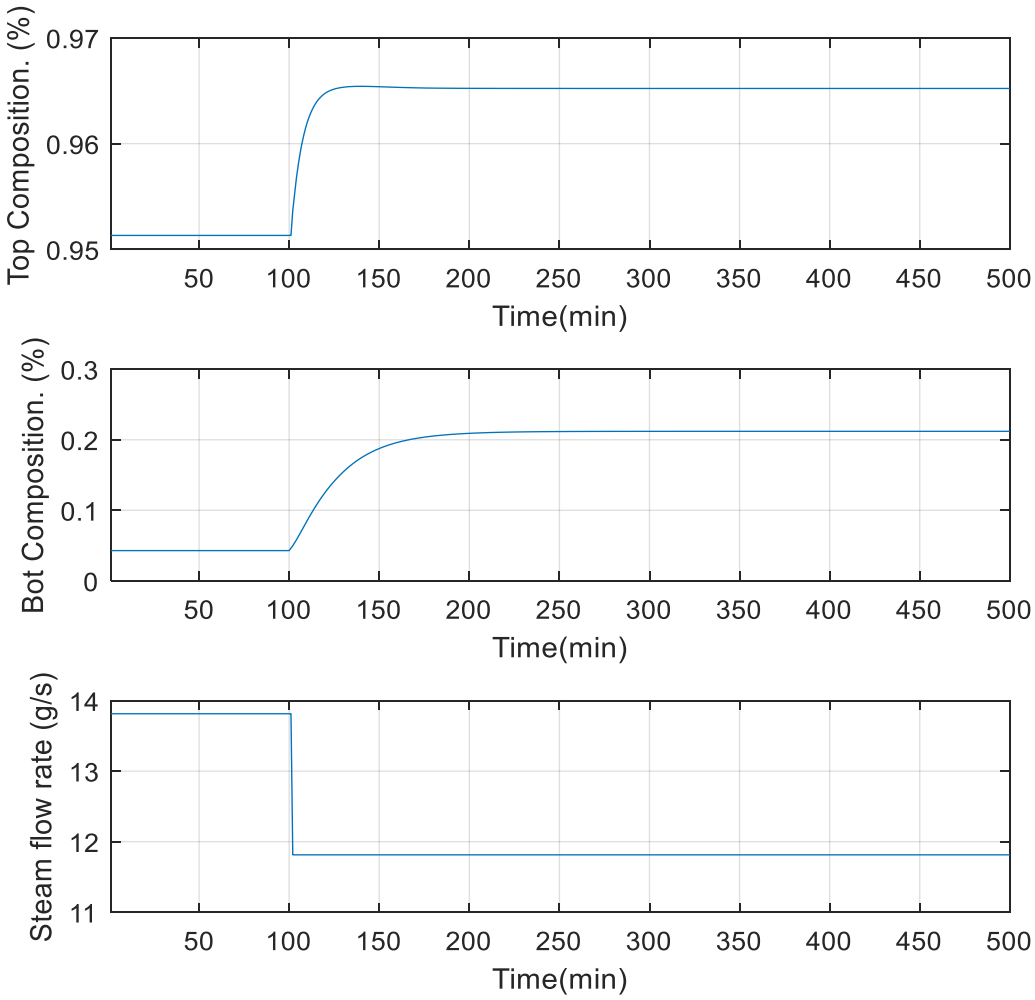

Figure 4.3: Process modelling with steam flow rate step changes

In addition, the identified process model is:

$$G_p = \begin{bmatrix} \frac{0.6651}{4.53s+1} & -\frac{0.693}{8.62s+1} \\ \frac{3.804}{19.7s+1} & -\frac{8.435}{21.3s+1} \end{bmatrix} e^{-10s} \quad (4.11)$$

It can be seen from the identified process model G_p that there is a direct relationship between the feed flow rate and the product compositions, while there is a reverse relationship between the steam rate and product compositions.

In order to obtain the transfer functions of G_d, step changes were applied individually on the external disturbance represented by feed flow-rate and feed composition as shown in Figures 4.4 and 4.5. It is assumed that there is a 10 min time delay in the composition analyser.

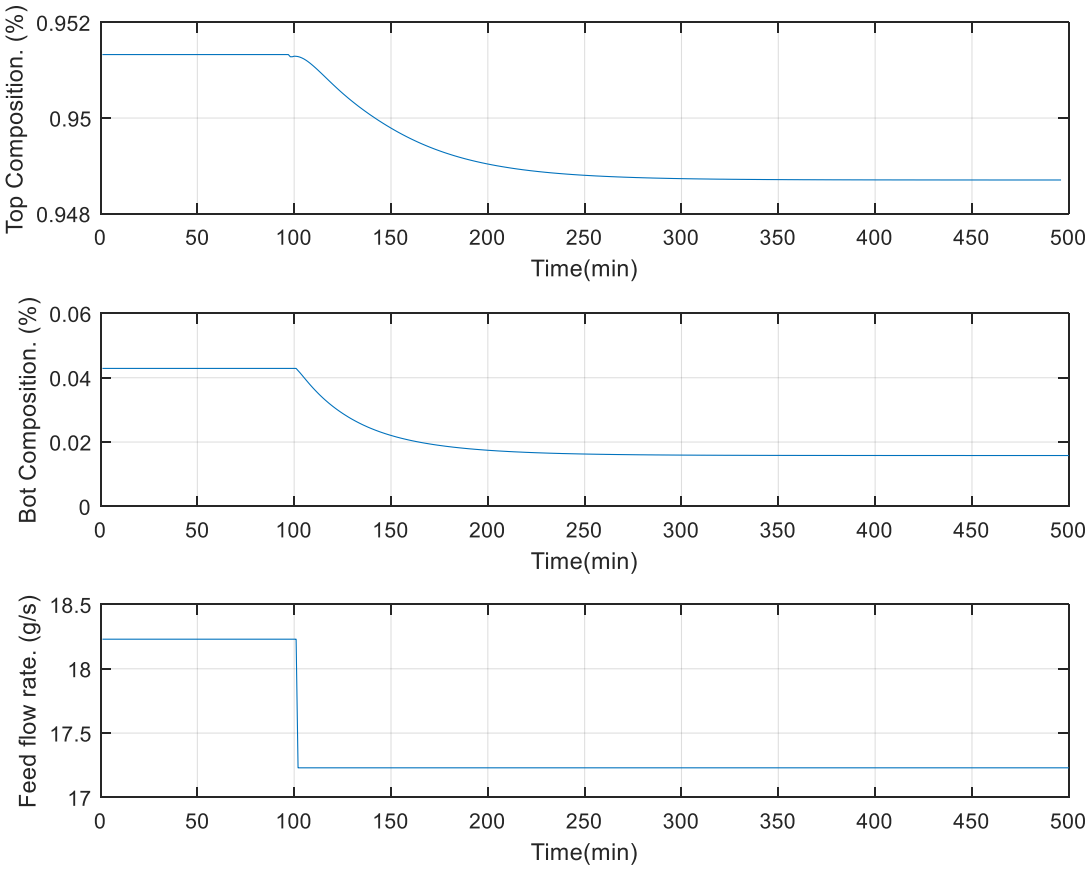

Figure 4.4: Disturbance modelling with feed flow rate step changes

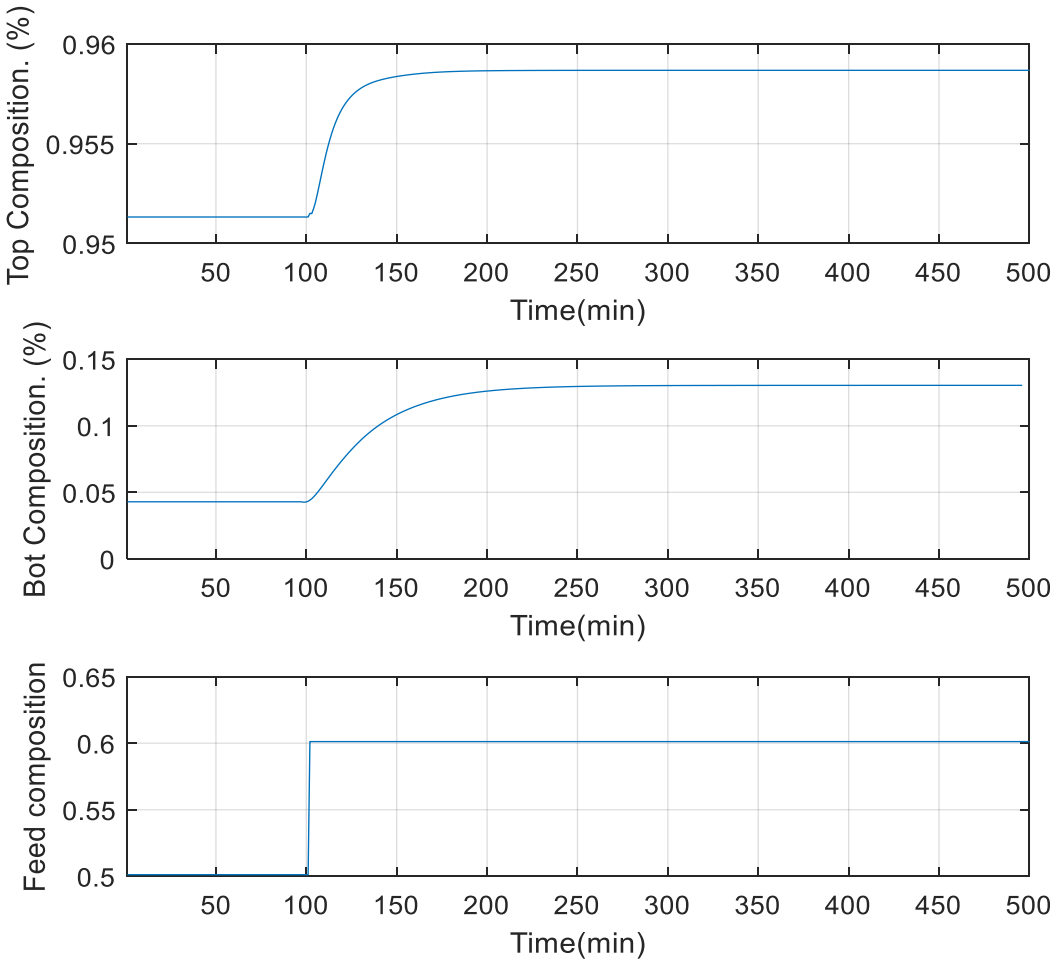

Figure 4.5: Disturbance modelling with feed composition step changes

The identified disturbance model is:

$$G_d = \begin{bmatrix} \frac{0.021}{64.7s+1} & \frac{0.63}{9.31s+1} \\ \frac{3.28}{17.4s+1} & \frac{86.5}{21.9s+1} \end{bmatrix} e^{-10s} \tag{4.12}$$

4.3 Multi-loop control of the distillation column

Since the main aim of this research is to make a suitable comparison between the common conventional multi-loop PI controller and the ADRC scheme, the parameters of the PI controller should be properly tuned.

4.3.1 Tuning the PI controller parameters

As in the previous chapter, the parameters of the PI controller are tuned by using the BLT tuning method. The multi-loop controller is given as:

$$G_c = \begin{bmatrix} G_{c1} & 0 \\ 0 & G_{c2} \end{bmatrix} \tag{4.13}$$

The transfer function P_{11} will be used to calculate the initial parameters of the first controller G_{c1} while P_{22} will be used to calculate the initial parameter of the second controller G_{c2} where G_c represents the PI controller.

Figures 4.6 and 4.7 show the Bode plot for P_{11} and P_{22} respectively.

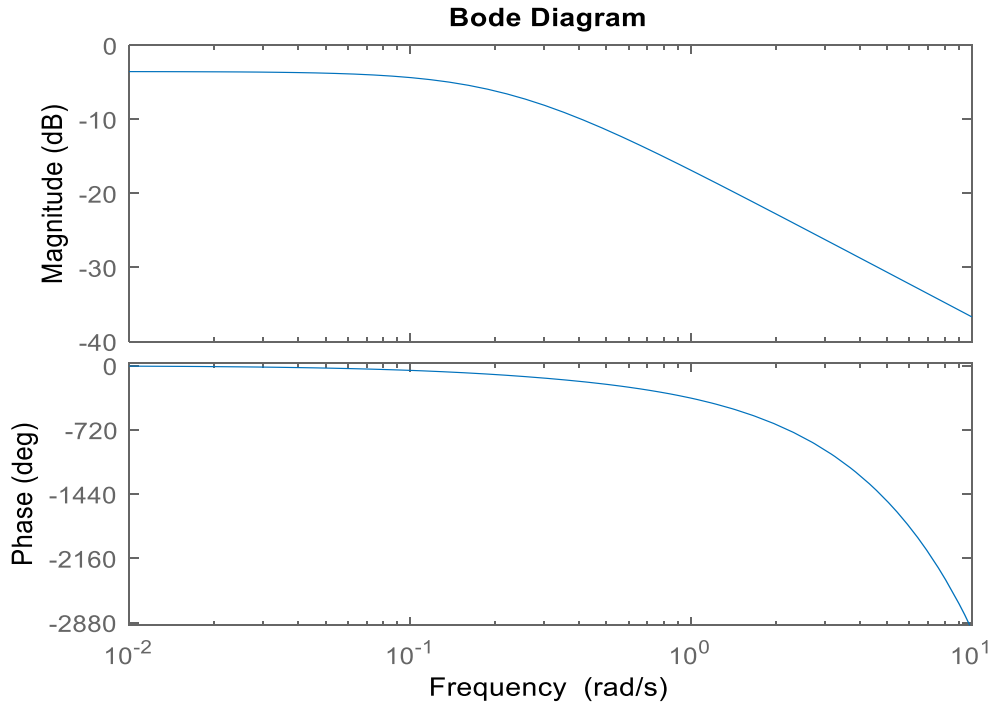

Figure 4.6: Bode plot of the top transfer function

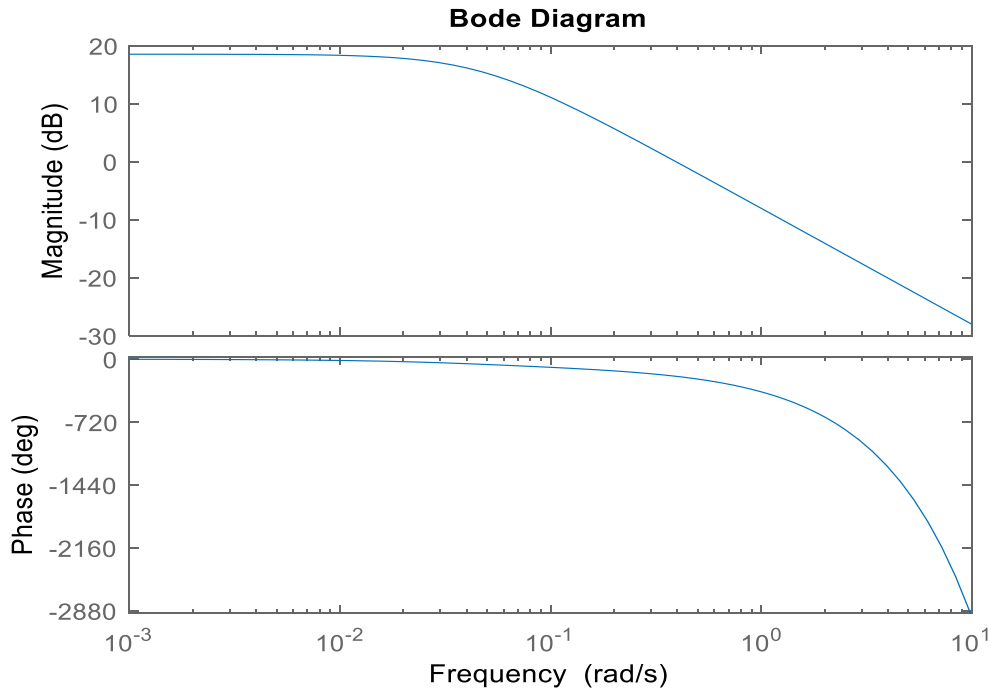

Figure 4.7: Bode plot of the bottom transfer function

Table 4.2 gives the G_M and w_G values and the corresponding initial PI controller parameters. These parameters were further detuned using the BLT method.

Table 4.2: ZN tuning setting for binary distillation column

Loop	Controller	G_M	w_G	K_C	τ_I
Y_1	G_{c1}	3.1867	0.4124	1.4485	12.6951
Y_2	G_{c2}	2.4076	0.9523	1.0944	5.4984

According to the transfer function in Equation 4.10, the binary distillation column is a 2×2 MIMO dynamic system, which should have a biggest log modulus of 4 under a properly tuned controller.

$$[L_{cm}]^{max} = 4 \tag{4.14}$$

The plot of L_{cm} with F = 2.698 is shown in Figure 4.8. It can be seen that under this detuning factor the biggest L_{cm} is approximately equal to 4.

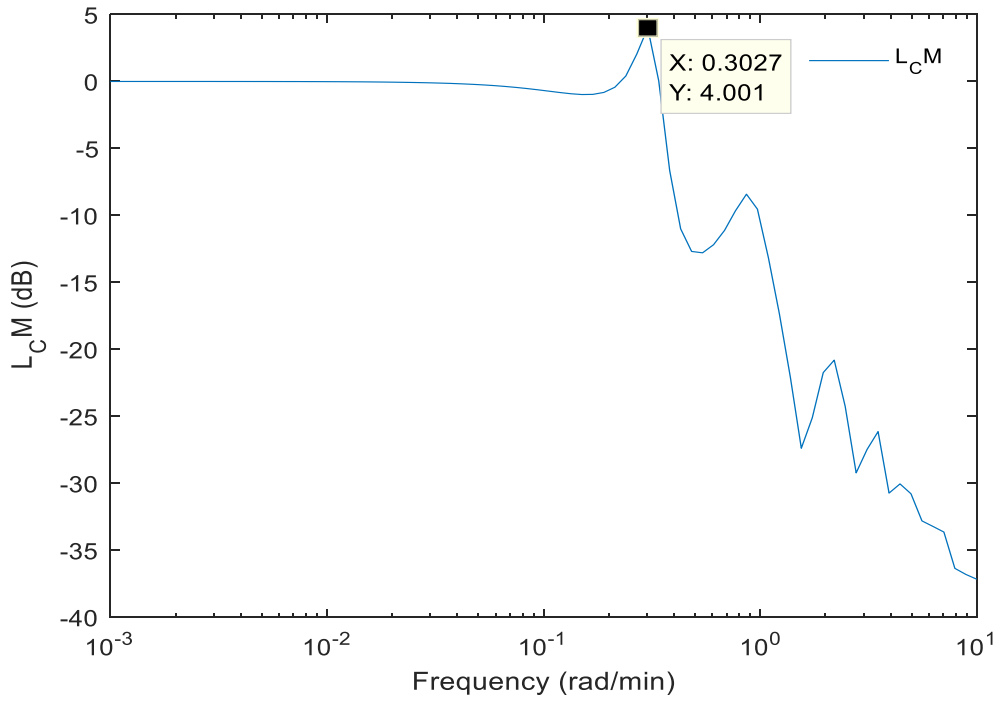

Figure 4.8: Closed-loop log modulus for binary distillation column

The initial PI controller parameters from ZN tuning are further tuned by this detuning factor, and final controller parameters are summarised in Table 4.3.

Table 4.3: BLT tuning setting for a binary distillation column

Loop	**Controller**	K_c	τ_I
Y_1	G_{c1} (reflux)	0.5369	34.2548
Y_2	G_{c2} (steam)	0.4056	14.8343

4.3.2 Implementing the components of ADRC scheme

Prior to applying the ADRC scheme on the mechanistic model of a binary distillation column, each component of the ADRC will be designed and tuned based on the equations given in Chapter 2.

i. TPG

Equations 2.12 and 2.13 were used to implement the discrete form of TPG. Table 4.4 gives the TPG tuning values. These values have been selected according to the recommended values for the TPG parameters introduced in Table 2.2. Furthermore, the initial value of the tuning parameter *r* should be approximately the inverse of the dominant time constant and then further modified as desired.

Table 4.4: Selected values for TPG tuning parameters *r* and *h*.

TPG tuning parameters	**Selected values**	
	Y_1	**Y_2**
r	10	10
h	0.004	0.004

ii. ESO

The ESO is designed by implementing equations shown in 2.14 and 2.15. The ESO tuning values are presented in Table 4.5. It can be observed from these equations that the gain parameters β_1, β_2 and β_3 are selected based on sampling interval *k*.

Table 4.5: Selected values for ESO tuning parameters.

ESO tuning parameters	**Selected values**	
	Y_1	**Y_2**
β_1	1	1
β_2	33.33	33.33
β_3	156.25	156.25
b	3.7	10

k	0.01	0.01

iii. N-LWS

The N-LWS is designed and implemented using equations 2.16, 2.17 and 2.18 to produce the effective suitable control signal u. Table 4.6 presents the suitable tuning values of N-LWS. These values have been selected based on the recommended values introduced in Chapter 2.

Table 4.6: selected values for N-LWS tuning parameters.

N-LWS tuning parameters	**Selected values**	
	$\boldsymbol{Y_1}$	$\boldsymbol{Y_2}$
α	0.05	0.5
δ	0.05	0.05
kp	90	-80
f_c	0.982	0.964

4.4 Investigating the performance of both control schemes

In order to evaluate and investigate the performance of both PI and ADRC control schemes, both control schemes are applied to the binary distillation column. In this section, the performance of both control schemes are investigated and analysed by conducting several common tests such as set-point tracking and external disturbance rejection. These types of experiments have been selected due to the existence of a sudden set-point change and undesired external disturbance in the MIMO system.

A. Set-point tracking performance

According to Murad et al. (1997), the simultaneous control of distillate and bottom compositions in a binary distillation column using the reflux and steam flow-rate as manipulated variables is usually quite difficult due to the inherent interaction between the control loops. Furthermore, any deviation from the desired set-point and steady state value in one loop will need quick and appropriate action or change in the controller signal of other interacting loops in order to maintain their respective set-points. As a result, loop interaction should be considered in the control system where a series of set-point changes are applied to both product compositions.

The performance of both control schemes will be investigated by applying various sudden set-point changes. The control performance is evaluated based on the SSE values of the control errors. The set-point tracking performance of Y_1 and Y_2 using ADRC and PI controllers are presented in Figures 4.9 and 4.11 respectively.

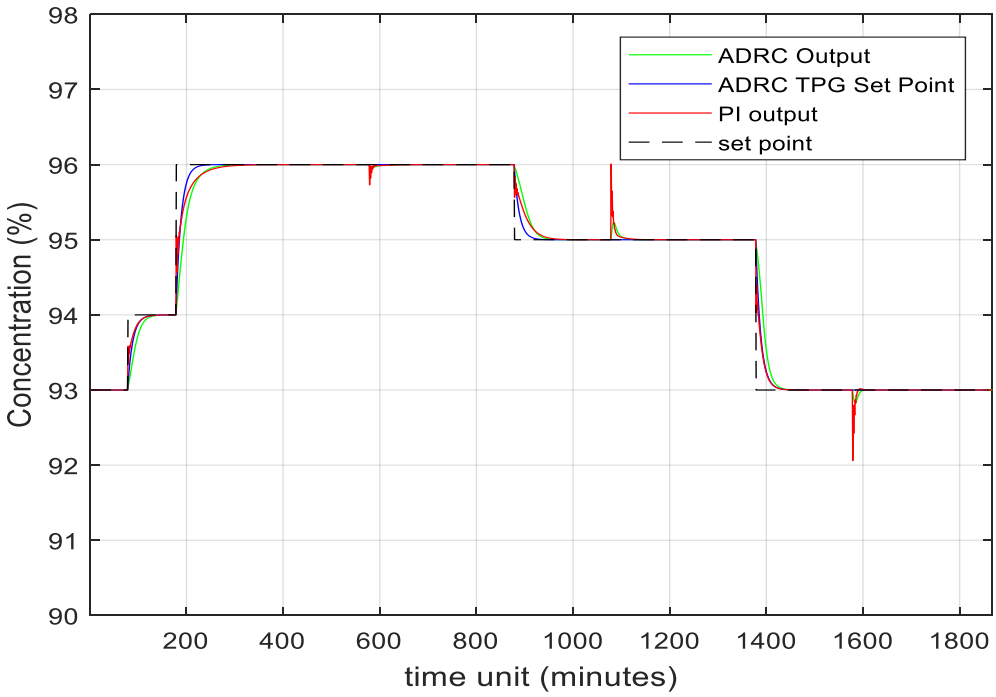

Figure 4.9: Performance of PI and ADRC schemes under the set-point tracking test for Y_1

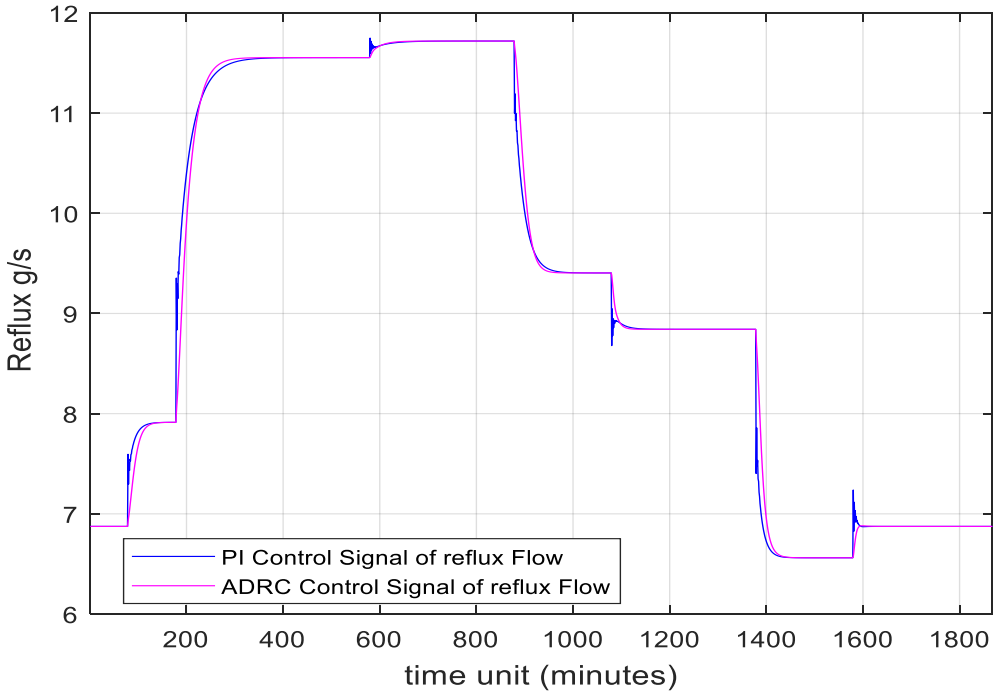

Figure 4.10: Control action of PI and ADRC schemes under the set-point tracking test for Y_1

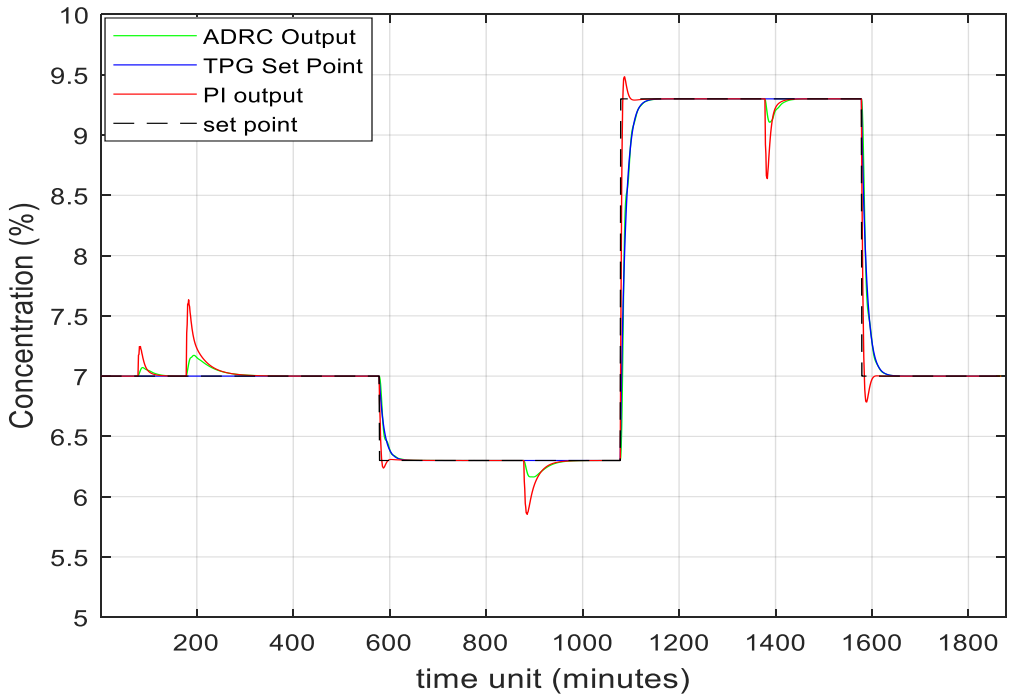

Figure 4.11: Performance of PI and ADRC schemes under the set-point tracking test for Y_2

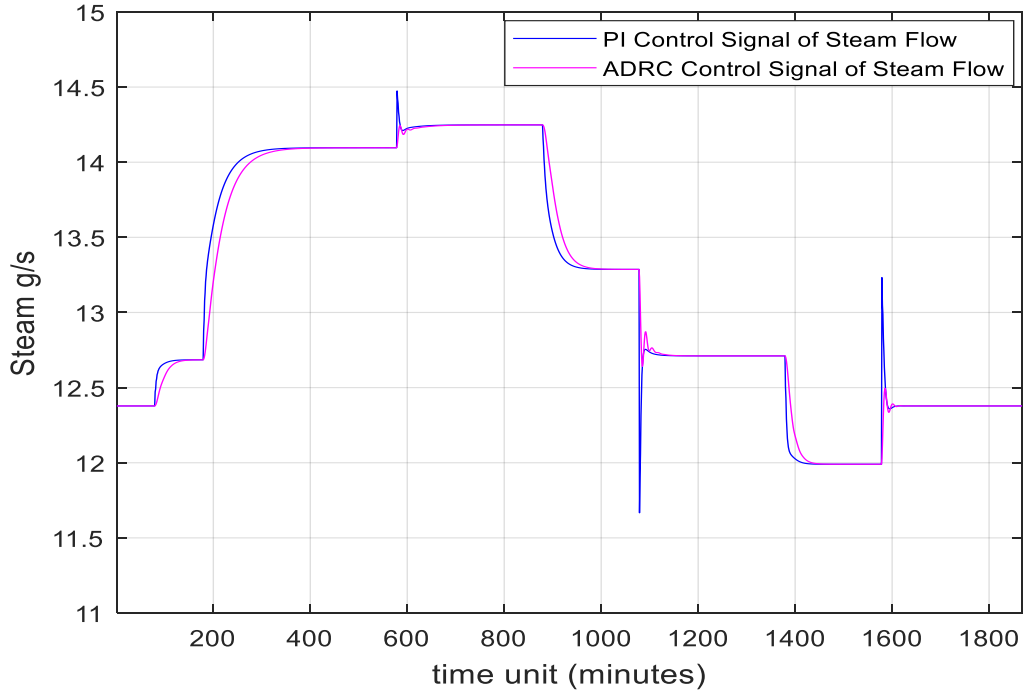

Figure 4.12: Control action of PI and ADRC schemes under the set-point tracking test for Y_2

Table 4.7 shows the SSE values associated with the set-point tracking performance of both control schemes. The SSE values associated with the PI controller are considerably greater than the SSE values.

Table 4.7: SSE values associated with both control schemes under the test of set-point tracking

Control Loops	***SSE (PI)***	***SSE (ADRC)***
Y_1	40.9622	10.665
Y_2	79.422	33.70

Furthermore, several points can be clearly observed from the above simulation results:

Set-point tracking capability

Referring to Figures 4.9 and 4.11, the ADRC scheme exhibits efficient control performance under set-point tracking. The controlled variables follow their set-points without any signs of overshoot or oscillation. This interesting result is due to the structure of the ADRC scheme: after the set-point signal change, the TPG generates a transient profile that forces the output signal to follow the desired set-point gradually, while the ESO is used in the path of a feedback loop to continuously observe the internal states in order to update the N-LWS and compensate for the error rapidly and efficiently. Based on accurate estimation from the ESO component, the product compositions of the binary distillation column track the desired reference input signal accurately. Moreover, and by referring to Figures 4.10 and 4.12, the ADRC control signal gives non-aggressive, non-sluggish and non-oscillating output performance due to the internal low-pass filter mentioned earlier, yielding an excellent set-point tracking performance.

Referring to Figures 4.9 and 4.11, the performance of the PI controller performs well at maintaining both product compositions close to their set-points with some variation or overshoot at both product compositions especially at bottom composition during the set-point change where more change in set-point will produce more overshoot. In most general cases, the suitable rates for both manipulated variables—reflux flow rate and steam flow rate—should be within their operating point 30–40% specified in Table 4.1. In this test, both the ADRC and PI control signals

are operating within the specified operating range except the bottom composition of the PI controller, which exceeds this range.

Strong loop interactions

The ADRC scheme produces efficient control performance under the effect of loop interactions. The response of the controlled variables follows the desired set-point successfully with little sign of overshoot when the set-point of any loop has been changed, especially at the bottom composition where there are small signs of overshoot during alteration of the top composition set-point. Reducing the impact of loop interaction proves the capability of the ADRC scheme to recover to the original steady state rapidly. The efficient performance of the ADRC scheme is due to its structure where the interaction between both loops are considered an external disturbance and can be estimated and compensated for by the ADRC algorithm in order to recover the output signal to the original steady state. Moreover, the control signal of the ADRC scheme shows smooth performance without any signs of oscillation, leading to excellent set-point tracking performance and conferring a practical ADRC control signal.

The performance of the PI controller under loop interaction is significantly compromised with a large variation and overshoot at both product compositions, especially at top composition, which has undesirable error under the PI controller. Moreover, the speed of the PI controller in compensating the disturbance is not as fast as the ADRC scheme and takes longer to become stable, resulting in a large overshoot. The control signal of the PI controller is not as practical as the ADRC control signal. This test highlights one of the major limitations of the PI controller.

B. External disturbance rejection

Several factors affect the desired product purity in the binary distillation column. External disturbances such as change in feed composition Z_L and feed flow rate F_L may cause a deviation in the top or distillate composition Y_1 and bottom composition Y_2 from their respective desired set-points. These kinds of external disturbance variations can disturb the steady state operations of the system and severely degrade the overall performance of the column. In order to eliminate the effect

of external disturbances on controlled variables and acquire the desired performance specifications, the controller must generate the corrective action rapidly and sufficiently. The impact of undesired unmeasured external disturbance on the performance of the controller is investigated by implementing periodic change in both feed flow rate and feed composition. A good controller is expected to suppress the disturbance introduced in both loops. Furthermore, the major control objective in this experiment is to keep both product compositions as close as possible to the desired set-points in spite of unexpected fluctuation in both feed composition and feed flow rate, which strongly impact product compositions.

In many existing publications, the disturbance of the binary distillation column is designed as an external random signal or a step signal (Zafiriou and Morari, 1987; Lee et al, 1991; Tham et al., 1991a; Skogestad, 1997). Nevertheless, this external disturbance varies persistently over a specific period of time. Hence, modelling it as a random signal could be unrealistic because the random signal rate and magnitude of change might be outside normal bounds in some instances. In addition, in order to test the noise suppression ability of both designed controller PI and ADRC, a random noise was introduced simultaneously by adding deviation changes in both common causes of disturbance, namely feed composition and feed flow rate. It is good to point here to point that the serious changes of the set-point signal in both compositions have been removed in order to investigate the efficiency of both controllers under the impact of external disturbances.

External disturbances in the form of changes in the feed flow rate

According to Table 4.1, the normal operating condition of the feed flow rate is 18.23 g/s. External disturbance can be generated by changing the feed stream flow rate while maintaining constant normal operating set-point values of Y_1 and Y_2. Figure 4.13 shows the series step changes that were introduced in the feed flow rate.

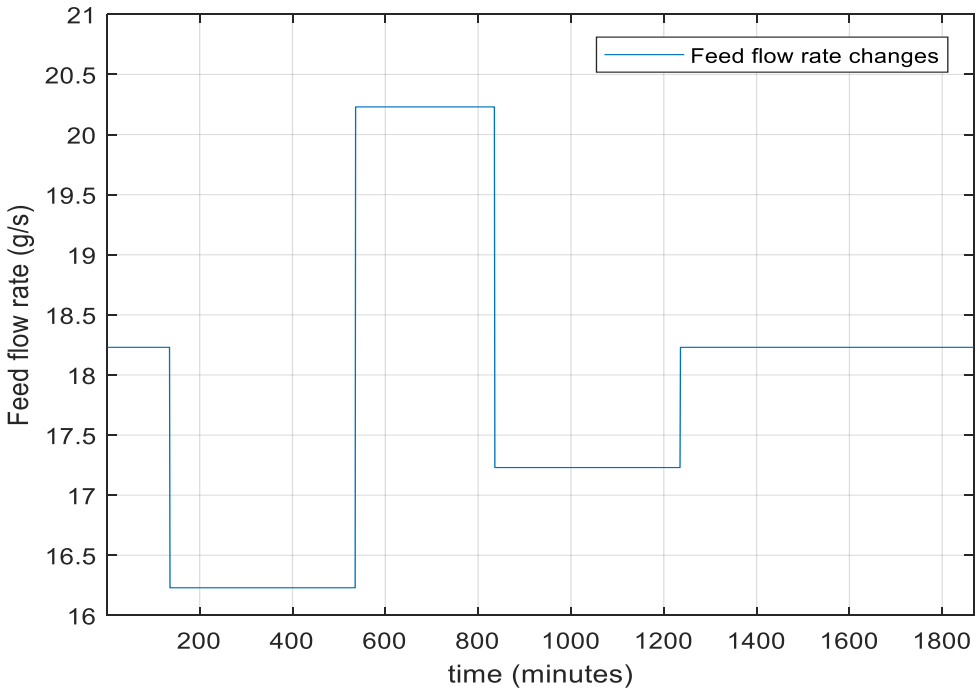

Figure 4.13: Changes in feed flow rate introduced to the system

Figures 4.14 to 4.17 represent the external disturbance rejection capability in both Y_1 and Y_2 for feed flow rate disturbance.

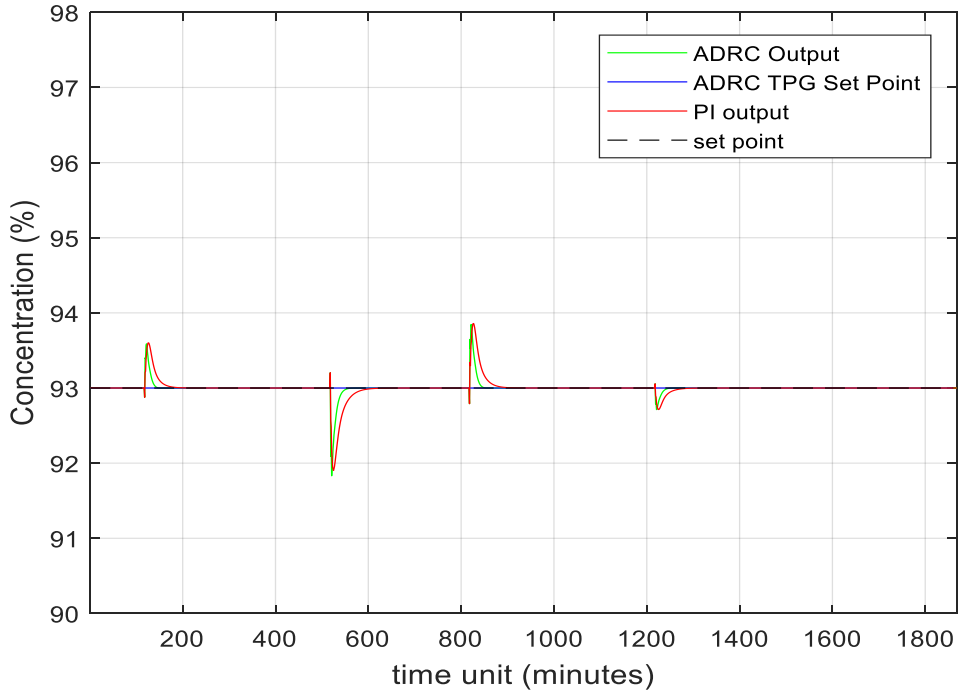

Figure 4.14: Performance of PI and ADRC schemes under the external disturbance test for Y_1

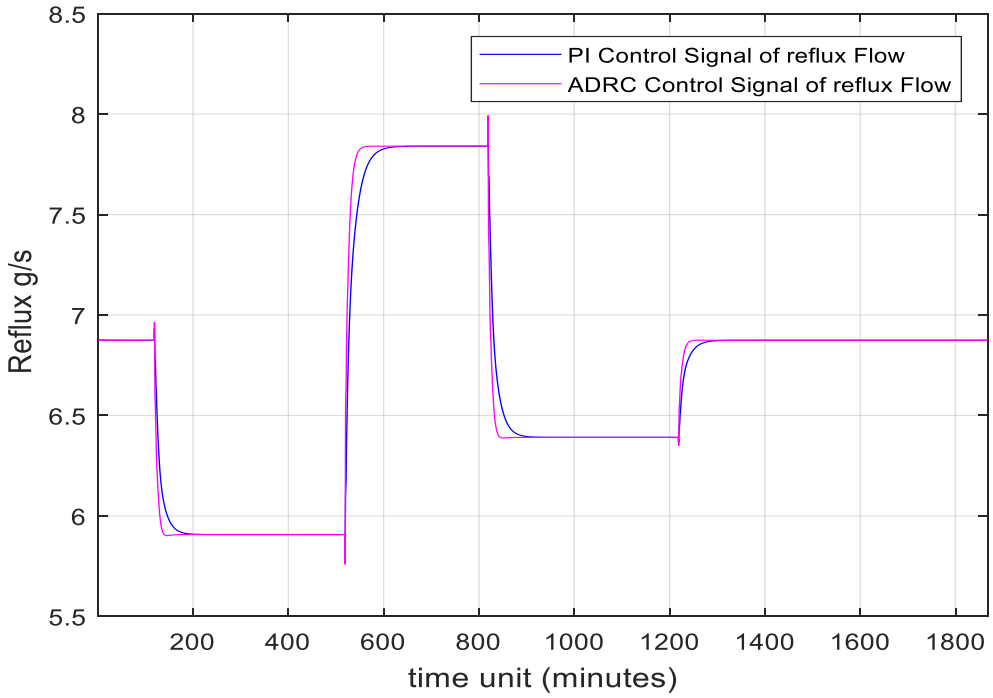

Figure 4.15: Control action of PI and ADRC schemes under the external disturbance test for Y_1

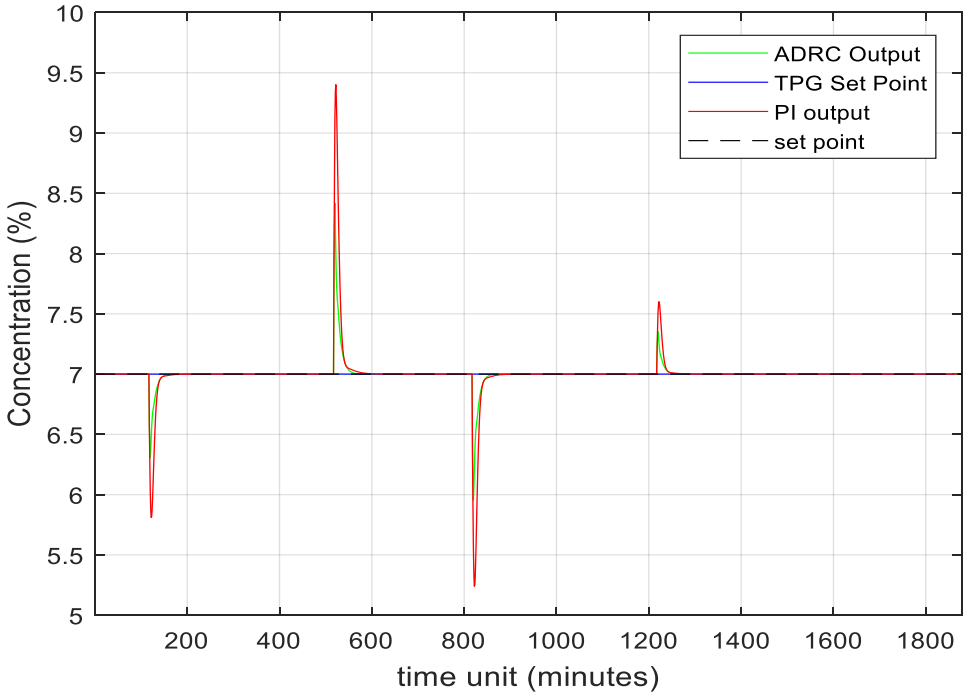

Figure 4.16: Performance of PI and ADRC schemes under the external disturbance test for Y_2

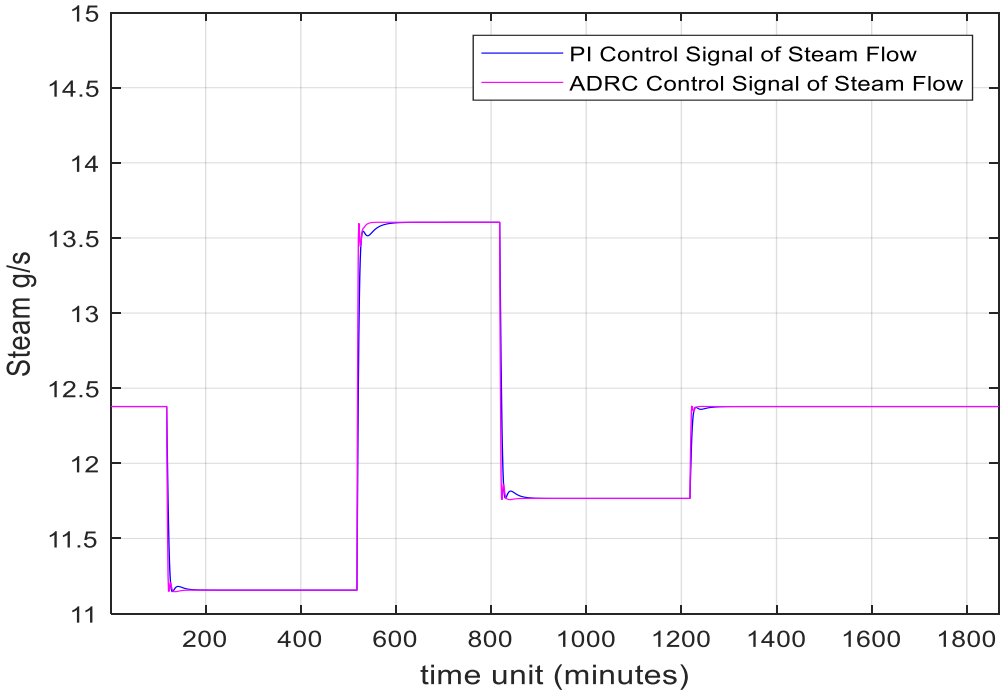

Figure 4.17: Control action of PI and ADRC schemes under the external disturbance test for Y_2

The results presented in Figures 4.14 and 4.16 show the successful and efficient external disturbance rejection performance of the ADRC scheme, where both product compositions quickly return to the desired original set point in a relatively smooth and non-oscillatory manner. Furthermore, and according to Figures 4.15 and 4.17, the control action of ADRC is found to be smooth. Correspondingly, the control performance of the PI controller is found not to be as efficient as the ADRC performance in terms of the magnitude of deviation away from the desired set-points. Moreover, according to Figures 4.15 and 4.17, the control signal of the PI controller under the effect of disturbance is non-smooth and aggressive.

External disturbances in the form of changes in the feed composition

According to Table 4.1, the nominal feed compositions is 0.5. The external disturbance can be generated by changing the feed composition while maintaining constant normal operating set-point values of Y_1 and Y_2. Figure 4.18 shows the series step changes introduced to the feed composition.

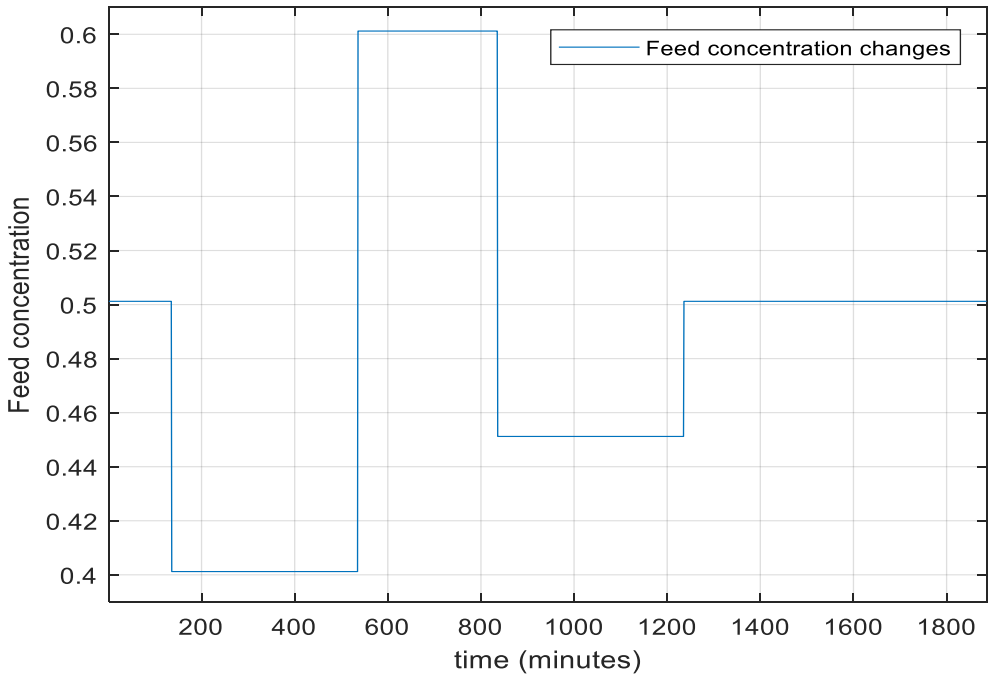

Figure 4.18: Changes in feed concentration introduced to the system

Figures 4.19 to 4.22 represents the external disturbance rejection capability in both Y_1 and Y_2 under feed composition disturbance.

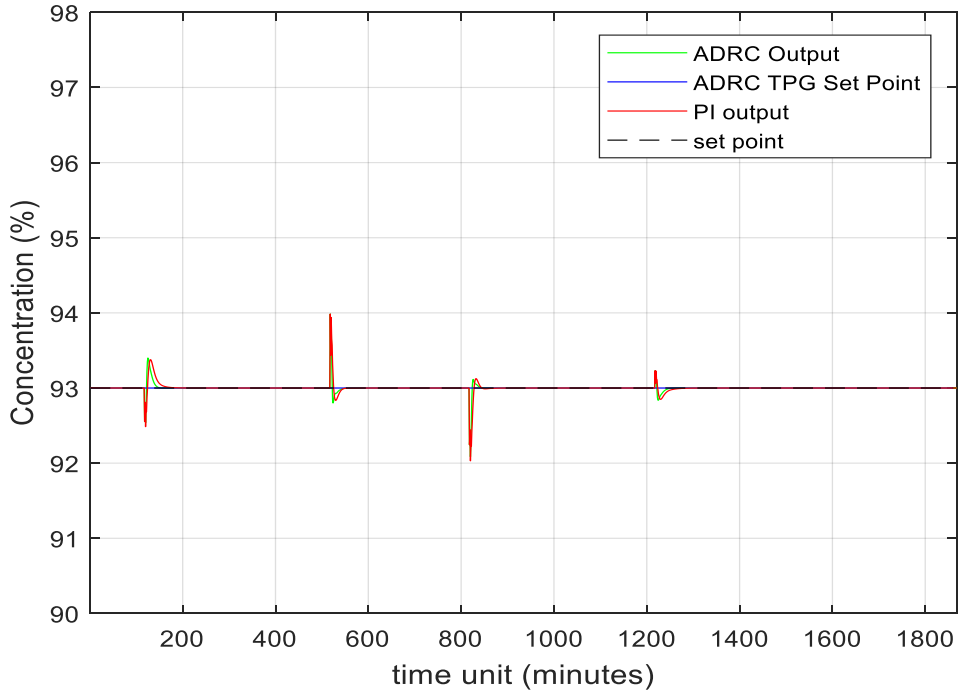

Figure 4.19: Performance of PI and ADRC schemes under the external disturbance test for Y_1

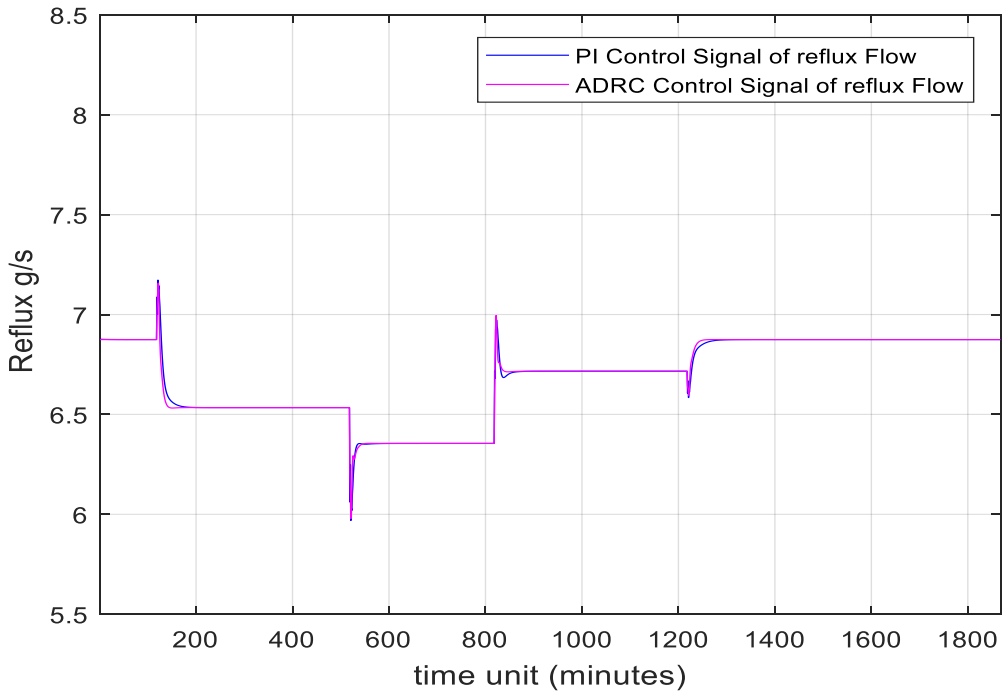

Figure 4.20: Control action of PI and ADRC schemes under the external disturbance test for Y_1

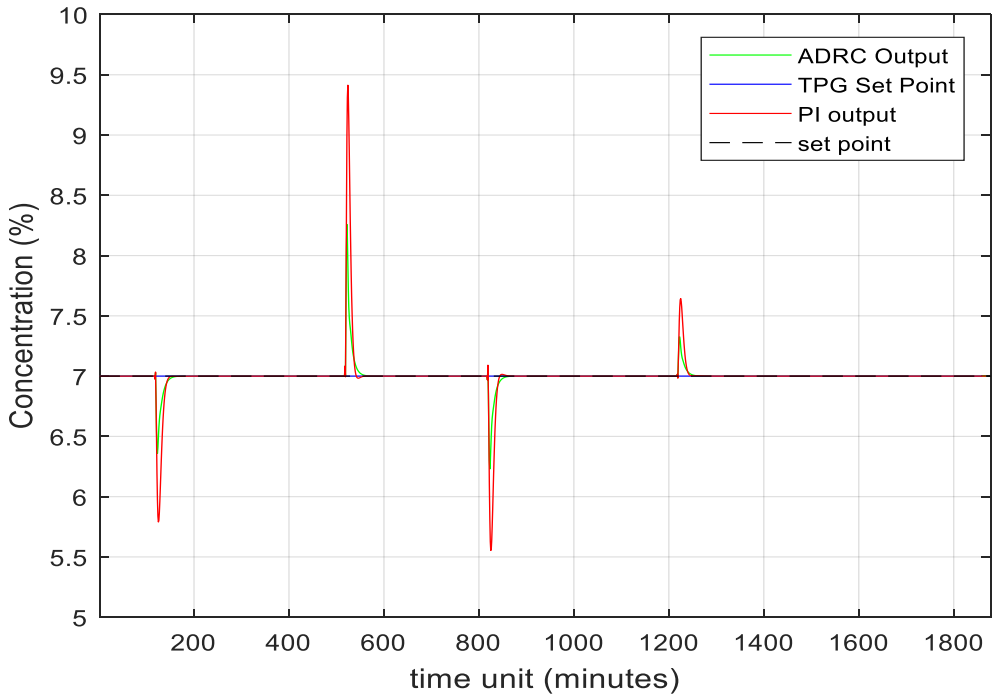

Figure 4.21: Performance of PI and ADRC schemes under the external disturbance test for Y_2

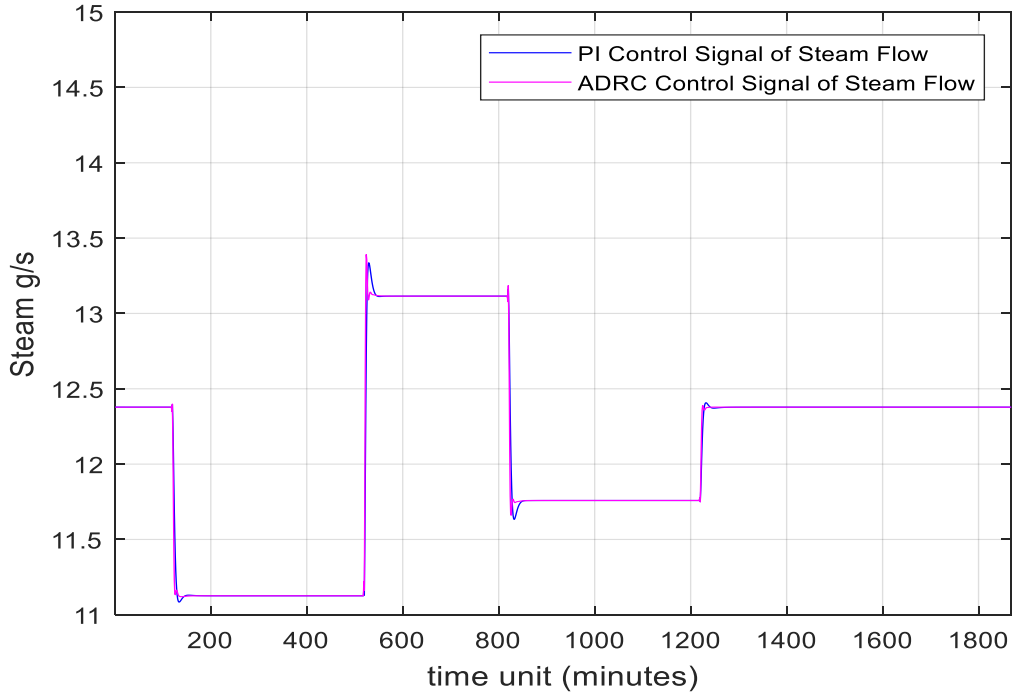

Figure 4.22: Control action of PI and ADRC schemes under the external disturbance test for Y_2

The results presented in Figures 4.19 and 4.21 show a similar efficient performance of the ADRC scheme, where both product compositions quickly return to the desired set point in a relatively smooth manner after the introduction of disturbance. This efficient performance of the ADRC scheme is due to the presence of the ESO component that estimates the external disturbance and reduces its effect. Furthermore, according to Figures 4.20 and 4.22, the control actions of the ADRC are found to be smooth and non-aggressive. On the other hand, the performance of the PI controller is found not to be as efficient as the ADRC in terms of the magnitude of deviation from the desired set-point, in addition to the speed of compensating for undesired disturbance where the speed of the PI controller in compensating the disturbance is not as fast as the ADRC scheme. Moreover, according to Figures 4.20 and 4.22, the control signals of the multi-loop PI controller under disturbance are non-smooth and aggressive. Table 4.8 shows the SSE values associated with both control schemes under both external disturbances. The SSE values associated with the PI controller are considerably greater than those of the ADRC.

Table 4.8: SSE values associated with external disturbance rejection performance

Control loop	**Feed flow rate disturbances**		**Feed concentration disturbances**	
	SSE of PI	**SSE of ADRC**	**SSE of PI**	**SSE of ADRC**
y_1	31.86	15.35	9.5677	6.7479
y_2	81.16	19.25	68.5131	13.5332

4.5 Conclusions

In this chapter, both the ADRC and multi-loop PI control are applied to a binary distillation column simulated by a detailed mechanistic model. The performance of both control strategies was investigated and demonstrated in terms of set-point tracking and external disturbance rejection capability. The simulation results indicate that the ADRC scheme has the ability to introduce fast and smooth dynamic performance under various amounts of disturbance. Compared with the PI scheme, ADRC has significantly better performance in terms of set-point tracking and disturbance rejection. In addition, the fact introduced in the existing literature that the ADRC scheme can overcome the total external undesired disturbance and perform well in tracking is confirmed where

it has capability to estimate the external disturbance and reject it prior to entering the dynamic system. However, efficient control performance from the ADRC in settling down to the setpoints quickly after the presence of disturbances and/or setpoint changes can also lead to energy saving as large variations in manipulated variables such as steam rate to reboiler and reflux rate, usually lead to more energy consumption. In addition, due to this promising result, it follows that the ADRC algorithm could be successfully applied in other complex chemical applications. In the next chapter, the ADRC scheme will be combined with inferential control, in order to estimate the product compositions and avoid the delay associated with current composition measurement tools.

Chapter 5 Inferential ADRC of a binary distillation column

5.1 Introduction

Inferential control of distillation columns using multiple tray temperature measurements as the secondery measured variables have been discussed and investigated in the existing literature (Mejdell and Skogestad 1991; Kaspar and Ray 1992; Zhang 2006; Jeffries et al. 2016). As mentioned in Chapter 2, soft sensors or inferential estimators are developed and used to overcome the issue of large measurement delay associated with composition analysers thus improving overall control performance because they are flexibile enough to be updated at any instant and have the capability to estimate the output quickley (Singh et al. 2016; Andrijić et al. 2017). However, in those studies the conventional PI controller is used and integrated with inferential estimators. It is expected that the overall control performance could be further enhanced and improved if an advanced control scheme is used in conjuction with soft sensors. This chapter proposes integrating inferential control into the ADRC scheme in order to control the binary distillation column.

The proposed inferential ADRC scheme for distillation column product composition control is presented in Figure 5.1, it can be seen from this figure that the top composition Y_1 and bottom composition Y_2 can be considered the primary controlled variables whereas the secondary measurements are tray temperatures x. In this control scheme, both top and bottom compositions will be estimated via multiple tray temperature measurements through soft sensors that are then used as feedback signals for the ADRC scheme in order to provide a continuous measurement for the product compositions. Designing the soft sensors can be done by using multivariate statistical techniques, which have became an indispensable part of current modern analytical chemistry.

Among these approaches are PCR and PLS. These approaches are similar in many ways and the theoretical relationship between both of them has been treated extensively in the literature (Kalivas 2001; Abdi 2003; Wentzell and Montoto 2003; Abdi 2010; Abdi 2010; Alibuhtto and Peiris 2015; Gagnon et al. 2017). The soft sensors in this research will be designed and implemented using PCR and PLS.

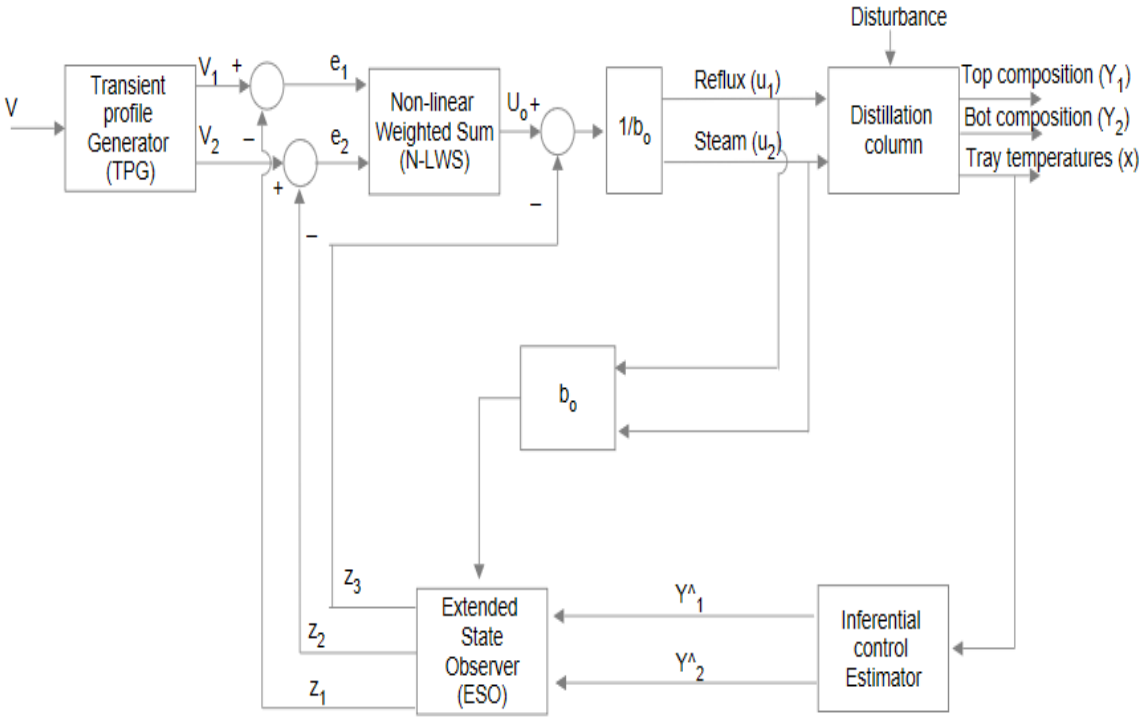

Figure 5.1: Inferential ADRC control scheme

This chapter is organised as follows: Section 5.2 provides a brief introduction on implementing the inferential estimator in the binary distillation column. Section 5.3 introduces the control structure with the PCR software sensor. In this section, the inferential models of $\hat{Y}_1$ and $\hat{Y}_2$ using static and dynamic PCR is introduced in order to integrate it within the ADRC schemes. Then, Section 5.4 details the control structure with the PLS software sensor. In this section, the inferential model of static and dynamic PLS is presented in order to integrate it with the ADRC schemes. Finally, conclusions are drawn in Section 5.5.

5.2 Software sensors based on the PCR model

The data generated from the mechanistic model of the binary column in the previous chapter is used here to build the estimation model. To generate data for building soft sensors several set-point changes are applied to the top and bottom product compositions. Moreover, several disturbances were applied to the simulated column. Figure 5.2 shows the top and bottom product compositions while the corresponding secondary measurements of tray temperatures are shown in Figure 5.3. Simulated measurement noises with normal distribution are added to both product

compositions. The mean and standard deviation of the noise are specified at 0 and 0.2% respectively.

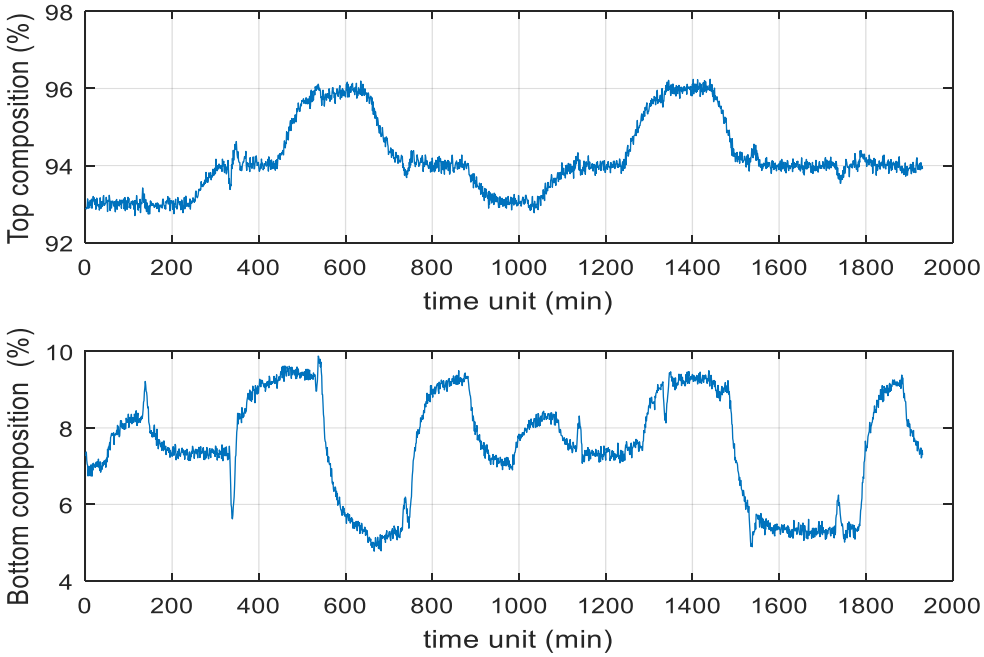

Figure 5.2: Top and bottom product compositions (primary variables)

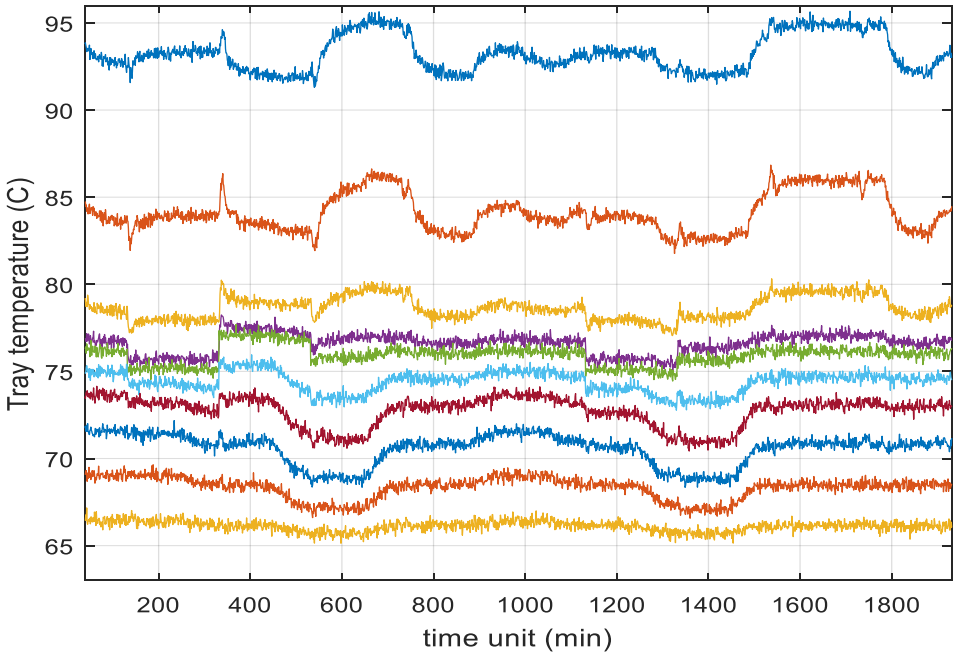

Figure 5.3: Tray temperatures (secondary variables)

It can be observed from Figure 5.3 that a strong correlation exists among tray temperature measurements. Since the tray temperature measurements are highly correlated, the multiple linear regression (MLR) is not efficient to build a reliable estimation model. As a result, PCR and PLS techniques can be used to build inferential estimation models (Weber and Brosilow 1972; Zhang 2006).

The data are scaled to zero mean and unit variance before building the model in order eliminate the influence of different magnitudes of model input and output variables. The complete set of tray temperatures and product composition data are divided into two parts: the training data set (samples 1 to 1000) and the testing data set (samples 1001 to 1982). PCR models with various numbers of principal components are developed on the training data and tested on the testing data which will be used to test the model performance (Hussain et al. 2017). Utilising the testing data to test the estimation model is a good way to determine whether the model can identify the right relationship in the data (Bolf et al. 2008). PCR models are created from principal components that are linear combinations of the original model input variables. It is essential to select the number of principal components appropriately. In this research, the cross-validation procedure is used as it is a statistically more suitable method to specify the number of PCs and avoid overfitting. This validation process can be executed by selecting the minimum value of SSE.

5.2.1 Static PCR models

The inferential model estimates the product compositions at time *t* with the tray temperatures at time *t*. Since the case study used in this research has 10 tray temperatures, the estimation model can be presented in the following form:

$$y(t) = \theta_1 T_1(t) + \theta_2 T_2(t) + \cdots + \theta_{10} T_{10}(t) \tag{5.1}$$

Where *y* denotes the product compositions, T_1 to T_{10} represent the tray temperatures from trays 1–10 respectively, θ_1 to θ_{10} correspond to model parameters, and *t* represents the discrete time. The data are scaled to zero mean and unit variance before model building. Figure 5.4 and Table 5.1 present SSE of different PCR models with different numbers of principal components on the training and testing data. The PCR model with the lowest error on the testing data is considered to have the most suitable number of principal components.

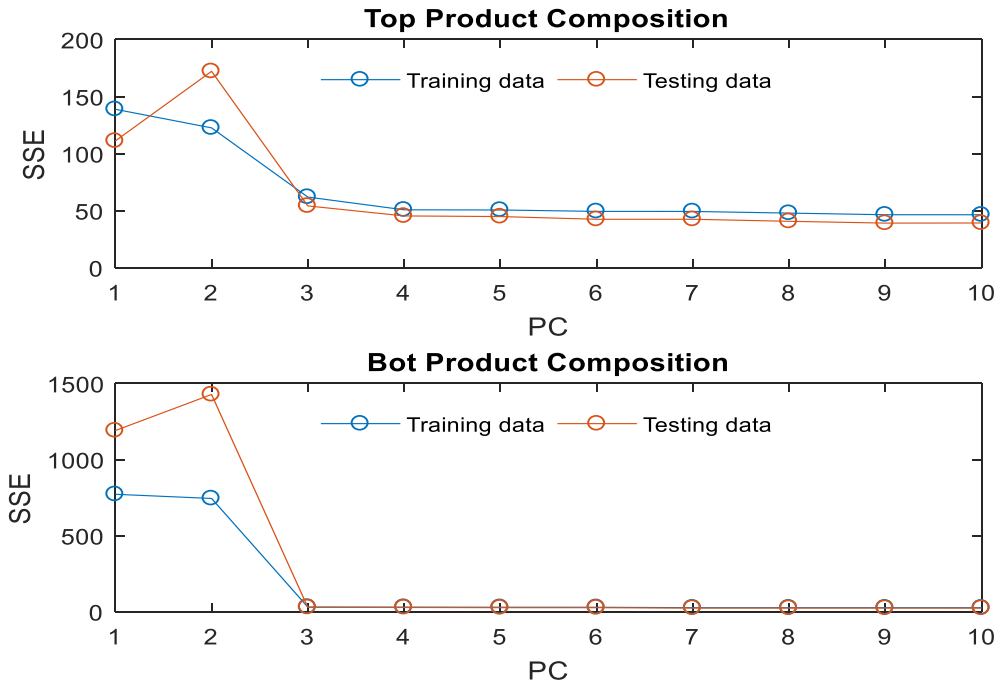

Figure 5.4: SSE of static PCR prediction of binary distillation

Table 5.1: SSE on training and testing data for static PCR models with different numbers of principal components

	Top composition		***Bottom composition***	
No. of PCs	***Training data***	***Testing data***	***Training data***	***Testing data***
1	138.826	111.052	771.4089	1190.25
2	122.526	172.096	744.052	1427.52
3	61.8852	54.1165	30.3316	28.2952
4	50.7095	45.3246	29.5166	27.2593
5	50.5490	44.7872	28.8777	26.0764
6	49.3117	42.3979	28.6747	25.8648
7	49.2793	42.4041	25.8739	23.3020
8	47.8213	40.6261	25.8065	23.2054

9	46.3866	39.0442	25.8038	23.1709
10	46.3540	39.1547	25.7536	23.0539

It can be noted from Table 5.1 that the PCR model with nine principal components provides the best performance for the top composition on the testing data and the one with ten principal components offers the best performance for the bottom compositions on the testing data. Therefore, nine principal components are used in the top composition model and ten principal components are used in the bottom composition model. The developed PCR models for the top and bottom product compositions in terms of PC's are as follows:

$$y_D = -0.47221\,PC_1 + 0.074952\,PC_2 - 0.18727\,PC_3 + 0.161918\,PC_4 + 0.035033\,PC_5 - 0.106035\,PC_6 - 0.019274\,PC_7 + 0.133379\,PC_8 + 0.156755\,PC_9 \quad (5.2)$$

$$y_B = 0.174896\,PC_1 - 0.097101\,PC_2 - 0.64249\,PC_3 + 0.043726\,PC_4 - 0.06989\,PC_5 + 0.042949\,PC_6 + 0.179119\,PC_7 - 0.0286766\,PC_8 - 0.006786\,PC_9 - 0.036186\,PC_{10} \quad (5.3)$$

The developed PCR models for the top and bottom product compositions can be converted in terms of tray temperatures as model inputs as follows:

$$y_D = 93 + 0.04500\Delta T_1 - 0.03572\Delta T_2 - 0.130424\Delta T_3 + 0.189102\Delta T_4 - 0.034529\Delta T_5 + 0.08806\Delta T_6 - 0.31151\Delta T_7 - 0.32551\Delta T_8 - 0.0666\Delta T_9 - 0.67369\Delta T_{10} \quad (5.4)$$

$$y_B = 7 - 0.39444\Delta T_1 + 0.071845\Delta T_2 - 0.22059\Delta T_3 + 1.356745\Delta T_4 + 0.21753\Delta T_5 + 0.88404\Delta T_6 - 0.98501\Delta T_7 - 0.87577\Delta T_8 - 1.75977\Delta T_9 - 0.71489\Delta T_{10} \quad (5.5)$$

Where y_D and y_B represent the top and bottom compositions (wt%) respectively, and ΔT is the deviation of a tray temperature from its nominal mean value.

5.3.2 Dynamic PCR models

The inferential estimation accuracy might be further enhanced and improved if dynamic PCR models are developed. In this chapter, dynamic PCR models with orders ranging from 1–7 were developed. The first order dynamic PCR models can be represented in the equation below:

$$y(t) = \theta_{1.1}T_1(t) + \theta_{1.2}T_2(t-1) + \theta_{2.1}T_2(t) + \theta_{2.2}T_2(t-1) \ldots + \theta_{10.1}T_{10}(t) + \theta_{10.2}T_{10}(t-1) \quad (5.6)$$

Data partition and data scaling are the same as in developing static PCR models. The suitable dynamic model was specified by the least SSE on the testing data. Table 5.2 presents the number of principal components and the corresponding SSE values on the testing data of these dynamic PCR models.

Table 5.2: Number of principal components and SSE on testing data of different dynamic PCR models

Model orders	**Product composition**	**SSE**	**No. of principal components**
Static PCR model	Top composition	40.5665	9
	Bot composition	46.5507	10
1st dynamic PCR model	Top composition	28.9446	19
	Bot composition	30.1110	19
2nd dynamic PCR model	Top composition	25.4500	24
	Bot composition	26.6627	28
3rd dynamic PCR model	Top composition	23.0394	30
	Bot composition	24.1184	28
4th dynamic PCR model	Top composition	22.5688	36
	Bot composition	22.4950	34
5th dynamic PCR model	Top composition	21.7144	49
	Bot composition	20.5285	39
6th dynamic PCR model	Top composition	21.4245	49
	Bot composition	19.6649	47

The table clearly shows that the dynamic PCR models significantly enhance the estimation accuracy compared to the static PCR model. The differences in SSE values between these models are not very significant. Hence, the 6^{th} order dynamic PCR model is used and integrated into the ADRC scheme to estimate the top and bottom compositions. Figures 5.5 and 5.6 and Figures 5.7 and 5.8 present, respectively, predictions from the static inferential PCR model and the 6^{th} dynamic inferential model. In these figures, the blue line represents the actual product composition response while the red solid line represents the corresponding estimation response.

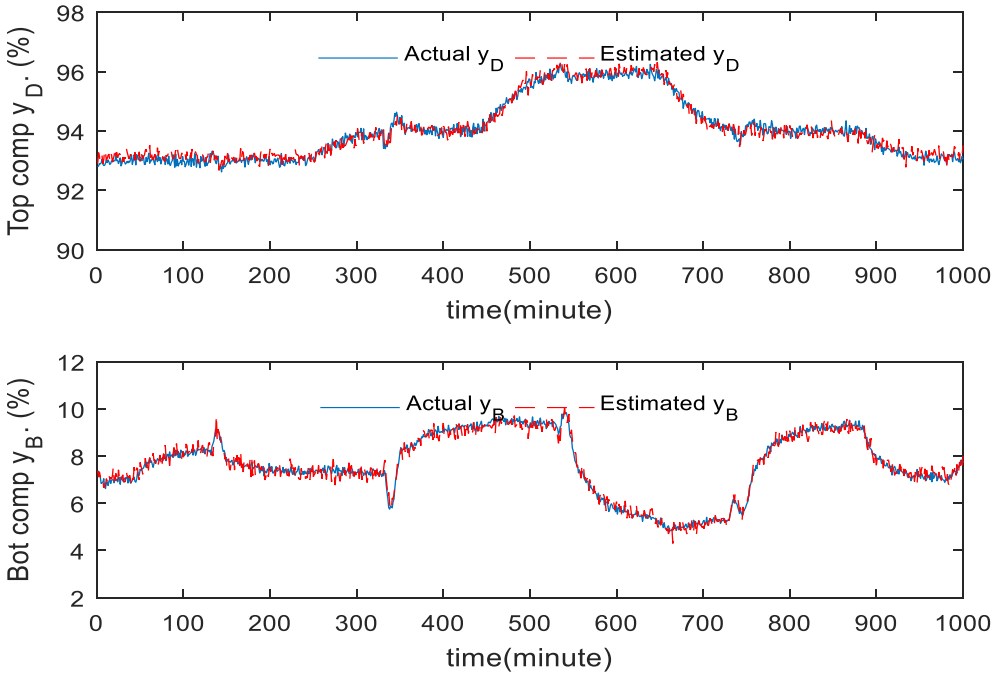

Figure 5.5: Model estimation of static PCR model (training data)

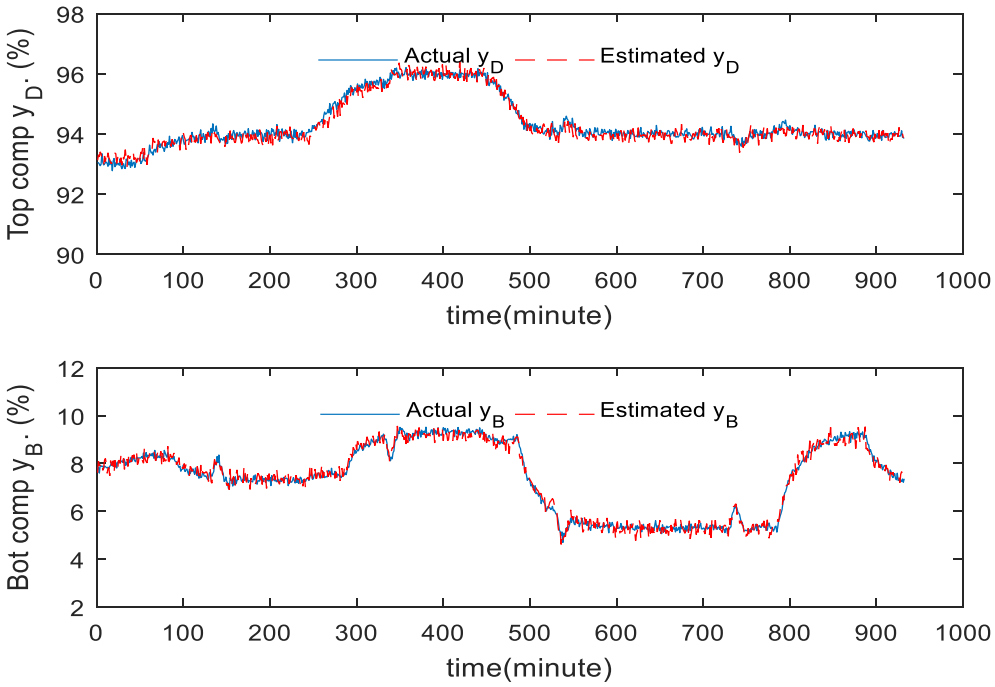

Figure 5.6: Model estimation of static PCR model (testing data)

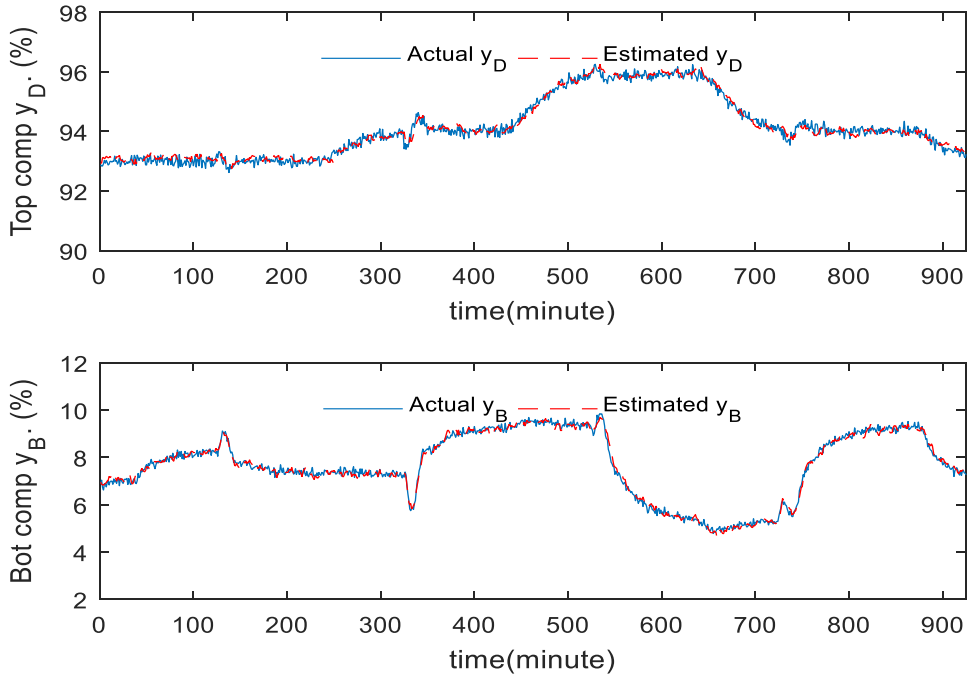

Figure 5.7: Model estimation of 6th order dynamic PCR model (training data)

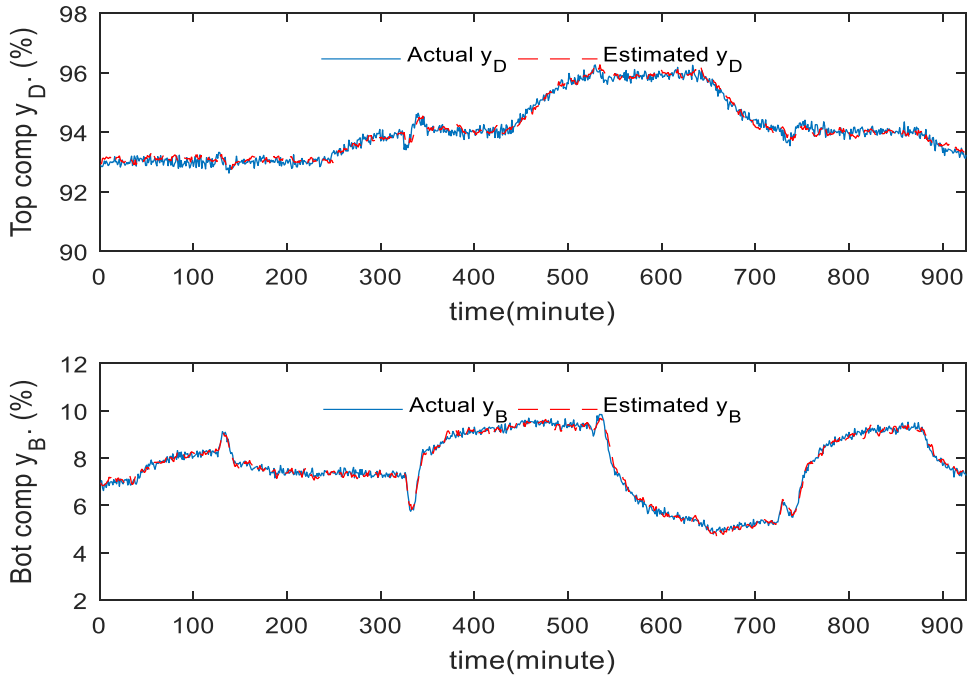

Figure 5.8: Model estimation of 6th order dynamic PCR model (testing data)

Figures 5.9 and 5.10 present estimation errors for both static and 6th dynamic PCR models. It can be noticed from this figure—and as expected—the 6th order dynamic PCR model shows better estimation performance than the static model.

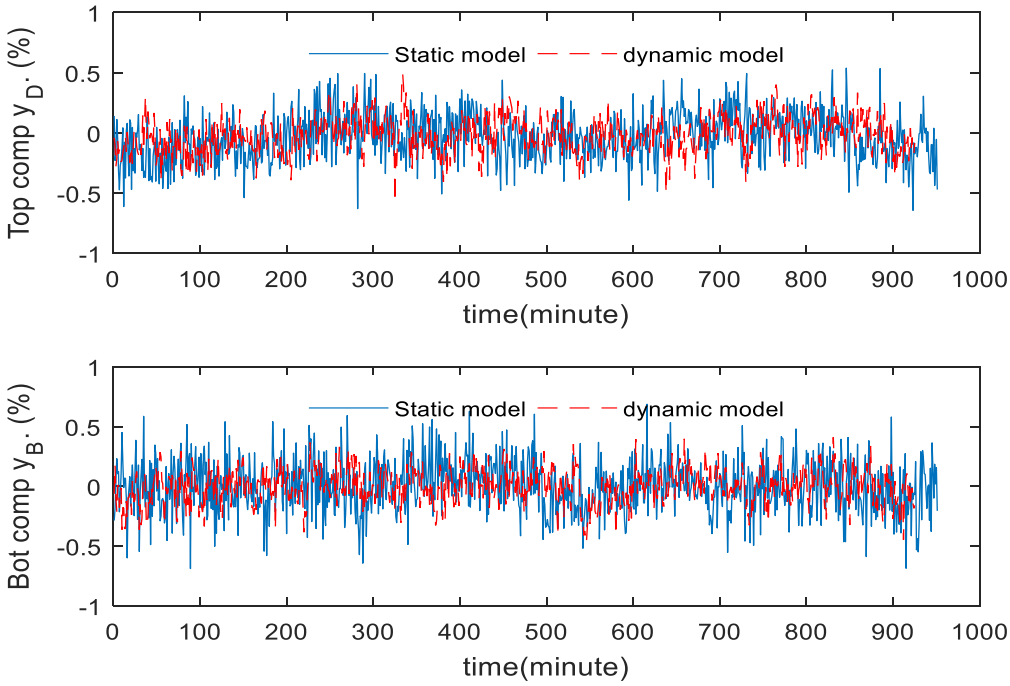

Figure 5.9: PCR Model estimation errors (training data)

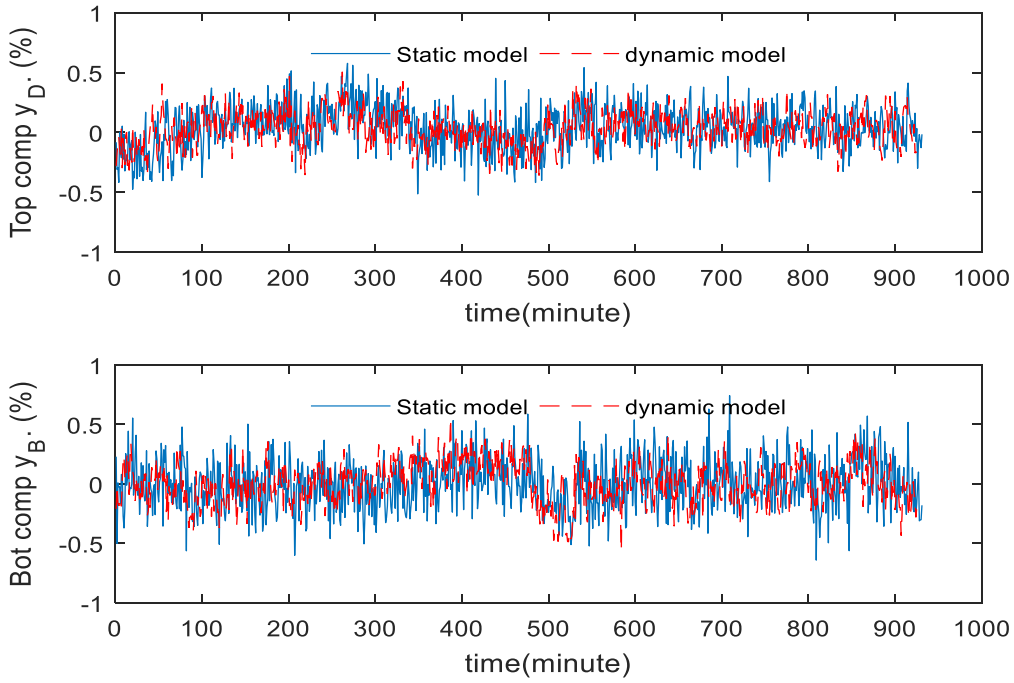

Figure 5.10: PCR Model estimation errors (testing data)

5.3 Inferential ADRC scheme based on PCR models

In the product composition control considered here, the manipulated variables for top and bottom compositions are reflux flow rate *L* and steam flow rate *V* to the reboiler respectively. The secondary measurements (tray temperatures) are fed to the PCR software sensors to estimate the top and bottom product compositions. The estimations are then used as a feedback signal to the ADRC scheme in order to provide an online measurement for the product compositions as shown in Figure 5.11. The availability of the continuous measurements of both compositions will allow the ADRC scheme to operate efficiently. The performance of both the ADRC and inferential ADRC control was investigated through simulation.

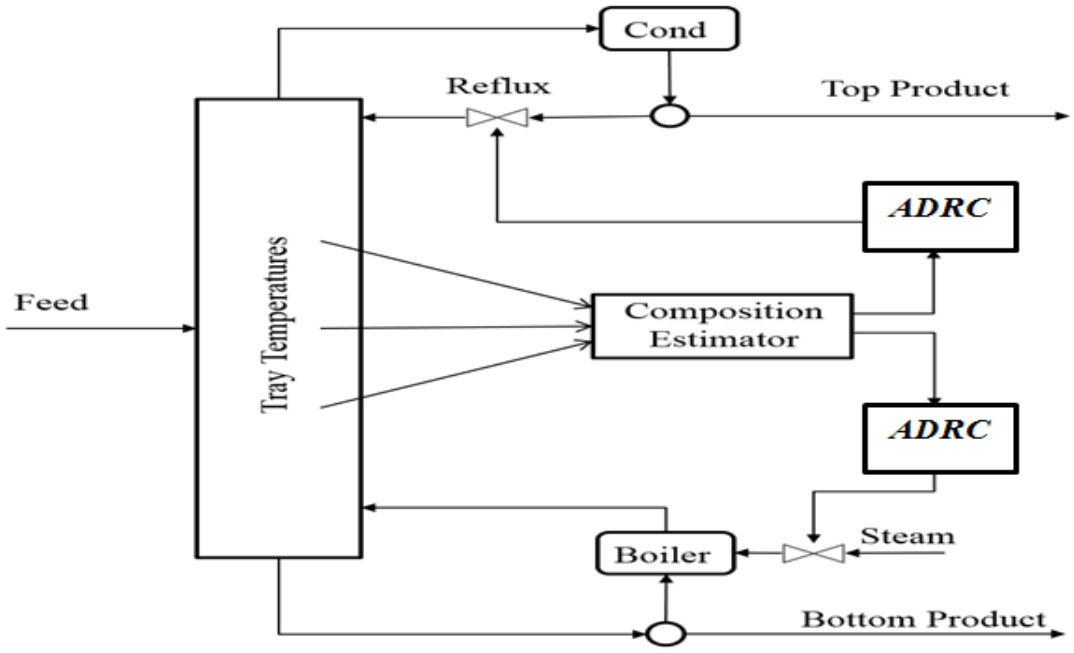

Figure 5.11: Inferential ADRC control of product compositions

The inferential ADRC control strategy is compared with single tray temperature control and composition analyser based control. After analysing the data used for building the inferential models, it was found that the temperature of the eighth tray (from the column bottom) has the largest correlation coefficient with the top product composition and the temperature of the second tray has the largest correlation coefficient with the bottom product composition. Hence, temperatures of the second and the eighth trays were controlled to indirectly control the bottom and top product compositions respectively. Temperatures at the second and the eighth trays correspond to the bottom composition of 7% and the top composition of 93% are 85.9°C and 70.5°C respectively. Hence, the set-points for the second and the eighth tray temperatures were set at 85.9° C and 70.5° C respectively. Temperature set-points corresponding to other product compositions were identified from simulated process operation data. A 10 min delay was added to both top and bottom compositions as the composition analyser typically possesses such a delay. Therefore, a uniform 10 min delay was added to all transfer functions introduced in Chapter 4 to simulate the delay of the composition analyser.

Figure 5.12 shows the control performance of tray temperature control and composition analyser based control. The solid, dash-dotted, and dashed lines represent the response of the single

tray temperature control, composition analyser based control, and the desired set-point signal. It can be seen from this figure that the composition analyser based control has a sluggish response.

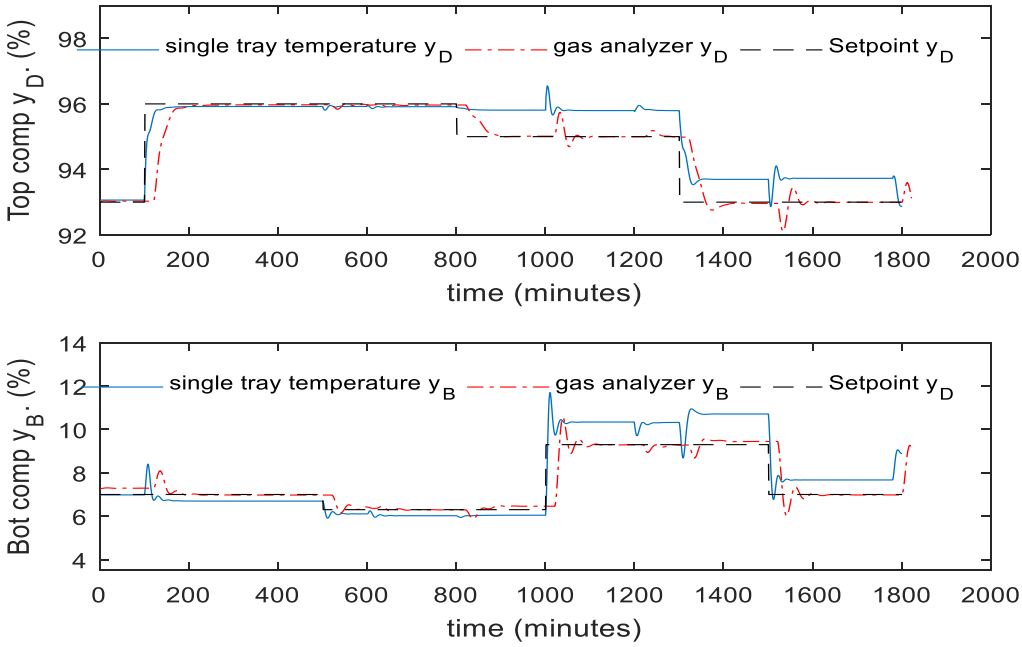

Figure 5.12: Control performance of tray temperature control and composition analyser based control

Figure 5.13 shows the set-point tracking and disturbance rejection performance of inferential ADRC with the static PCR model across a broad range of set-point changes, feed flow rate and feed composition disturbance. The set-point signal was smoothed by TPG to avoid undesired overshoot. It can be seen that the top composition is controlled quite well with small control offsets, but large control errors exist for the bottom product composition. These control errors are due to the estimation errors of the PCR models, which can get worse when operating conditions change such as during set-point change and or disturbance changes. In addition, more deviation from the introduced estimated signal will lead to more un-accurate actual output composition. Figure 5.14 shows the set-point tracking and disturbance rejection performance of inferential ADRC with the sixth order dynamic PCR model for the same set-point changes, feed flow rate and feed composition disturbance. It can be seen that the control performance improved under the dynamic PCR model. Furthermore, the control offsets in the dynamic PCR are smaller than the control offset in the static one. In addition, more accurate estimation of product compositions leads to better control performance.

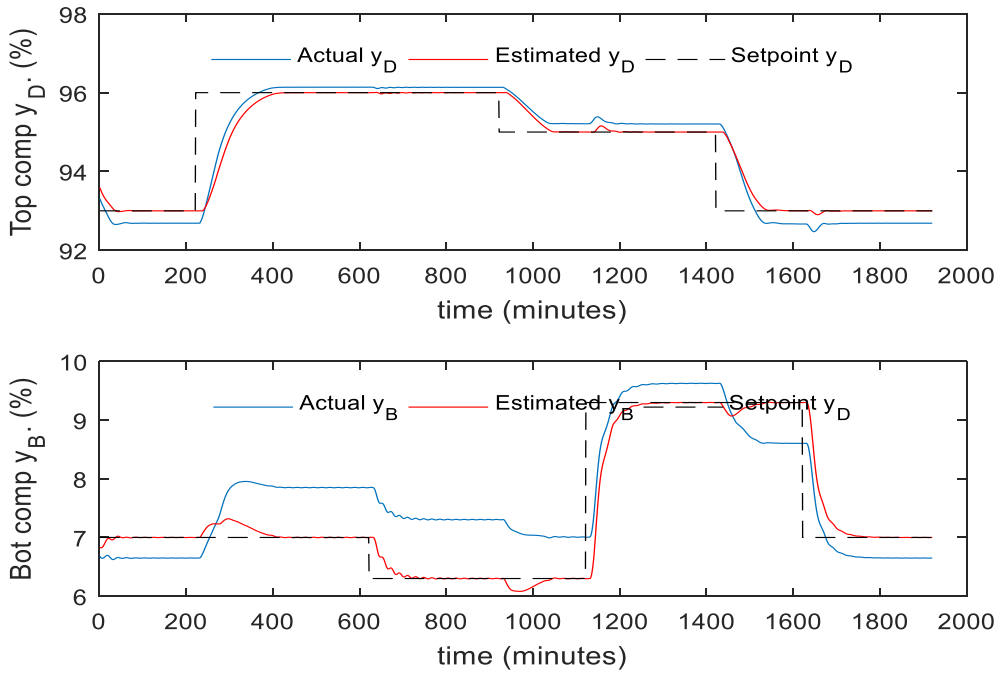

Figure 5.13: Responses of actual and estimated product compositions under inferential ADRC with static PCR model (without mean updating)

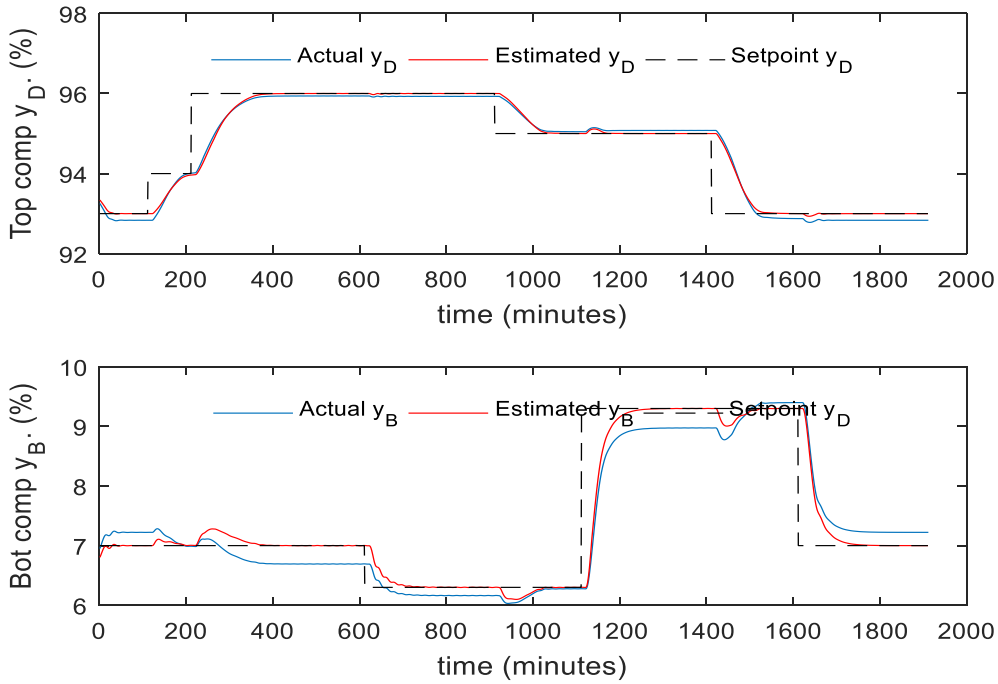

Figure 5.14: Responses of actual and estimated product compositions under inferential ADRC with sixth order dynamic PCR models (without mean updating)

To overcome the control offset issue due to the variation in process operating conditions, the intermittent process variable mean updating strategy proposed by Zhang (2006) is used here. When a new steady state is reached, the static values of product compositions and tray temperatures are used to replace the mean values of these variables in the PCR models. It can be seen here that only intermittent product composition measurements are required. Figures 5.15 and 5.16 present the control performance with the mean updating technique. It can be observed from these figures that mean updating is an efficient technique that can significantly reduce static control offsets. Moreover, the SSE of control errors has been reduced dramatically after using the mean updating technique as shown in Table 5.3.

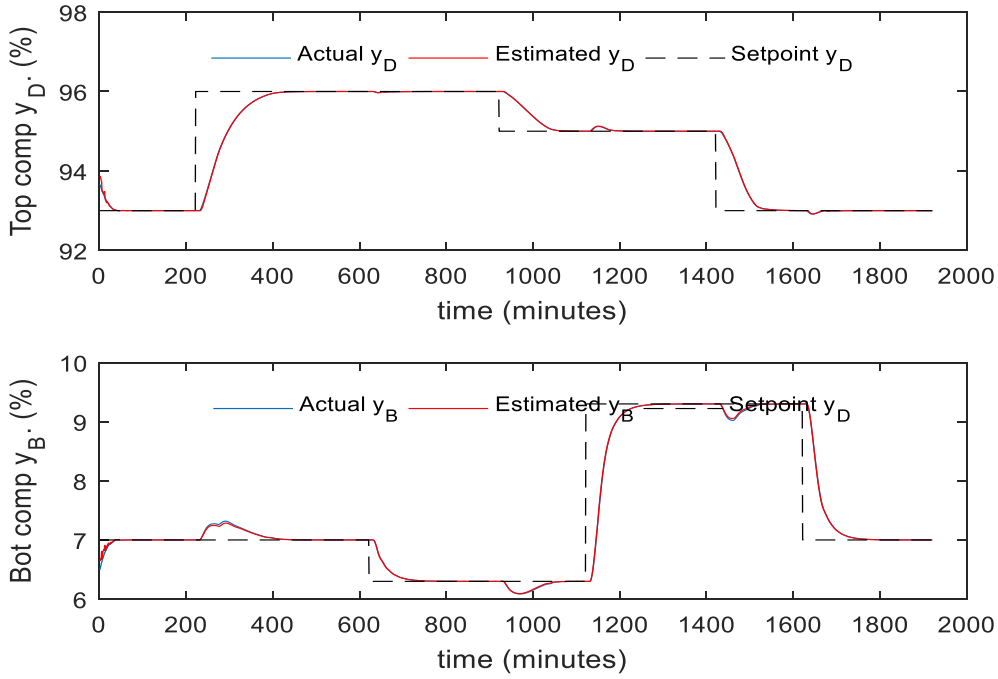

Figure 5.15: Responses of actual and estimated product compositions of static inferential ADRC (with mean updating)

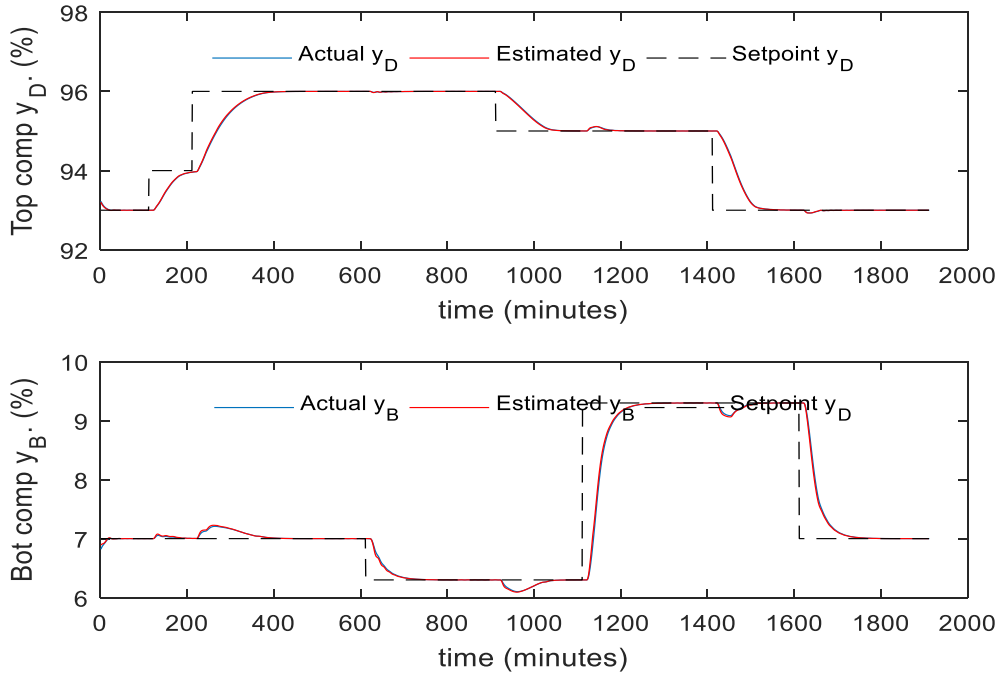

Figure 5.16: Responses of actual and estimated product compositions of inferential ADRC using the 6th order dynamic PCR model (with mean updating)

Table 5.3: SSE of different control schemes

Control schemes		**Top Comp**	**Bottom Comp**
Inferential ADRC with static PCR model	Without mean updating	100.8368	828.3034
	With mean updating	0.0642	0.1516
Inferential ADRC with sixth order dynamic PCR model	Without mean updating	18.6386	92.7922
	With mean updating	0.0436	0.0295

It can be seen from the above figures that the resulting control offsets and steady state model estimation bias have been eliminated successfully through the mean updating technique. Moreover, it can be noticed from Table 5.3 that the dynamic PCR model has much smaller

estimation offsets than the static PCR model when the operating condition is changed. This leads to the conclusion that the dynamic PCR model is more robust than the static PCR model for processing operating condition variations. As a result, the dynamic inferential ADRC scheme provides better control performance than the static inferential ADRC.

5.4 Inferential ADRC scheme based on PLS models

Historically, PCR predates the PLS technique, with the latter introduced in the chemical literature around 1983 (Wold et al. 2001; Wentzell and Montoto 2003). Since its introduction however, the PLS approach appears to have become the technique of choice among chemometricians. The reasons for this are due to a number of advantages (Wentzell and Montoto 2003):

i. PLS can estimate better because the correlations with the *y* variable are required in specifying the latent variables.
ii. PLS requires fewer latent variables than the PCR approach.

This section presents the implementation of static and dynamic soft sensors for predicting the product compositions using the PLS approach.

5.4.1 Static PLS model

As mentioned previously, PLS techniques can be used to build an estimation model with correlated data. Similar to the PCR approach, data partition and data scaling are the same as in developing static PCR models. In this research, the PLS model was designed and developed by selecting the suitable number of latent variables (LVs) based on the minimum SSE on the testing data set as shown in Figure 5.17.

.

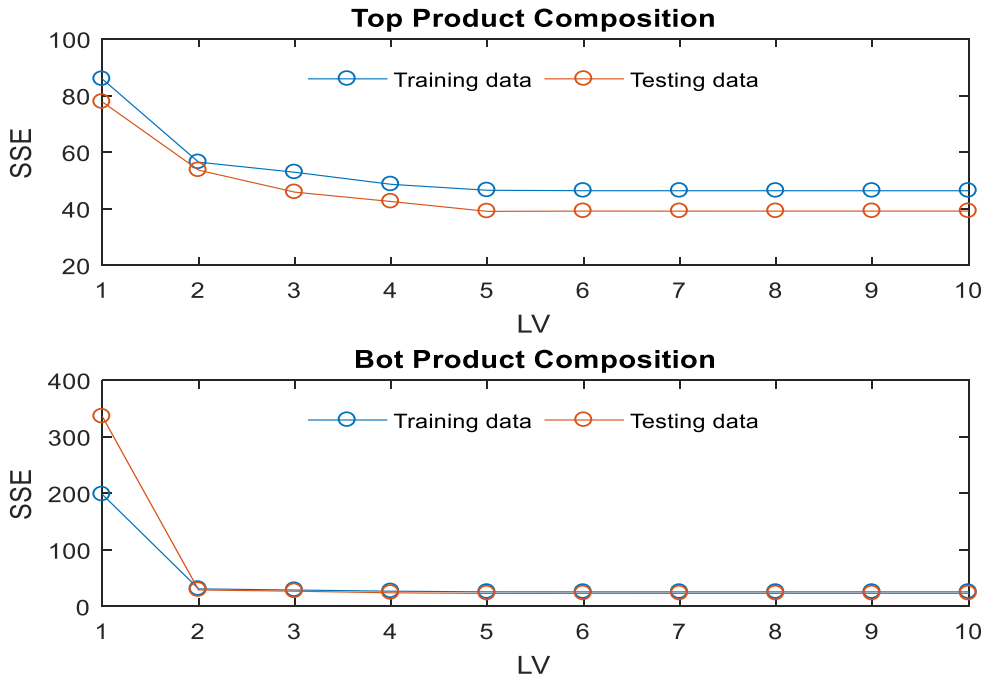

Figure 5.17: SSE of static PLS prediction

Table 5.4 presents the SSE of different PLS models on the training and testing data. The PLS model with the lowest SSE on the testing data is considered to have a suitable number of LVs.

Table 5.4: SSE on training and testing data for static PLS models with different numbers of LVs

	Top composition		***Bottom composition***	
No. of LVs	***Training data***	***Testing data***	***Training data***	***Testing data***
1	85.8460	77.7726	198.0767	335.817
2	56.4557	53.6429	31.0883	29.1430
3	52.8871	45.8497	29.0368	26.9307
4	48.6229	42.5458	26.9729	24.1009
5	46.5161	39.0638	25.8117	22.9674
6	46.3635	39.1601	25.7595	23.0993

7	46.3548	39.1348	25.7540	23.0563
8	46.3541	39.1468	25.7536	23.0527
9	46.3540	39.1548	25.7536	23.0538
10	46.3540	39.1547	25.7536	23.0539

It can be seen from Table 5.4 that the PLS model with five latent variables provides the best performance for the top composition on the testing data, and five latent variables offer the best performance for the bottom compositions on the testing data. Therefore, five latent variables are used in both the top and bottom composition models. This proves the fact that PLS requires fewer latent variables than PCR. The developed PLS models for the top and bottom product compositions in terms of LVs as model inputs are as follows:

$$y_D = 0.3896\, LV_1 + 0.8230\, LV_2 + 0.5142\, LV_3 + 0.9145\, LV_4 + 0.2214\, LV_5 \quad (5.7)$$

$$y_B = 0.0311\, LV_1 + 0.9121\, LV_2 + 0.4850\, LV_3 + 0.6776\, LV_4 + 0.0603\, LV_5 \quad (5.8)$$

The developed PLS models for both top and bottom product compositions can be re-expressed using the tray temperatures as model inputs as follows:

$$y_D = 93 - 0.02546\Delta T_1 + 0.02926\Delta T_2 + 0.007075\Delta T_3 + 0.44464\Delta T_4 - 0.33676\Delta T_5 + 0.04521\Delta T_6 + 0.15891\Delta T_7 - 1.25635\Delta T_8 - 0.18726\Delta T_9 - 0.08926\Delta T_{10} \quad (5.9)$$

$$y_B = 7 - 0.18163\Delta T_1 - 0.048632\Delta T_2 + 0.08601\Delta T_3 + 0.00591\Delta T_4 - 0.07168\Delta T_5 + 0.05474\Delta T_6 - 0.018416\Delta T_7 - 0.04858\Delta T_8 - 0.04047\Delta T_9 - 0.060867\Delta T_{10} \quad (5.10)$$

Where y_D and y_B represent the top and bottom compositions (wt%) respectively, and ΔT is the deviation of a tray temperature from its nominal mean value.

5.4.2 Dynamic PLS models

Similar to the dynamic PCR model, it is expected that the inferential estimation accuracy could be further enhanced if dynamic PLS models are developed. In this research, dynamic PLS models with orders ranging from 1– 6 were designed.

Data partition and data scaling are the same as when developing static PLS models. A suitable number of LVs was once again determined by the least SSE on the testing data. Table 5.5 presents the number of latent variables and the corresponding SSE values on the testing data of these dynamic PLS models.

Table 5.5 Number of latent variables and SSE on testing data of different dynamic PLS models

Model orders	**Product compositions**	**SSE**	**No. of LVs**
Static PLS model	Top composition	40.5380	5
	Bot composition	49.8400	5
1st dynamic PLS model	Top composition	28.8752	8
	Bot composition	30.1748	5
2nd dynamic PLS model	Top composition	25.3334	5
	Bot composition	26.9182	8
3rd dynamic PLS model	Top composition	22.9115	5
	Bot composition	24.3736	9
4th dynamic PLS model	Top composition	22.2474	5
	Bot composition	23.1856	8
5th dynamic PLS model	Top composition	21.6017	5
	Bot composition	22.4371	9
6th dynamic PLS model	Top composition	21.2488	6
	Bot composition	19.7109	9

The data in the table shows that the dynamic PLS models significantly enhance the estimation accuracy compared to the static PLS model especially at the sixth order model. Thus, the sixth order dynamic PLS model was selected and used due to its lowest SSE value. This sixth

order dynamic PLS was integrated with the ADRC scheme to estimate the primary variables of top and bottom compositions.

Figures 5.18 and 5.19 and Figures 5.20 and 5.21 present, respectively, predictions from the static inferential PLS model and the sixth order dynamic inferential model. In these figures, the blue line represents the actual product compositions while the red solid line represents the corresponding estimations.

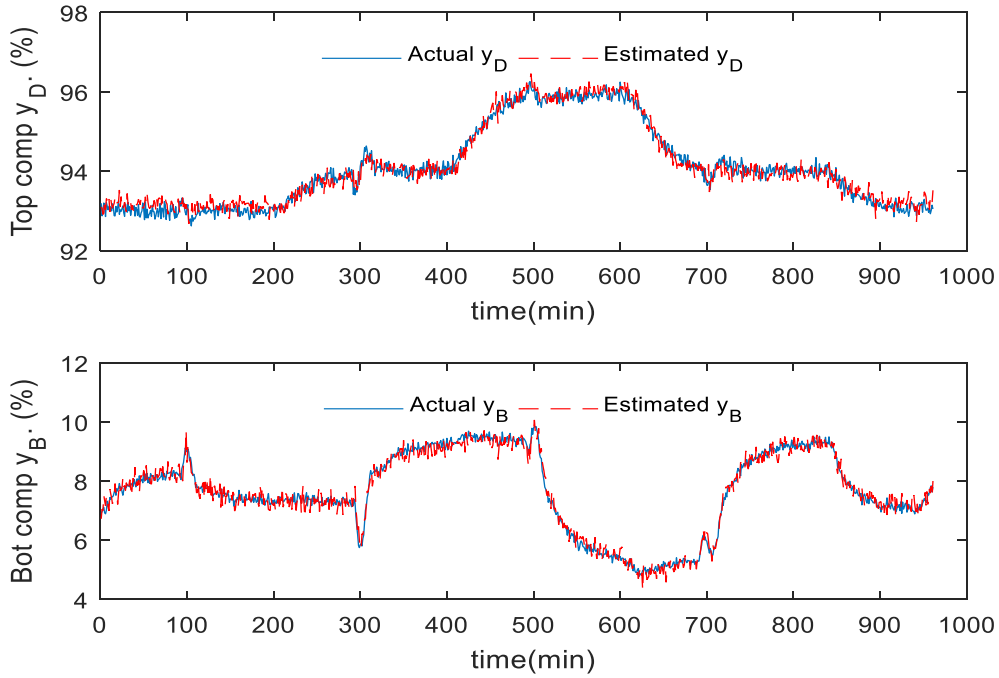

Figure 5.18: Model estimation of static PLS model (training data)

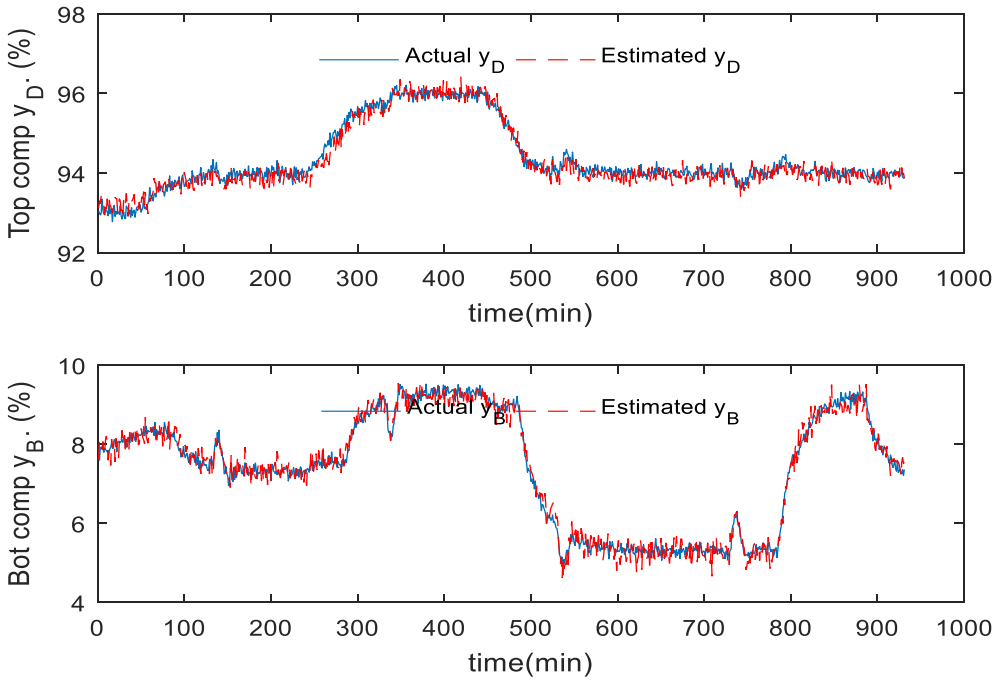

Figure 5.19: Model estimation of static PLS model (testing data)

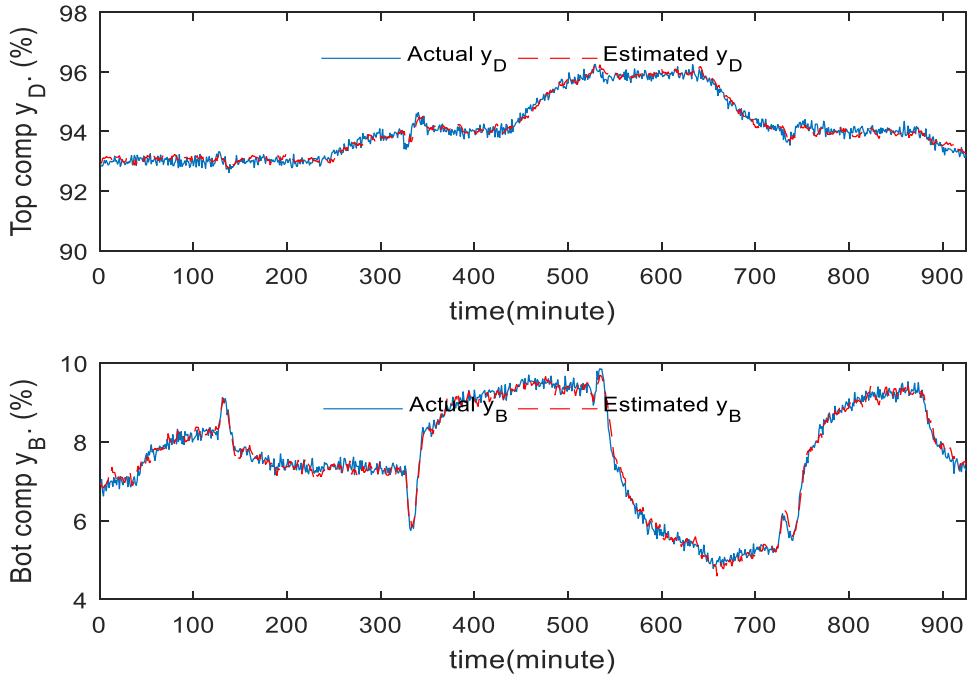

Figure 5.20: Model estimation of 6th order dynamic PLS model (training data)

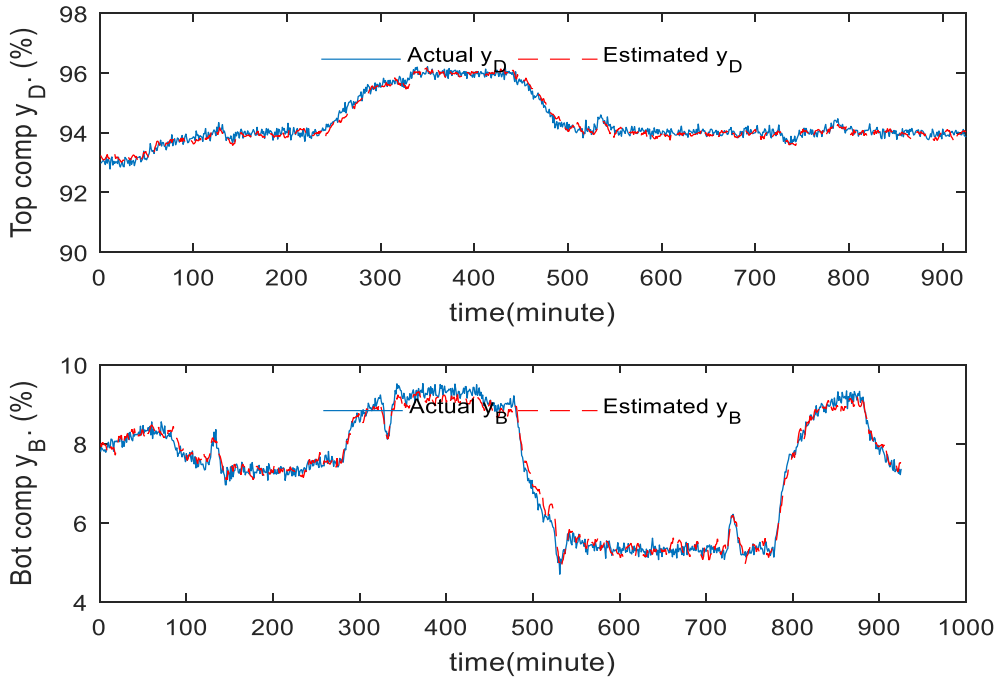

Figure 5.21: Model estimation of 6th order dynamic PLS model (testing data)

Figure 5.22 and 5.23 presents estimation errors for both the static and 6^{th} dynamic PLS model. It can be noticed from this figure and as expected, the 6^{th} order dynamic PLS model shows better estimated performance than the static model.

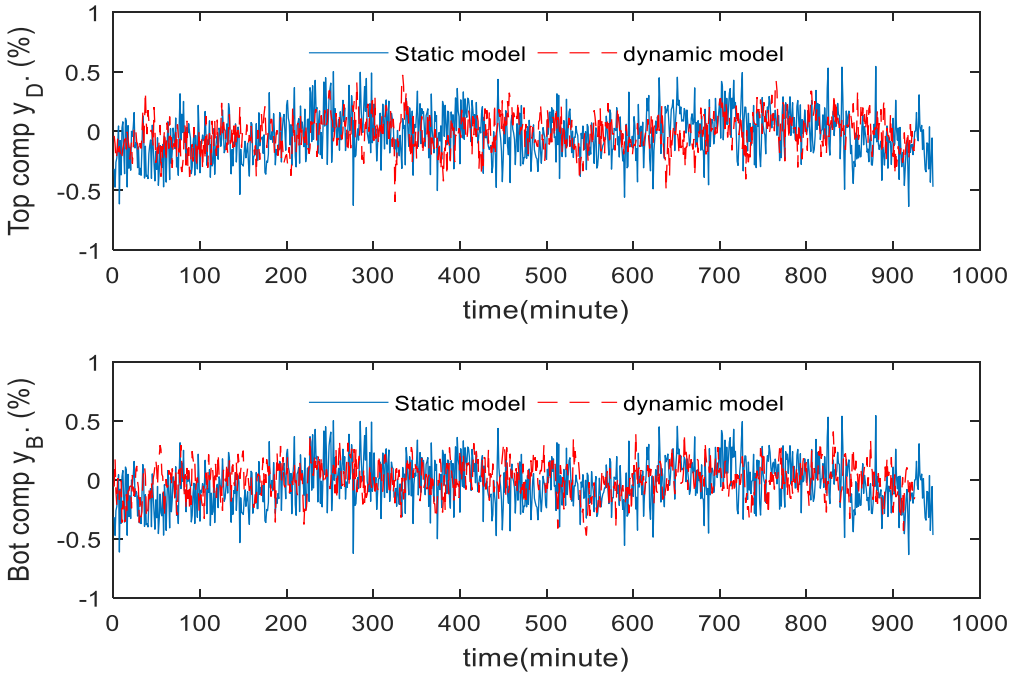

Figure 5.22: PLS Model estimation errors (training data)

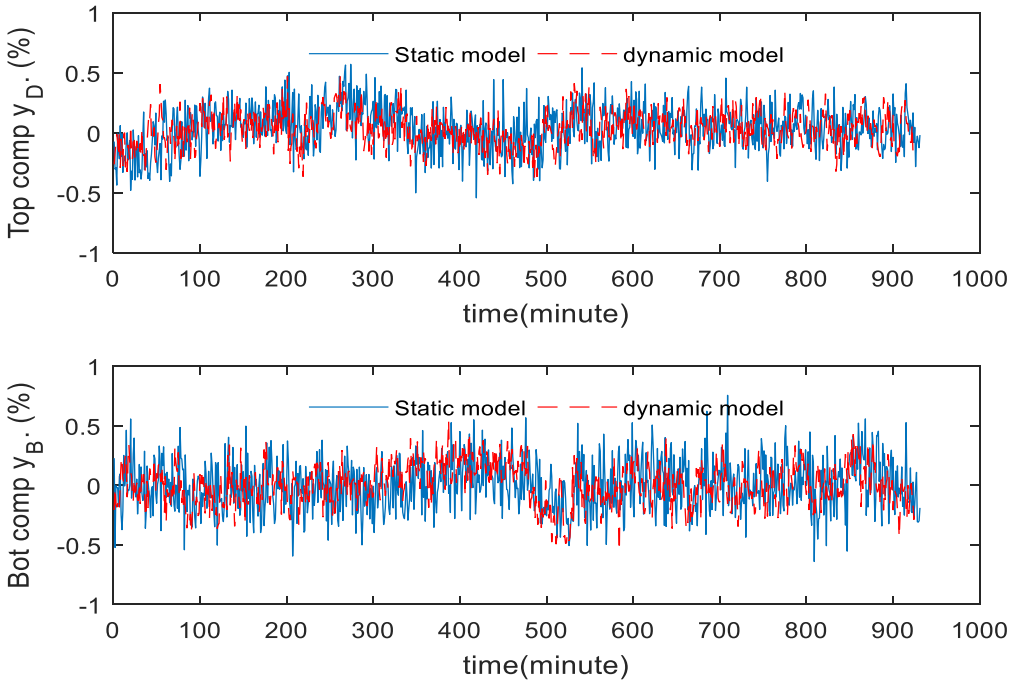

Figure 5.23: PLS Model estimation errors (testing data)

5.5 Inferential ADRC scheme based on PLS models

Similar to the inferential ADRC scheme based on PCR models, the manipulated variables for top and bottom compositions are: reflux flow rate L and steam flow rate V to the reboiler respectively. The only difference is that the secondary measurements and tray temperatures here are passed to the PLS inferential estimator instead of the PCR software sensors to estimate the product compositions. The predicted product compositions are then used as feedback signals to the ADRC scheme in order to provide an online measurement for both product compositions as shown in Figure 5.11. The performance of the inferential ADRC will be investigated through simulation. The simulated distillation column is subjected to external disturbance introduced by the feed flow rate and feed composition.

Figure 5.23 shows the set-point tracking and disturbance rejection performance of the inferential ADRC with static PLS model across a wide range of set-point changes, feed flow rates and feed composition disturbance. It can be seen that both product compositions have large control offsets due to the estimation errors of the static PLS model that can get worse when operating conditions change such as set-point changes and or disturbance changes. In addition, large estimation offsets will lead to large control offsets. Figure 5.24 shows the set-point tracking and disturbance rejection performance of inferential ADRC with the 6^{th} order dynamic PLS model for the same set-point changes, feed flow rate and feed composition disturbances. It can be seen that the control performance improved under the dynamic PLS model with small control offsets at both actual product compositions. In addition, accurate inferential estimations will lead to better control performance.

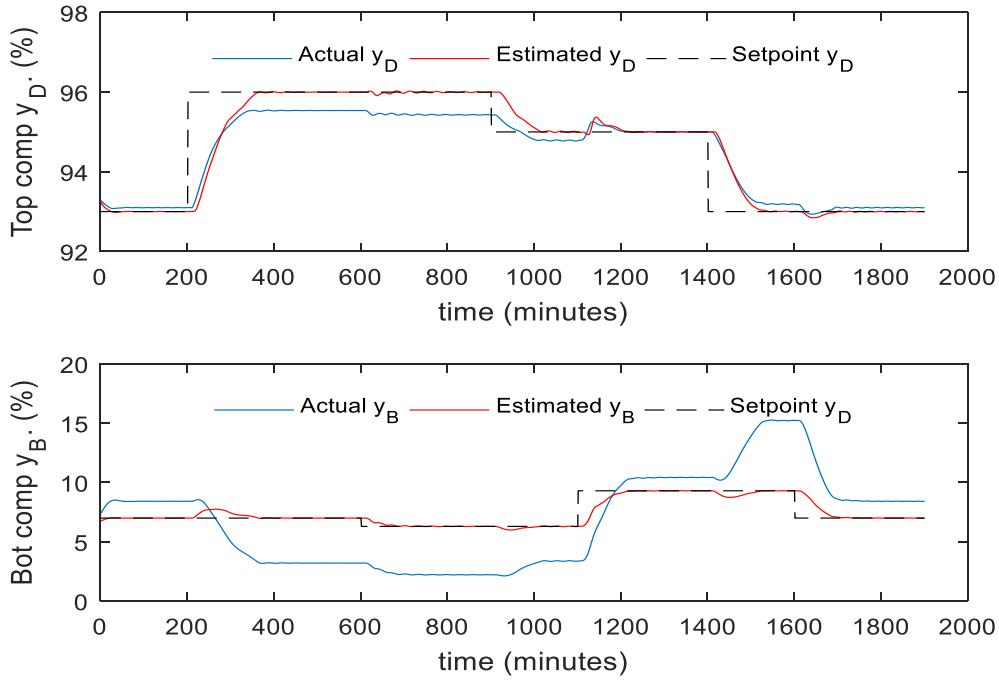

Figure. 5.24: Responses of actual and estimated product compositions under the inferential ADRC with static PLS model (without mean updating)

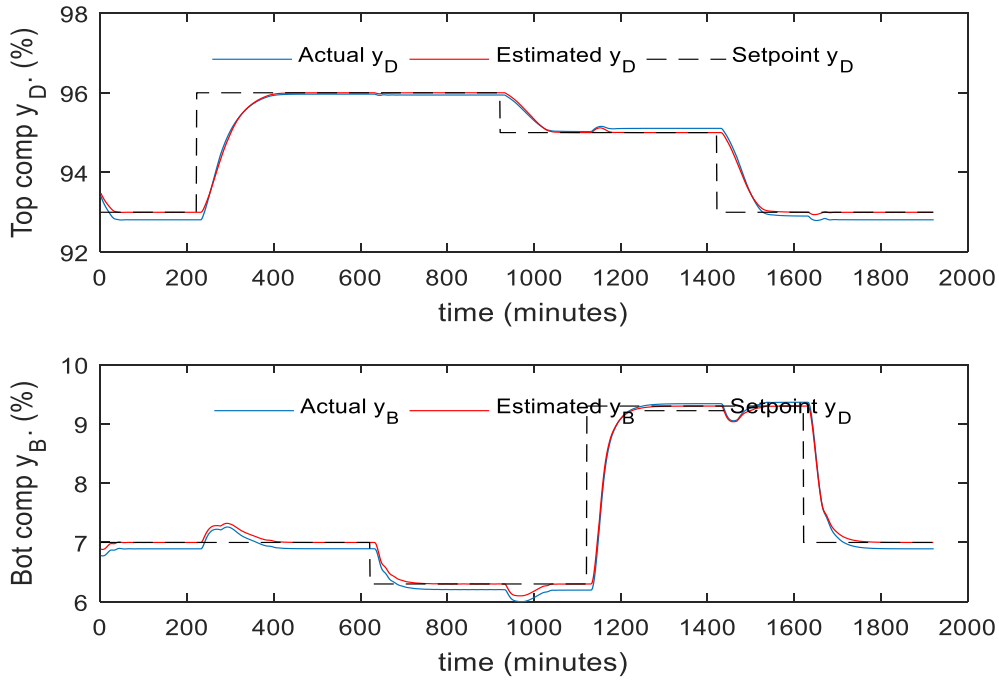

Figure 5.25: Responses of actual and estimated product compositions under inferential ADRC with 6th order dynamic PLS models (without mean updating)

The control offset in both the static and dynamic inferential ADRC will again be eliminated by implementing the mean updating technique in order to improve the overall performance of the inferential ADRC. Figures 5.26 and 5.27 present the control performance with the mean updating technique. It can be seen from these figures that mean updating is an efficient and successful technique that can eliminate the effects of undesired control offsets. The SSE of control errors has been reduced significantly after implementing and utilising the mean updating technique as shown in Table 5.6.

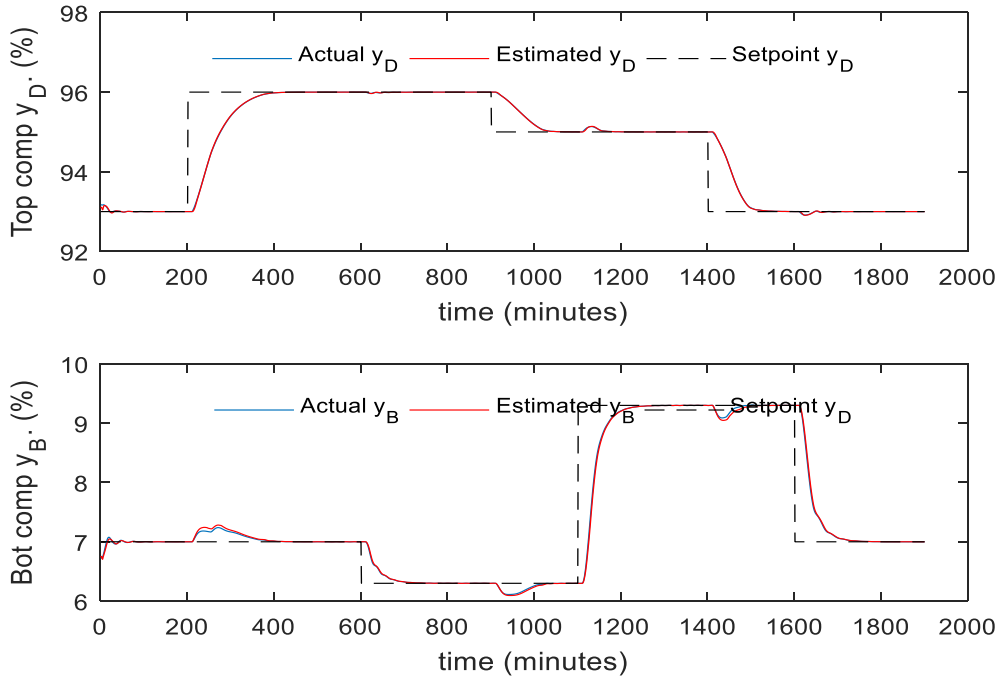

Figure 5.26: Responses of actual and estimated product compositions of static inferential ADRC (with mean updating)

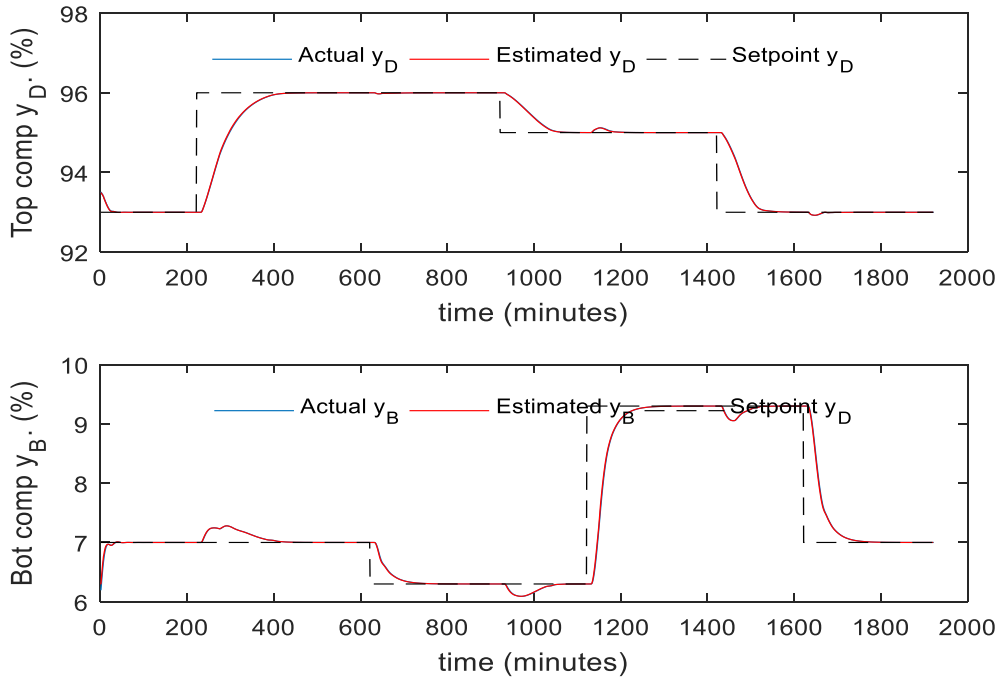

Figure 5.27: Responses of actual and estimated product compositions of inferential ADRC using the sixth order dynamic PLS model (with mean updating)

Table 5.6: SSE of different control schemes

Control schemes		Top Comp.	Bottom Comp.
Inferential ADRC with static PLS model	Without mean updating	190.572	958.4365
	With mean updating	0.5129	0.8197
Inferential ADRC with eighth order dynamic PLS model	Without mean updating	24.4268	15.1448
	With mean updating	0.0431	0.0557

It can be observed from the above figures that control off-sets and steady state model estimation bias have been eliminated successfully through the technique of mean updating. Furthermore, it can be noted from Table 5.6 that there is a large difference between the SSE of the dynamic inferential ADRC scheme and the static inferential ADRC scheme, where the dynamic PLS model has much smaller estimation off-sets than the static PLS model when the operating conditions change. This is due to the efficient performance of dynamic over static estimation. In addition, the dynamic PLS model provides more robust performance than the static PLS model to process operating condition variations. As a result, the dynamic inferential ADRC scheme provides better control performance than the static inferential ADRC. Moreover, the inferential ADRC scheme based on the PLS model provides good overall performance as the inferential ADRC scheme is based on the PCR model under correlated data.

5.6 Conclusions

Inferential ADRC control schemes with static and dynamic PCR and PLS models are proposed for product composition control in distillation columns. Inferential estimation models for product compositions are developed from the process operational data using both PCR and PLS. The estimated product compositions are used as the controlled variables in the ADRC controller. The mean updating technique is used to eliminate steady state model estimation bias and resulting control off-sets. The proposed control method is applied to a simulated methanol–water separation column. Simulation results indicate the effectiveness and success of the proposed dynamic

inferential ADRC control method over the static inferential ADRC control method. Furthermore, no significant differences were observed from the simulation results in the prediction errors reported by both PCR and PLS. The PLS approach however always required fewer LVs than the PCR technique, but this did not appear to influence predictive ability.

Chapter 6 ADRC of a heat integrated distillation column simulated using a mechanistic model

6.1 Introduction

The control system for a HIDiC is considered a MIMO system with model plant mismatches, time delay, strong loop interactions and significant sensitivity to external disturbance including feed composition and feed rate fluctuations. Model plant mismatches commonly exist due to several reasons (Cong, 2015a):

- Model parameters are only known approximately.
- Measurement devices have some limitations or imperfections.
- Model parameters may vary with operating conditions.

However, to the author's knowledge the issues of how to compensate for control loop coupling, undesired disturbance and model uncertainties in HIDiC have not yet been fully investigated. These issues obstruct attempts to control product compositions and might result in degradation in product quality and over-consumption of energy. Thus, the main objectives for controlling a HIDiC can be described as follows (Olujić *et al*., 2008):

- To maintain stable operation of the distillation column.
- To control conditions in the distillation column in order to make product compositions always meet desired specifications despite internal and/or external disturbance.

This chapter is organised as follows: Section 6.2 introduces the control structure of HIDiC. In this section, the nominal operating conditions of the considered HIDiC with the assumptions made are introduced prior to implementing both multi-loop PI and ADRC schemes. It will also introduce the 2×2 transfer function matrix for the purpose of PI controller tuning. Section 6.3 presents the multi-loop PI controller using the BLT technique. It will also show the selected parameters for the ADRC scheme. After that, both control schemes will be implemented, investigated and evaluated by performing various tests such as set-point tracking and external disturbance rejection in Section 6.4. Section 6.5 gives an overview of the inferential ADRC for HIDiC. Section 6.6 introduces the control structure with the PCR software sensor. In this section, the static and dynamic PCR inferential models are introduced and integrated with the ADRC

schemes. Then, Section 6.7 introduces the control structure with the PLS software sensors. The static and dynamic PLS inferential models are integrated with the ADRC schemes. Finally, conclusions are drawn in Section 6.8.

6.2 The ADRC control structure of a HIDiC

Currently, most industrial distillation columns are controlled by using multi-loop PID. In this research, ADRC is applied to the HIDiC in order to control the product compositions. The performance of ADRC is compared to that of PID control. Both control schemes are implemented individually in order to assess and compare their performance and efficiency under common process conditions such as set-point tracking and disturbance rejection.

6.2.1 The considered distillation column

The heat integrated distillation column is one of the most complex distillation columns around the world due to its challenging process characteristics such as non-linearity and strong loop interactions. ADRC and PI control algorithms are applied to control both top and bottom product compositions of a simulated HIDiC for separating a benzene-toluene mixture. The non-linear HIDiC dynamic simulation is based on a rigorous mechanistic model consisting of tray-by-tray energy and mass balances. Table 6.1 gives the nominal operating conditions of the simulated HIDiC.

The mechanistic model of a HIDiC is formulated under the following assumptions: negligible vapour holdups, perfect mixing of vapour and liquid on each tray, constant liquid molar holdups on each tray, uniform composition and the temperature on each tray, negligible pressure drop in each column, instantaneous heat transfer from the rectifying section to the stripping section, negligible heat capacity change and heat loss of the separation process, negligible time delay in thermal feed condition and column pressures changes,, constant and equal latent heat of each component, constant relative volatility, no liquid and vapour side stream withdrawn, instantaneous control for the top and bottom composition, and finally instantaneous pressure control.

The mechanistic model of the HIDiC can be represented by the following equations (Takamatsu et al. 1996; Cong et al. 2015b; Bisgaard et al. 2017):

- The heat transferred between stage *j* in the rectifying section and stage *j*+*f*-1 in the stripping column is:

$$Q_j = UA\,(T_j - T_{j+f-1}) \qquad (j = 1, \ldots, f-1) \tag{6.1}$$

Where *UA* represents the heat transfer rate and T_j is the stage temperature, which can be calculated according to the Antoine equation, Raoult's law and Dalton's law:

$$T_j = \frac{b}{(a - \ln p_{vp,j}) - c} \tag{6.2}$$

$$p_{vp,j} = \frac{P}{\left[X_j + \frac{1 - X_j}{\alpha}\right]} \tag{6.3}$$

Where *a*, *b*, and *c* are the coefficients of the Antoine equation, $p_{vp,j}$ represents the vapour saturated pressure of the stage *j*, *P* represents the pressure of either rectifying column P_r or the stripping column P_s, X_j is the mole fraction of the liquid at stage *j*, α is the relative volatility.

- Liquid flow rates in the rectifying section are:

$$L_j = \sum_{k=1}^{j} \frac{Q_k}{\lambda} \qquad (j = 1, \ldots, f-1) \tag{6.4}$$

Where λ represents the latent heat.

The vapour flow rates in the rectifying section can be calculated by:

$$V_{j+1} = V_1 + L_j \qquad (j = 1, \ldots, f-1) \tag{6.5}$$

Where V_1 represents the vapour flow rate of the top product leaving the first stage that can be derived from the total mass equation:

$$V_1 = F(1 - q) \tag{6.6}$$

Where *F* is the feed flow rate and *q* represents the feed thermal condition.

- Liquid flow rates in the stripping section are calculated as:

$$L_{f+j-1} = L_{f-1} + Fq - \sum_{k=1}^{j} \frac{Q_k}{\lambda} \qquad (j = 1, \ldots, f-1) \tag{6.7}$$

$$L_n = F - V_1 \tag{6.8}$$

- The vapour flow rates in the stripping section are:

$$V_{f+j} = V_f - F(1-q) - \sum_{k=1}^{j} \frac{Q_k}{\lambda} \qquad (j = 1, \ldots, f-1) \tag{6.9}$$

- Component mass balances are:

$$H\frac{dX_1}{dt} = V_2Y_2 - V_1Y_1 - L_1X_1 \tag{6.10}$$

$$H\frac{dX_j}{dt} = V_{j+1}Y_{j+1} - V_jY_j + L_{j-1}X_{j-1} - L_jX_j \qquad (j = 2, \cdots, n-1 \text{ and } j \neq f) \tag{6.11}$$

$$H\frac{dX_f}{dt} = V_{f+1}Y_{f+1} - V_fY_f + L_{f-1}X_{f-1} - L_fX_f + FZ_f \tag{6.12}$$

$$H\frac{dX_n}{dt} = -V_nY_n + L_{n-1}X_{n-1} - L_nX_n \tag{6.13}$$

Where H represents the stage holdup, Z_f is the mole fraction of the feed and Y_j is the mole fraction of the vapour at stage j.

- Vapour–liquid equilibrium relationships:

$$Y_j = \frac{\alpha X_j}{[(\alpha-1)X_j+1]} \qquad (j = 1, \ldots, n) \tag{6.14}$$

Typical values of the model parameters are shown in Table 6.1 (Bisgaard et al. 2017):

Table 6.1 Model variables and parameters

Property	Numerical value
Number of stages	54
Feed stage	27
Feed flow rate	83.33 kmol h^{-1}
Top composition (benzene)	99.5%
Bottom composition (toluene)	0.5%
Feed thermal condition (q)	0–1
Feed composition (d_1)	50%
Pressure of stripping section (P_s)	0.1013 MPa
Pressure of rectifying section (P_r)	2.3385 MPa
Heat transfer rate	9803 W K^{-1}
Latent heat of vaporisation	30001.1 kJ $kmol^{-1}$
Relative volatility	2.317

Simulations were conducted to verify the effectiveness of the ADRC scheme compared to the conventional PI controller in terms of set-point tracking and disturbance rejection. SSE is used as a control performance indicator. The controlled variables are the top and bottom product compositions and the corresponding manipulated variables are the rectifying pressure P_r (u_1) and feed thermal condition q (u_2). The undesired disturbance will be introduced by adding some changes to the feed composition z_f (D) as shown in Figure 6.1.

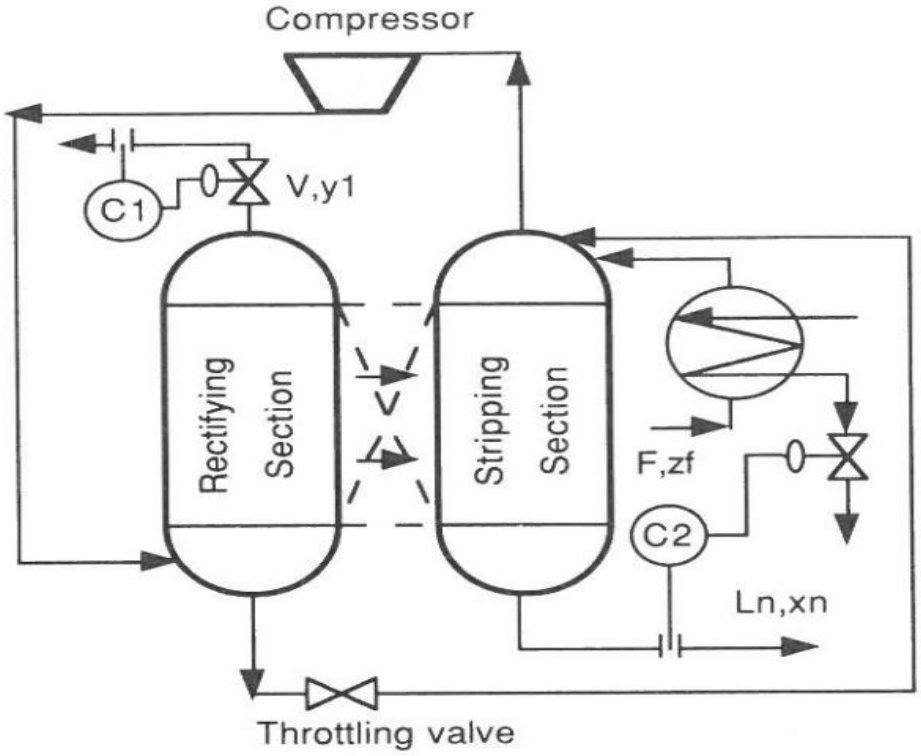

Figure 6.1 Schematic of the HIDiC

6.2.2 Modelling the considered distillation column

First of all, and prior to implementing and applying the multi-loop PI controller on the HIDiC, its transfer function model should be obtained first in order to tune the PI controller efficiently. The form of the transfer function model is given in Equation (6.15).

$$\begin{bmatrix} Y_1(s) \\ Y_2(s) \end{bmatrix} = \begin{bmatrix} G_{11} & G_{12} \\ G_{21} & G_{22} \end{bmatrix} \begin{bmatrix} u_1(s) \\ u_2(s) \end{bmatrix} + \begin{bmatrix} d_1 \\ d_2 \end{bmatrix} [Z(s)] \tag{6.15}$$

Where the process model is represented by the transfer function G_p and the disturbance model is represented by G_d:

$G_p = \begin{bmatrix} G_{11} & G_{12} \\ G_{21} & G_{22} \end{bmatrix}$, and $G_d = \begin{bmatrix} d_1 \\ d_2 \end{bmatrix}$

According to equation 6.15, in order to obtain the transfer function of G_{11} and G_{21}, a step change was applied to the rectifying pressure P_r and feed thermal q, which correspondingly changes both Y_1 and Y_2. Both top and bottom composition models were obtained using these step test data.

Since the mechanistic model of a HIDiC is quite complicated, the process reaction curve method will be used to obtain the transfer function. Prior to using the process reaction curve to produce the transfer function G_p, two step changes have been made in both manipulated variables P_r and q individually and the corresponding changes in both Y_1 and Y_2 were recorded in Figures 6.2 and 6.3. Product compositions are measured and it is assumed that there is a 10 min time delay in the composition analyser.

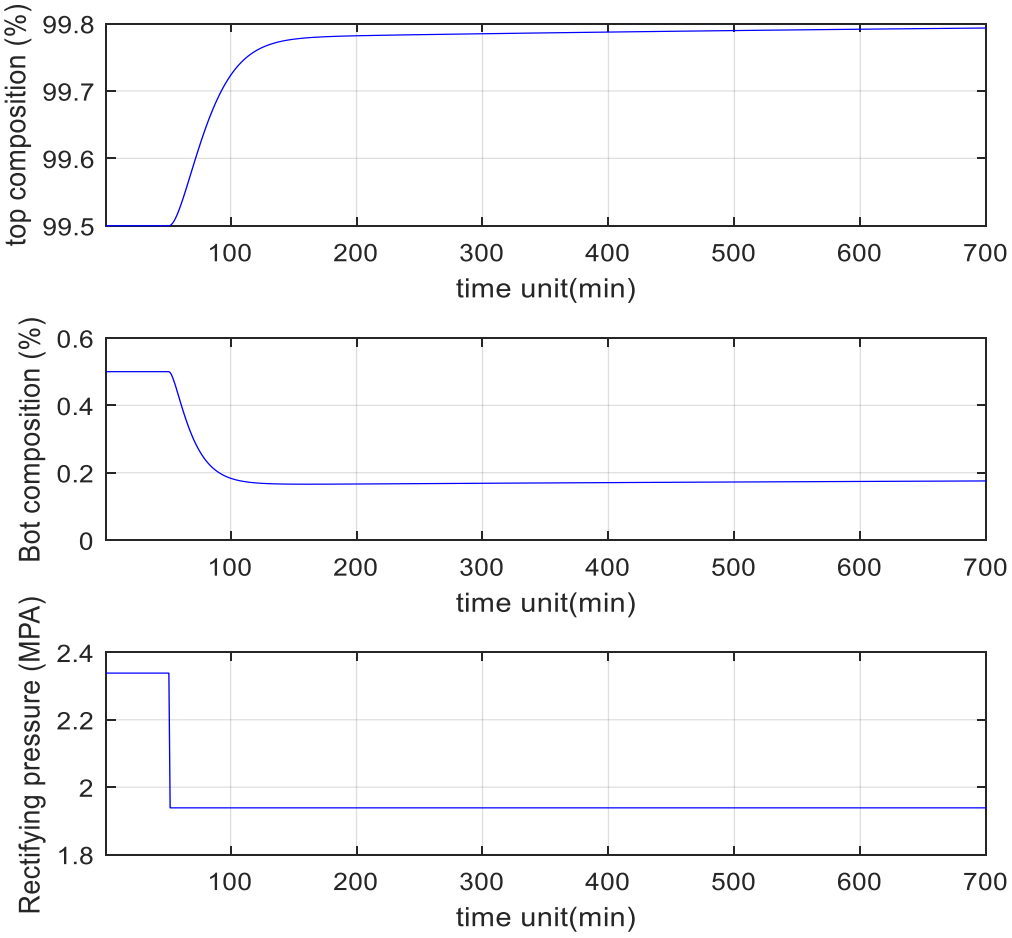

Figure 6.2: Process modelling with rectifying pressure step change

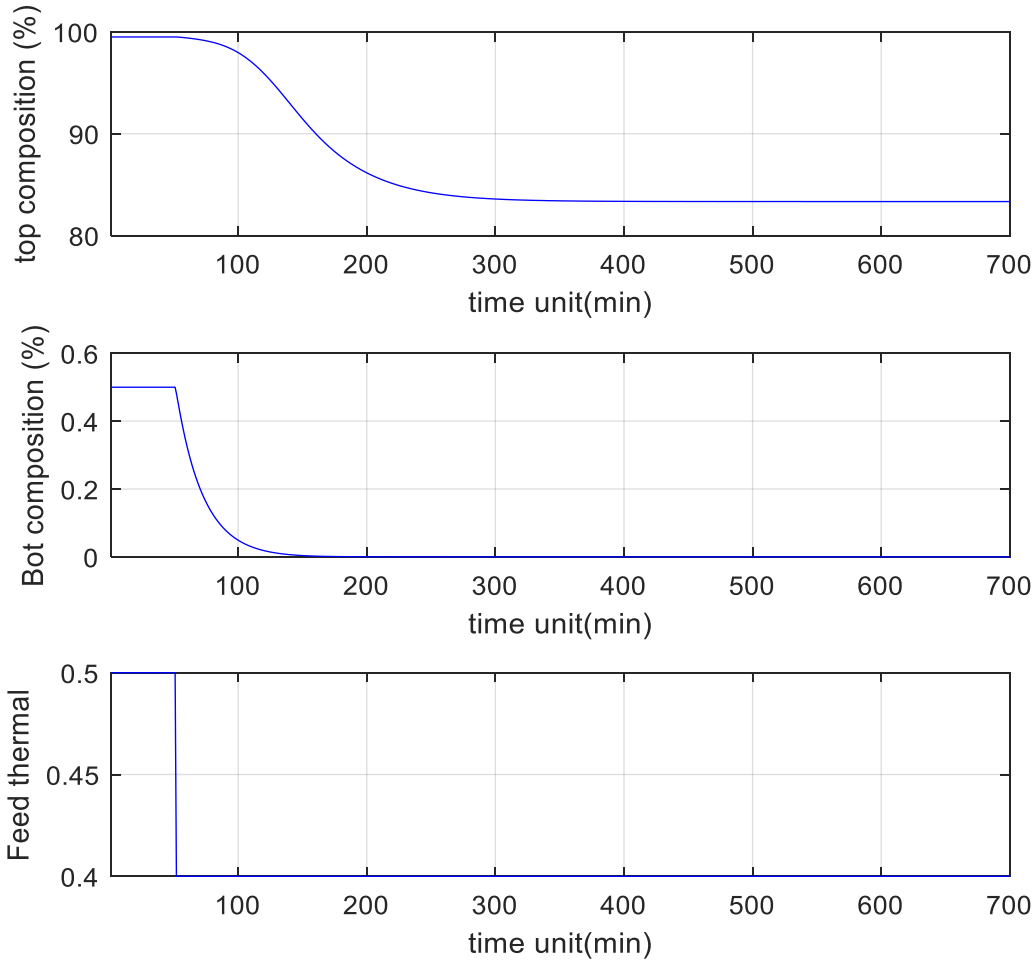

Figure 6.3: Process modelling with feed thermal step change

The identified process model is:

$$G_p = \begin{bmatrix} -\frac{0.84}{34.1s+1} & \frac{152\,e^{-9.75s}}{109.2s+1} \\ \frac{0.8325}{18.7s+1} & \frac{4.98}{20.3s+1} \end{bmatrix} e^{-10s} \tag{6.16}$$

It can be seen from the identified process model G_p that there is a direct relationship between both rectifying pressure u_1 and feed thermal u_2 with the bottom composition and product compositions respectively while there is a reverse relationship between the rectifying pressure u_1 and the top composition.

In order to obtain the transfer functions of G_d, a step change was applied to the feed composition as shown in Figure 6.4.

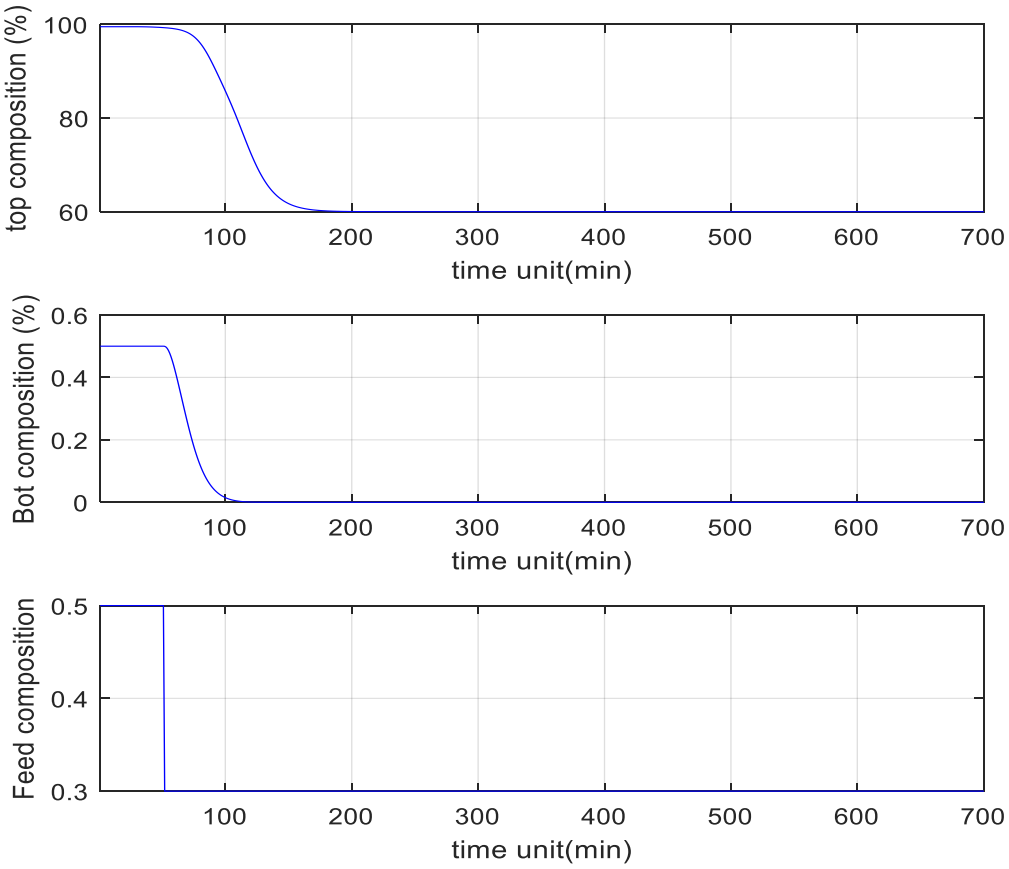

Figure 6.4: Disturbance modelling with feed composition step changes

Furthermore, the identified disturbance model is:

$$G_d = \begin{bmatrix} \frac{197.2\, e^{-3.4\, s}}{47.5s+1} \\ \frac{2.499}{23.7s+1} \end{bmatrix} e^{-10s} \tag{6.17}$$

6.3 Closed loop control of the case study

6.3.1 Tuning the PI controller parameters

In the transfer function model G_{11} will be used to tune the first controller and G_{C1} and G_{22} will be used to tune the second controller G_{C2}. Figures 6.5 and 6.6 show Bode plots for G_{11} and G_{22} respectively.

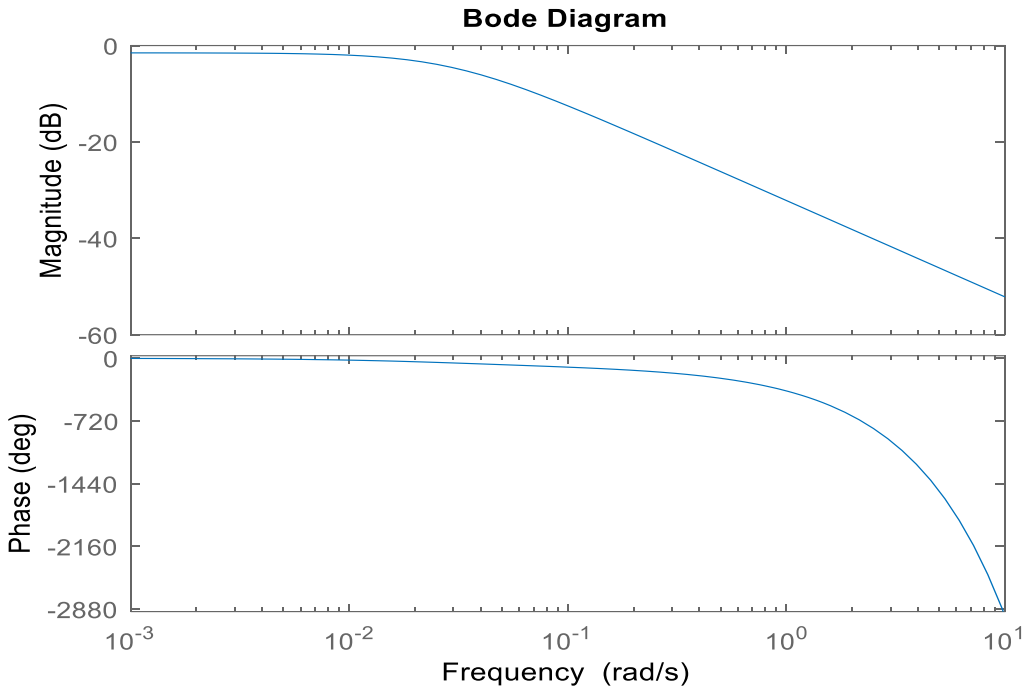

Figure 6.5: Bode plot of the top transfer function

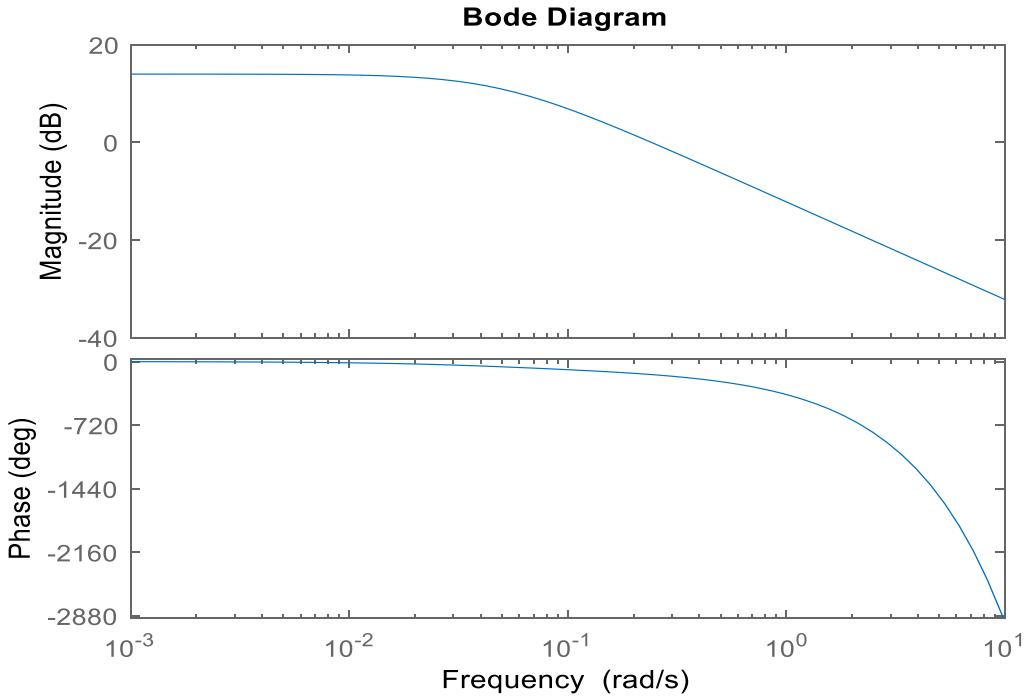

Figure 6.6: Bode plot of the bottom transfer function

From these Bode plots, both G_M and w_G were obtained and the corresponding controller parameters are given in Table 6.2.

Table 6.2: ZN tuning settings for the HIDiC

Loop	***Controller***	G_M	w_G	K_C	τ_I
Y_1	G_{c1}	13.4842	0.3318	6.1292	15.7787
Y_2	G_{c2}	1.4082	0.3426	0.6401	15.2814

As the HIDiC is a 2×2 MIMO dynamic system that should have a BLT of 4, the plot of L_{cm} with F=4.9 is shown in Figure 6.7. It can be seen that the BLT is approximately 4 when the detuning factor F is 4.9.

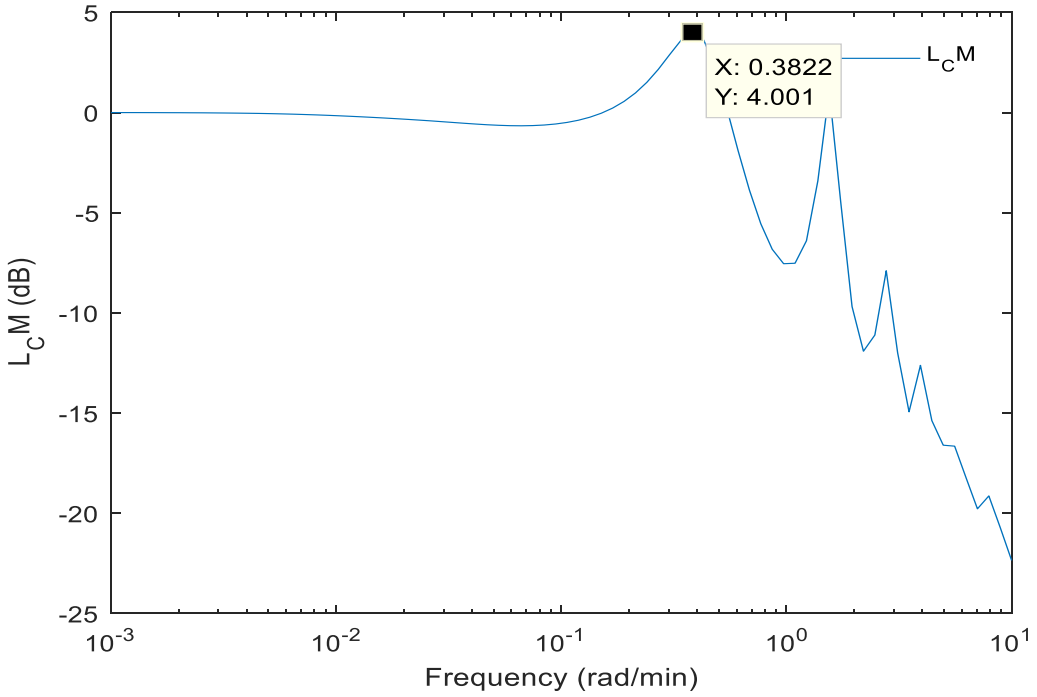

Figure 6.7: Closed-loop log modulus for HIDiC

In addition, the gain parameters introduced from ZN tuning approach in Table 6.2 are further tuned using the detuned factor *F*, and summarised in Table 6.3.

Table 6.3: BLT tuning setting for HIDiC

Loop	**Controller**	K_c	τ_I
Y_1	G_{c1} (P_r)	1.2509	77.3247
Y_2	G_{c2} (q)	0.1304	74.8872

6.3.2 Implementing the components of the ADRC scheme

Prior to applying the ADRC scheme on the mechanistic model of HIDiC, each component of ADRC will be designed and tuned based on the equations introduced in Chapter 2. Table 6.4 presents the tuned suitable value of the components of the ADRC scheme:

Table 6.4: Selected values for the ADRC approach.

ADRC tuning parameters	Selected values	
	Y_1	Y_2
r	10	10
h	0.004	0.004
b	0. 292999	27.74
k	0.04	0.04
α	0.4	0.09
δ	0.07	0.045
kp	2.45	0.045
f_c	0.1999589	0.039999

6.4 Investigation of the performance of both control schemes

Set-point tracking, model uncertainty, control signal response, and disturbance rejection are the most important behavioural characteristics of any multivariable control system. These factors will be analysed and discussed in order to investigate the efficiency of both controllers.

A. Set-point tracking performance

The overall performance of both control schemes will be investigated and analysed based on their performance under the impact of set-point tracking. A good controller should produce desired performance without any undesired overshoot and large settling time.

The performance of both control schemes was investigated by applying a series of set-point changes. The control performance was assessed based on SSE values of the control errors. The set-point tracking performance of Y_1 and Y_2 using ADRC and PI controllers are presented in

Figures 6.8 and 6.10 with their corresponding control actions presented in Figures 6.9 and 6.11 respectively.

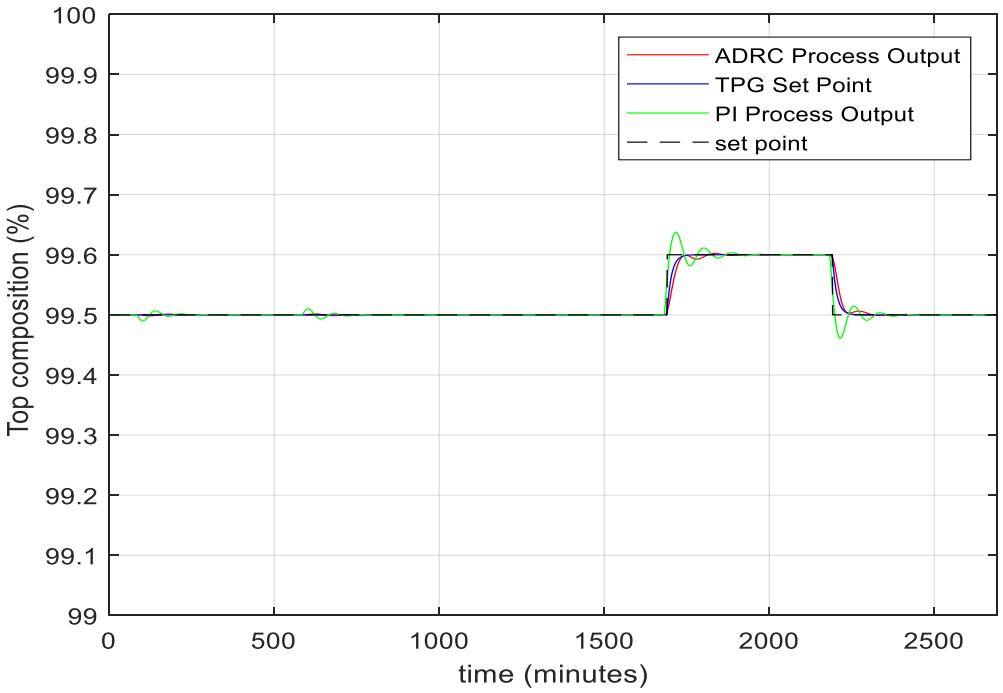

Figure 6.8: Performance of PI and ADRC schemes under the set -point tracking test for Y1

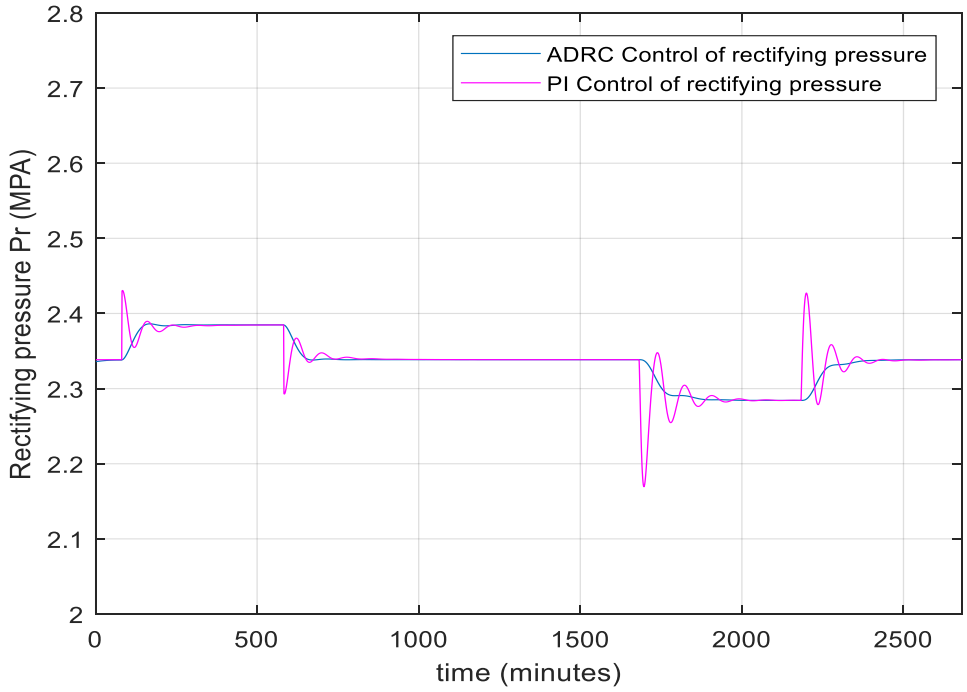

Figure 6.9: Control action of PI and ADRC schemes under the set-point tracking test for Y1

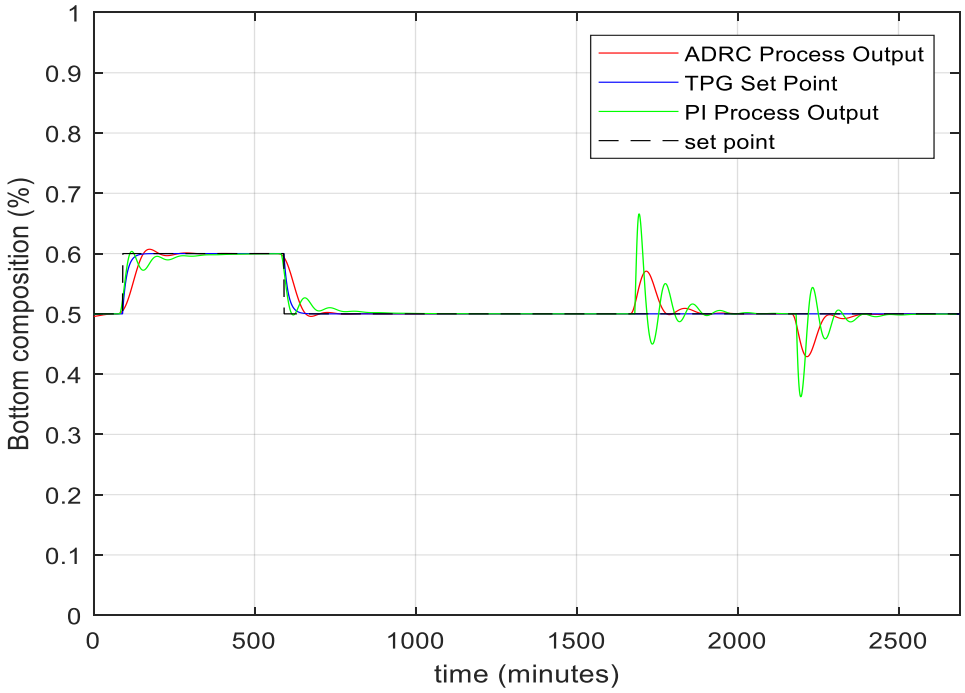

Figure 6.10: Performance of PI and ADRC schemes under the set-point tracking test for Y2

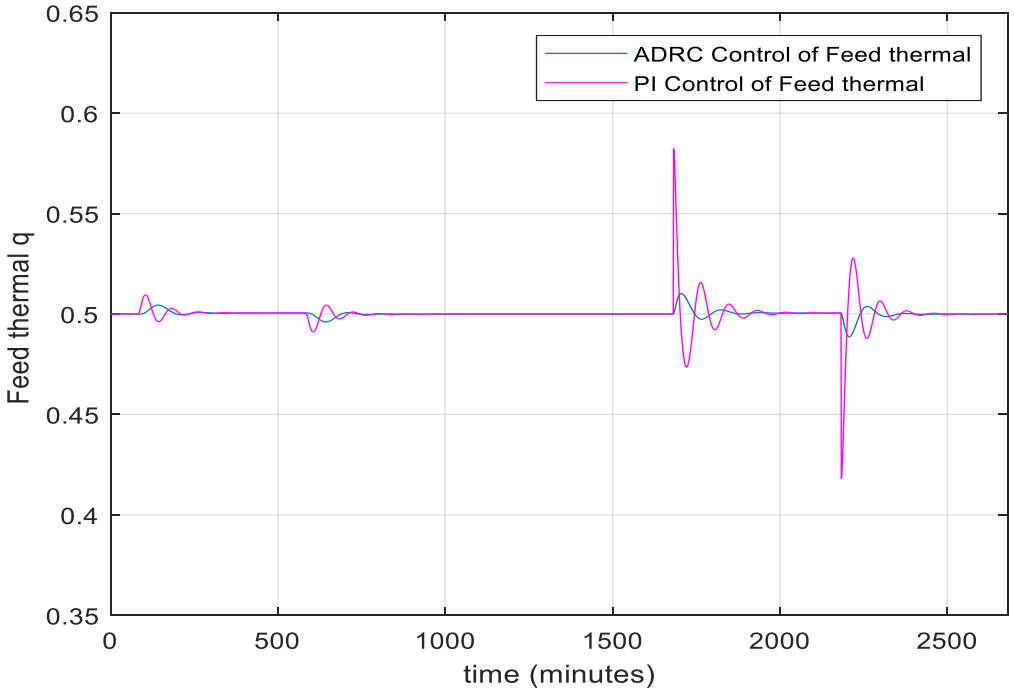

Figure 6.11: Control action of PI and ADRC schemes under the set-point tracking test for Y2

Several points can be clearly observed from the above simulation results:

Set-point tracking capability

In terms of set-point tracking and by referring to Figures 6.8 and 6.10, both the ADRC and PI schemes show an efficient and successful control performance under a sudden set-point changes but the ADRC gives better control performance than the PI. In the ADRC scheme, the controlled process outputs follow their set-points tightly without producing any signs of overshoot or sluggishness in both product compositions. Furthermore, it produces a smooth response, small maximum deviation and short settling time. This amazing performance of the ADRC scheme is due to the structure of the ADRC scheme. The TPG produces a transient profile that smoothens the set-point signal and makes it follow the desired set-point gradually and successfully, while the ESO component is utilised at the feedback loop to continuously monitor the internal states that are represented by the product compositions in order to update the N-LWS and compensate for the error rapidly and efficiently. Based on accurate estimation from the ESO component, the product compositions of the HIDiC track the desired set-point accurately. Figures 6.9 and 6.11 indicate that the ADRC control signal gives smooth control performance due to the structure of ADRC, which has an internal low-pass filter.

The suitable rates for both manipulated variables—rectifying pressure P_r and feed thermal q—should be within their operating point 30–40% specified in Table 6.1. In this test, ADRC control signals are operating within the specified operating range but the PI control signals are operating beyond the specified range.

Strong loop interactions

It can be seen that the interaction between both individual loops is very strong but the ADRC scheme reduces its impact. Despite the strength of the interaction in the HIDiC, the controlled process outputs follow strictly and successfully the desired set-points with small signs of overshoot when the set-point of any loop changes, especially at the bottom composition where there are signs of variation during set-point changes of the top composition. The ADRC scheme shows its superiority to recover and tackle this situation successfully. The efficient performance of the ADRC scheme is due to the integral performance of its components where the interaction between

both loops is considered an external disturbance and can be estimated and compensated for by the ADRC algorithm.

The performance of the conventional PI controller under the impact of loop interactions also efficient but not as the ADRC performance. Moreover, the speed of the PI controller in recovering the loop interaction impact is slower than the ADRC scheme and takes longer to settle down to a steady state, causing a large overshoot at the same time. The control signal of the PI controller is impractical, unlike the ADRC control signal.

Table 6.5 gives the SSE values of both control schemes for set-point tracking. It can be seen that the SSE values associated with the PI controller are considerably greater than the SSE values associated with ADRC.

Table 6.5: SSE values associated to both control schemes under the test of set-point tracking

Control Loops	***SSE (PI)***	***SSE (ADRC)***
Y_1	12.6581	1.1178
Y_2	14.8429	4.8943

B. External disturbance rejection capability

Getting the desired product purity in a HIDiC is always affected by several factors such as the external disturbance introduced by feed composition *Z*. This type of disturbance adds another challenge to the controller. According to Table 6.1, the normal value of the feed composition is 50%. In order to illustrate the disturbance rejection capability of a closed loop system, some external disturbances were generated and introduced by adding series step changes in the feed composition.

<u>External disturbance conferred by changes in feed composition from the feed stream</u>

According to Table 6.1, the normal operating conditions of the feed composition is 50%. External disturbance can be generated by changing the feed composition whilst maintaining

constant normal operating set-point values of Y_1 and Y_2. Figure 6.12 shows the series step changes that were introduced to the feed composition.

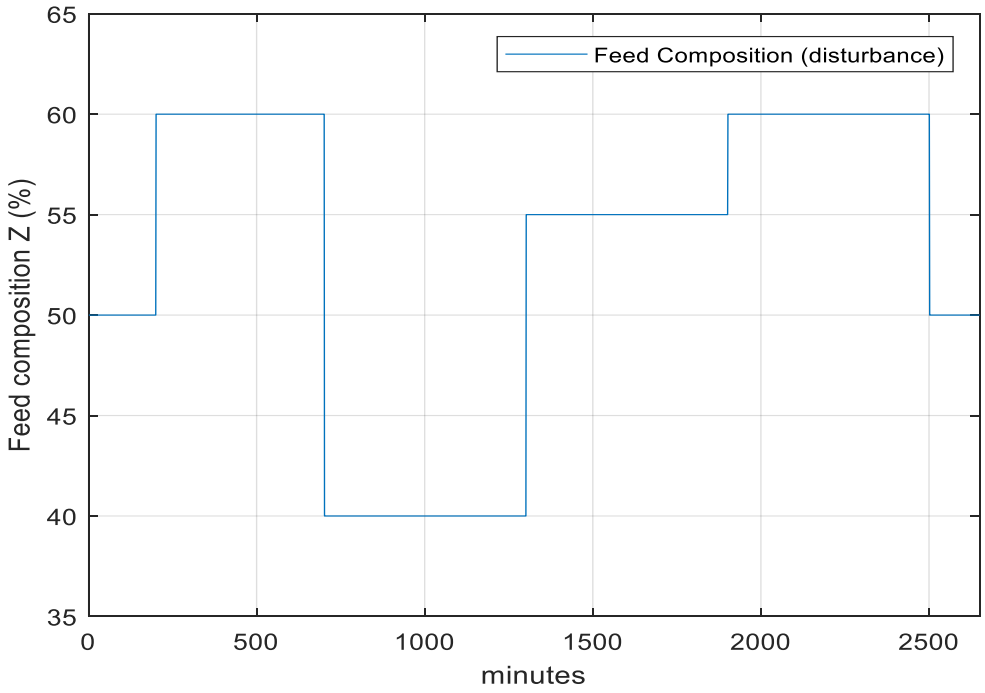

Figure 6.12: Changes in feed composition introduced to the HIDiC system

The disturbance rejection performance of Y_1 and Y_2 using ADRC and PI controllers are presented in Figures 6.13 and 6.15 with their corresponding control actions at Figures 6.14 and 6.16 respectively.

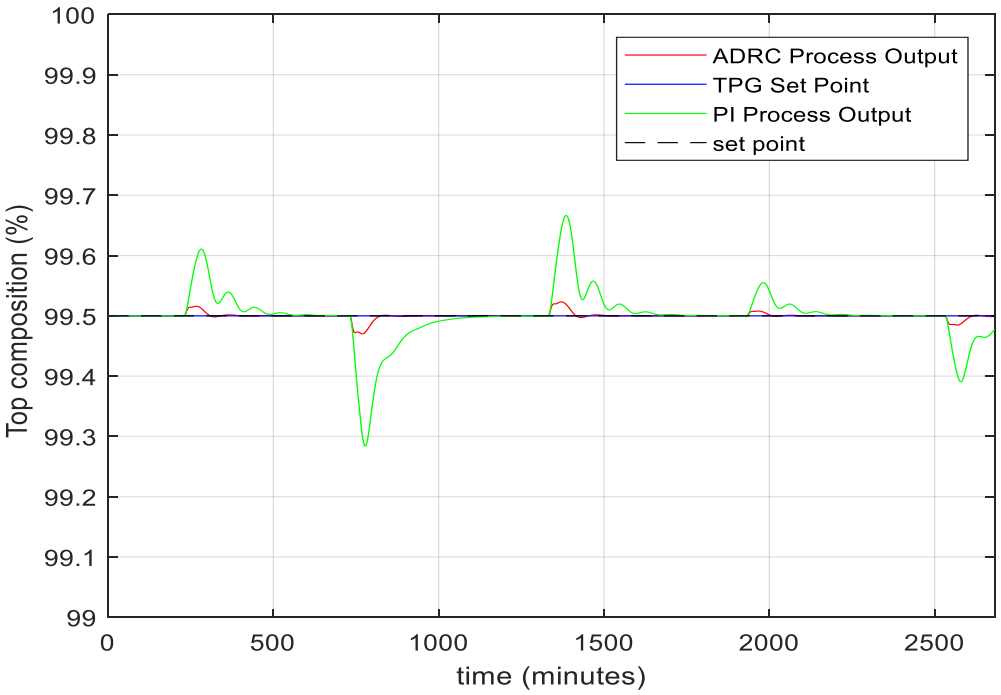

Figure 6.13: Performance of PI and ADRC schemes under the external disturbance rejection test for Y1

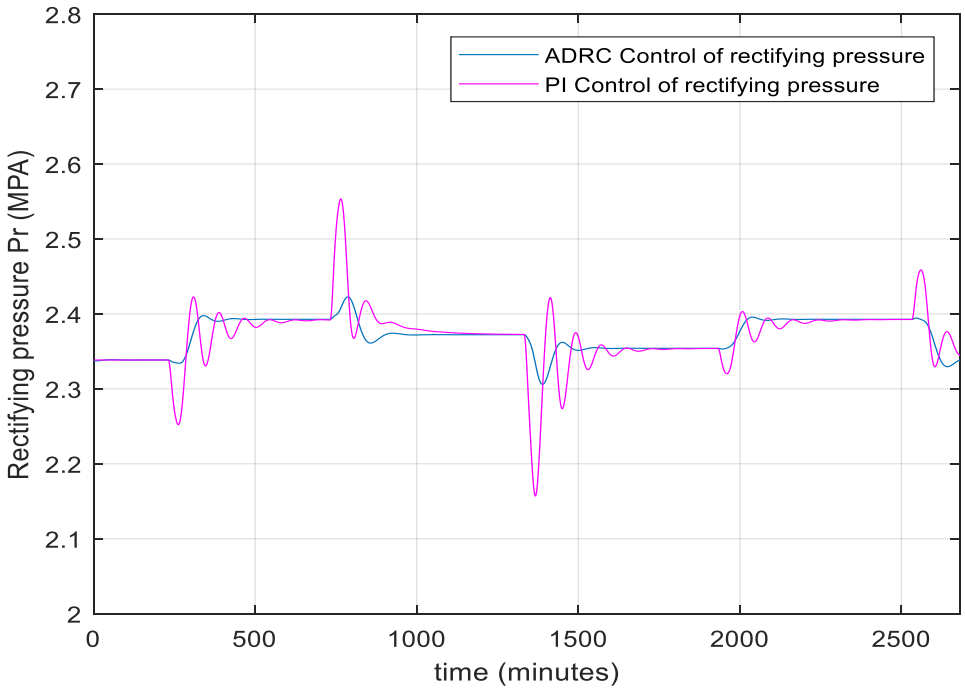

Figure 6.14: Control action of PI and ADRC schemes under the external disturbance rejection test for Y1

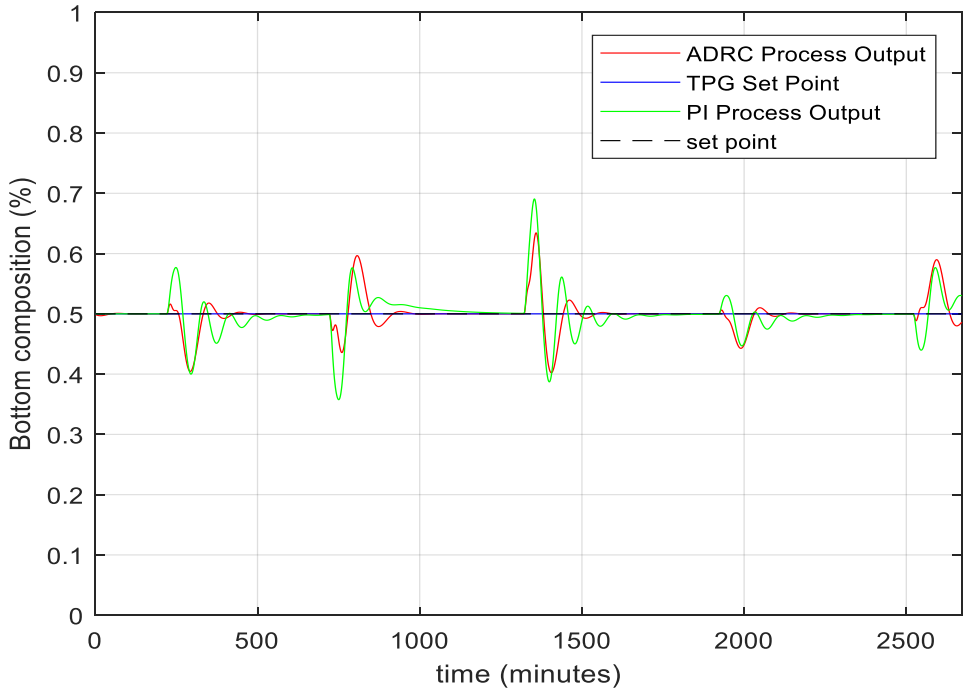

Figure 6.15: Performance of PI and ADRC schemes under the external disturbance rejection test for Y2

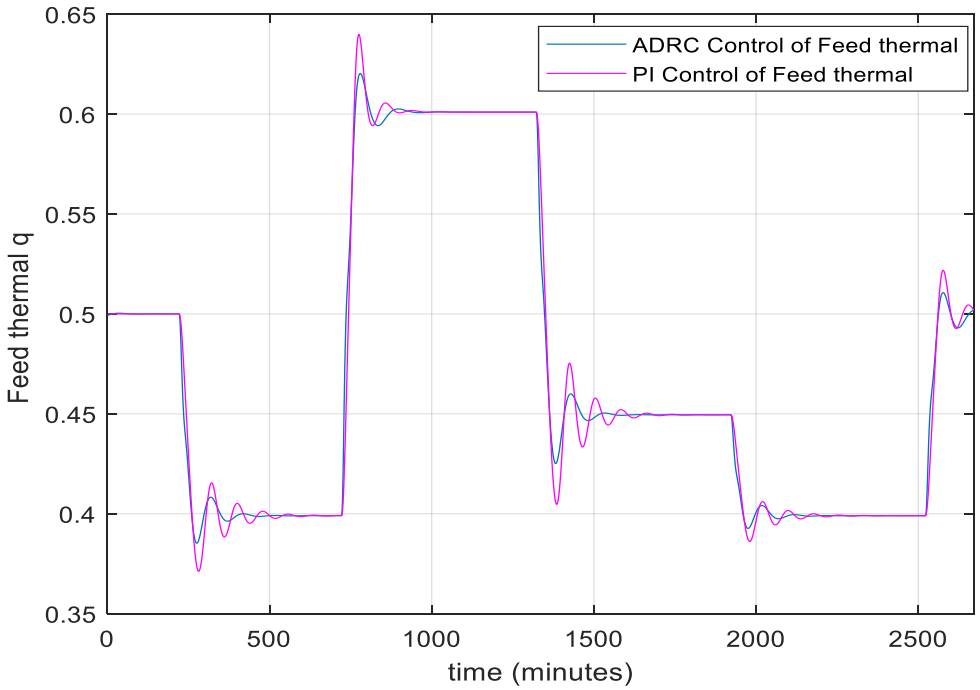

Figure 6.16: Control action of PI and ADRC schemes under the external disturbance rejection test for Y2

Several points can be clearly seen from the above simulation results:

Referring to Figures 6.13 and 6.15, the ADRC scheme produces better performance than the PI control under the feed composition disturbance *Z*. Furthermore, the speed of the PI controller in compensating for the disturbance is slower than the ADRC scheme. In the ADRC scheme, the controlled product composition follows their set-points with small signs of variations especially at the bottom composition. The ADRC scheme shows its superiority in recovering the controlled process outputs to their original steady state rapidly. This good performance of the ADRC scheme is due to efficient integration of its components where the ESO component estimates external disturbance. Subsequently, this estimated output is compared with the output of TPG in order to produce the control signal by N-LWS that reduces the impact of external disturbance in order to eliminate its impact before it enters the plant system. Moreover, and according to Figures 6.14 and 6.16, the ADRC control signal is smooth and without any sign of oscillation and overshoot due to the presence of an internal low-pass filter that removes signals with a frequency higher than the cut-off frequency f_c specified in Table 6.4 for both Y_1 and Y_2. The control signal of the PI controller however is non-smooth and not desirable in practice due to large oscillation and variation at both product compositions.

Table 6.6 gives the SSE values of both control schemes under the impact of external disturbance. The SSE values of the PI controller are considerably greater than those of the ADRC. The large value of SSE associated with the PI controller shows the efficiency of the ADRC scheme in dealing with external disturbances compared to the conventional PI controller.

Table 6.6: SSE values associated with external disturbance rejection capability

Control Loops	***SSE (PI)***	***SSE (ADRC)***
Y_1	33.5723	1.1695
Y_2	35.0912	18.315

Controlling the product composition of the HIDiC is a significant challenge due to undesired delay associated with product composition measurements. Delay is introduced by current measurement devices such as gas analysers. As a result, the delayed online composition

measurements used in the feedback control loop of the ideal HIDiC will impact the overall performance of the ADRC scheme significantly.

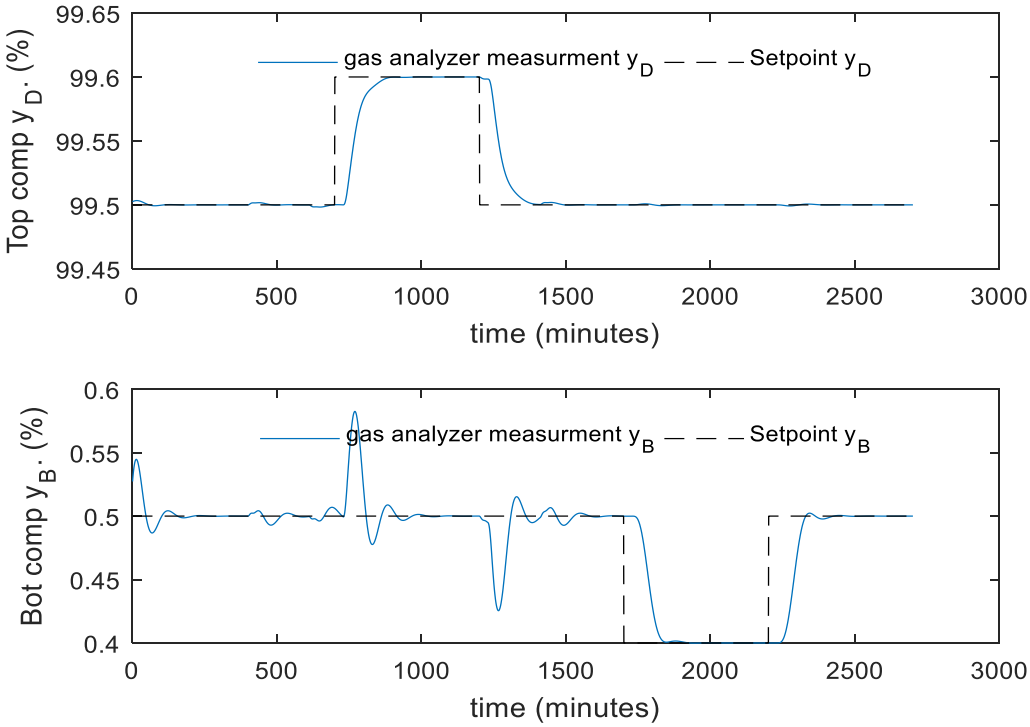

Figure 6.17: Control performance under the influence of composition analyser

As in Chapter 5, this issue can be solved by using inferential control, which will produce an online estimation of the product compositions.

The application of soft sensors for estimating the unmeasured primary variables is of particular interest in the processing industry, where many secondary variables are measured quickly and continuously and can be used as input signals for an inferential estimator. Moreover, since inferential estimation is being implemented by a computer, values can be estimated quickly compared to the hardware sensors with measurement delay (Willis et al. 1992). In HIDiC, a single tray temperature is not efficient enough to infer the composition of one product (Mejdell and Skogestad 1991; Baratti et al. 1995; Yeh et al. 2003). In this chapter, the tray temperatures of HIDiC will be used as secondary variables in order to estimate product compositions. The estimated compositions will be used directly in the ADRC scheme similarly to that shown in Figure 5.2.

6.5 Overview of inferential ADRC for HIDiC

The designed inferential ADRC scheme for a HIDiC consists of three main parts:

i. Inferential estimators: Due to stringent environmental laws and a highly competitive industrial market, strict quality control of distillation column products is essential. As a result, many variables should be effectively measured online so that the key process parameters can be successfully monitored and controlled through a feedback mechanism. In order to achieve this, inferential estimators, sometimes called soft sensors, are introduced. Inferential estimators are developed by utilising the relationship between the difficult-to-measure primary variables and the easy-to-measure secondary variables. The secondary variables are used to infer the values of the primary variables at a continuous frequent sampling rate. The inferential estimator is designed in an adaptive framework with the parameters of the primary model and updated whenever the secondary variable value becomes available. The soft sensors designed in this experiment use tray temperatures as secondary measurements to estimate the product composition (Bahar et al. 2006). However, there are various advantages of using inferential control (Deshpande and Deshpande 2012):

- Due to the large measurement delay associated with composition analysers, inferential control of product composition is a suitable approach as it depends on measurements of secondary variables that have no or relatively low dead time.
- In case of sensor failure for a particular plant, the performance of the controller will deteriorate and finally may affect the productivity and safety of a plant. In this case the estimated signal can be used for retaining the controller performance (Xie et al. 2010).
- Due to the huge amount of maintenance cost associated with online analysers, inferential estimators that measure the secondary variables typically eliminate the maintenance costs and are easier to implement. Furthermore, they keep the control loops working properly without any unexpected off-time.
- In many cases, online analysers for measuring primary variables are not accessible at all, making the inferential control technique the only suitable option.

Currently, there are many soft sensor techniques such as artificial neural networks and the Kalman filter (Zhang and Agustriyanto 2001).

ii. ADRC Controller: the ADRC scheme here receives the inferential estimator via ESO in order to estimate the internal and external undesired disturbance. Then, the N-LWS will compare the output estimation signals of ESO with the TPG output signal in order to produce the control signal u to compute the manipulated variables. In this plant, the top product purity is controlled by manipulating the rectifying pressure, while the bottom product purity is controlled by manipulating the feed thermal rate. The complete list of manipulated variables and control variables is shown in Figure 6.18.

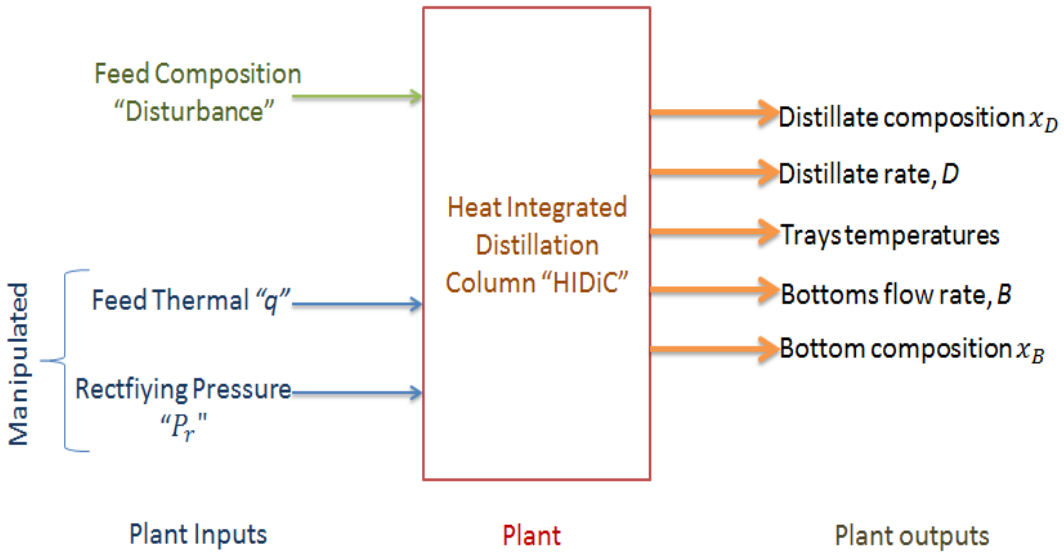

Figure 6.18: MIMO control of HIDiC

iii. Process: the distillation column used in this study is a HIDiC for separating a benzene and toluene mixture. A mechanistic nonlinear tray-by-tray dynamic model has been developed using mass and energy balances (Bisgaard et al. 2013).

6.6 Software sensors based on PCR models

Data for building soft sensor models are generated from simulations using the mechanistic model by adding some changes to the manipulated variables in open-loop. The following disturbances are also applied to the simulated column: feed composition increased by 15% at 200 and 2100 minutes, Simulated measure noises with normal distribution are added to the product compositions. The mean and standard deviation of the noise are 0 and 0.1% respectively.

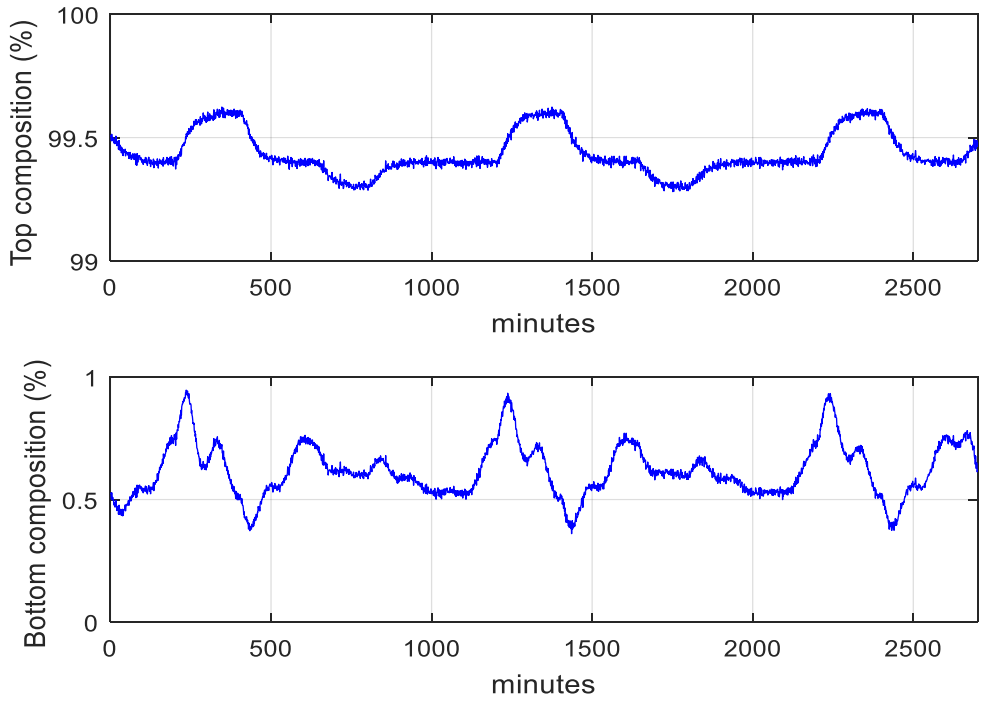

Figure 6.19: Product composition of HIDiC

The 54 tray temperatures generated from the dynamic simulation of the HIDiC were used to estimate the product compositions. Random measurement noises of the distribution N($0°C, 0.1°C$) were added to the tray temperature measurements in order to represent the practical situations where measurement noises always exist. Data are scaled to unit variance and zero mean prior to the model building. The data set (2700 samples) is divided into two sets:

- The training data set is the set of samples used to build and fit the model parameters. The training data set used in this study contains samples 1–1400.
- The testing data set is the set of samples used as part of the model building process to prevent any over-fitting. It is also used to identify the number of principal components used in the PCR model. The testing data set used in this study contains samples 1401–2700.

According to Figure 6.20, the tray temperatures of HIDiC exhibit strong correlation, making multiple linear regression inappropriate. As a result, PCR and PLS will be used in order to overcome the issue of correlation among the predictor variables (Kresta et al. 1991; Min et al. 1994). These methods address the collinearity issue by projecting the original model input variables into a low dimensions space forming orthogonal LVs (Zhang and Agustriyanto 2001;

Zhang (2006). PCR was originally introduced by analytical chemists to deal with the issues associated with multivariable calibration applications (Geladi and Kowalski 1986). It generally results in a well-conditioned model with good estimation performance. Implementing the PCR model in a HIDiC will calculate the linear relation between the primary and both manipulated and secondary variables over a wide range of operating conditions (Budman et al. 1992).

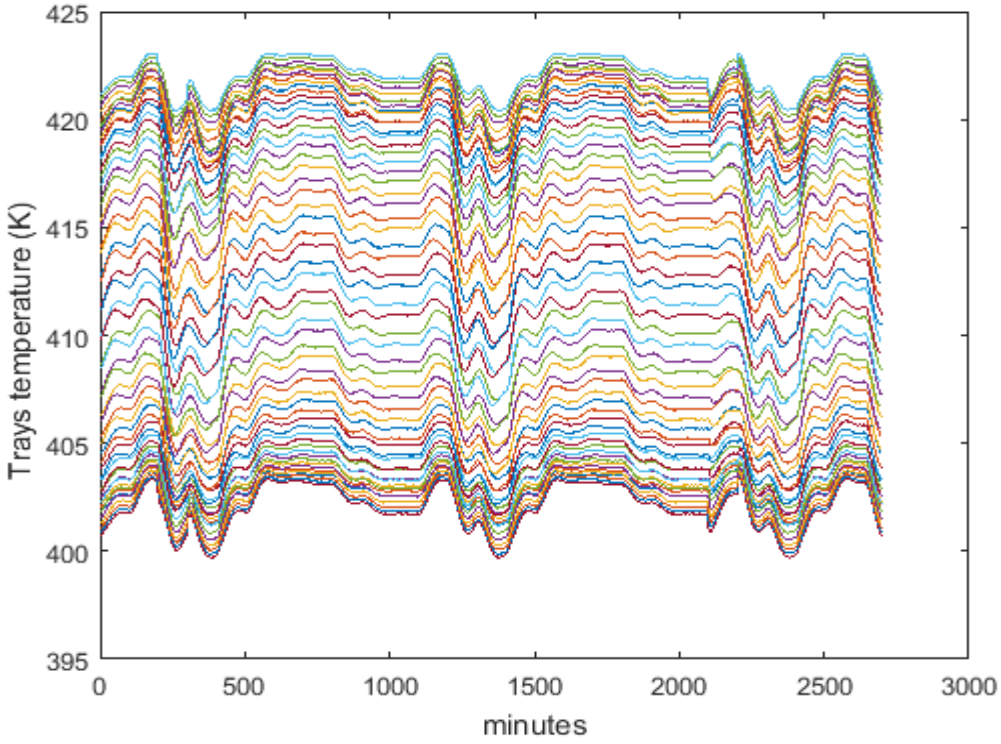

Figure 6.20: Tray temperatures of the HIDiC

6.6.1 Static inferential model

Again, the static inferential model of the HIDiC will be developed using Equation (5.2). The secondary variables tray temperatures of the HIDiC from trays 1–54 is used as an input signal of soft sensors in order to be used to estimate the primary variables. In this section, a PCR model was developed by selecting the suitable number of PCs based on the minimum SSE on the testing data set as shown in Figure 6.21.

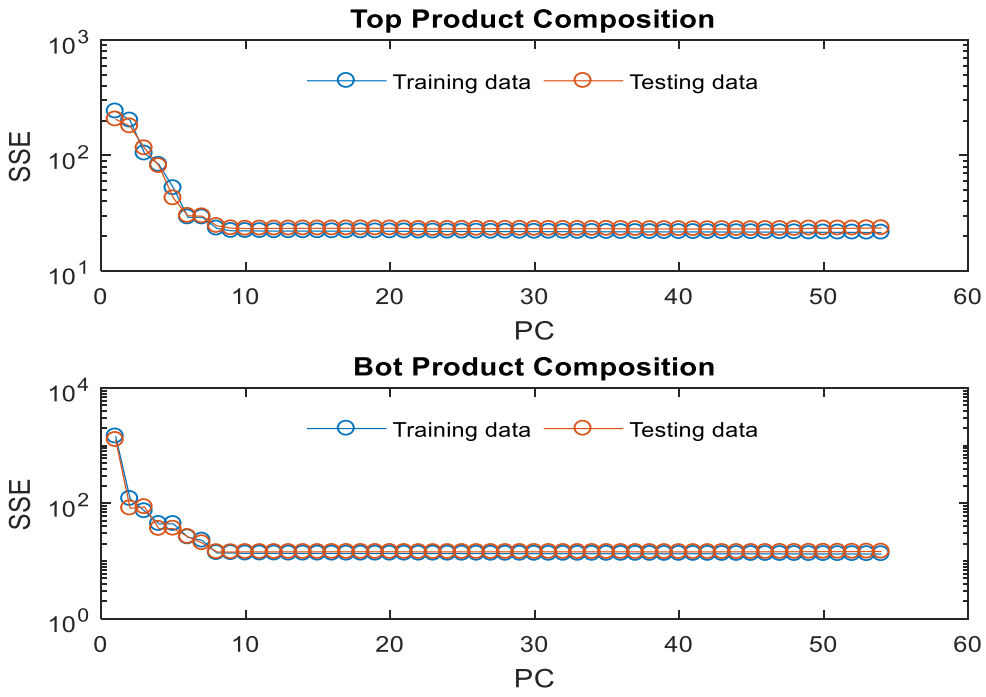

Figure 6.21: SSE of static PCR models

It can be seen from Figure 6.21 that the PCR model with 8 PCs gives the best performance for the top composition on the testing data, and 8 PCs produces the best performance for the bottom compositions on the testing data. Therefore, 8 PCs are used in both the top and bottom composition models. The developed PCR models for the top and bottom product compositions in terms of PCs are as follows:

$$y_D = 0.0998\ PC_1 - 0.1790\ PC_2 + 0.6588\ PC_3 + 0.5940\ PC_4 + 1.2163\ PC_5 - 1.3716\ PC_6 - 0.0045\ PC_7 + 1.5119\ PC_8 \quad (6.2)$$

$$y_B = -0.0095\ PC_1 + 0.4966\ PC_2 - 0.4402\ PC_3 + 0.2198\ PC_4 - 0.5411\ PC_5 - 1.1518\ PC_6 + 0.6654\ PC_7 + 1.7234\ PC_8 \quad (6.3)$$

6.6.2 Dynamic inferential model

The relationship between the easy-to-measure process variables and the difficult-to-measure product quality variables can be dynamic. In such cases, dynamic soft sensors would be more

appropriate. In order to enhance the estimation accuracy of the inferential estimator, seven dynamic models have been developed.

Data division and scaling are kept the same as for building static PCR models. The appropriate dynamic model can be recognised by identifying the lowest SSE value on the testing data. Eight inferential feedback control schemes with seven different soft sensors (static and seven dynamic inferential PCR models) were developed and implemented. Table 6.7 presents the SSE values of different inferential models.

Table 6.7: Number of PCs with corresponding SSE on the testing data of different dynamic PCR models.

Order of dynamic model	**Product compositions**	**No of PC**	**SSE**
Static inferential model	Top Comp	8	21.1013
	Bot comp	8	13.2801
1st order dynamic PCR model	Top Comp	10	17.9134
	Bot comp	27	11.1365
2nd order dynamic PCR model	Top Comp	22	16.6029
	Bot comp	25	10.3346
3rd order dynamic PCR model	Top Comp	26	15.7191
	Bot comp	26	9.7464
4th order dynamic PCR model	Top Comp	31	14.6439
	Bot comp	13	9.1311
5th order dynamic PCR model	Top Comp	37	13.7126
	Bot comp	25	8.5876
6th order dynamic PCR model	Top Comp	17	12.2620

	Bot comp	21	7.5707
7^{th} order dynamic PCR model	Top Comp	18	12.9932
	Bot comp	18	8.0464

According to Table 6.7, the estimation accuracy of the dynamic model has been significantly enhanced compared to the static inferential PCR model, especially in the 6^{th} order models. In addition, the 6^{th} dynamic model is selected and integrated with the ADRC controller as it gives better performance than the rest. Figures 6.22 and 6.23 and Figures 6.24 and 6.25 present, respectively, predictions from the static inferential PCR model and the 6^{th} order dynamic inferential model. In these figures, the blue line represents the actual product composition response while the red solid line represents the corresponding estimation response.

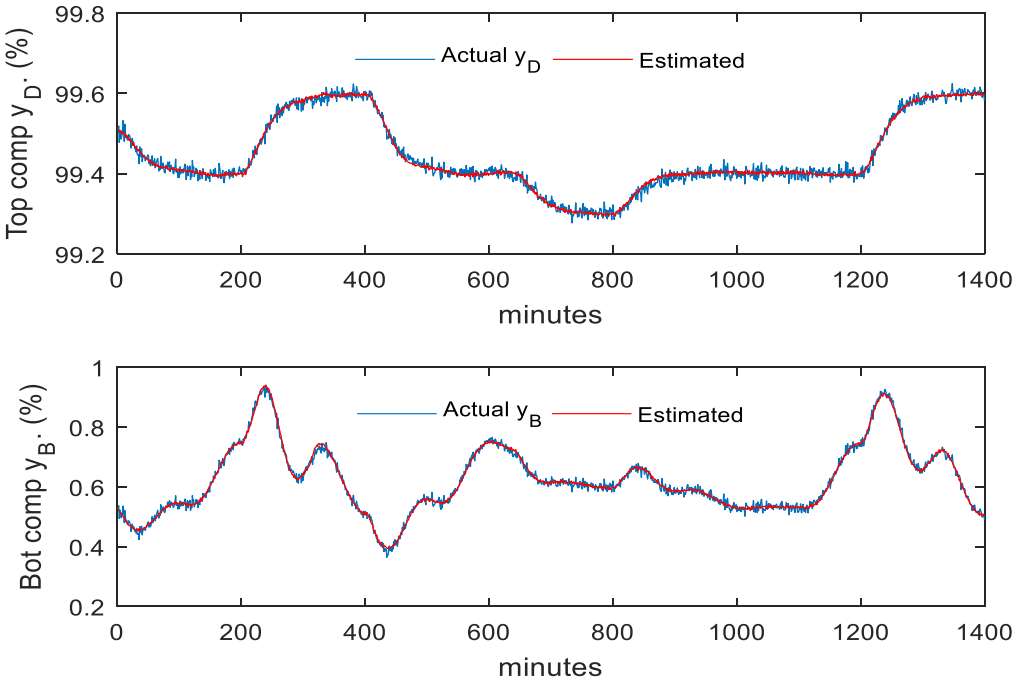

Figure 6.22: Model estimation of static PCR model (training data)

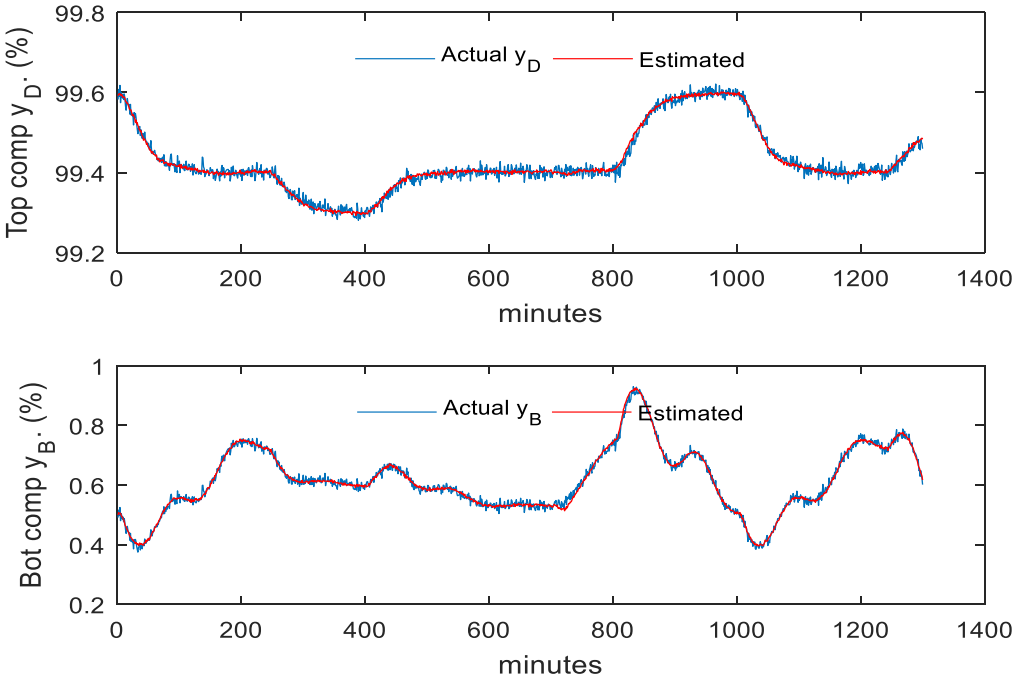

Figure 6.23: Model estimation of static PCR model (testing data)

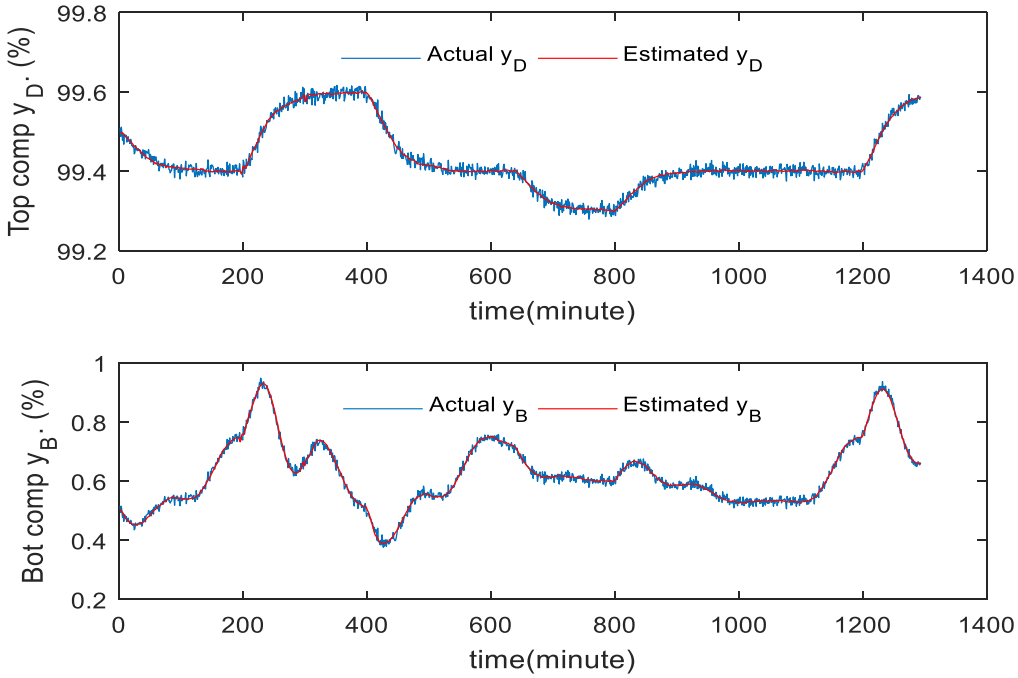

Figure 6.24: Model estimation of 6th order dynamic PCR model (training data)

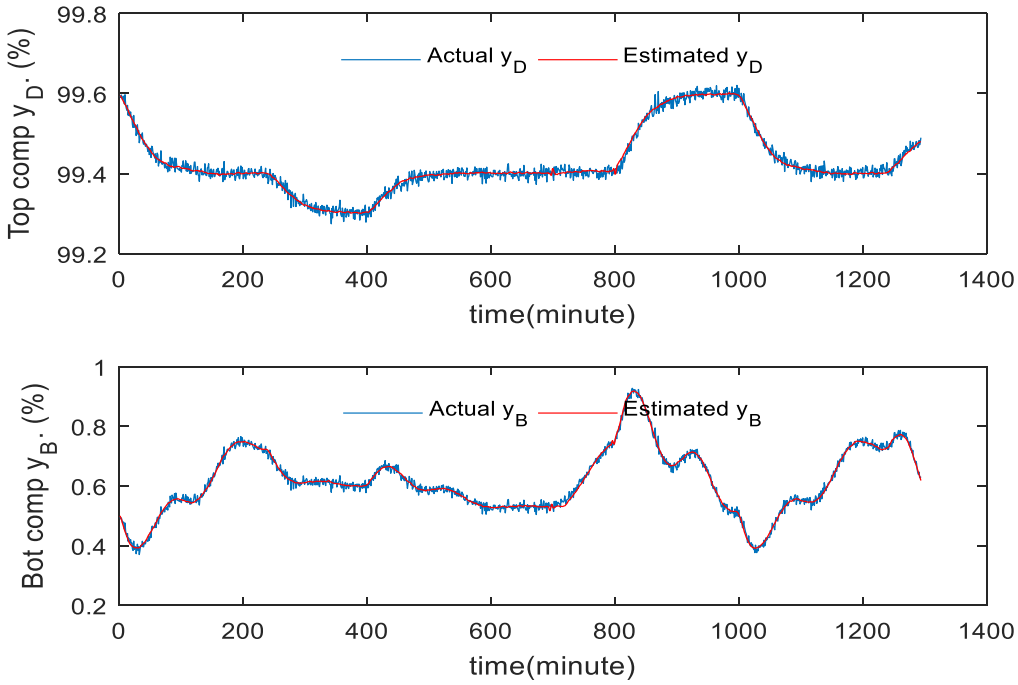

Figure 6.25: Model estimation of 6th order dynamic PCR model (testing data)

Figures 6.26 and 6.27 present the estimation errors for both the static and 6th dynamic PCR model. It can be noticed from this figure and as expected, the 6th order dynamic PCR model shows better estimation performance than the static model.

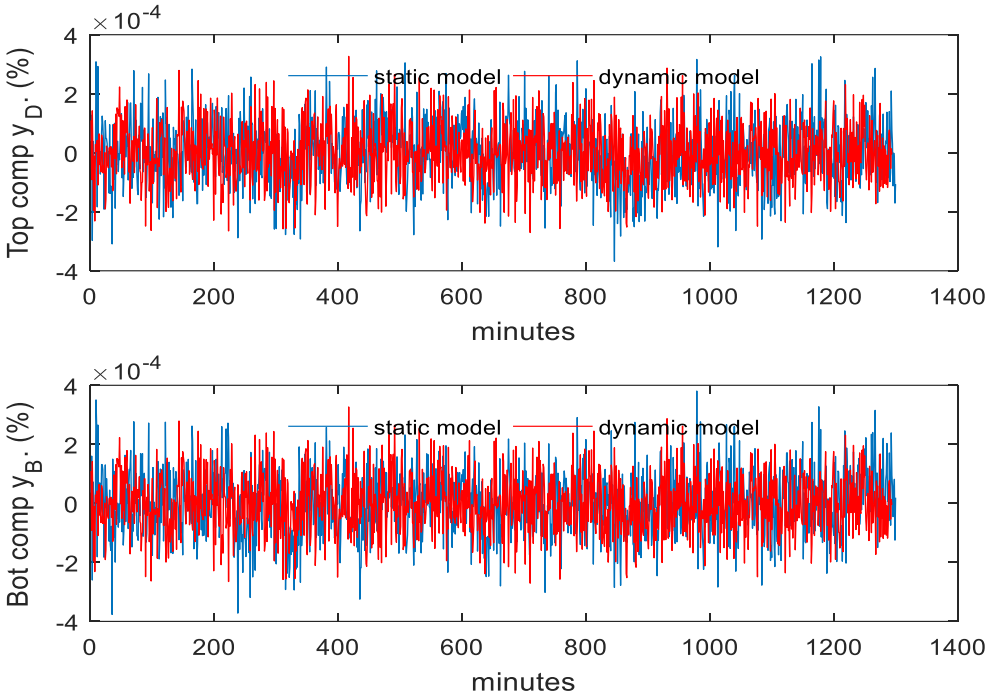

Figure 6.26: Model estimation errors (training data)

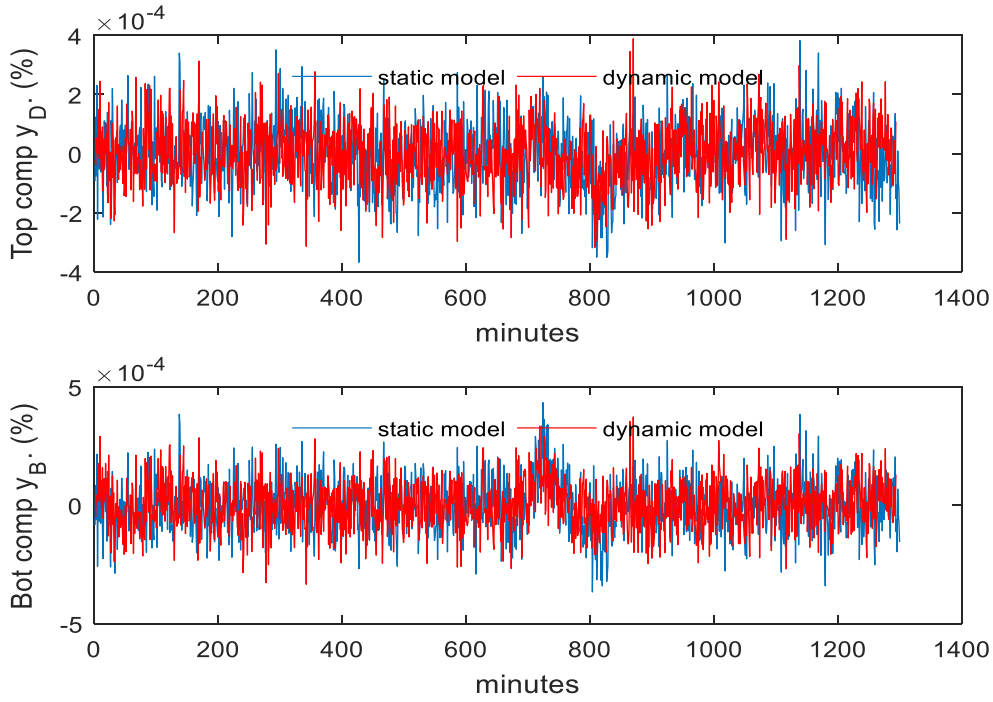

Figure 6.27: Model estimation errors (testing data)

6.6.3 Inferential control performance

Since the dynamic inferential models give better performance than the static inferential models, especially the 6th dynamic inferential ADRC schemes, the 6th order dynamic inferential model will be combined with the ADRC scheme in order to introduce the inferential ADRC scheme.

Figures 6.28 and 6.29 respectively show the responses of both static and dynamic inferential ADRC schemes over a wide range of feed composition disturbance and set-point changes. It can be seen from both figures that the set-point signal was smoothed by the ADRC scheme in order to make the controlled variables follow the smoothed set-point signal gradually without any overshoot. Furthermore, the dynamic inferential ADRC gives better performance than the static inferential scheme despite large offset errors existing at the bottom composition. The existence of offset error in both the static and dynamic inferential ADRC schemes is due to bias in the soft sensor that increases when operating conditions change.

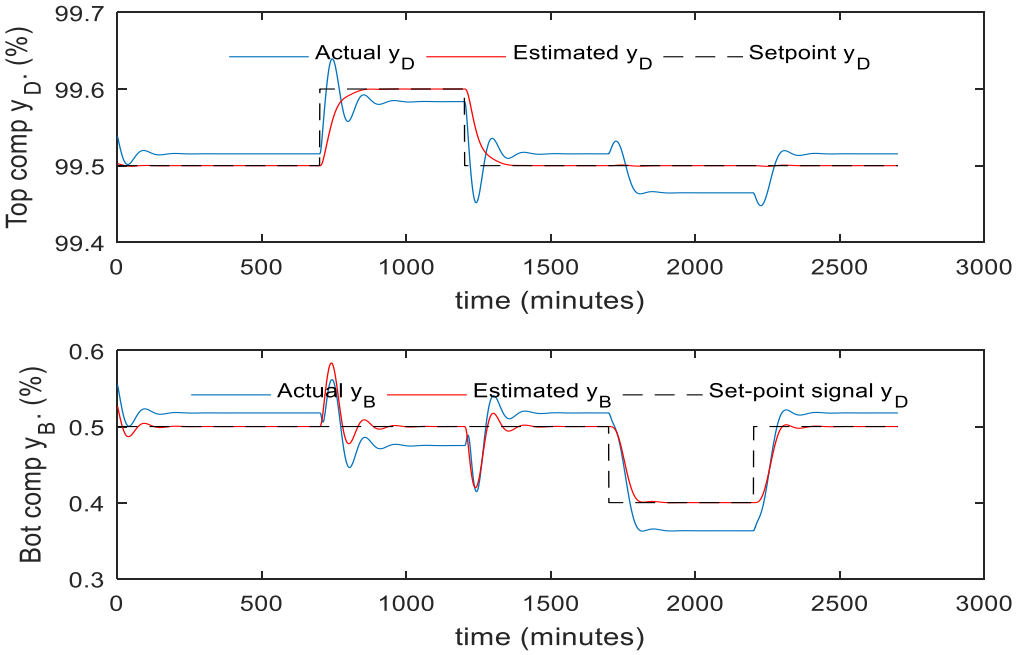

Figure 6.28: Responses of actual and estimated product composition of the static inferential scheme (without the mean updating technique)

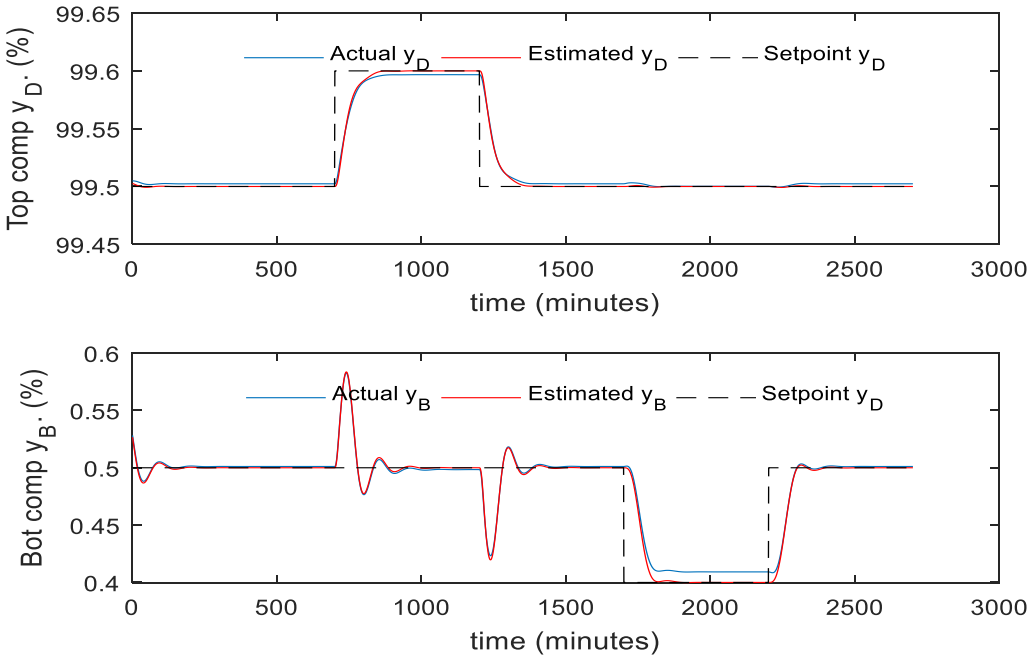

Figure 6.29: Responses of actual and estimated product composition of 6th dynamic inferential scheme (without the mean updating technique)

In order to improve the estimation accuracy and remove the existence of control offsets due to estimation bias, the mean updating strategy introduced by Zhang (2006) is implemented. The main principle of the mean updating technique is that when a new steady state is reached, the new steady values of the process variables are used as the new mean values of these variables. Hence, the estimation accuracy of the estimated signal is improved.

Figures 6.30 and 6.31 show the control performance of inferential ADRC scheme with mean updating strategy. It can be seen from both figures that the control offsets have been eliminated by using the mean updating technique.

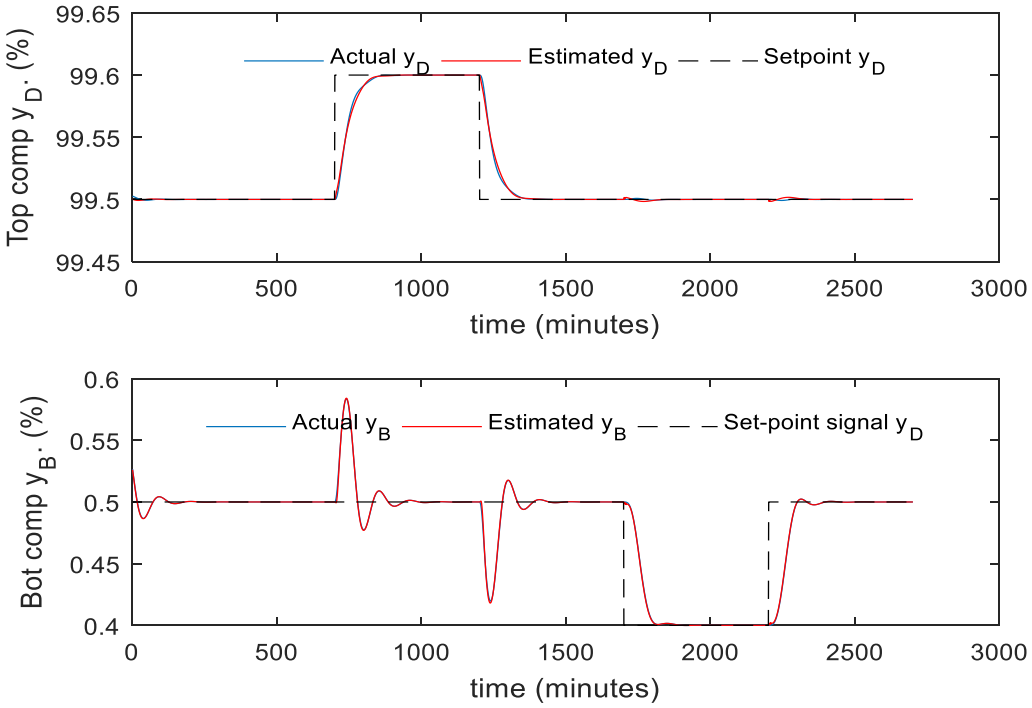

Figure 6.30: Responses of actual and estimated product compositions of static inferential scheme (with the mean updating technique)

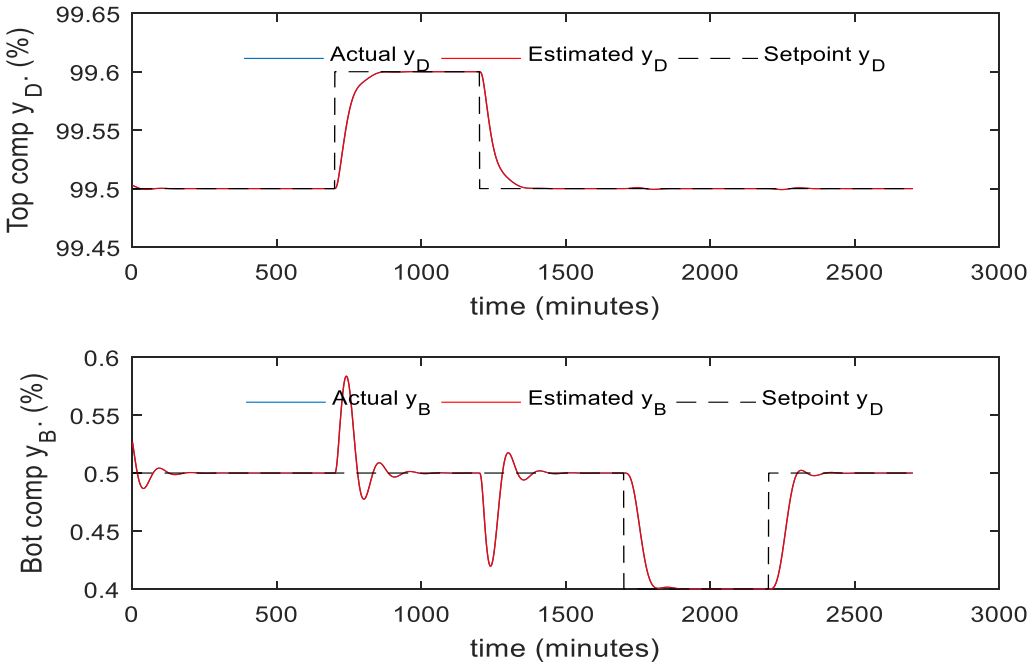

Figure 6.31: Responses of actual and estimated product composition of 6th dynamic inferential scheme (with the mean updating technique)

Table 6.8: SSE of static and dynamic inferential ADRC schemes

Control schemes	**Product composition**	**Top comp**	**Bot comp**
Static inferential ADRC	Without mean updating	10.2497	21.2276
	With mean updating	2.9371×10^{-5}	1.0010×10^{-5}
6^{th} dynamic inferential ADRC	Without mean updating	0.5809	1.4160
	With mean updating	1.0396×10^{-7}	1.1987×10^{-7}

It can be seen from Table 6.8 that the mean updating strategy reduces the SSE value. Table 6.9 also demonstrates the efficiency of dynamic inferential ADRC compared to the static one with and without the existence of the mean updating technique.

6.7 Inferential ADRC scheme based on PLS models

6.7.1 Static PLS model

The PLS method can also be used to deal with collinear model input variables. In building static PLS soft sensors, data partition and data scaling are the same as in building static PCR models. In this research, PLS models are developed by selecting the suitable number of LVs based on the minimum SSE on the testing data set as shown in Figure 6.32.

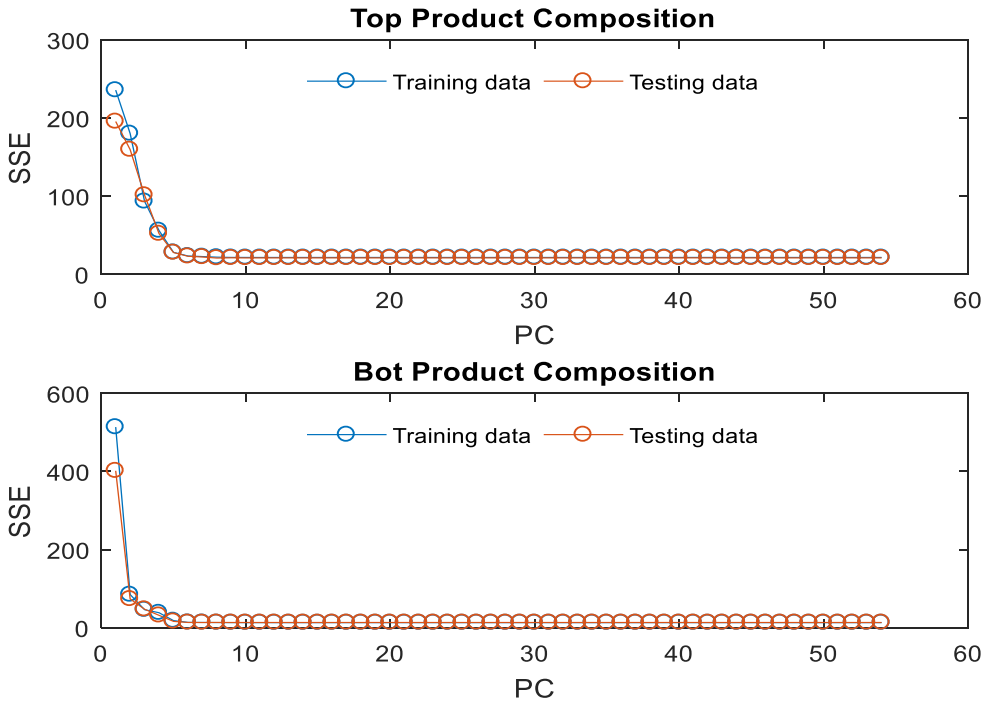

Figure 6.32: SSE of static PLS prediction of HIDiC

The PLS model with the lowest SSE on the testing data set is considered to have the most suitable number of LVs. According to this table, the PLS model with six LVs gives the best performance for both top and bottom compositions on the testing data. The developed PLS models for the top and bottom product compositions in terms of the latent variables are as follows:

$$y_D = 0.0329\,LV_1 + 0.1783\,LV_2 - 0.1848\,LV_3 + 0.0837\,LV_4 + 0.0572\,LV_5 + 0.1869\,LV_6 \quad (6.4)$$

$$y_B = 0.0002\,LV_1 + 0.0615\,LV_2 - 0.0530\,LV_3 + 0.0228\,LV_4 + 0.0234\,LV_5 + 0.1039\,LV_6 \quad (6.5)$$

Therefore, six latent variables were used to build both top and bottom composition models.

Figures 6.33 and 6.34 shows the estimations of the static PLS model. It can be seen from this figure that the model estimations of static PLS are very accurate where the estimation signal follows the actual compositions precisely.

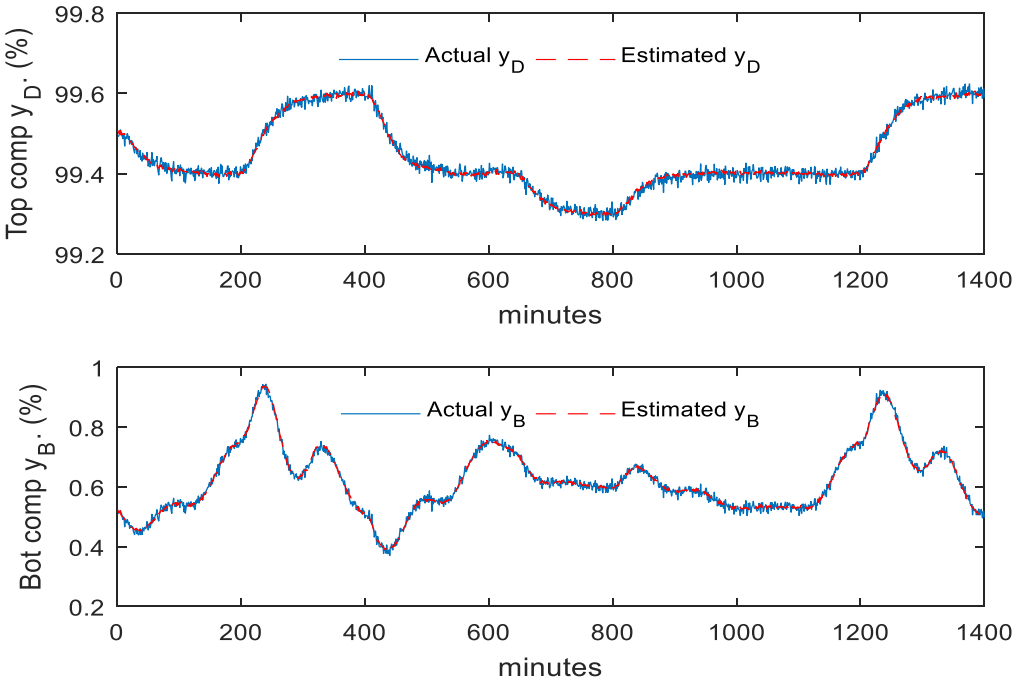

Figure 6.33: Model estimation of static PLS model (training data)

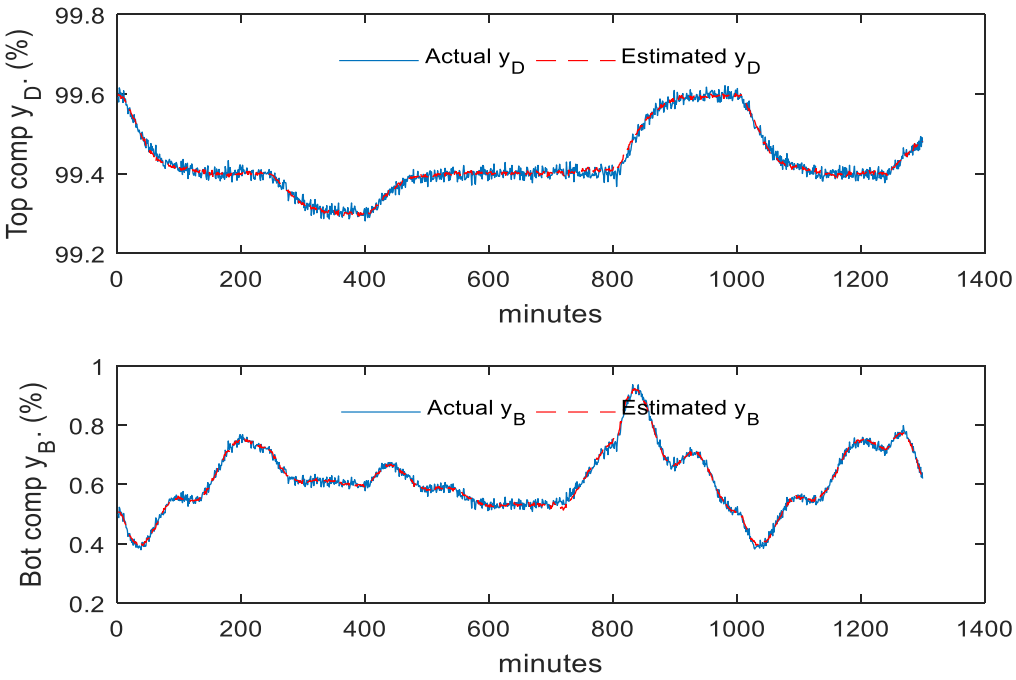

Figure 6.34: Model estimation of static PLS model (testing data)

6.7.2 Dynamic PLS models

In order to further improve the estimation of the static PLS model, dynamic PLS models are developed. In this research, dynamic PLS models with orders ranging from 1–5 were built.

Data partition and data scaling are the same as in developing static PLS models. Table 6.9 presents the number of latent variables and the corresponding SSE values on the testing data of nine dynamic PLS models.

Table 6.9: SSE of different dynamic PLS models on the testing data

Order of dynamic model	**Product compositions**	**No of LV**	**SSE**
Static PLS model	Top Comp	6	21.5957
	Bot comp	6	13.1389

1st order dynamic PLS model	Top Comp	7	20.5056
	Bot comp	8	12.9832
2nd order dynamic PLS model	Top Comp	15	18.8667
	Bot comp	18	11.3227
3rd order dynamic PLS model	Top Comp	19	17.5135
	Bot comp	21	10.6982
4th order dynamic PLS model	Top Comp	16	16.4601
	Bot comp	23	10.0834
5th order dynamic PLS model	Top Comp	22	15.3769
	Bot comp	21	9.4759

It can be seen from this table that the estimation accuracy of the dynamic PLS models have been significantly enhanced compared to the static PLS model, especially at the 5th order. In addition, the 5th order dynamic PLS model was selected since it has the lowest SSE value. This dynamic PLS model was integrated with the ADRC scheme to control the product compositions using tray temperature measurements. The estimations from the 5th order dynamic PLS model are shown in Figures 6.35 and 6.36. Again, in this figure the red solid lines represent the actual measured compositions while the blue solid lines represent the corresponding model estimations.

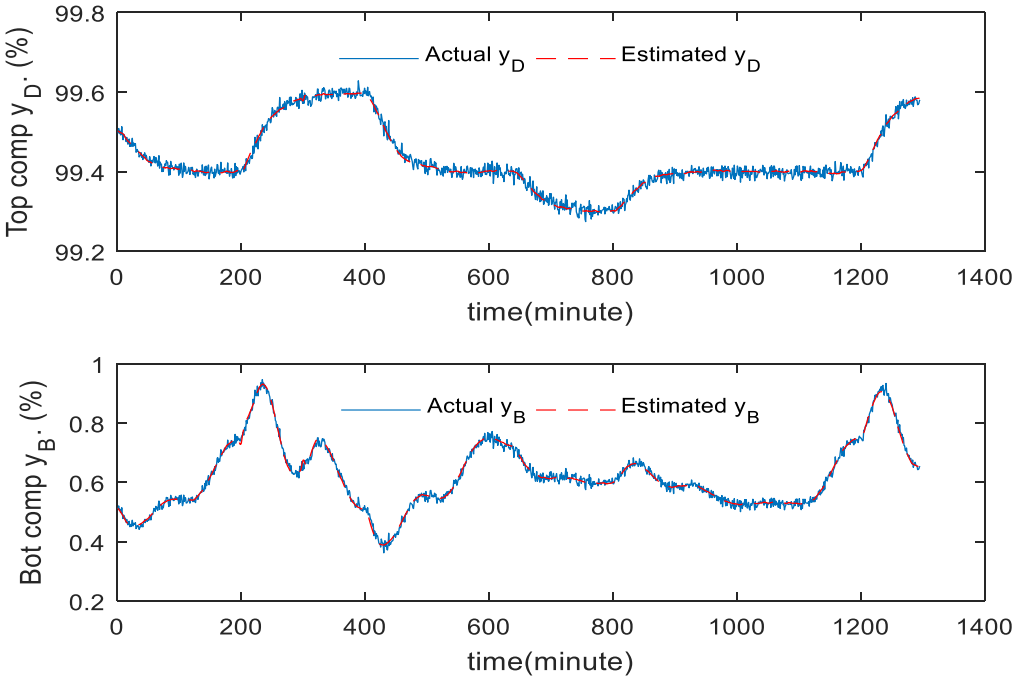

Figure 6.35: Model estimation of dynamic PLS model (training data)

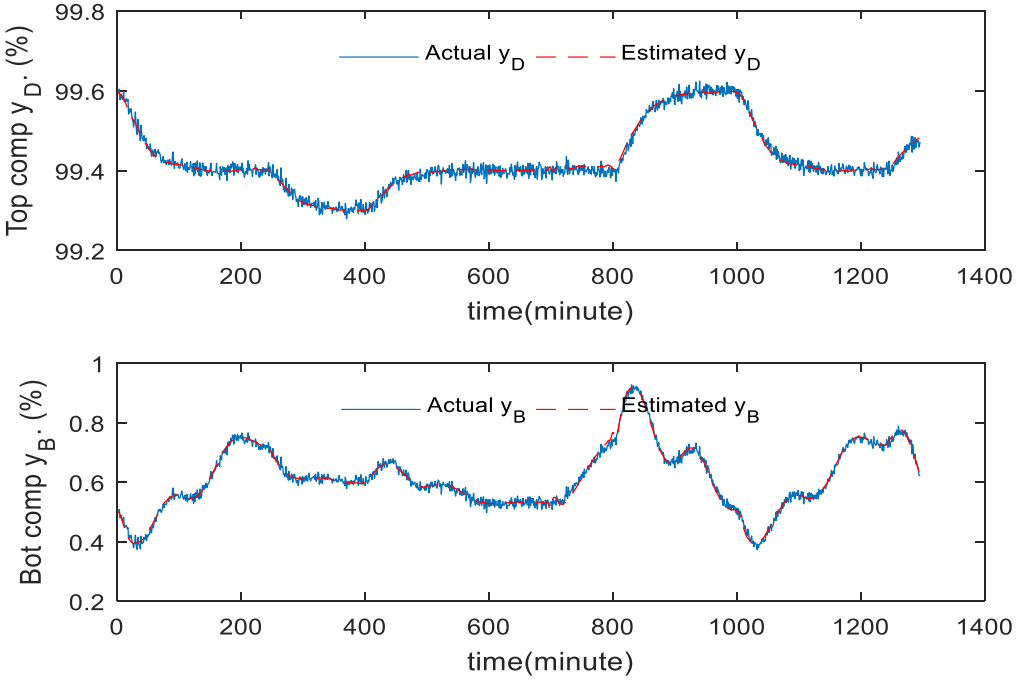

Figure 6.36: Model estimation of dynamic PLS model (testing data)

Figures 6.37 and 6.38 present the estimation errors for both the static and 5th order dynamic PLS models. It can be noticed from this figure and as expected, the 5th order dynamic PLS model shows better estimation performance than the static model.

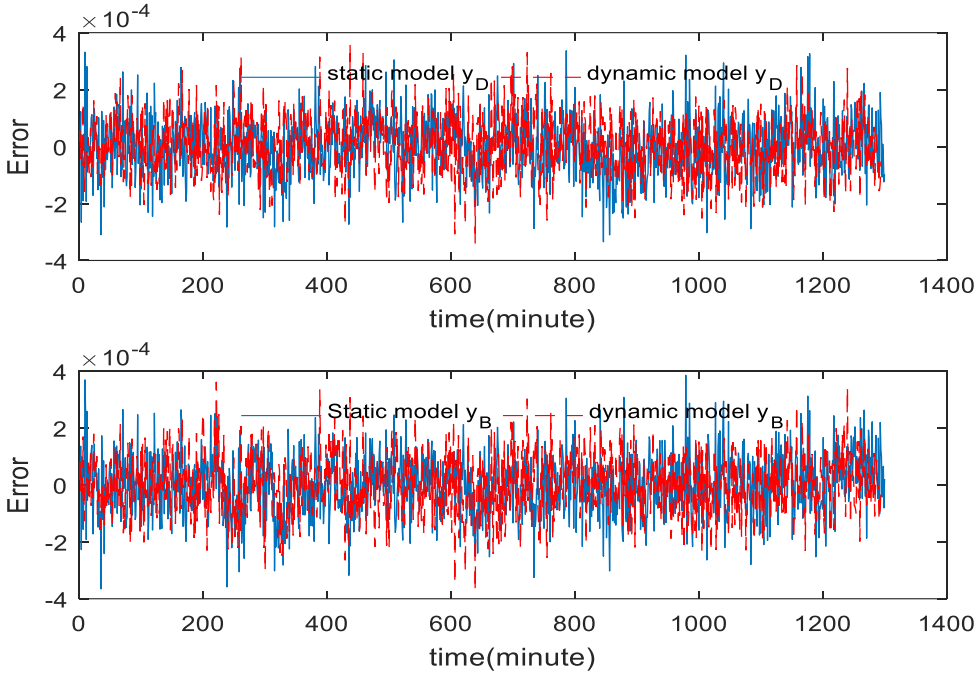

Figure 6.37: Model prediction error (training data)

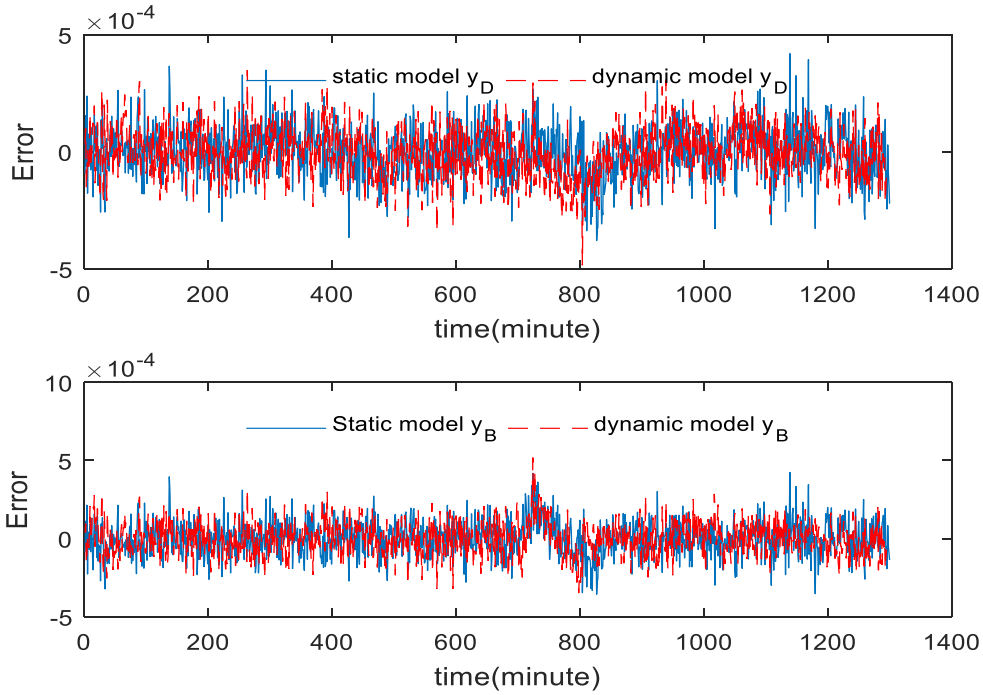

Figure 6.38: Model prediction error (testing data)

6.7.3 Inferential control performance

Figure 6.39 shows the control performance of the inferential ADRC with the static PLS model across a wide range of set-point changes. It can be seen from this figure that large control offsets exist at both product compositions due to the estimation errors of the static PLS model, which become worse when operating conditions change, such as during a set-point change. Figure 6.40 shows the control performance of the inferential ADRC with the 5^{th} order dynamic PLS model for the same set-point changes and feed composition disturbance. It can be seen from this figure that the control performance improved under the dynamic PLS model with small control offsets at both product compositions.

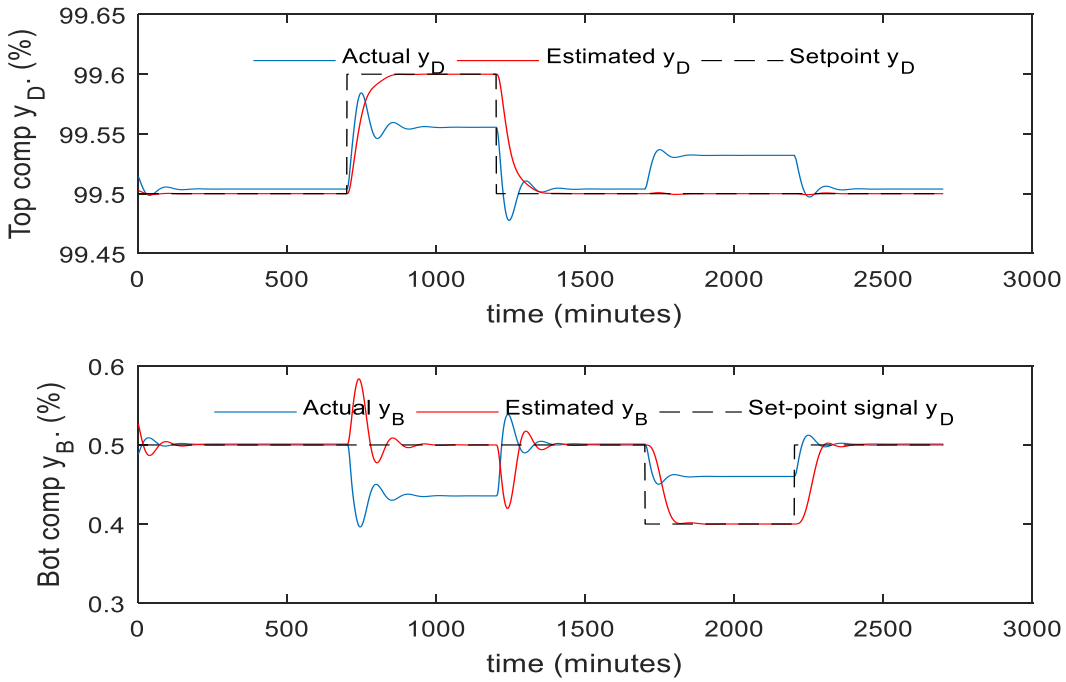

Figure 6.39: Responses of actual and estimated product composition of the static inferential scheme (without the mean updating technique)

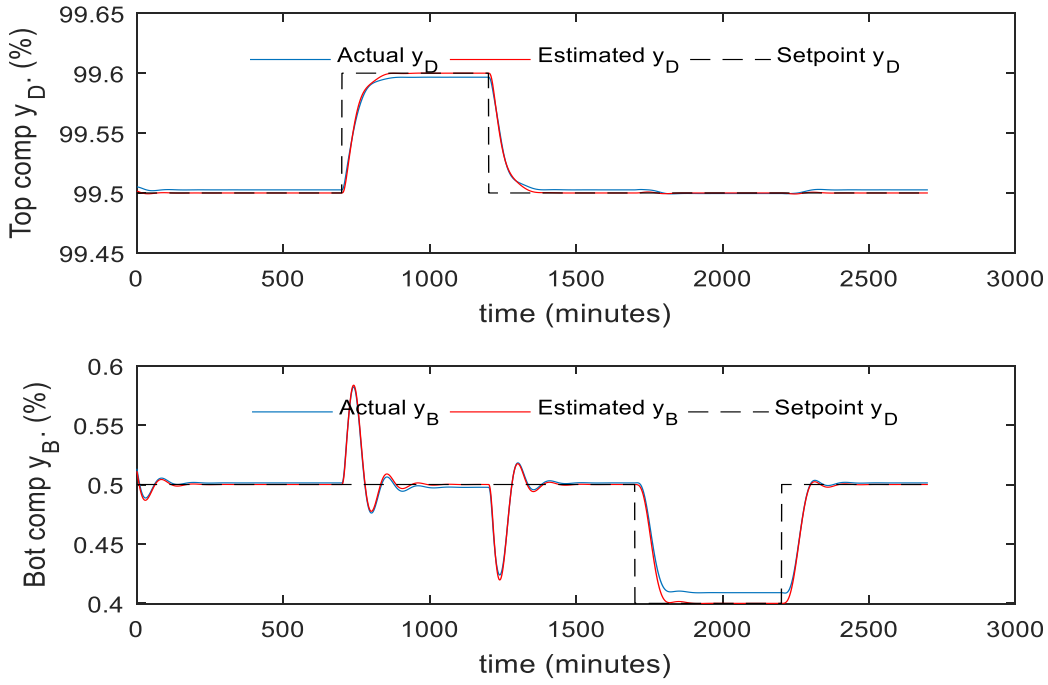

Figure 6.40: Responses of actual and estimated product composition of the 5th dynamic inferential scheme (without the mean updating technique)

The existence of undesired control offset in both the static and dynamic inferential ADRC schemes will be again reduced and/or removed by applying the mean updating technique introduced by Zhang (2006) in order to enhance overall product composition performance. Figures 6.41 and 6.42 show the control performance of the inferential ADRC scheme with the mean updating technique. It can be seen from these figures that the mean updating technique is an effective means of eliminating steady state control offsets. Moreover, the SSE of control errors have been reduced considerably after implementing this method as shown in Table 6.10.

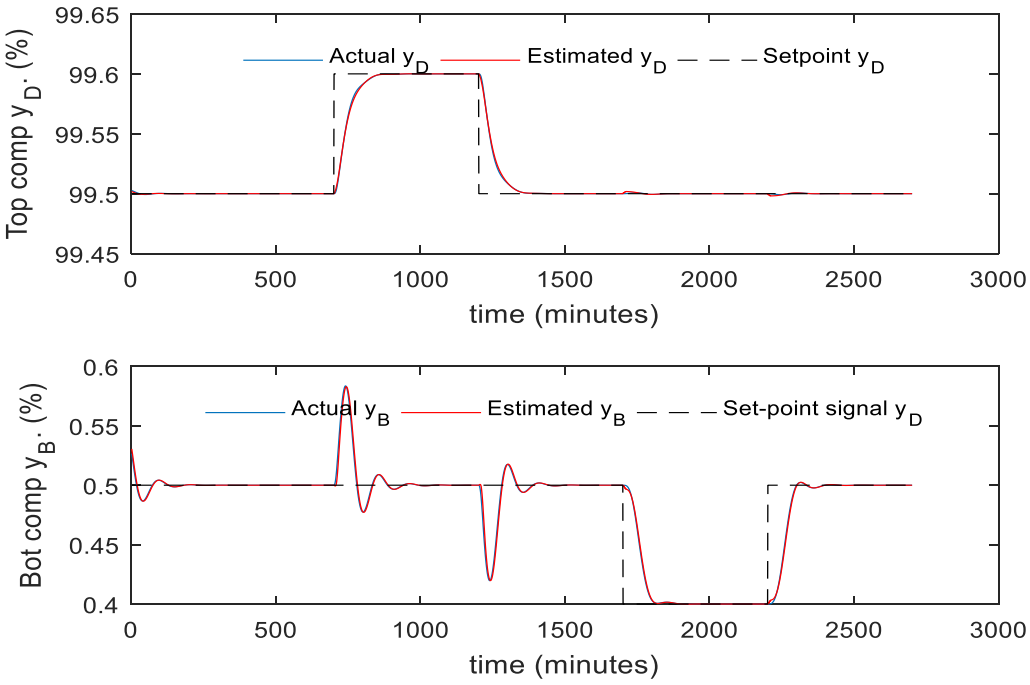

Figure 6.41: Responses of actual and estimated product composition of the static inferential scheme (with the mean updating technique)

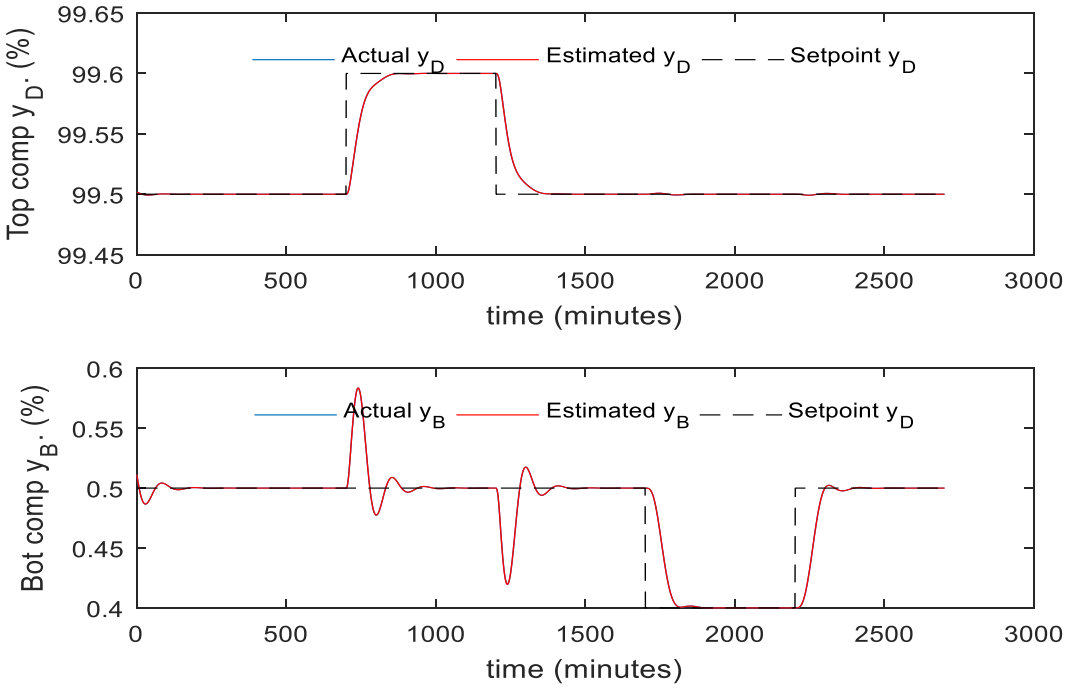

Figure 6.42: Responses of actual and estimated product composition of the 5th inferential scheme (with the mean updating technique):

Table 6.10: SSE of static and dynamic inferential PLS schemes

Control schemes		Top Comp.	Bottom Comp.
Inferential ADRC with static PLS model	Without mean updating	8.33	16.690
	With mean updating	7.6392×10^{-4}	8.9755×10^{-5}
Inferential ADRC with 5^{th} order dynamic PLS model	Without mean updating	2.31	4.73
	With mean updating	1.4154×10^{-7}	1.5614×10^{-7}

It can be seen from the above figures that the control offsets and steady state estimation biases were completely eliminated by using the mean updating technique. Furthermore, it can be observed from Table 6.11 that the dynamic estimation model improved over the static model significantly with a large reduction in SSE of control errors. Moreover, the inferential ADRC

scheme based on the PLS model gives as good overall performance as the inferential ADRC scheme based on the PCR model under correlated data.

6.8 Conclusions

The ADRC and conventional multi-loop PI control schemes have been applied here in the HIDiC in order to investigate their performance for set-point tracking and disturbance rejection. Prior to the performance comparison, the 2×2 transfer function matrix was obtained from the mechanistic model based simulation of a HIDiC. The transfer function introduced here was used for identifying the parameters of the PI controller using the BLT approach. Simulation results clearly indicate that the ADRC scheme exhibits a much better dynamic control performance than the traditional PI controller in terms of set-point tracking and disturbance rejection. Moreover, the ADRC control signal in both tests is smooth, non-oscillatory and non-aggressive compared to the control signal of the PI control.

The inferential ADRC control scheme was then proposed for the HIDiC process in order to overcome the problems of large time delay associated with composition analysers. Due to existence of strong correlation in temperature trays of the HIDiC, the product compositions are estimated from multiple tray temperatures using PCR and PLS techniques. Both static and dynamic soft sensors were developed. The soft sensor outputs were operated as an inferential estimator that then feeds back its estimation to the ADRC scheme as a feedback signal to provide online measurements of the product compositions. Excellent control performance was obtained with both types of soft sensors, but the dynamic PCR and PLS soft sensor gave better control performance than the static one. Moreover, the mean updating technique was used to eliminate steady state estimation bias and the resulting control offsets.

Chapter 7 Conclusions and recommendations for future work

7.1. Conclusions

This thesis has examined the advantages of applying the ADRC scheme to a common chemical process: distillation columns. The thesis starts by providing some recent statistics in terms of energy consumption in the chemical industry worldwide. It is shown that distillation columns consume approximately 45% of the energy consumed by the chemical industry, which leads to an increase in production costs. In order to reduce energy consumption in distillation columns, some options have been introduced such as changing the operating conditions, changing the design of the column, preheating the feed rate and implementing some optimal control solutions. In addition, this has motivated control researchers to develop various control schemes for distillation columns to reduce energy consumption and associated costs. It has been identified through the existing literature that the PID control scheme is the most common control scheme applied to distillation columns. Moreover, it has been argued by some researchers that the simplicity of the PID controller leads to some major limitations such as sudden set-point jumps, noise degeneration in the derivative control '*D*', oversimplification in the form of linear weighted sum control law, and complications due to the integral term '*I*'. It was also found that some existing control theories are not practical because they require an accurate mathematical model of the controlled plant, which may not be easy to obtain in the real world, especially for complex industrial processes. As a result, it was expected that the ADRC scheme could overcome these limitations due to its independence from the mathematical model of the controlled plant. Therefore, the core aim and contribution of this research was to design and develop an inferential ADRC technique to control conventional distillation columns and HIDiCs. Chapter 2 presents comprehensive background information about the characteristics, design and advantages of the ADRC components and the inferential control.

Since the Wood–Berry distillation column model has been considered as a classical process control example that has been widely used in many previous research papers concerned with MIMO process control, it has been adopted as the first case study used in this research. Control of the Wood–Berry distillation column using ADRC is presented in Chapter 3, where all its basic features are explained. First, the BLT tuning method was applied to MIMO transfer function of

the Wood–Berry model in order to specify the parameters of the multi-loop PI controller. Then, PI and ADRC schemes were applied to the MIMO system. Both control schemes were analysed and investigated through several tests such as set-point tracking, robustness capability and disturbance rejection. The controlled variables specified are the top and bottom product compositions, while the manipulated variables are reboiler boil up rate and reflux flow rate. The simulation results clearly indicate that the ADRC scheme provides better performance than the PI controller in terms of set-point tracking, disturbance rejection, robustness, and coping with loop interactions.

A binary distillation column for separating methanol and water simulated using rigorous mechanistic model was selected and used as a second case study. The mechanistic model of this column is presented in Chapter 4. The reflux flow-rate (L) and vapour flow rate (v) are used as manipulated variables to control the product composition of binary distillation columns. Furthermore, the feed flow-rate (F) and feed composition (x_f) are considered external disturbances to which the binary column is subjected. Prior to applying the PI controller, a process reaction curve technique is used to generate the 2×2 MIMO transfer function using simulated step test data for the purpose of PI tuning. Simulation results show that the ADRC scheme has the ability to provide fast and smooth dynamic performance under various amounts of disturbance, where it has the capability to force the output signal to follow the desired set-point signal rapidly and avoid any unexpected undesired overshoot. The SSE values of the ADRC scheme are much lower than those of the PI controller, demonstrating the efficiency of ADRC compared to the conventional PI controller.

Like any control scheme, the ADRC technique needs measurements of the controlled variables without much delay. Unfortunately, obtaining delay-free measurements for the product compositions is not possible via current measurement tools, such as gas analysers. These tools have some drawbacks such as high maintenance costs and a large measurement delay of around 5–20 min as explained in Chapter 5. This chapter proposes integrating inferential control with the ADRC scheme to control the binary distillation column. In this scheme, the top composition (Y_1) and bottom composition (Y_2) were considered the primary controlled variables whereas the secondary measurements are the tray temperatures (x). Due to the existence of correllation among the tray temperature measurements, static inferential estimation models were designed and implemented via PCR and PLS techniques. Then, the developed inferential estimation models

were integrated with the ADRC scheme. The static estimation bias and the resulting static control offset due to the variation in process operating conditions were eliminated via the mean updating technique introduced by Zhang (2006). In order to futher improve the inferential estimation performance, dynamic inferential PCR and PLS models were developed and integrated with the ADRC scheme to form the dynamic inferential ADRC scheme. Based on the simulation results, this scheme provided a more accurate estimation compared to the static inferential ADRC scheme. It can be concluded that the inferential ADRC scheme provides better control performance compared to the single tray temperature control and direct composition control using measurements from gas analysers. It can be also observed that there is no difference between PCR and PLS approaches in terms of estimation accuracy except that the PLS techniques required fewer LVs compared to the PCR technique.

Due to the promising results achieved from applying the ADRC scheme to the simple binary distillation column, it was of significant importance to further investigate the efficiency of this control scheme in controlling more complex distillation columns such as the HIDiC. The HIDiC is a new distillation technology introduced to reduce energy consumption in the distillation process. However, it is difficult to control due to strong loop interactions and time delay associated with product composition measurements. The mechanistic model of the HIDiC for seperating a benzene and toluene mixture was adopted and presented in Chapter 6 where all characteristics and assumptions were explained. The rectifiying pressure (P_r) and feed thermal condition (q) are used as manipulated variables to control the product compositions of the HIDiC. The feed composition (z) is considered an external disturbance to the HIDiC. Before operating and controlling the HIDiC by PI controller, the 2×2 MIMO transfer function was identified first for the PI tuning purpose. The tuning parameters of the PI controller were then altered using the BLT tuning method. After that, PI and ADRC schemes were analysed and specified individually. Simulation results clearly show that the ADRC scheme produces much better dynamic control performance than the traditional PI controller in terms of set-point tracking, loop interaction and disturbance rejection. Moreover, the control signal of the ADRC scheme in both tests is practical, smooth, non-oscillating and non-aggressive compared to the control signal of the PI scheme. An inferential ADRC control scheme was proposed to overcome the problem of long time delays in composition measurements. The 54 tray temperatures (x) of the HIDiC were considered secondary variables to estimate the top composition (Y_1) and bottom composition (Y_2). First, the static inferential model was designed and

implemented using both PCR and PLS techniques to overcome the strong correlation among tray temperatures., The static inferential ADRC scheme was then implemented with mean updating in order to reduce estimation bias. It is believed that the estimation model can be further enhanced and improved by implementing the dynamic inferential ADRC scheme. The suitable dynamic model was selected based on the lowest SSE. Finally, the dynamic model was combined with the ADRC to form the dynamic inferential ADRC scheme. The mean updating technique was used again to eliminate the undesired static control offset. Overall, performance of the dynamic inferential ADRC scheme is better than the static one.

7.2 Recommendations for future work

The work presented in this thesis shows the efficiency and success of the ADRC control scheme in controlling non-linear distillation columns compared to the PI controller over a wide range of operating conditions. Furthermore, it also shows the ability of the inferential ADRC scheme in eliminating undesired measurement delays introduced from the current measurement tools. In this section, some recommendations on possible guidelines for future work are presented.

i. Robustness analysis of ADRC on distillation column control

As mentioned in Chapter 2, the ADRC scheme needs little information about the dynamic plant system where the discrepancy between the mathematical model and the dynamic system is considered a generalised disturbance that will be estimated by ESO and then successfully compensated in the control law. In this research, and due to the time limitation, the model uncertainty and its impact on ADRC control performance for the Wood–Berry distillation column has been investigated in the time domain. In addition, and as future research, the model uncertainty and its effect on ADRC control performance should be investigated in the frequency domain using some robustness analysis techniques such as structured singular value analysis (μ-analysis).

ii. Implementation of the inferential ADRC scheme in the chemical and oil and gas industries

In this thesis, the inferential ADRC controller shows successful, efficient and promising results. It can be further enhanced and applied to other oil and gas industries and similar industrial processes in which the controlled or primary variables are inaccessible or cannot be measured directly online

and depend on laboratory assays associated with long-time analysis. It can also be applied on non-linear and time-varying industrial processes that are associated with strong loop interactions, external disturbance and continuous set-point changes.

In my country, Oman, the Oil Refineries and Petroleum Industries Company (ORPIC) for example, use both the Crude Distillation Unit (CDU) and Vacuum Distillation Unit (VDU) to distil and separate valuable distillates such as oil, naphtha, kerosene, diesel and atmospheric gas oil (AGO) from the crude feedstock stream. They use the multi-loop PI control scheme to control these distillation columns. They also use gas chemography and lab samples to measure product compositions. The average production cost in Oman is approximately 28 $ per barrel. In the future, it is essential to implement the inferential ADRC scheme in their processes to improve overall control performance and consequently reduce the huge amount of energy consumption and associated production costs.

Bibliography

Abdi, H. (2003) Partial Least Squares (PLS) Regression, in *Encyclopedia for research methods for the social sciences*, pp. 792–795.

Abdi, H. (2010) Partial least squares regression and projection on latent structure regression (PLS Regression). *Wiley Interdisciplinary Reviews: Computational Statistics*, 2 (1), pp. 97–106.

Abolpour, B., Abolpour, R., Shamseddini, A., Kamyabi, S. & Hamzehee, F. (2013) Optimization of the reflux ratio for methanol-water stage distillation column. *Research on Chemical Intermediates*, 39 (2), pp. 681–692.

Abusnina, A., Kudenko, D. & Roth, R. (2014) 'Improving robustness of gaussian process-based inferential control system using kernel principle component analysis', in *Proceedings - 2014 13th International Conference on Machine Learning and Applications, ICMLA 2014*, pp. 99–104.

Acharya, P., Dumpa, G. & Dan, T.K. (2016) Modelling and control of distillation column, in *Computation of Power, International Conference on* e*nergy Information and Commuincation (ICCPEIC)*, pp. 123–128.

Adel, I.M., Elamvazuthi, I. & Hanif, N.H.H.B.M. (2009) Monitoring and controlling system for binary distillation column, in *SCOReD2009 - Proceedings of 2009 IEEE Student Conference on Research and Development*, pp. 453–456.

Ahuja, A., Narayan, S. & Kumar, J. (2016) Optimal two degrees of freedom decoupling smith control for MIMO systems with multiple time delays, 2016 *IEEE International Conference*

on Power Electronics, Intelligent Control and Energy Systems (ICPEICES), pp. 1–5.

Al-Dunainawi, Y. & Abbod, M.F. (2016) Evolutionary based optimisation of multivariable fuzzy control system of a binary distillation column, *2016 UKSim-AMSS 18th International Conference on Computer Modelling and Simulation*, pp. 127–132.

Al-Muslim, H., Dincer, I. & Zubair, S.M. (2003) Exergy analysis of single-and two-stage crude oil distillation units. *Transaction of American Society of Mechanical Engineering, Journal of Energy Resources Technology*, 125 (3), pp. 199–207.

Alhajji, M. & Demirel, Y. (2015) Energy and environmental sustainability assessment of a crude oil refinery by thermodynamic analysis. *International Journal of Energy Research*. 39 (14), pp. 1925–1941.

Alibuhtto, M.C. & Peiris, T.S.G. (2015) *Principal component regression for solving multicollinearity problem*.

Almodaresi, E. & Bozorg, M. (2017) k P-stable regions in the space of PID controller coefficients. *IET Control Theory & Applications*, pp. 1642-1647.

Andrijić, Ž.U., Mohler, I., Bolf, N. & Dorić, H. (2017) Development of inferential models for fractionation reformate unit, *2017 21st International Conference in Process Control (PC),*. pp. 143–148.

Åström, K. and Hägglund, T. (1995) PID controllers: theory, design, and tuning, *Instrument society of America Research Triangle Park*, pp. 343-343.

De Assis, A.J. & Maciel Filho, R. (2000) Soft sensors development for on-line bioreactor state estimation, *in Computers and Chemical Engineering*, pp. 1099–1103.

Bahar, A., Güner, E., Ozgen, C., Engineering, C. & Technical, M.E. (2006) Design of State Estimators for the Inferential Control of an Industrial Distillation Column, *International Joint Confernce On Neural Network*, pp. 1112–1115.

Baratti, R., Bertucco, A., Da Rold, A. & Morbidelli, M. (1995) Development of a composition estimator for binary distillation columns. Application to a pilot plant, *Chemical Engineering Science*. 50 (10), 1541–1550.

Bendib, R., Bentarzi, H. & Zennir, Y. (2015) Investigation of the effect of design aspects on dyanamic control of a binary distillation column, *2015 IEEE 4th International Conference In Electrical Engineering (ICEE)*, pp. 1–5.

Bisgaard, T., Huusom, J.K. & Abildskov, J. (2013) A modeling framework for conventional and heat integrated distillation columns', in *IFAC Proceedings Volumes (IFAC-PapersOnline)*. pp. 373–378.

Bisgaard, T., Skogestad, S., Abildskov, J. & Huusom, J.K. (2017) Optimal operation and stabilising control of the concentric heat-integrated distillation column (HIDiC). *Computers and Chemical Engineering*. 96196–211.

Biyanto, T.R., Rahman, J.A., Laila, H.N., Abdurrakhman, A. & Darwito, P.A. (2017) Techno Economic Optimization of Petlyuk Distillation Column Design Using Duelist Algorithm. *Procedia Engineering*, pp. 520–527.

Bolder, J., Oomen, T. & Steinbuch, M. (2014) Aspects in inferential Iterative Learning Control: A 2D systems analysis', *in Proceedings of the IEEE Conference on Decision and Control*. . 2014 pp. 3584–3589.

Bolf, N., Ivandic, M. & Galinec, G. (2008) Soft sensors for crude distillation unit product properties estimation and control', *in 2008 Mediterranean Conference on Control and Automation - Conference Proceedings,* pp. 1804–1809.

Budman, H.M., Webb, C., Holcomb, T.R. & Morari, M. (1992) Robust Inferential Control for a Packed-Bed Reactor, *Industrial and Engineering Chemistry Research*. 31 (7), pp. 1665–1679.

Cao, S., Shi, L., Ze, X. & Zhang, H. (2008) Continuously sintering furnace temperature control system based on intelligent PID adjustment, *in Proceedings of the 2008 International Conference on Computer and Electrical Engineering ICCEE* ,pp. 190–193.

Chen, C., Wang, Y., Zhang, Y., & Zhai, Y. (2017) Indoor Positioning Algorithm Based on Nonlinear PLS Integrated With RVM, *IEEE Sensors Journal*, *18*(2), pp. 660-668.

Chen, J., Omidvar, M.N., Azad, M. & Yao, X. (2017) Knowledge-based particle swarm optimization for PID controller tuning, *2017 IEEE Congress in Evolutionary Computation (CEC)*, pp. 1819–1826.

Chen, W.H., Yang, J., Guo, L. & Li, S. (2016) Disturbance-Observer-Based Control and Related Methods - An Overview, *IEEE Transactions on Industrial Electronics*, 63 (2), pp.1083–1095.

Chen, Z.., Zheng, Q. & Gao, Z. (2007) Active Disturbance Rejection Control of Chemical Processes. *2007 IEEE International Conference on Control Applications*, pp. 1–3.

Chong, Y and Zhang, K. (2010) Study on the active disturbance rejection control of servo system, *2010 International Conference on Computer and Communication Technologies in*

Agriculture Engineering, pp. 364-367.

Chunzhe, Z., Donghai, L., Li, S. & Lingling, T. (2015) Parameter tuning for decentralized low-order active disturbance rejection control scheme', *2015 IEEE 54th Annual Conference in Society of Instrument and Control Engineers of Japan (SICE),* pp. 422–427.

Cominos, P. & Munro, N. (2002) PID controllers : recent tuning methods and design to specification, *IEEE proceedings Control Theory and Application*. 149 (1), pp. 46–53.

Cong, L. (2015a) Nonlinear wave modeling and generic model control of heat integrated distillation column, *2015 10th Asian Control Conference (ASCC)*, pp. 1-6.

Cong, L., Chang, L. & Liu, X. (2015b) Nonlinear-wave based analysis and modeling of heat integrated distillation column. *Separation and Purification Technology*, pp. 119–131.

Contreras-Zarazúa, G., Vázquez-Castillo, J.A., Ramírez-Márquez, C., Segovia-Hernández, J.G. & Alcántara-Ávila, J.R. (2016) Multi-objective optimization involving cost and control properties in reactive distillation processes to produce diphenyl carbonate, *Computers and Chemical Engineering*, pp. 185-196.

Costa, B., de Almeida, J.. & Angélico, B.. (2012) Application of optimization heuristics in tuning decentralized PID controllers, *2012 10th IEEE/IAS International Conference on Industry Applications (INDUSCON),* pp. 1–8.

De, J., Barçante, G., Cavalcante, M., Da, O. & Torrico, B. (2010) PI multivariable control applied to temperature and humidity neonate incubators, *2010 9th IEEE/IAS International Conference on Industry Applications, INDUSCON 2010*, pp. 1-6.

Dekemele, K., Ionescu, C.-M., De Doncker, M. & De Keyser, R. (2016) Closed loop control of

an electromagnetic stirrer in the continuous casting process, *2016 IEEE European Control Conference (ECC),* pp. 61–66.

Demirel, Y. (2013) Sustainable operations for distillation columns. *Chem. Eng. Process Tech.* 11005.

Desai, R., Patre, B. & Pawar, S. (2018) Active disturbance rejection control with adaptive rate limitation for process control application', in *2018 IEEE Indian Control Conference (ICC)*, pp. 131–136.

Deshpande, P. & Deshpande, A. (2012) Inferential control of DC motor using Kalman Filter, *2012 2nd International Conference on Power, Control and Embedded Systems (ICPCES)*, pp. 1–5.

Deshpande, P (1989) *Multivariable process control*. Instrument Society of America.

Deshpande, P & Ash, R. (1983) *Elements of computer process control, with advanced control applications*. Instrument society of America.

Díaz, S., Pérez-Correa, J.R., Cipriano, A. & Fernández-Fernández, M. (2016) Intelligent control applications on a binary distillation column, *2016 IEEE International Conference on Automatica (ICA-ACCA)*, pp. 1–8.

Dinh, H. Truong, D. Nguyen, T. Truong, X and Nguyen, C. (2017) Active disturbance rejection control design for integrated guidance and control missile based SMC and extended state observer, *2017 International Conference on System Science and Engineering (ICSSE)*, pp. 476-481.

Dong, L. Zheng, q and Gao, Z. (2008) On Control System Design for the Conventional Mode of

Operation of Vibrational Gyroscopes, *in IEEE Sensors Journal*, 8, pp. 1871-1878.

Dong, Z. & Zhang, J. (2015) An active disturbance rejection controller design for ball and plate system, in *Chinese Control Conference*, pp. 928–933.

Du, Y, del Villar, R. & Thibault, J. (1997) Neural net-based softsensor for dynamic particle size estimation in grinding circuits. *International Journal of Mineral Processing*. 52 (3), pp. 121–135.

Dumpa, G., Acharya, P. & Dan, T.K. (2016) Comparative analysis of different control techniques for a distillation column, *2016 IEEE International Conference on Computation of Power, Energy Information and Commuincation (ICCPEIC)*, pp. 52–57.

Fazlali, A., Hosseini, S., Yasini, B. & Moghadassi, A. (2009) Optimization of operating conditions of distillation columns: An energy saving option in refinery industry. *Songklanakarin Journal of Science and Technology*. 31 (6), pp. 661–664.

Feng, J., Jacy, Q., Hamaguchi, T., Ota, Y. & Hashimoto, Y. (2006) Design and control of HIDiC, *in 2006 SICE-ICASE International Joint Conference*, pp. 5727–5730.

Fernandez De Canete, J., Garcia-Cerezo, A., Garcia-Moral, I., Del Saz, P. & Ochoa, E. (2013) Object-oriented approach applied to ANFIS modeling and control of a distillation column. *Expert Systems with Applications*. 40 (14), pp. 5648–5660.

Forbes, R. (1970) *A short history of the art of distillation: from the beginnings up to the death of Cellier Blumenthal*. Brill.

Fortuna, L., Graziani, S. & Xibilia, M. (2005) Soft sensors for product quality monitoring in debutanizer distillation columns. *Control Engineering Practice*, 13 (4), pp. 499–508.

Freshwater, D. (1961) The heat pump in multi-component distillation. *British Chem,* 6, pp. 388–391.

Freshwater, D & Pike, K. (1967) Vapor-Liquid Equilibrium Data For Systems Of Acetone-Methanol-Isopropanol. *Journal of Chemical and Engineering Data*, 12 (2), pp. 179–183.

Fuentes, C. & Luyben, W.(1983) Control of High-Purity Distillation Columns. *Industrial and Engineering Chemistry Process Design and Development*, 22 (3), pp. 361–366.

Fukushima, T., Kano, M. & Hasebe, S. (2006) Dynamics and control of heat integrated distillation column (HIDiC), *Journal of Chemical Engineering of Japan*. 39 (10), pp. 1096–1103.

Funk, G., Houston, B & Stacy, G. (1978) Making energy-conservation pay through automation. *Chemical Engineering Progress*, 74 (5), pp. 66–70.

Gagnon, E., Pomerleau, A. & Desbiens, A. (2003) A new representation of the generalized relative dynamic gains, *AIAA Guidance, Navigation and Control Conference and Exhibit*, pp. 1–4.

Gagnon, P., Bédard, M. & Desgagné, A. (2017) An Efficient Bayesian Robust Principal Component Regression. *arXiv preprint arXiv:1711.06341*.

Gao, Z. (2015) Active disturbance rejection control: from an enduring idea to an emerging technology, *2015 IEEE 10th International Workshop on Robot Motion and Control (RoMoCo),* pp. 269–282.

Gao, Z. (2014) On the centrality of disturbance rejection in automatic control. *ISA Transactions*, 53 (4).pp. 850–857.

Gao, Z. (2006a) Active disturbance rejection control: a paradigm shift in feedback control system design, *in 2006 American Control Conference*, pp 7 - 13.

Gao, Z. (2006b) Scaling and bandwidth-parameterization based controller tuning, *in Proceedings of the American control conference*, pp. 4989–4996.

Gao, Z., Huang, Y. & Han, J. (2001) An alternative paradigm for control system design. *Proceedings of the IEEE Conference on Decision and Control* ,5, pp. 4578–4585.

Garcia, D., Karimi, A. & Longchamp, R. (2007) Robust proportional integral derivative controller tuning with specifications on the infinity-norm of sensitivity functions. *IET Control Theory & Applications*. 1 (1), pp. 263–272.

Garrido, J., Vázquez, F. & Morilla, F. (2011) An extended approach of inverted decoupling. *Journal of Process Control*. 21 (1), pp. 55–68.

Geladi, P. & Kowalski, B. (1986) Partial least-squares regression: a tutorial. *Analytica Chimica Acta*. 185 (C), pp. 1–17.

Glenchur, T. & Govind, R. (1987) Study on a continuous heat integrated distillation column. *Separation Science and Technology*. 22 (12), pp. 2323–2338.

Goforth, F. (2004). On motion control design and tuning techniques, *Proceedings of the 2004 American Control Conference*,1, pp. 716-721.

Gong, X., Bai, Y., Peng, C., Zhao, C. & Tian, Y. (2012) Trajectory tracking control of a quad-rotor UAV based on command filtered backstepping, *2012 3rd International Conference on Intelligent Control and Information Processing ICICIP*, pp. 179–184.

Grosdidier, P. & Morari, M. (1987) A computer aided methodology for the design of

decentralized controllers. *Computers and Chemical Engineering*. 11 (4), pp. 423–433.

Gross, F., Baumann, E., Geser, A., Rippin, D.W.T. & Lang, L. (1994) Modelling, simulation and controllability analysis of an industrial heat-integrated distillation process, *in Integration of Process Design and Control*, pp. 73–78.

Guilandoust, M., Julian Morris, A. & Tham, M. (1988) An Adaptive Estimation Algorithm for Inferential Control. *Industrial and Engineering Chemistry Research*, 27 (9), pp. 1658–1664.

Han, J. (2009) From PID to active disturbance rejection control, *in IEEE Transactions on Industrial Electronics*, pp. 900–906.

Harmsen, J. (2010) Process intensification in the petrochemicals industry: Drivers and hurdles for commercial implementation. *Chemical Engineering and Processing: Process Intensification*. 49 (1), pp. 70–73.

Haselden, G (1958) An approach to minimum power consumption in low temperature gas separation. *Chem. Eng. Res*, pp. 36, 123–132.

Hou, Y., Gao, Z., Jiang, F. & Boulter, B. (2001) Active disturbance rejection control for web tension regulation. *Proceedings of the 40th IEEE Conference on Decision and Control (Cat. No.01CH37228)*, 5, pp. 4974–4979.

Huang, K., Nakaiwa, M., Akiya, T., Aso, K. & Takamatsu, T. (1996) A numerical consideration on dynamic modeling and control of ideal heat integrated distillation columns. *Journal of Chemical Engineering of Japan*, 29 (2), pp. 344–351.

Huang, Y. & Xue, W. (2014) Active disturbance rejection control: Methodology and theoretical analysis. *ISA Transactions*. 53 (4), pp. 963–976.

Hussain, T., Siniscalchi, S.M., Lee, C.-C., Wang, S.-S., Tsao, Y. & Liao, W.-H. (2017) Experimental Study on Extreme Learning Machine Applications for Speech Enhancement. *IEEE Access*, *5*, pp. 25542-25554.

Jain, M. & Lakshminarayanan, S. (2007) Estimating performance enhancement with alternate control strategies for multiloop control systems. *Chemical Engineering Science*. 62 (17), pp. 4644–4658.

Jana, A.K. (2010) Heat integrated distillation operation. *Applied Energy*. 87 (5), pp. 1477–1494.

Jeffries, S, Al-Abri, S. & Zhang, J. (2016) Inferential disturbance observer based control of a binary distillation column, *IECON 2016-42nd Annual Conference of the IEEE Industrial Electronics Society*, pp. 190–195.

Jogwar, S. & Daoutidis, P. (2010) Dynamics and control of energy integrated distillation column networks. *Proceedings of the 2010 American Control Conference*, pp. 2835–2840.

Kadhar, K., Baskar, S. & Amali, S. (2015) Diversity Controlled Self Adaptive Differential Evolution based design of non-fragile multivariable PI controller. *Engineering Applications of Artificial Intelligence*, 46, pp. 209–222.

Kadlec, P and Gabrys, B. (2008) Adaptive Local Learning Soft Sensor for Inferential Control Support, *2008 International Conference on Computational Intelligence for Modelling Control & Automation*, pp. 243-248.

Kai, S. & Yanlei, Z. (2010) A speed observer for speed sensorless control of induction motor, *2010 2nd International Conference on Future Computer and Communication (ICFCC)*, 3, pp. 257-263.

Kalivas, J.(2001) Basis sets for multivariate regression. *Analytica Chimica Acta*. 428 (1), pp. 31–40.

Kalpana, D., Thyagarajan, T. & Venkatachalam, N. (2017) Design of fractional order PI controller for MIMO system using relay feedback', *Trends in Industrial Measurement and Automation (TIMA)*, pp. 1–7.

Kano, M., Showchaiya, N., Hasebe, S., & Hashimoto, I. (2003). Inferential control of distillation compositions: selection of model and control configuration. *Control Engineering Practice*, 11(8), pp 927-933.

Kaspar, M & Ray, W (1992) Chemometric methods for process monitoring and high-performance controller design. *AIChE Journal*, 38 (10), pp. 1593–1608.

Keller, H & Humphrey, J. (1997) Separation Process Technology. *McGrawHill, New York*.

King, C.J. (2013) *Separation processes*. Courier Corporation.

Kiss, A (2013) *Advanced distillation technologies: design, control and applications*. John Wiley & Sons.

Kiss, A. (2014) Distillation technology - still young and full of breakthrough opportunities. *Journal of Chemical Technology and Biotechnology*, 89 (4), pp. 479–498.

Kiss, A.A. & Bildea, C.S. (2011) A control perspective on process intensification in dividing-wall columns. *Chemical Engineering and Processing: Process Intensification*. 50 (3), pp. 281–292.

Kiss, A.A., Landaeta, S.J.F. & Ferreira, C.A.I. (2012) Towards energy efficient distillation technologies–Making the right choice. *Energy*, 47 (1), pp. 531–542.

Kögel, M. & Findeisen, R. (2013) Set-point tracking using distributed MPC, *IFAC Proceedings Volumes (IFAC-PapersOnline*), pp. 57–62.

Koivo, H. & Tanttu, J. (1991) Tuning of PID Conrollers: Survey of Siso and Mimo Techniques. *IFAC Proceedings Volumes*. 24 (1), pp. 75–80.

Kotina, R. Zheng, Q. van den Bogert, J and Gao, Z. (2011) Active disturbance rejection control for human postural sway, *Proceedings of the 2011 American Control Conference*, pp. 4081-4086.

Kresta, J., Macgregor, J. & Marlin, T. (1991) Multivariate statistical monitoring of process operating performance. *The Canadian Journal of Chemical Engineerging*, pp. 6935–6947.

Lee, J. Kesavan, P and Morari, M. (1997) Control structure selection and robust control system design for a high-purity distillation column,' in *IEEE Transactions on Control Systems Technology*, vol. 5, pp. 402-416.

Lee, J. Morari, M and Garcia, C. (1991) State-Estimation-Based Model Predictive Control with On-Line Robustness Tuning Parameters, *1991 American Control Conference*, pp. 2373-2378.

Li, J., Qi, X., Xia, Y., Ma, D., Li, S. & Xu, Y. (2015) On the absolute stability of nonlinear ADRC for SISO systems', *2015 34th Chinese Control Conference (CCC)*, pp. 1571–1576.

Li, J., Xia, Y., Qi, X., Gao, Z., Chang, K. & Pu, F. (2015) Absolute stability analysis of non-linear active disturbance rejection control for single-input–single-output systems via the circle criterion method. *IET Control Theory & Applications*. 9 (15), pp. 2320–2329.

Liao, Z. & Dexter, A. (2010) An inferential model-based predictive control scheme for

optimizing the operation of boilers in building space-heating systems. *IEEE Transactions on Control Systems Technology*. 18 (5), pp. 1092–1102.

Limon, D., Pereira, M., Munoz De La Pena, D., Alamo, T., Jones, C.N. & Zeilinger, M.N. (2016) MPC for Tracking Periodic References. *IEEE Transactions on Automatic Control*. 61 (4), pp. 1123–1128.

Liu, L., Ling, D., Wu, Y. & Zheng, Y. (2017) 'Process model quality monitoring of model predictive controller', *2017 36th Chinese Control Conference (CCC)*, pp. 4391–4396.

Lu, X. & Wang, Y. (2012) Active disturbance rejection guidance for ascent using quadratic transition, in *Proceedings - 2012 International Symposium on Computer, Consumer and Control, IS3C 2012*, pp. 268–271.

Lueprasitsakul, V., Hasebe, S., Hashimoto, I. & Takamatsu, T. (1990) Study of energy efficiency of a wetted-wall distillation column with internal heat integration. *Journal of Chemical Engineering of Japan*. 23 (5), pp. 580–587.

Luyben, W. (1986) Simple Method for Tuning SISO Controllers in Multivariable Systems. *Industrial and Engineering Chemistry Process Design and Development*. 25 (3), pp. 654–660.

Madoński, R. & Herman, P. (2011) An experimental verification of ADRC robustness on a cross-coupled Aerodynamical System, *in Proceedings - ISIE 2011: 2011 IEEE International Symposium on Industrial Electronics*, pp. 859–863.

Manikandan, P., Thangaganapathy, P. & Manamalli, D. (2017) 'Selection of control structure and dual composition control for ethanol-water distillation column', *Trends in Industrial*

Measurement and Automation (TIMA), pp. 1–6.

Mantz, R & De Battista, H. (2002) Sliding Mode Compensation for Windup and Direction of Control Problems in Two-Input−Two-Output Proportional−Integral Controllers. *Industrial & Engineering Chemistry Research*. 41 (13), pp. 3179–3185.

Masoumi, M. & Kadkhodaie, S. (2012) Optimization of energy consumption in sequential distillation column. *World Academy of Science, Engineering and Technology*, 6 (1), pp. 67-80.

Maurya, R. & Bhandari, M. (2016) Fractional Order PID Controller with an Improved Differential Evolution Algorithm', *2016 International Conference on Micro-Electronics and Telecommunication Engineering (ICMETE).* pp. 550–554.

Mejdell, T. & Skogestad, S. (1991) Estimation of Distillation Compositions from Multiple Temperature Measurements Using Partial-Least-Squares Regression, *Industrial and Engineering Chemistry Research* , 30 (12), pp. 2543–2555.

Miccio, M. & Cosenza, B. (2014) Control of a distillation column by type-2 and type-1 fuzzy logic PID controllers. *Journal of Process Control* ,24 (5), pp. 475–484.

Miklosovic, R., Radke, a. & Gao, Z. (2006) Discrete implementation and generalization of the extended state observer. *2006 American Control Conference*, pp. 2209–2214.

Min, Y., Yun, H. & Jeong, H. (1994) Studies on the distillation operation of Baikha-ju. *Journal of the Korean Society for Applied Biological Chemistry*, 37 (1), pp. 9–13.

Mishra, R., Khalkho, R., Kumar, B. & Dan, T (2013) Effect of tuning parameters of a model predictive binary distillation column, *2013 IEEE International Conference on Emerging*

Trends in Computing, Communication and Nanotechnology ICE-CCN. pp. 660–665.

Mohammadzaman, I. & Jamab, A. (2006) Adaptive predictive control of an electromagnetic suspension system with LOLIMOT identifier', *14th Mediterranean Conference on Control and Automation*, pp. 1-6.

Murad, G., Postlethwaite, I., and Gu, D. (1997) A discrete-time internal model-based controller and its application to a binary distillation column. *Journal of Process Control*, 7(6), pp. 451-465.

Nair, R. & Raykar, A. (2017) Performance investigation of vapour recompressed batch distillation for separating ternary wide boiling constituents. *Resource-Efficient Technologies*, pp. 452-458.

Naito, K., Nakaiwa, M., Huang, K., Endo, A., Aso, K., Nakanishi, T., Nakamura, T., Noda, H. & Takamatsu, T. (2000) Operation of a bench-scale ideal heat integrated distillation column (HIDiC): an experimental study. *Computers & Chemical Engineering*. 24 (2–7), pp. 495–499.

Nakaiwa, M., Huang, K., Naito, K., Endo, A., Owa, M., Akiya, T., Nakane, T. & Takamatsu, T. (2000) A new configuration of ideal heat integrated distillation columns (HIDiC). *Computers & Chemical Engineering*. 24 (2), pp. 239–245.

Nandong, J. & Zang, Z. (2014) Multi-loop design of multi-scale controllers for multivariable processes. *Journal of Process Control*. 24 (5), pp. 600–612.

Null, H. (1976) Heat pumps in distillation. Chemical Engineering Progress ,72 (7) pp.58–64.

O'dwyer, A. (2006) Handbook of PI and PID controller tuning rules, pp. 92-93.

Olesen, D., Huusom, J & Jørgensen, J (2013) A tuning procedure for ARX-based MPC, in *Proceedings of the IEEE International Symposium on Computer-Aided Control System Design*. pp. 188–193.

Olujic, Z., Fakhri, F., De Rijke, A., De Graauw, J., & Jansens, P (2003) Internal heat integration–the key to an energy-conserving distillation column. *Journal of Chemical Technology and Biotechnology*, 78(2-3), pp. 241-248.

Oomen, T., Grassens, E., Hendriks, F., Van Herpen, R. & Bosgra, O. (2011) Inferential motion control: Identification and robust control with unmeasured performance variables, *in Proceedings of the IEEE Conference on Decision and Control*, pp. 964–969.

Orozco, G., Cortés, B., Heras, M., Téllez, A. & Anzurez, J. (2016) Analysis and comparison of distillation column models considering constant and variable relative volatility, *2016 IEEE International Autumn Meeting on Power, Electronics and Computing (ROPEC)*, pp. 1–6.

Parvat, B., Deo, S. & Kadu, C. (2015) Mathematical Modeling of Interacting and Non Interacting Tank System. *International Journal of Application or Innovation in Engineering and Management (IJAIEM)*, 4 (1), pp. 86–92.

Peng, H. Wang, J. Shen, W. Zhao, J and Hao, R. (2017) Active disturbance rejection control for electrical cylinder, *2017 36th Chinese Control Conference (CCC)*, pp. 629-633.

Petlyuk, F, Platonov, V & Slavinskii, D.(1965) Thermodynamically optimal method for separating multicomponent mixtures. *International Chemical Engineering*, 5 (3), pp. 555–561.

Ponce, G., Alves, M., Miranda, J., Maciel Filho, R. & Wolf Maciel, M.(2015) Using an

internally heat-integrated distillation column for ethanol-water separation for fuel applications. *Chemical Engineering Research and Design*, 95, pp. 55–63.

Precup, R.., Tomescu, M., Preitl, S. & Petriu, E (2009) Fuzzy logic-based stabilization of nonlinear time-varying systems. *International Journal of Artificial Intelligence*, 3 (9 A), pp. 24-36 .

Qiao, L. & Jie, W. (2005) Application of Auto-Disturbance Rejection Control for a Shunt Hybrid Active Power Filter', *Proceedings of the IEEE International Symposium on Industrial Electronics ISIE.* pp. 627–632.

Rahman, A. & Shoukat Choudhury, M. (2011) Detection of control loop interactions and prioritization of control loop maintenance. *Control Engineering Practice*. 19 (7), pp. 723–731.

Rakkiyappan, R., Balasubramaniam, P. & Krishnasamy, R. (2011) Delay dependent stability analysis of neutral systems with mixed time-varying delays and nonlinear perturbations. *Journal of Computational and Applied Mathematics*. 235 (8), pp. 2147–2156.

Rehm, A. (2009) Binary distillation control in a descriptor system set-up, *in IFAC Proceedings Volumes (IFAC-PapersOnline)*, pp. 102–107.

Rencher, A.C. (1998) *Multivariate statistical inference and applications*, 338, Wiley-Interscience.

Ribeiro, M. (2004) Kalman and Extended Kalman Filters : Concept , Derivation and Properties. *Institute for Systems and Robotics Lisboa Portugal*. (February), 42.

Rivero, R., Rendón, C. & Gallegos, S. (2004) Exergy and exergoeconomic analysis of a crude oil

combined distillation unit. *Energy*. 29 (12), 1909–1927.

Ruiz, G., Kim, S., Moon, J., Zhang, L. & Linninger, A. (2010) Design and optimization of energy efficient complex separation networks. *Computers and Chemical Engineering*. 34 (9), pp. 1556–1563.

Schmidt-Traub, H. & Górak, A. (2006) *Integrated reaction and separation operations: Modelling and experimental validation*.Berlin: springer.

Selvi, J, Radhakrishnan, T. & Sundaram, S. (2007) Performance assessment of PID and IMC tuning methods for a mixing process with time delay. *ISA Transactions*. 46 (3), pp. 391–397.

Shao, X. & Wang, H. (2015) Active disturbance rejection based trajectory linearization control for hypersonic reentry vehicle with bounded uncertainties. *ISA Transactions*. pp. 5427–5438.

Sharma, N. & Singh, K. (2010) Control of reactive distillation column: A review. International Journal of Chemical Reactor Engineering 8.

Shepard, R., Carroll, J. & Krishnaiah, P. (1966) Multivariate analysis. *PR Krishnaiah . Academic Press, New York*. 561.

Shimizu, K., Holt, B., Morarl, M. & Richard Mah, S. (1985) Assessment of Control Structures for Binary Distillation Columns with Secondary Reflux and Vaporization. *Industrial and Engineering Chemistry Process Design and Development*, 24 (3), pp. 852–858.

Shimizu, K. & Mah, R.S.H. (1983) Dynamic characteristic of binary srv distillation systems. *Computers & Chemical Engineering*. 7 (2), 105–122.

Shin, J., Yoon, S. & Kim, J. (2015) Application of exergy analysis for improving energy efficiency of natural gas liquids recovery processes. *Applied Thermal Engineering*, 75, pp. 967–977.

Shridhar, R. & Cooper, D. (1997) A tuning strategy for unconstrained SISO model predictive control. *Industrial & Engineering Chemistry Research* , (36), pp. 729–746.

Singh, S., Rani, A., Singh, V. & Yadav, J. (2016) Soft sensor for inferential control in non-isothermal CSTR, *2016 International Conference on Advances in Computing, Communications and Informatics ICACCI 2016*, pp. 1785–1790.

Singh, V., Gupta, I. & Gupta, H.O. (2005) ANN based estimator for distillation - Inferential control, *Chemical Engineering and Processing: Process Intensification* , 44 (7), pp. 785–795.

Skogestad, S. (1997) Dynamics and Control of Distillation Columns: A tutorial introduction. Chemical Engineering Research and Design, 75 (6) ,pp. 539–562.

Skogestad, S. (2001) Probably the best simple PID tuning rules in the world. *Journal of Process Control* ,21–27.

Skogestad, S. (2003) Single analytic rules for model reduction and PID controller tuning. *Journal of Process control* ,13 (4), 291–309.

Soares Pinto, F., Zemp, R., Jobson, M. & Smith, R. (2011) Thermodynamic optimisation of distillation columns. *Chemical Engineering Science*. 66 (13), pp. 2920–2934.

Soave, G. & Feliu, J.A. (2002) Saving energy in distillation towers by feed splitting, *in Applied Thermal Engineering* ,2002 pp. 889–896.

Sun, Z., Zheng, J., Man, Z., Wang, H. & Lu, R. (2017) Sliding mode-based active disturbance rejection control for vehicle steer-by-wire systems. *IET Cyber-Physical Systems: Theory & Applications*., 3(1), pp. 1-10.

Sundmacher, K., Kienle, A. & Seidel-Morgenstern, A. (2005) *Integrated Chemical Processes: Synthesis, Operation, Analysis, and Control*.

Suphanit, B. (2010) Design of internally heat-integrated distillation column (HIDiC): uniform heat transfer area versus uniform heat distribution. *Energy journal*, 35 (3), pp. 1505–1514.

Suphanit, B. (2011) Optimal heat distribution in the internally heat-integrated distillation column (HIDiC). *Energy journal* ,36 (7), pp. 4171–4181.

Takamatsu, T., Nakaiwa, M. & Nakanishi, T. (1996) The concept of an ideal heat integrated distillation column (HIDiC) and its fundamental properties, *Kagaku Kogaku Ronbunshu* ,22 (5), pp. 985–990.

Tan, W. & Fu, C. (2015) Analysis of active disturbance rejection control for processes with time delay', in *American Control Conference (ACC)*, pp. 3962–3967.

Tarjani, J., Toth, A., Nagy, T., Haaz, E. & Mizsey, P. (2017) Dynamic controllability comparison of conventional distillation sequences and dividing-wall columns with upper and lower partitions using the desirability function, *Industrial & Engineering Chemistry Research* , 56 (4), pp. 952–959.

Tavakoli, S., Griffin, I. & Fleming, P. (2006) Tuning of decentralised PI (PID) controllers for TITO processes. *Control Engineering Practice*, 14 (9), pp. 1069–1080.

Tham, M, Montague, G, Glassey, J. & Willis, M.(2002) Practical inferential estimation using

artificial neural networks. *Measurement and Control*, 35 (1), pp. 5-9 .

Tham, M, Montague, G., Julian Morris, A & Lant, P (1991a) Soft-sensors for process estimation and inferential control, *Journal of Process Control*, 1 (1), pp. 3–14.

Tham, M, Vagi, F., Morris, A. & Wood, R. (1991b) Multivariable and multirate self-tuning control: a distillation column case study, *in IEE Proceedings D (Control Theory and Applications)*, pp. 9–24.

Tham, M., Vagi, F., Morris, A & Wood, R. (1991c) On-line multivariable adaptive control of a binary distillation column., *The Canadian Journal of Chemical Engineering*. 69 (4), 997–1009.

Tian, G. & Gao, Z. (2009) From Poncelet's invariance principle to Active Disturbance Rejection. *2009 American Control Conference*,pp. 2451–2457.

Tufa, L. & Ka. (2016) Effect of Model Plant Mismatch on MPC Performance and Mismatch Threshold Determination, *in Procedia Engineering*, pp. 1008–1014.

Tyreus, B & Luyben, W. (1976) Controlling Heat Integrated Distillation Columns, pp. 59-66.

Uddin, F., Tufa, L., Yousif, S. & Maulud, A.(2016) Comparison of ARX and ARMAX Decorrelation Models for Detecting Model-Plant Mismatch. *Procedia Engineering*, pp. 985–991.

Vazquez–Castillo, J., Venegas–Sánchez, J., Segovia–Hernández, J., Hernández-Escoto, H., Hernández, S., Gutiérrez–Antonio, C. & Briones–Ramírez, A. (2009) Design and optimization, using genetic algorithms, of intensified distillation systems for a class of quaternary mixtures, *Computers & Chemical Engineering* , 33 (11), pp. 1841–1850.

Waheed, M., Oni, A, Adejuyigbe, S., Adewumi, B. & Fadare, D. (2014) Performance enhancement of vapor recompression heat pump, *Applied Energy* ,114, pp. 69–79.

Waller, K., Häggblom, K., Sandelin, P. & Finnerman, D. (1988) Disturbance sensitivity of distillation control structures. *AIChE Journal*, 34 (5), pp. 853–858.

Wang, L. Zhang, H. Cai, M and Luo, Z. (2017) Active disturbance rejection power control for a floating wind turbine, *2017 29th Chinese Control And Decision Conference (CCDC)*, pp. 559-564.

Weber, R. & Brosilow, C. (1972) The use of secondary measurements to improve control. *AIChE Journal* , 18 (3), pp. 614–623.

Welch, G. & Bishop, G. (2006) An Introduction to the Kalman Filter. *In Practice*, 7 (1), pp. 1–16.

Weitz, O. and Lewin, D. (1996) Dynamic controllability and resiliency diagnosis using steady state process flowsheet data, *Computers and Chemical Engineering*, 20(4), pp. 325-335.

Wentzell, P. & Montoto, L.(2003) Comparison of principal components regression and partial least squares regression through generic simulations of complex mixtures. *Chemometrics and Intelligent Laboratory Systems*, 65 (2), pp. 257–279.

White, D.C. (2012) Optimize energy use in distillation. *Chemical Engineering Progress* ,108 (3), pp. 35–41.

Willis, M., Montague, G., Di Massimo, C., Tham, M. & Morris, A. (1992) Artificial neural networks in process estimation and control. *Automatica*. , 28 (6), pp. 1181–1187.

Wold, S., Trygg, J., Berglund, A. & Antti, H. (2001) Some recent developments in PLS

modeling. *Chemometrics and intelligent laboratory systems*. 58 (2), pp. 131–150.

World Energy Council (2016) *World Energy Resources 2016*.

Wright, R.O. (1949) Fractionation apparatus. *Standard Oil Dev Co*. 7 (11).

Xia, Y., Shi, P., Liu, G, Rees, D. & Han, J. (2007) Active disturbance rejection control for uncertain multivariable systems with time-delay, *IET Control Theory & Applications*, 1 (1), pp. 75–81.

Xie, L., Liu, Y., Yang, H. & Ding, F. (2010) Modelling and identification for non-uniformly periodically sampled-data systems ,*IET Control Theory & Applications*, 4 (5), pp. 784-794.

Xie, L., Yang, H. & Ding, F. (2011) Inferential adaptive control for non-uniformly sampled-data systems, in *American Control Conference (ACC),* pp. 4177–4182.

Xie, Y. & Long, Z. (2009) A high-speed nonlinear discrete tracking-differentiator with high precision. *Control Theory & Applications*. 26 (2), 127–132.

Xiong, Q. & Cai, W. (2006) Effective transfer function method for decentralized control system design of multi-input multi-output processes. *Journal of Process Control* ,16 (8), pp. 773–784.

Xu, X. & Wang, Q. (2017) Speed control of hydraulic elevator by using PID controller and self-tuning fuzzy PID controller, *in Proceedings - 2017 32nd Youth Academic Annual Conference of Chinese Association of Automation* ,pp. 812–817.

Yeh, T, Huang, M. & Huang, C (2003) Estimate of process compositions and plantwide control from multiple secondary measurements using artificial neural networks, *Computers and Chemical Engineering*, 27 (1), pp. 55–72.

Zafiriou, E and Morari, M. (1987) Setpoint Tracking vs. Disturbance Rejection for Stable and Unstable Processes,*1987 American Control Conference,* pp. 649-651.

Zhang, D. & Liu, G. (2017) Integration of heat exchanger network considering the pressure variation of distillation column, *Applied Thermal Engineering*,116, pp. 777–783.

Zhang, J. (2001) Inferential feedback control of distillation composition based on PCR and PLS models, *Proceedings of the American Control Conference,* pp. 1196–1201.

Zhang, J. (2006) Offset-free inferential feedback control of distillation compositions based on PCR and PLS models, *Chemical Engineering and Technology*, 29 (5), pp. 560–566.

Zhang, J. & Agustriyanto, R. (2001) Inferential feedforward control of a distillation column, *in Proceedings of the American Control Conference,* 4, pp. 2555-2560.

Zhang, Y., Xue, Y., Yang, H., Li, D., Sun, L., Niu, H., and Huang, H. (2017) Low-order active disturbance rejection control on furnace pressure of 1000MW power plant, *2017 36th Chinese Control Conference (CCC),* pp. 4453-4458.

Zhao, Y., Zhao, Z., Zhao, B. & Li, W. (2011) Active disturbance rejection control for manipulator flexible joint with dynamic friction and uncertainties compensation, in *Proceedings - 2011 4th International Symposium on Computational Intelligence and Design, ISCID 2011*.pp. 248–251.

Zheng, L., Cai, W., Zhang, X. & Wang, Y. (2017) Design and control of reactive dividing-wall column for the synthesis of diethyl carbonate. *Chemical Engineering and Processing: Process Intensification*, pp. 127–140.

Zheng, Q., Chen, Z. & Gao, Z. (2009) A practical approach to disturbance decoupling control.

Control Engineering Practice. 17 (9), pp. 1016–1025.

Zheng, Q., Dong, L.L., Lee, D.H. & Gao, Z. (2009) Active Disturbance Rejection Control for MEMS Gyroscopes. *Ieee Transactions on Control Systems Technology*. 17 (6), 1432–1438.

Zheng, Q., Gao, L.& Gao, Z. (2012) On Validation of Extended State Observer Through Analysis and Experimentation, *Journal of Dynamic Systems, Measurement, and Control*. 134 (2), 24505.

Zheng, Q. & Gao, Z. (2014) Predictive active disturbance rejection control for processes with time delay. *ISA Transactions*. 53 (4), pp. 873–881.

Zheng, W. Liu, W. Dong, W. Deng, Z and Yang, Y. (2017) Monte-Carlo tuning of PMSM servo system based on active-disturbance rejection controller, *2017 36th Chinese Control Conference (CCC)*, pp. 6090-6093.

Zhou, W and Gao, Z . (2007) An Active Disturbance Rejection Approach to Tension and Velocity Regulations in Web Processing Lines, *2007 IEEE International Conference on Control Applications*, pp. 842-848.

Zhu, D., Qiu, X., Wang, K. & Hou, Y. (2011) Study on friction compensation for gun control system of tank based on ADRC, *2011 Second International Conference on Mechanic Automation and Control Engineering (MACE)*. pp. 1672–1675.

Zhu, X., Hong, W. & Wang, S. (2004) Implementation of advanced control for a heat-integrated distillation column system. 30th *Annual Conference of IEEE* on *Industrial Electronics Society IECON*. Vol. 3. pp. 2006–2011..

Abbreviations

ADRC: Active Disturbance Rejection Control

ARMAX: Auto Regressive Moving Average with Exogenous Input.

ARX: Autoregressive with Exogenous Input

BLT: Biggest Log-Modulus

CDU: Crude Distillation Unit

DCSaDE-LS: Diversity Controlled Self Adaptive Differential evolution with Local Search

EPA: Environmental Protection Agency

ESO: Extended State Observer

FIS: Fuzzy Inference System

FQL: Fuzzy Q-learning Algorithm

GA: Genetic Algorithm

GPC: Generalised Predictive Controller

GUI: Graphical User Interface

HGA: Hierarchical Genetic Algorithm

HIDiC: Heat Integrated Distillation Column

IAE: Integrate Absolute Error

ICI: Imperial Chemical Industry

i-HIDiC: ideal Heat Integrated Distillation Column

IMC: Internal Model Controller

ITAE: Integral of Time – Weighted Absolute Error

LV: Latent Variables

MIMO: Multi-Input Multi-Output

MLR: Multiple Linear Regression

MPC: Model Predictive Control

MPM: Model Plan Mismatch

NIR: Near-Infrared

N-LWS: Non-Linear Weighted Sum

NN: Neural Networks

OIE: Overall Integral Error

OLS: Ordinary Least Square

ORPIC: Oil Refineries and Petroleum Industries

PCR: Principal Component Regression.

PID: Proportional-Integral-Derivative controller

PLS: Partial Least Square

PSO: Particle Swarm Optimization

RTO: Real Time Optimization

SCADA: Supervisory Control and Data Acquisition

SMC: Sliding Mode Control

SNR: Signal to Noise Rate

SRV: Secondary Reflux and Vaporization

SSE: Sum of Squared Errors

TAC: Total Annual Cost

TITO: Two-Inputs, Two-Outputs

TPG: Transient Profile Generator

VDU: Vacuum Distillation Unit

ZoH: Zero Order Hold